Multi-layered Space Frequency Time Codes

Samir Al-Ghadhban

Dissertation submitted to the Faculty of
the Virginia Polytechnic Institute and State University
in partial fulfillment of the requirement for the degree of

Doctor of Philosophy
In
Electrical Engineering

Brian Woerner (Co-Chair)

R. Michael Buehrer (Co-Chair)

William Tranter

Sedki Riad

James Holub

Nov. 4. 2005
Blacksburg, Virginia

Keywords: MIMO Wireless Systems, Space Frequency Time Codes, Multi-layered Space Time Codes, Uplink MIMO Scheduling.

Multi-layered Space Frequency Time Codes

by

Samir Al-Ghadhban

Abstract

This dissertation focuses on three major advances on multiple-input multiple-output (MIMO) systems. The first studies and compares decoding algorithms for multi-layered space time coded (MLSTC) systems. These are single user systems that combine spatial multiplexing and transmit diversity. Each layer consists of a space time code. The detection algorithms are based on multi-user detection theory. We consider joint, interference nulling and cancellation, and spatial sequence estimation algorithms. As part of joint detection algorithms, the sphere decoder is studied and its complexity is evaluated over MIMO channels. The second part contributes to the field of space frequency time (SFT) coding for MIMO-OFDM systems. It proposes a full spatial and frequency diversity codes at much lower number of trellis states. The third part proposes and compares uplink scheduling algorithms for multiuser systems with spatial multiplexing. Several scheduling criteria are examined and compared.

The capacity and error rate study of MLSTBC reveals the performance of the detection algorithms and their advantage over other open loop MIMO schemes. The results show that the nulling and cancellation operations limit the diversity of the system to the first detected layer in serial algorithms. For parallel algorithms, the diversity of the system is dominated by the performance after parallel nulling. Theoretically, parallel cancellation should provide full receive diversity per layer but error propagations as a result of cancellation prevent the system from reaching this goal. However, parallel cancellation provides some gains but it doesn't increase the diversity. On the other hand, joint detection provides full receive diversity per layer. It could be practically implemented with sphere decoding which has a cubic complexity at high SNR.

The results of the SFT coding show the superiority of the IQ-SFT codes over other codes at the same number of sates. The IQ-SFT codes achieve full spatial and frequency diversity at much lower number of trellis states compared to conventional codes. For V-BLAST scheduling, we propose V-BLAST capacity maximizing scheduler and we show that scheduling based on optimal MIMO capacity doesn't work well for V-BLAST. The results also show that maximum minimum singularvalue (MaxMinSV) scheduling performs very close to the V-BLAST capacity maximizing scheduler since it takes into account both the channel power and the orthogonality of the channel.

All praises goes to Allah, the Creator and Lord of the Universe

To my beloved mother and father

To Amal, my lovely wife, your love and care give me the patience

To Munirah and Lma, your smiles and hugs give me the spirit

To my great family

To my special friends

Acknowledgment

In the name of Allah the most Compassionate and the most Merciful, who has favored me with countless blessings. May Allah accept our good deeds and forgive our shortcomings.

I would like to express my high gratitude to my advisors, Dr. Brian Woerner and Dr. Richard Buehrer. I had the great pleasure of working with them. Under their supervision, they gave me the chance to work independently and be creative.

My greatest thanks are to Dr. Sedki Riad, Dr. William Tranter and Dr. James Holub. They have been very helpful in improving my proposal and dissertation. I am grateful to them for sharing their time and expertise.

I am thankful for King Fahd University of Petroleum and Minerals (KFUPM) and Saudi Arabia Cultural Mission (SACM) for their great support. They gave me the chance to join one of the greatest universities in the US, Virginia Tech. I like to thank my advisors in SACM, Dr. Jamil Makhadmi and Dr. Abdullah Sbeih. I also like to express my high gratitude to my advisor in KFUPM, Dr. Saud Al-Semari.

My greatest gratitude and thankfulness are to my family. My mother with her love and prayers backed me up and helped me to reach my goal. My father taught me the respect of science and encouraged me to seek knowledge and get higher education. My greatest love and thanks are to my wife. Her love, care, and prayers were of great motivation and inspiration. My special thanks are to my brothers and sisters. They were of great motivation and inspiration.

My special thanks is to Maruf Mohammed. His assistance and partnership were of great pleasure. His comments and views were very insightful and helpful. I like to thank MPRG students and staff for creating a healthy research environment.

My high gratitude is to all my friends in US and in Saudi Arabia. They were backing me up technically and emotionally. I enjoyed their friendship and their sincere advices.

Table of Content

List of Acronyms

AM	Amplitude Modulation
AWGN	Additive White Gaussian Noise
BLAST	Bell Labs Space Time
DSTM	Differential Space Time Modulation
DUSTM	Differential Space Time Modulation
FSC	Frequency Selective Channel
IQ	Inphase-Quadrature
MIMO	Multiple Input Multiple Output
MISO	Multiple Input Multiple Output
MLSTTC	Multi-layered Space Time Trellis Codes
MLSTBC	Multi-layered Space Time Block Codes
OFDM	Orthogonal Frequency Division Multiplexing
QAM	Quadrature Amplitude Modulation
SD	Sphere Decoder
SFT	Space Frequency Time
SIMO	Single Input Multiple Output
SISO	Single Input Single Output
STBC	Space time Trellis Code
STBE	Space Time Trellis Encoder
STTC	Space Time Trellis Code
STTE	Space Time Trellis Encoder
TCM	Trellis Coded Modulation
USTM	Unitary Space Time Modulation
V-BLAST	Vertical-Bell Labs Space Time

List of Tables

List of Figures

Chapter 1

Introduction and Literature Survey

Motivated by information theory results [Tel95][Fos98], multiple-input multiple-output (MIMO) wireless fading channels have attracted a lot of attention in the past few years. Information theorists proved that MIMO channels can boost the information capacity of wireless systems by orders of magnitude. To exploit this potential, several MIMO communication systems that have multiple-transmit and multiple-receive antennas were designed [Fos96][Tar98][Ala98][Wol98][Tar99a]. Instead of mitigating the effect of multipath propagation like traditional systems, MIMO systems take advantage of space and time propagation characteristics. They can provide transmit and receive antenna diversity and high data rates without any bandwidth expansion. For the scarce spectrum of mobile and cellular communications, MIMO systems are an excellent cost-effective candidate.

1.1 Scope and Motivation

This dissertation focuses on bandwidth efficient advances for MIMO systems, covering three major areas. The first area considers a layered architecture that has transmit diversity at each layer [Tar99], termed a multi-layered space time code. This architecture combines spatial multiplexing and transmit diversity and it bridges the gap between these two MIMO systems. The focus in this part is to how the multi-layered system compares to other MIMO systems, such as V-BLAST[1] and space time block codes. Furthermore, we propose and compare multi-layered detection algorithms which are based on multi-user detection theory. We also evaluate the outage capacity of these detection algorithms.

The second part of the dissertation focuses on space-frequency-time (SFT) coding for MIMO-OFDM[2] systems. SFT coding applies spatial coding across multiple antennas, frequency coding across OFDM subcarriers and temporal coding across successive OFDM symbols. In [Ben00], it was shown that the maximum achievable diversity for a MIMO-OFDM system is $M_T L M_R$, where L is the number of paths in a frequency selective channel, termed the length of the channel. Also, M_T and M_R are the number of transmit and receive antennas, respectively. In order to achieve this diversity, the minimum effective length of the SFT code should be at least equal to $M_T L$. The motivation of our work in this part is to reduce the complexity of the design, in terms of number of states, while achieving full diversity without any bandwidth expansion.

The last part of this dissertation studies uplink scheduling criteria for multiuser systems with spatial multiplexing. Scheduling is a channel-aware process that assigns transmission to selected users based on certain criteria. Our focus is to select a criterion that maximizes uplink

---

[1] Vertical- Bell Labs LAyered Space Time
[2] Orthogonal Frequency Division Multiplexing

capacity for practical detection algorithms. Scheduling provides multi-user diversity to the system while spatial multiplexing increase the data rate of the user.

1.2 Literature Survey

Information theory results show that the capacity of MIMO system increases linearly with min(M_R,M_T), where M_R and M_T are the number of receive and transmit antennas respectively [Tel95][Fos98]. However, for single-input single-output (SISO) channels, the capacity increases logarithmically with signal-to-noise ratio (SNR). Thus, a significant capacity increase can be achieved by MIMO systems without adding power and without expanding the bandwidth.

Spatial Multiplexing

The first high data rate architecture was the Bell-labs layered space time architecture (BLAST) and it was proposed by [Fos96]. In BLAST, multiple parallel data streams are spatially multiplexed and transmitted simultaneously on the same frequency through all transmit antennas. With rich multipath propagation, these different streams are separated at the receiver based on their distinct spatial signatures. However, this architecture is a full spatial multiplexing scheme and it doesn't provide any transmit diversity while receive diversity is achieved on some streams depending on the receiver architecture.

Space Time Codes

A unique joint design of transmit diversity, modulation and coding was proposed by [Tar98]. They extended the delay transmit diversity scheme proposed by [Wit93] to a space time trellis code (STTC). This scheme provides full rate, full transmit diversity and coding gains without any bandwidth expansion. One main drawback is that the decoding complexity increases

exponentially with increasing number of transmit antennas. In order to reduce the complexity of STTC, [Tar98b] illustrated that by using principal ratio combining, which is a nontrivial extension of the maximum ratio combining for multiple transmit antennas, the complexity was reduced by almost a factor of M_T. However, the complexity still increases exponentially with the number of transmit antennas. Another attempt by Tarokh was in [Tar99] where he proposed a spatial multiplexing structure to support high data rate applications with a transmit diversity at each layer. It is a generalized version of BLAST and it is called multi-layered space-time architecture. This architecture is the basis of our work in this dissertation.

To achieve linear processing at the receiver, Alamouti in [Ala98] proposed a novel transmit diversity scheme where the transmitted symbols are mapped to a 2×2 space time orthogonal transmission matrix. The orthogonal design achieves maximum likelihood decoding with linear processing per transmitted symbol. Extending Alamouti's work, [Tar99a] designed space time block codes (STBC) for more than two transmit antennas. They showed that the orthogonal design couldn't provide full transmission rate for more that two transmit antennas with complex modulation. The rate-diversity tradeoff is investigated in [Jaf01], where they designed quasi-orthogonal STBC that achieves full transmission rates for more than two transmit antennas but at half the transmit diversity. However, the decision statistics can't be uncoupled and ML detection is performed over each pair of symbols. In [Sha03], they rotated the constellation of one of the symbols in order to improve the distance properties of the decision statistics. It turns out that this rotation made the quasi-orthogonal STBC full rank. That is a full-rate full-diversity STBC for four transmit antennas. Also, full-rate full-diversity nonorthogonal designs were proposed in [Dam03]. In [Ahm03], a full rate nonorthogonal design with simplified maximum likelihood detection was proposed for eight transmit antennas.

The performance of the above space time codes is highly dependent on channel estimation. Differential transmit diversity schemes eliminate the need for channel estimation, thus reducing receiver complexity and increasing system throughput. A differential STBC for two transmit antennas was proposed in [Tar98c].

One of the recent advances in MIMO communication systems is the concept of space time modulation (STM). Instead of mapping transmitted symbols to a space time transmission matrix (as in STBC), the information bits select a matrix from the space time signal constellation. In order to detect these space time matrices without channel state information, [Hoc00a] showed that signal matrices should be unitary and they proposed a unitary space time modulation (USTM) in [Hoc00a][Hoc00c]. A differential encoding and decoding scheme for STM was proposed independently by [Hoc00b][Hug00].

Another MIMO scheme that achieves full transmit and receive diversity without coding or MIMO processing is MIMO antenna selection [Tho01][Che03]. This approach requires a feedback of channel state information to select the best set of transmit and receive antennas which limits its application in high mobility environments.

MIMO Application in Cellular Systems

A majority of existing cellular systems deploy receive antenna diversity at the base station in order to improve the performance of the uplink (mobile unit to base station). On the other hand, deploying receive diversity at the mobile unit may not be feasible due to the additional cost and battery limitations. Also, due to the small size of mobile units, high spatial correlation between the receiving antennas may limit the diversity gains. Therefore, transmit diversity has attracted significant attention for improving downlink performance.

Transmit diversity has been proposed for third generation (3G) CDMA systems [Tex98][Luc99]. One of the attractive transmit diversity schemes is Alamouti's STBC with two transmit antennas. This code is simple to implement with very low complexity and it provides full transmission rate and full transmit diversity. In the literature, they referred to this scheme as space time transmit diversity (STTD). A similar scheme was proposed by Lucent for CDMA 2000 and is termed space time spreading (STS) [Pap99][Hoc99][Son04]. Another candidate is orthogonal transmit diversity (OTD) originally proposed by [Roh97]. This scheme uses orthogonal spreading sequences to spread signals transmitted from different antennas and relies on coding and interleaving to provide transmit diversity. The above three schemes are termed "open loop" schemes because the transmitter doesn't require knowledge of the channel.

Closed loop schemes were also proposed for third generation systems [DaS01][Ste00]. Transmit adaptive antenna (TxAA) is a scheme originally proposed for the frequency division duplex (FDD) mode of UMTS[3] and then adapted to the time division duplex (TDD) mode [3GPP99]. The main difference between applying TxAA for these two modes is that in the FDD mode, the mobile unit has to send TxAA weights to the base station via a feedback channel. On the other hand, for TDD mode, the feedback mechanism is not needed since uplink and down link frequency bands coincide. The base station can assume that the uplink and the downlink propagation channels are identical provided that the channel doesn't change too rapidly.

Several comparison studies between different transmit antennas schemes applied to 3G systems had been reported in the literature. For example, open loop transmit diversity schemes had been compared in [Jal99][Dab00][Son04]. In [Jal99], they compared the performance of STTD and OTD over third generation CDMA environment. They showed that STTD is slightly

[3] Universal Mobile Telecommunications System

better than OTD. The gain is around 0.2dB. Furthermore, [Dab00] compared between STTD, OTD and STS. They showed that STS is similar to STTD but with a signal constellation expansion. Thus, STS has higher peak to average ratio. Also, they showed that the performance of STTD is 0.3 to 0.5 dB better than OTD. [Son04] compared STS and OTD for IS-2000 systems.

Comparing open loop transmit diversity schemes with closed loop schemes is done by [Roh99] and [Ong01]. It was shown in [Rah99] that closed loop schemes, such as TxAA, improve the signal to noise ratio at the receiver by a factor of two compared to OTD. This is due to the fact that transmitted symbols are received coherently at the mobile station, forming a beam with maximum gain in the direction of the desired mobile.

MIMO Multi-user Detection

In a multi-user environment, multi-user interference (MUI) greatly limits the performance of communication systems. Multi-user detection (MUD) techniques are used to mitigate the effect of MUI. In the context of CDMA wireless systems, several investigation evaluated MUD receivers for users with multiple antennas. For, example, [Xia00] proposed and evaluated the performance of four MUD receivers for STBC systems over MC-CDMA[4] systems. The considered receivers detect the information bearing bits of the desired user while suppressing interference. The four schemes were a maximum ratio combiner, an orthogonal resorting combiner, a minimum mean square error combiner, and a minimum mean square error multiuser detector. Furthermore, [Zhi01] developed novel space time multiuser transceivers for multiple access systems over frequency-selective channels. Each user transmits from multiple transmit antennas but only one receive antenna is needed.

[4] Multi-Carrier Code Division Multiple Access

In order to improve the performance of STBC over CDMA systems, many researchers proposed and evaluated the performance of concatenating STBC with turbo or convolutional codes [Yum00] [Cha01] [Her02]. In [Yum00], they developed a reduced complexity multi-user receiver for turbo coded STBC users in CDMA systems. The receiver is a multistage receiver that implements non-linear MMSE estimation and parallel interference cancellation schemes. Another concatenated turbo-coded STBC system was proposed in [Cha01]. The receiver consisted of linear MUD such as a decorrelator and a MMSE detectors followed by soft interference cancellation and decoders for each user. A low complexity soft-iterative multiuser receiver was proposed by [Her02]. Each transmitter serially concatenated a convolutional encoder, interleaver, STBC and spreading. The proposed receiver used a soft-input soft-output (SISO) multiuser detector, which is a soft interference canceller for space time wideband code division multiple access (WCDMA) signals.

It is well known in MUD theory that joint detection is the best in terms of performance and near-far resistance. However, the price is very large receiver complexity. Trying to implement joint detection with reduced complexity has attracted several researchers. In [Jay01], the joint optimal maximum likelihood (ML) multiuser detector for trellis space time coded synchronous CDMA systems was derived. In order to obtain a better trade-off between performance and complexity, they proposed a suboptimal low complexity iterative ST-MUD based on iterative SISO interference cancellation. For applications that can't handle delays associated with iterative processing, [Cor02] proposed noniterative joint detection scheme for space time trellis coded asynchronous DS-CDMA systems. The receiver is based on a reduced state multiuser sequence detection algorithm. The main advantage is near optimum performance with low decoding delays. However, the receiver's complexity grows exponentially with the

number of users and the constraint length of the users' encoder. Thus, it is suitable for high data rate users that have low processing gains.

Blind multiuser detectors had also attracted several researchers [Mis02][Rey02] [Xug01]. Blind MUD has the advantage that the receiver requires knowledge of only the signature waveform and timing of the desired user. [Rey02] developed blind adaptive MUD for synchronous and asynchronous space time coded CDMA systems. Also, [Xug01] proposed a linear blind MUD for space time coded CDMA systems. The receiver was called a Capon receiver and it suffered from slow convergence and scalar ambiguity associated with its blind channel estimates. To solve this drawback, [Hon02] proposed a semi-blind Capon receiver by capitalizing on periodically inserted training symbols.

The above MUD schemes were applied to space time coded CDMA systems where each user and possibly each transmit antenna of each user had a different spreading sequence. However, few researchers considered the case where all the space time coded users transmit on the same frequency and time and without any signature waveform assignment. A similar case would be that if some users had been assigned the same spreading sequence or an interferer happened to have the same spreading sequence. In both cases, the receiver could not apply the normal CDMA multiuser detectors. This introduces some challenges that must be considered. First, MUI is very high and it dramatically degrades the performance of the receiver if ignored. Another consideration is that the performance highly depends on accurate estimation of the spatial signature of each user to be able to separate them. [Nag98] considered the system of K synchronous space time block coded users each transmitted through M_T antennas. They developed an MMSE interference suppression technique that suppresses the interference from the K-1 co-channel users and provides a diversity order of $M_T \times (M_R - K + 1)$. To further improve the

performance of the multiuser receiver, [Ben00a] proposed an iterative SISO MMSE MUD followed by parallel MAP decoders for each user. The previous two schemes require a number of receive antennas greater than or equal to the number of users ($M_R \geq K$). In order to reduce the number of receive antennas, [Tra02] proposed a novel multi-user receiver for space time coded systems. The users are divided into groups where each group is assigned a group signature. The receiver consists of group interference cancellation followed by trellis decoding for each user. MUD and trellis decoding are performed jointly in an iterative manner. The idea of using group signatures greatly simplifies the group interference cancellation and it reduces the number of receive antennas. Furthermore, the receiver is less complex than [Ben00a] but with the cost of bandwidth expansion.

MIMO-OFDM

Concatenating space time codes with orthogonal frequency division multiplexing (OFDM) is known as space frequency time (SFT) codes. SFT coding applies spatial coding across multiple antennas, frequency coding across OFDM subcarriers and temporal coding across successive OFDM symbols. The first space frequency coding study was done by [Aqr98] where they adapted Tarokh's space time codes [Tar98] to OFDM with multiple transmit antennas. However, these codes were designed for quasi-static fading channels. Thus, they were not optimized for OFDM channels and couldn't benefit from the available frequency diversity. In [Ben00], it was shown that the maximum achievable diversity for a MIMO-OFDM system is $M_T L M_R$, where L is the frequency selective channel length and M_T and M_R are the number of transmit and receive antennas, respectively. In order to achieve this diversity, the minimum effective length of the SFT code should be equal to $M_T L$. Thus, the trellis code design criterion is similar to the design over rapidly fading channels, which is the maximization of the minimum

effective length. However, the coding gain depends on the channel and thus optimizing the coding gain is not visible [Ben00]. Furthermore, since the OFDM channel in the frequency domain is highly correlated and slowly varying, interleaving across frequency tones is a vital requirement that allows the code to exploit the available frequency diversity. To achieve full spatial-frequency diversity, trellis code design needs large number of states. In order to simplify the design and reduce the complexity of the code, [Gon03] proposed to concatenate TCM with STBC. The spatial diversity is guaranteed by STBC while the frequency diversity is achieved by TCM. This separation allows for a less complex, lower number of states, TCM design.

MIMO-Scheduling

In a multi-user environment, scheduling transmission to or from the best user at a time leads to a form of selection diversity known as multiuser diversity. In single-input single-output systems, where each mobile and the base station have one antenna, it was shown that selecting the user with the maximum signal to noise ratio maximizes the total information capacity of the uplink system [Kno95]. Similar results were also found for the downlink from the base station to the mobile unit [Tse97]. This scheduler is known as MaxSNR scheduling. Over MIMO channels, most of the studies were based on theoretical information capacity [Hea01] [Air03] [Rea04] and on the downlink. It was shown in [Goz03] that STBC and scheduling weren't a good match. In fact, scheduling to a user with single antenna outperformed scheduling using STBC. The reason is that STBC averages the fades while the scheduler tends to benefit from high peaks in the fading channel. In addition, multiuser diversity obtained from scheduling is much higher than the spatial diversity of STBC. On the other hand, spatial multiplexing schemes match perfectly with scheduling. This is because they provide high data rates while the scheduler compensates for the lack of diversity by providing multiuser selection diversity.

In a MIMO system, scheduling can be done to a single user or multiple users. Scheduling to multiple users, i.e allowing more than one user to transmit or receive at the same time, was shown to be optimal in terms of maximizing system capacity and throughput. In [Hea01], downlink scheduling to multiple users improved the average throughput compared to a single user scheduling. Furthermore, the optimal uplink MIMO scheduling based on an information theoretical approach was considered in [Lau02]. They showed that it should allocate all the power to at most M_R users, where M_R is the number of receive antennas at the base station. Also, they found that the optimal power resource allocation is water-filling in space and time. In [Air03], the authors found that multiuser scheduling reduces the average delay experienced by the users compared to single-user scheduling. In [Shi03], the scheduler selects K users at a time and it cycles through groups of users in a round robin (RR) fashion. Thus, it provides diversity through multiple antennas while it insures fairness through RR scheduling.

The literature didn't focus much on multi-layered space-frequency-time systems. These systems are important in the field of MIMO systems since they combine spatial multiplexing and frequency and spatial diversity. Thus, further investigation is needed and advanced design of detection algorithms are required. Furthermore, advantage of multi-layered systems compared to V-BLAST and other open loop MIMO systems must be investigated. In addition, low complexity designs for full spatial and frequency diversity codes for MIMO-OFDM systems are needed since conventional designs require large number of states for practical values. Uplink scheduling criteria for practical MIMO systems are needed to address the high data rate challenge of future wireless systems. Detailed contribution of this work is given in next section.

1.3 Contributions

The main contributions of this work are:

- Development of new detection algorithms for multi-layered space time trellis codes. These algorithms are based on multi-user detection techniques. They are based on joint detection, interference nulling and cancellation algorithms, and spatial sequence estimation.
- A unique outage capacity study of multi-layered space time block codes that shows the optimal performance and tradeoffs of different detection algorithms.
- Outage capacity comparison of open loop MIMO systems with multi-layered space time black codes. It shows the advantage of multi-layered codes and the preferred region of operation compared to V-BLAST and STBC.
- Complexity study of the sphere decoder for MIMO systems. The study examines the effect of number of antennas, signal to noise ratio, signal set constellation size, and initial search radius on the complexity of the sphere decoder.
- A modified sphere decoder design for non-rectangular and rotated constellations.
- Evaluation of detection algorithms for multi-layered space time block coded OFDM systems. The results show that the performance of group interference nulling and cancellation algorithms is dominated by the first detected layer. The best performance is obtained with the sphere decoder with moderate complexity.
- A reduced complexity space-frequency-time code, based on IQ-trellis codes, for MIMO-OFDM systems. In addition, we examine the effect of interleaving on the diversity and performance of space frequency time coded systems.

- Development and comparison of scheduling criteria for uplink V-BLAST users. We propose a V-BLAST capacity maximizing scheduler and we show that optimal MIMO capacity maximization doesn't work well for V-BLAST. Also, we examine suboptimal scheduling criteria that require less computation.

So far, we have the following publications based on this work:

- S. Al-Ghadhban and B. Woerner, "Iterative Joint and Interference Nulling/Cancellation Decoding Algorithms for Multi-Group Space Time Trellis Coded Systems," *WCNC. 2004 IEEE* ,vol. 4 , pp.2317 – 2322, 21-25 March 2004.
- M. Mohammad, S. Al-Ghadhban, B. Woerner, and W. Tranter, "Comparing Decoding Algorithms for Multi-Layer Space-Time Block Codes," *SoutheastCon, 2004. Proceedings. IEEE,* Pages:147 – 152
- S. Al-Ghadhban, M. Mohammad and B. Woerner, "Iterative Spatial Sequence Estimator for Multi-Group Space Time Trellis Coded Systems" *VTC2004-Fall. 2004 IEEE 60th* , vol. 2, pp.1353 – 1357, 26-29 Sept. 2004.
- M. Mohammad, S. Al-Ghadhban and B. Woerner, "Spatial Sequence Estimator Based Decoding Algorithm for V-BLAST*". VTC2004-Fall. 2004 IEEE 60th ,* vol. 3, pp. 1875 – 1879, 26-29 Sept. 2004.
- S. Al-Ghadhban, M. Mohammad, B. Woerner and R. M. Buehrer, "Performance Evaluation of Decoding Algorithms for Multi-Layered STBC-OFDM System" *Signals, Systems and Computers, 2004. Conference Record of the Thirty-Eighth Asilomar Conference on,* vol. 1, pp.1208 – 1212, Nov. 7-10, 2004.

- S. Al-Ghadhban, R. M. Buehrer and B. D. Woerner, "Outage Capacity Comparison of Multi-Layered STBC and V-BLAST Systems," Presented at VTC Fall 2005, Dallas, Tx.

Recent submissions:

- S. Al-Ghadhban, R. M. Buehrer and M. Robert, "Uplink Scheduling Criteria for Multiuser V-BLAST Systems," Submitted to IEEE Communications Letter.
- S. Al-Ghadhban, R. M. Buehrer and B. D. Woerner, "IQ Space Frequency Time Codes for MIMO-OFDM Systems," Submitted to IEEE VTC Spring 2006.
- S. Al-Ghadhban, R. M. Buehrer and M. Robert, "Uplink Scheduling Criteria Comparison for V-BLAST Users," Submitted to IEEE VTC Spring 2006.

1.4 Outline of Dissertation

The dissertation starts with an overview of basic MIMO capacity and systems in Chapter 2. It also contains a simulation study of space time trellis and block codes.

The original work of this dissertation starts in Chapter 3. Chapter 3 focuses on the development of decoding algorithms for multi-layered space time trellis coded (MLSTTC) systems. This architecture considers a single user who transmits through K parallel space time trellis coders without any signature waveforms. It is a spatial multiplexing system with transmit diversity and coding gains for each layer. Since there is no signature waveforms assigned, the interference for this architecture is very high and the receiver must relay on the spatial signature of each encoder in order to successfully detect all encoders. We develop and compare three MLSTTC detection algorithms; joint detection, group interference nulling and cancellation, and spatial sequence estimation. The joint decoders perform the best and provide full receive

diversity to the system. The interfere nulling and cancellation algorithms suffer from diversity reduction caused by nulling and error propagation caused by cancellation. In order to avoid cancellation, a soft-input soft-output spatial sequence estimator is proposed in this chapter. The spatial sequence estimator algorithm has the flexibility to tradeoff complexity with receive diversity and it doesn't suffer from error propagation. The algorithm outperforms group interference nulling and cancellation algorithms.

Chapter 4 examines the outage capacity of multi-layered space time block coded (MLSTBC) systems and compares it to other open loop MIMO architectures, such as V-BLAST and STBC. The first part of this chapter evaluates and compares the information capacity of different detection algorithms. This study gives useful insight into the optimal performance of these algorithms and on the spatial multiplexing-diversity tradeoffs of these systems. The second part compares the capacity of MLSTBC to other open loop MIMO architectures, such as V-BLAST and STBC. The results of this study show that for the same number of transmit-receive antennas, MLSTBC is more power efficient than V-BLAST, since it provides more diversity. Furthermore, at low SNR and low outage probabilities, MLSTBC is more spectrally efficient. Thus, it is more suitable for low power high data rate wireless applications.

A joint detector that is easily applied to MLSTBC with moderate complexity is a sphere decoder. Thus, Chapter 5 studies the complexity of the sphere decoder for MIMO systems. The complexity is measured in flops (floating point operations). Its performance is evaluated for V-BLAST, full-rate full-diversity space time block codes, and MLSTBC systems. The results show a large gain in performance with moderate complexity. Also, this chapter contains a modified sphere decoder to handle non-rectangular and rotated constellations.

Chapter 6 investigates a MLSTBC system over frequency selective channels (FSC). To mitigate the effect of FSC, we concatenate MLSTBC with OFDM. This transforms a MIMO FSC into parallel MIMO flat fading channels. The study evaluates and compares the OFDM symbol error rate performance of several decoders for MLSTBC-OFDM systems. The results show that the performance of group interference nulling and cancellation algorithms is dominated by the first detected layer. The best performance with moderate complexity is obtained with the sphere decoder.

Chapter 7 studies concatenated coding for MIMO-OFDM systems. The proposed concatenated system achieves full spatial and frequency diversity at a substantially reduced complexity in terms of number of states. In general, coding for MIMO-OFDM systems is known as space frequency time (SFT) coding since coding is done in the frequency domain. The chapter starts with an overview of a concatenated trellis coded modulation (TCM) and STBC systems over fading channels. Then, we illustrate and describe the benefits of IQ-trellis codes, which are the focus of the study. After that, concatenated SFT codes are compared and evaluated. The results show the performance improvement of IQ-TCM compared to conventional designs at the same number of states. In addition, a multi-layered SFT coded system is presented. It combines spatial multiplexing with frequency and spatial diversity.

Finally, we study in Chapter 8 uplink scheduling for MIMO users. The scheduler selects one user at a time based on a certain criterion that depends on the detection algorithm. Each user spatially multiplexes his data over the transmit antennas. This spatial multiplexing (SM) scheme provides high data rates while a multi-user diversity obtained from scheduling improves the performance of the uplink system. The main results of this study show that the scheduler that maximizes the optimal MIMO capacity doesn't work well for a V-BLAST system. Instead, we

find a scheduler that maximizes the V-BLAST capacity which is derived specifically from the V-BLAST detection algorithm. Furthermore, we investigate suboptimal schedulers and their performances. In addition, we look into scheduling for SM with sphere decoding and we find that in this case, using MIMO capacity as the scheduling criterion is the best.

Chapter 2

Overview of MIMO Communication Systems

This chapter gives an overview of MIMO channel models, MIMO capacity and the basic open loop MIMO communication systems. It covers Bell Labs Space Time (BLAST) architecture, space time trellis and block codes, and space time modulation schemes.

2.1 MIMO Channel Models

A MIMO channel is a wireless link between M_T transmit and M_R receive antennas. It consists of $M_T M_R$ elements that represent the MIMO channel coefficients. The multiple transmit and receive antennas could belong to a single user modem or it could be distributed among different users. The later configuration is called distributed MIMO and cooperative communications. Figure 2.1 shows conceptual diagram of MIMO channels.

Statistical MIMO channel models offer flexibility in selecting the channel parameters, temporal and spatial correlations. MIMO channel simulation tools are implemented based on these models. Several statistical MIMO channel models were proposed in [Ped00] and [Vie01].

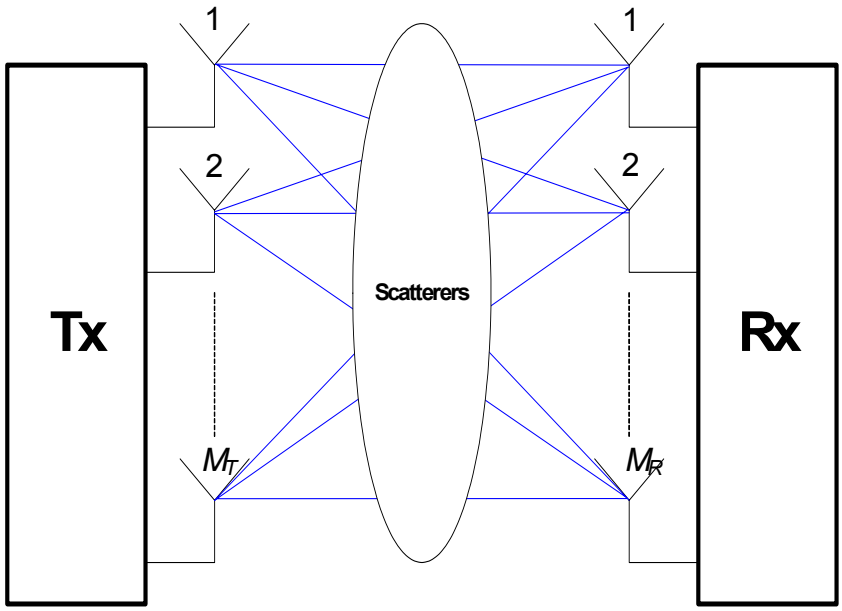

Figure 2.1: A MIMO wireless channel

Both models introduced spatial correlation by multiplying a matrix of uncorrelated random variables by a square root of a covariance matrix and both are based on similar assumptions. However, they differ in their approach. In [Ker02], the authors validate the statistical model of [Ped00] based on measurements in picocells and microcells. They showed that the eigenvalue distribution of the model matches the measurements.

Uncorrelated MIMO channel model

To evaluate the optimal performance of MIMO systems, an independent identically distributed (i.i.d) MIMO channel model is typically assumed ($\mathbf{H}_{unc}$). For non-line-of-sight communications with a large number of scatterers, the elements of $\mathbf{H}_{unc}$ are i.i.d zero mean

complex Gaussian random variables with Rayleigh distributed envelope and uniformly distributed phase.

Correlated MIMO channel model

Let $\mathbf{R}_T$ and $\mathbf{R}_R$ be the normalized spatial covariance matrices of the transmitter and receiver elements, respectively. Assuming independence between the transmitter and the receiver and for a large number of scatterers, the spatial covariance matrix of the MIMO channel is written as [Vie01][Ker02]:

$$\mathbf{R}_{MIMO} = E\{vec(\mathbf{H}) \cdot vec(\mathbf{H})^H\} = \mathbf{R}_R \otimes \mathbf{R}_T \qquad (2.1)$$

where $\mathbf{R}_{MIMO}$ is an $M_R M_T \times M_R M_T$ spatial covariance matrix

$vec(\mathbf{H})$ is the vector operator that stacks the columns of the $M_R \times M_T$ matrix **(H)** into an $M_R M_T \times 1$ column vector .

$\mathbf{H}$ is the $M_R \times M_T$ MIMO channel matrix.

$\mathbf{H}^H$ the superscript (^{H}) denotes the complex conjugate transpose, known as the Hermitian conjugate.

$E\{\bullet\}$ is the expectation operator.

$\otimes$ is the Kronecker product. The Kronecker product between two matrices is defined as:

$$\mathbf{A}_{m\times n}\otimes\mathbf{B}_{p\times q}=\begin{bmatrix}\mathbf{A}(1,1)\mathbf{B} & \mathbf{A}(1,2)\mathbf{B} & \cdots & \mathbf{A}(1,n)\mathbf{B}\\ \mathbf{A}(2,1)\mathbf{B} & \mathbf{A}(2,2)\mathbf{B} & \cdots & \mathbf{A}(2,n)\mathbf{B}\\ \vdots & \vdots & \ddots & \vdots\\ \mathbf{A}(m,1)\mathbf{B} & \mathbf{A}(m,2)\mathbf{B} & \cdots & \mathbf{A}(m,n)\mathbf{B}\end{bmatrix}_{mp\times nq}$$

Since the covariance matrix is nonnegative definite, it can be factorized using Cholesky decomposition [Sch97]:

$$\mathbf{R}_T=\mathbf{L}_T^H\cdot\mathbf{L}_T \tag{2.2}$$

$$\mathbf{R}_R=\mathbf{L}_R^H\cdot\mathbf{L}_R \tag{2.3}$$

where **L** is a lower triangular matrix.

It is shown in [Vie01] that the spatially correlated MIMO channel matrix ($\mathbf{H}_{cor}$) can be modeled as:

$$\mathbf{H}_{cor}=\mathbf{L}_R^H\cdot\mathbf{H}_{unc}\cdot\mathbf{L}_T^* \tag{2.4}$$

Note that the superscript (*) in (2.4) denotes the complex conjugate operator.

To introduce temporal correlation in the model, the power spectrum of the uncorrelated channel samples in $\mathbf{H}_{unc}$ can be shaped by an appropriate Doppler spectrum as illustrated in [Ped00] [Ker02][Rap96].

$\mathbf{R}_T$ and $\mathbf{R}_R$ can be obtained from reported measurements, such as [Ker02], or from closed form or approximated spatial correlation functions, such as [Bue02][Tsa02].

2.2 MIMO Capacity

Channel capacity is the maximum information rate that can be transmitted and received with arbitrarily low probability of error. A common representation of the channel capacity is

within a unit bandwidth of the channel and can be expressed in bps/Hz. This representation is also known as spectral (bandwidth) efficiency. Early capacity analysis of single-input single-output (SISO) flat Rayleigh fading channels showed that the channel capacity in bps/Hz can be expressed as:

$$C_{SISO} = E_h\{\log_2(1+\mathrm{SNR}\left|h\right|^2)\} \tag{2.5}$$

where $E_h\{\cdot\}$ is the expectation operator with respect to the channel coefficient (h), which is a complex Gaussian random variable with zero mean and a variance of 0.5 per dimension, and SNR is the average signal to noise ratio for each receiving antenna. This is often termed ergodic capacity. For a given h, there is only one way to increase the capacity of the SISO channel and that is by increasing SNR. Also, the capacity increases logarithmically with increasing SNR. At high SNR, an additional 1 bps/Hz to the capacity is achieved with a 3dB increase in SNR.

The need to transmit high data rates over wireless channels pushed researchers to investigate new communication systems. One of the promising ways to boost the capacity of wireless channels by an order of magnitude is transmission through MIMO channels. For M_T transmit antennas and M_R receive antennas, [Tel95] and [Fos98] showed that the MIMO flat fading channel capacity can be expressed as:

$$C_{MIMO} = E_H\left\{\log_2\left(\det\left[\mathbf{I}_{M_R} + \frac{\mathrm{SNR}}{M_T}\mathbf{H}\mathbf{H}^H\right]\right)\right\} \text{ bps/Hz} \tag{2.6}$$

It is interesting to express the channel capacity in terms of the eigenvalues of $\mathbf{H}\mathbf{H}^H$ as illustrated in [Tel95]. The rank of $\mathbf{H}$ is defined as the number of linear independent columns or rows and it is equal to the number of nonzero eigenvalues of $\mathbf{H}\mathbf{H}^H$ [Sch97]:

$$\mathrm{rank}(\mathbf{H}) = \mathrm{rank}(\mathbf{H}\mathbf{H}^H) = r \le \min(M_R, M_T) \tag{2.7}$$

Using singular value decomposition (SVD), the channel matrix **H** can be decomposed as:

$$\mathbf{H} = \mathbf{U}\mathbf{D}\mathbf{V}^{H} \tag{2.8}$$

where **D** is an $M_R \times M_T$ diagonal matrix having the singular values on its diagonal. **U** is an $M_R \times M_R$ unitary[5] matrix that spans the column space of **H** and **V** is an $M_T \times M_T$ unitary matrix that spans the row space of **H**. The singular values are nonnegative real numbers and defined as the square roots of the eigenvalues of $\mathbf{H}\mathbf{H}^{H}$. Thus, the diagonal matrix **D** is equal to $diag(\sqrt{\lambda_1},\cdots,\sqrt{\lambda_r},0,\cdots,0)$, where *r* is the rank of **H** and λ_i is the i^{th} eigenvalue of $\mathbf{H}\mathbf{H}^{\text{H}}$.

The received samples at time *t* on the M_R receive antennas can be written as:

$$\mathbf{y} = \mathbf{H}\mathbf{x} + \boldsymbol{\eta} \tag{2.9}$$

where **x** is the $M_T \times 1$ transmitted vector and $\boldsymbol{\eta}$ is the $M_R \times 1$ additive white Gaussian noise (AWGN) vector. Decomposing **H** and applying a unitary transformation to (2.9) results in:

$$\begin{aligned} \mathbf{y} &= \mathbf{U}\mathbf{D}\mathbf{V}^{H}\mathbf{x} + \boldsymbol{\eta} \\ \mathbf{U}^{H}\mathbf{y} &= \mathbf{D}\mathbf{V}^{H}\mathbf{x} + \mathbf{U}^{H}\boldsymbol{\eta} \\ \tilde{\mathbf{y}} &= \mathbf{D}\tilde{\mathbf{x}} + \tilde{\boldsymbol{\eta}} \end{aligned} \tag{2.10}$$

Since **U** and **V** are unitary matrices, the statistics of **y**, **x** and $\boldsymbol{\eta}$ are preserved. Thus, the MIMO communication channel is equivalent to *r* parallel SISO channels. The i^{th} channel has a power of λ_i. By using the parallel Gaussian channel capacity formula with uniform power distribution [Cov91], the MIMO flat fading capacity is written as:

$$C_{MIMO} = E_{\lambda}\left\{\sum_{i=1}^{r}\log_2\left(1+\frac{\text{SNR}}{M_T}\cdot\lambda_i\right)\right\} \text{ bps/Hz} \tag{2.11}$$

Representing the capacity of MIMO channels in terms of the singular values of the channel matrix (**H**) clearly shows the effect of spatially correlated or rank deficient MIMO channels on

[5] a Unitary matrix $\mathbf{A} \in \mathbb{C}^{N\times N}$ is defined as any matrix where $\mathbf{A}\mathbf{A}^{H} = \mathbf{A}^{H}\mathbf{A} = \mathbf{I}$.

the capacity. Correlated MIMO channels have lower rank than independent channels. Therefore, they have a lower number of nonzero singular values resulting in reduced channel capacity.

The MIMO channel capacity could be further increased by optimally allocating power at the transmitter using the water filling principle [Tel95][Kha01]. Estimated channel state information (CSI) is fed back to the transmitter in order to perform the water filling. This could be done if the channel is slowly varying and the fading doesn't change much over two or more frames. At a low number of antennas and at low SNR, the capacity will significantly increase compared to uniform power allocation [Kha01].

To get some insight into the advantages of MIMO channels, we look at some special cases.

Case 1: orthogonal parallel (uncoupled) channels

Let's assume that $M_R = M_T = M$ and the channel matrix $\mathbf{H} = \mathbf{I}_M$. Thus the MIMO channels are uncoupled and each channel has a gain of one and there is no interference at the receiver. The channel capacity is [Fos98]:

$$C_{MIMO_{|\text{Uncoupled}}} = M \cdot \log_2(1 + \frac{\text{SNR}}{M}) \rightarrow \frac{\text{SNR}}{\ln(2)} \text{ as } M \rightarrow \infty \qquad (2.12)$$

Note that unlike the SISO capacity, the MIMO capacity scales linearly, rather than logarithmically, with increasing SNR for large number of antennas.

Case 2: Increase M_R and fix M_T

When M_T is large, by the law of large numbers $\frac{1}{M_T}\mathbf{H}\mathbf{H}^H \rightarrow \mathbf{I}_{M_R}$. Thus, (2.6) is reduced to [Tel95]:

$$C_{MIMO_{|\text{Large } M_T}} = M_R \cdot \log_2(1+\text{SNR}) \tag{2.13}$$

Thus, the capacity increases linearly with the number of receive antennas. As $M_R \to \infty$, $C_{MIMO_{|\text{Large } M_T}} \to \infty$.

Case 3: Increase M_T and fix M_R

Since the eigenvalues of $\mathbf{HH}^H$ and $\mathbf{H}^H\mathbf{H}$ are the same, (2.6) can be written as:

$$C_{MIMO} = E_H \left\{ \log_2 \left(\det \left[\mathbf{I}_{M_T} + \frac{SNR}{M_T} \mathbf{H}^H \mathbf{H} \right] \right) \right\} \text{ bps/Hz} \tag{2.14}$$

At large M_R and by the law of large numbers, $\frac{1}{M_T}\mathbf{H}^H\mathbf{H} \to \frac{M_R}{M_T}\mathbf{I}_{M_T}$. Therefore, the MIMO capacity is:

$$C_{MIMO_{|\text{Large } M_R}} = M_T \cdot \log_2\left(1+\frac{M_R}{M_T}\text{SNR}\right) \tag{2.15}$$

The above capacity increases logarithmically with increasing M_T. However, it has an upper bound that depends on the value of M_R.

$$\text{When } M_T \to \infty,\ C_{MIMO_{|\text{Large } M_R}} \to \frac{M_R \text{SNR}}{\ln 2}$$

Also, the rate of increase depends on the value of M_R compared to M_T. As shown in Figure 2.2, when $M_R \geq M_T$, the increase in capacity with increasing M_T is more than the linear relation in case 2. However, the rate of increase gets much slower (similar to a logarithmic increase) when $M_R < M_T$. Therefore, to achieve at least a linear increase in the capacity of MIMO channels with increasing number of antennas, M_R must be greater than or equal to M_T.

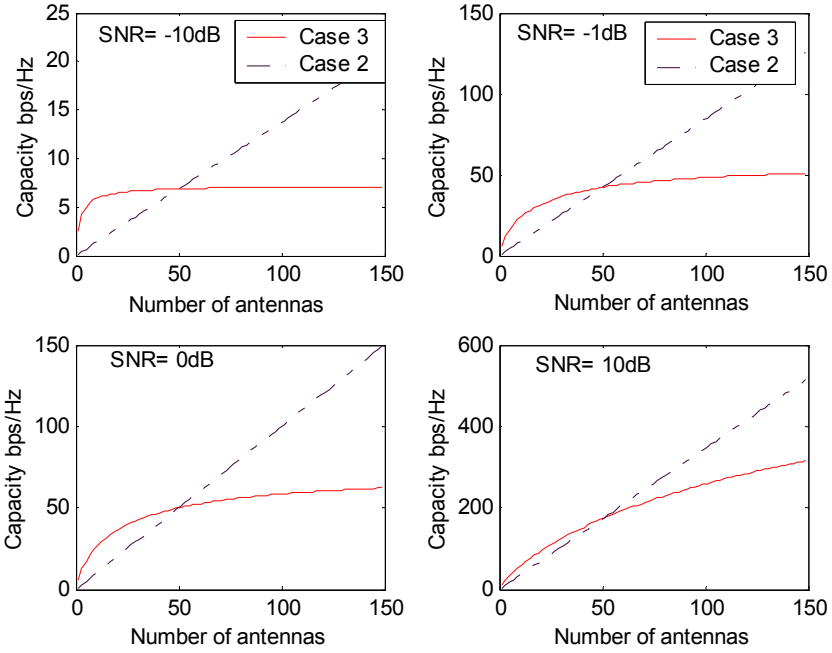

Figure 2.2: Capacity comparison between case 2 and case 3 for different SNR. The number of fixed receive antennas for case 3 is 50 antennas.

Capacity of other channels can be derived from the MIMO channel capacity. For a single-input multiple-output (SIMO) channel (receive diversity systems) with one transmit and M_R receive antennas, the MIMO capacity in (2.14) is reduced to:

$$C_{SIMO} = E_h \left\{ \log_2 \left(1 + \mathrm{SNR} \sum_{i=1}^{M_R} |h_i|^2 \right) \right\} \text{ bps/Hz} \qquad (2.16)$$

The above capacity corresponds to maximum ratio combining of the received signals.

Also, the capacity of multiple-input single-output (MISO) channels (transmit diversity systems) with M_T transmit and one receive antenna can be written as:

$$C_{MISO} = E_h \left\{ \log_2 \left(1 + \frac{\mathrm{SNR}}{M_T} \sum_{i=1}^{M_T} |h_i|^2 \right) \right\} \text{ bps/Hz} \qquad (2.17)$$

Since the total power of the transmitter is fixed irrespective of the number of transmit antennas, the SIMO capacity becomes larger than MISO at a given SNR.

Since there is no closed form expression for the MIMO capacity, we turn to computer simulation to estimate the MIMO capacity. Upper bounds on the MIMO capacity are derived in [Ge02] and [Kie02]. Based on a Monte Carlo simulation, a large number of channel realizations (10000 for our case) is generated and the instantaneous channel capacity is calculated using (2.6) . From these values, we estimate the mean capacity and the complementary cumulative distribution function (CCDF).

The average MIMO capacity is shown in Figure 2.3 for four different comparisons. The mean capacity is estimated over a range of SNR in Figures 2.3.a and c. The plot in Figure 2.3.a compares three antenna configurations. It is apparent that when $M_R > M_T$, the mean capacity is greater than the case for which $M_R < M_T$. This is mainly due to the constraint on transmitted power which is fixed regardless of the number of transmit antennas. Figure 2.3.c compares the mean capacity between four flat fading channels. It shows the huge capacity increase of MIMO channels over SIMO, MISO and SISO channels. Figures 2.3.b and d illustrate the effect of changing the number of receive and transmit antennas on the capacity of MIMO channels. It is apparent from Figures (b) and (d) that increasing the number of receiving antennas has a more significant impact on MIMO capacity than increasing the number of transmitting antennas.

Another useful tool used for evaluating MIMO capacity is the outage capacity. Since the capacity over fading channels is random, some realizations fall below a capacity threshold (the outage capacity) for which reliable decoding of a block of information is impossible. The probability that the channel capacity falls below the outage capacity is called the outage probability. Mathematically speaking,

$$\text{Outage Probability} = \mathrm{P}\left\{C \le C_{Outage}\right\} = q \quad \text{;where } C_{Outage} \text{ is the outage capacity} \tag{2.18}$$

For example, assume that 4 bps/Hz is transmitted over a fading channel. If the instantaneous capacity of the channel falls below 4 bps/Hz, the transmission will violate Shannon's capacity theorem and decoding the transmitted signal with arbitrarily low number of errors is impossible.

The complement of the outage probability is the probability that the capacity is greater than the outage capacity. In other words, the percentage of good channels over which reliable communication is possible at a given outage capacity.

The estimated CDF and Complementary CDF are used to find the outage probability and the complement of the outage probability, respectively. Figure 2.4 shows four different plots of the complementary CDF for different wireless channels. Figure 2.4.a compares the complement of the outage probability for MIMO, MISO, SIMO and SISO channels. At a given outage probability, the MIMO channel boosts the capacity by an order of magnitude. For example, at SNR=10dB and at a 10% outage probability, the SISO capacity is approximately 1bps/Hz whereas the MIMO capacity with four transmit and four receive antennas jumps to 9.25 bps/Hz. Figures 2.4.(b,c,d) show the effect of doubling the number of antennas for the MIMO, MISO and SIMO channels, respectively. The most significant increase in capacity is achievable with MIMO channels for which doubling the number of antennas results in doubling the capacity. On the other hand, the largest outage capacity gain in MISO channels is observed when going from SISO to a 2x1 channel. After that, diminishing capacity gains are observed. This suggests that for transmit diversity schemes, a small number of transmit antennas is enough to provide most of the capacity of MISO channels.

Figure 2.5 shows the outage probability as a function of SNR. The results indicate that the MIMO channel requires less power to transmit the same information compared to other channels. Thus, it is very suitable in power limited applications such as cellular and personal communication systems (PCS), ad-hock networks and wireless local area networks (WLAN).

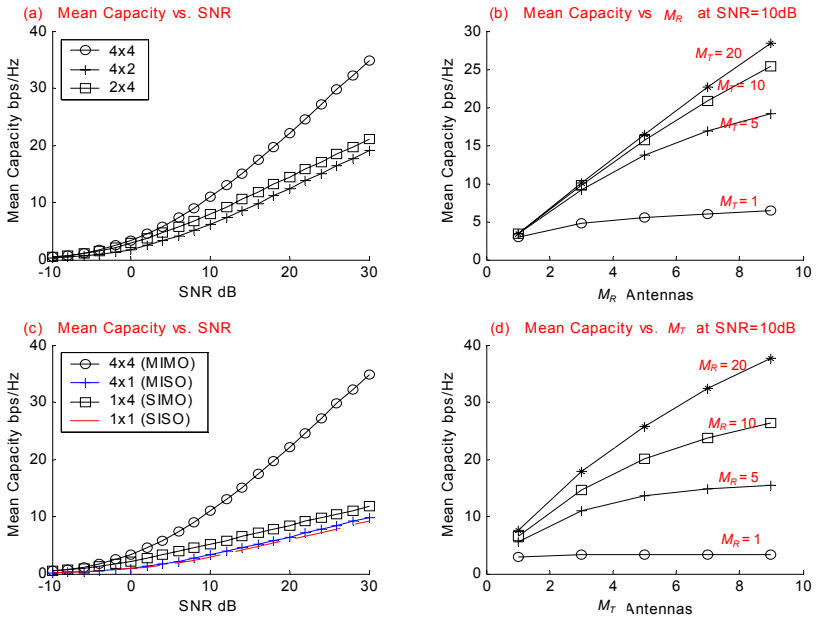

Figure 2.3: Mean capacity comparisons for MIMO channels.

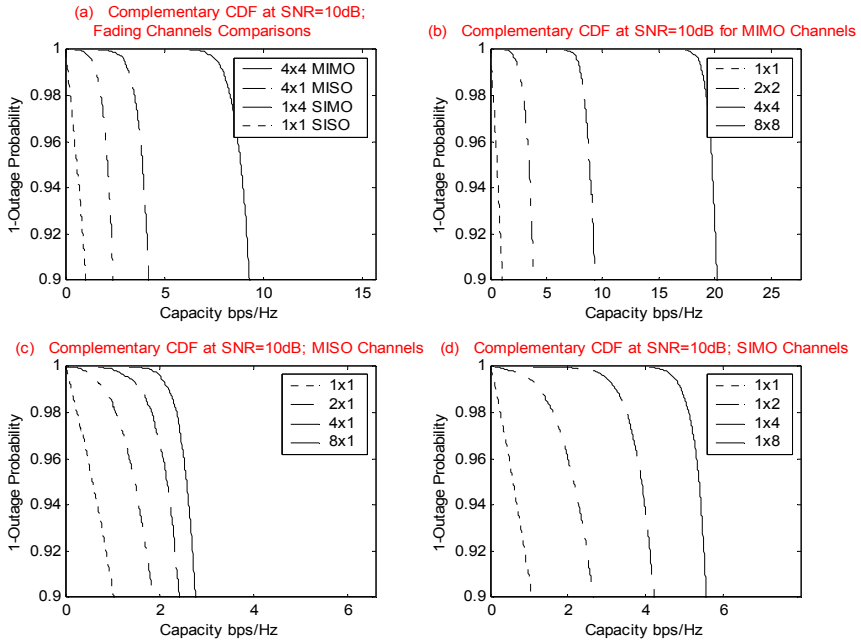

Figure 2.4: Complementary CDF comparison for flat fading channels

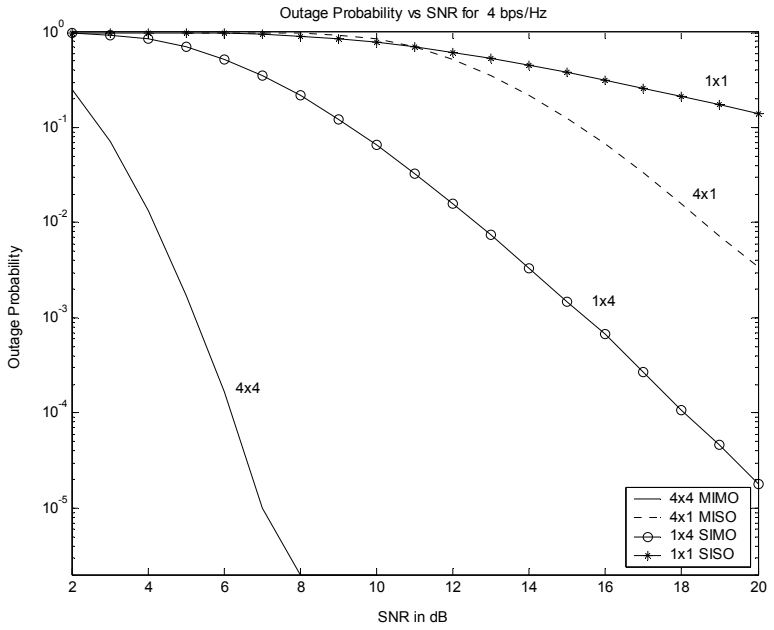

Figure 2.5: Outage probability vs. SNR for flat fading channels.

2.3 Open Loop MIMO Communication Systems

This chapter presents an overview of open loop communication schemes designed to operate over MIMO channels. These schemes don't require channel knowledge at the transmitter. Space time coding or modulation is a coding or modulation scheme designed for multiple transmit antennas. The target design of some schemes, such as layered space time architecture, is to provide high data rates through spatial multiplexing. Other schemes, such as space time block codes, are focused on designing codes that provide diversity at the transmitter with simple detection algorithm at the receiver. A summary chart of these schemes is given in Figure 2.6.

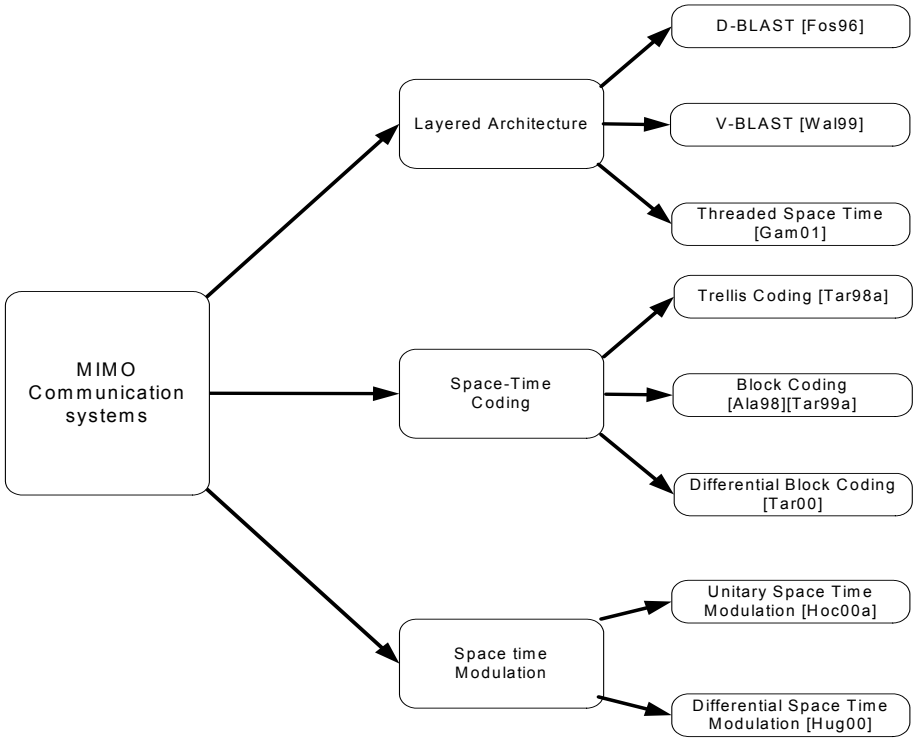

Figure 2.6: Summary chart of MIMO communication systems

2.3.1 Layered Space Time Architecture

This section presents an overview of layered space time architectures. The transmitted symbols are arranged into layers- diagonal, horizontal or threaded- before transmission. Symbols are transmitted simultaneously through all transmit antennas. The receiver applies multi-user detection algorithms to detect symbols and eliminate interference from other transmitted layers.

Bell-Labs Layered Space Time Architecture

One of the earliest communication systems that was proposed to take advantage of the promising capacity of MIMO channels is the Bell-Labs Layered Space Time (BLAST) architecture. It achieves high spectral efficiencies by spatially multiplexing coded or uncoded symbols over the MIMO fading channel. M_T symbols are transmitted through M_T antennas. Each receive antenna receives a superposition of M_T faded symbols. The maximum likelihood (ML) decoder would select the set of symbols that are closest in Euclidean distance to the received M_R signals. However, it is hard to implement due to its exponential complexity. More practical decoding architectures were proposed in the literature. They can be classified under two categories; D-BLAST and V-BLAST.

The diagonal (D) BLAST architecture was originally proposed by Foschini in 1996 [Fos96]. The target application was for fixed and low mobility wireless networks, such as WLAN. The vertical version of the BLAST was proposed by [Wol98] as a simplification of D-BLAST.

The transmission is described as follows. A data stream is demultiplexed into M_T substreams termed layers. For D-BLAST at each transmission time, the layers circularly shift across the M_T transmit antennas resulting in a diagonal structure across space and time. On the

other hand, the layers are arranged horizontally across space and time for V-BLAST and the cycling operation is removed before transmission.

At the receiver, as mentioned previously, the received signals at each receive antenna is a superposition of M_T faded symbols plus additive white Gaussian noise (AWGN). Assuming a flat fading MIMO channel, the discrete received vector at each time will be:

$$\mathbf{y} = \mathbf{H}\mathbf{x} + \boldsymbol{\eta} \tag{2.19}$$

Although the layers are arranged differently for the two BLAST systems across space and time, the detection process for both systems is performed vertically for each received vector. Without loss of generality, assume that the first symbol is to be detected. The detection process consists of two main operations:

1- Interference suppression (nulling): the suppression operation nulls out interference by projecting the received vector onto the null subspace (perpendicular subspace) of the subspace spanned by the interfering signals. After that, normal detection of the first symbol is performed.

2- Interference cancellation (subtraction): the contribution of the detected symbol is subtracted from the received vector.

The interference suppression and cancellation are serially repeated until all symbols are detected as shown in Figure 2.7.

BLAST detection algorithm combines linear (interference suppression) and nonlinear (serial cancellation) algorithms. This is similar to the decorrelating decision feedback multiuser detection algorithm. A drawback of BLAST algorithms is the propagation of decision errors. Also, the interference nulling operation requires that the number of receive antennas be grater than or equal to the number of transmit antennas. Furthermore, due to the interference

suppression, early detected symbols benefit from lower receive diversity than later ones. Thus, the algorithm results in unequal diversity advantage for each symbol.

There are few differences between V-BLAST and D-BLAST. While the layers of the V-BLAST can be coded or uncoded, the D-BLAST is intended to be used only with coded layers. This is the reason behind cycling which provides more spatial diversity for each layer particularly over slowly fading channels [Shi99]. Further, due to the diagonal structure of D-BLAST, each layer benefits from the same diversity advantage while V-BLAST layers have unequal diversity advantages. However, D-BLAST requires advanced interstream coding techniques to optimize the performance of the code across space and time [Fos99]. Finally, some space-time is wasted at the start and the end of the burst for D-BLAST.

Threaded Space Time Architecture

A threaded space time (TST) architecture is a layered space time architecture that combines efficient algebraic code design with iterative signal processing techniques. It was proposed by El Gamal in [Gam01]. It combines the concepts of space time trellis coding (STTC) and D-BLAST. By relaxing the bandwidth efficiency requirement of STTC, the TST architecture provides more flexibility in the tradeoff between power efficiency, bandwidth efficiency and receiver complexity. The encoder consists of M_T parallel convolutional codes, where each encoder creates a layer. The layering approach is called threaded layering and is designed to maximize spatial and temporal diversity for a given transmission rate. The receiver concatenates soft-input soft-output (SISO) detection and SISO parallel convolutional decoders in an iterative processing procedure.

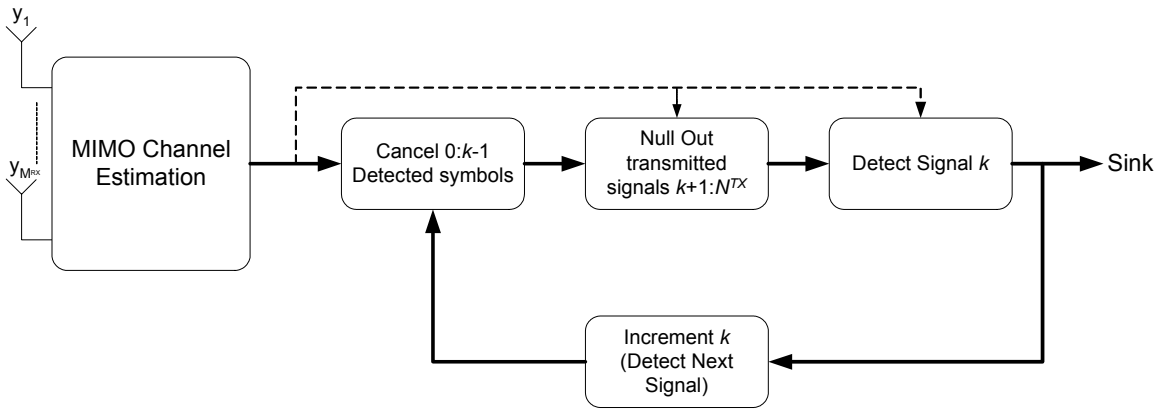

Figure 2.7: Block diagram of a BLAST receiver: Serial interference suppression and cancellation algorithm

2.3.2 Space Time Trellis Codes

The pioneering work on space time trellis codes (STTC) using multiple transmit and receive antennas was done by Tarokh in [Tar98]. It was an extension to the delay transmit diversity scheme proposed by [Wit93]. Space time trellis coding integrates the design of channel coding and modulation with multiple transmit antennas. It provides coding gains and diversity to combat fading without any bandwidth expansions.

STTC are an important extension of trellis coded modulation (TCM) schemes to the spatial dimension. A TCM scheme jointly combines the design of a convolutional code with a bandwidth efficient modulation scheme. It was proposed by [Ung82] and it was a revolutionary design in the sense that redundancy was added to the signal set rather than adding more bits to the information block. According to the design criterion, the signal set is partitioned and symbols are assigned carefully to the trellis branches resulting in a coding gain compared to uncoded systems without any bandwidth expansion. For Gaussian channels, the design criterion is to maximize the minimum Euclidean distance between any two codewords [Ung82]. For Rayleigh flat fading channels, maximizing the length of the shortest error event path and maximizing the product of branch distances along this path are the main design criteria [Jam94]. The length of

the shortest error event path is known as the minimum effective length of the code and is sometimes referred to as the time diversity of the code. For conventional[6] TCM, the temporal diversity of the code increases by preventing parallel transitions and increasing the number of encoder states. Another way to increase the temporal diversity of the code is to assign more than one symbol per trellis branch. This was proposed by [Div88] and is referred to as multiple trellis coded modulation (MTCM). Furthermore, another approach to increase the time diversity of TCM schemes was proposed by Al-Semari in [Als97] where two parallel high time diversity TCM encoders were used to separately encode the Inphase and Quadrature components of the transmitted symbols. The scheme was called I-Q TCM and it showed a huge improvement in performance compared to conventional TCM schemes over Rayleigh fading channels.

Over static, quasi-static or very slow time varying fading channels, such as fixed wireless backbone routers and low mobility users, time diversity will not be able to compensate the effect of fading. Long interleavers greatly improve the performance of TCM schemes over slowly fading channels. They break the temporal correlated fading and that improves the performance of the soft Viterbi decoder used to decode TCM. On the other hand, space diversity is the best way to compensate for fading over static, quasi-static and block fading channels. Therefore, transmit and receive diversity has been the focus of research for the past few years.

A complete coverage of the design and performance criterion of STTC over Rician and Rayleigh fading channels is presented in Tarokh's paper [Tar98]. In this overview, we emphasize the design criteria over quasi-static and rapidly fading Rayleigh channels.

---

[6] Conventional TCM means that each trellis branch is assigned one symbol.

Before going through the design criteria of STTC, we will define some design parameters in this paragraph. STTC transmits M_T trellis coded symbols simultaneously at each symbol interval. For a frame length of L, consider the two different transmitted codewords:

$$\mathbf{x}^T = \underbrace{x_1^1 x_2^1 \cdots x_{M_T}^1}_{\left[\underline{x}^1\right]^T} x_1^2 x_2^2 \cdots x_{M_T}^2 \cdots x_1^L x_2^L \cdots x_{M_T}^L \tag{2.20}$$

$$\mathbf{q}^T = \underbrace{q_1^1 q_2^1 \cdots q_{M_T}^1}_{\left[\underline{q}^1\right]^T} q_1^2 q_2^2 \cdots q_{M_T}^2 \cdots q_1^L q_2^L \cdots q_{M_T}^L \tag{2.21}$$

Note that the codewords are represented in column vectors and $\underline{x}^t$ and $\underline{q}^t$ are two possible vectors of transmitted symbols at time t from the M_T antennas. The transmitted symbols are drawn from a signal set Q of size 2^b. The *distance matrix* $\mathbf{A}$ is defined as an $M_T \times M_T$ matrix that represents the sum of Euclidean distances between the symbols of the two codewords. It is defined as:

$$\mathbf{A}\left(\underline{\mathbf{x}}, \underline{\mathbf{q}}\right) = \sum_{t=1}^{L} \left(\underline{x}^t - \underline{q}^t\right)\left(\underline{x}^t - \underline{q}^t\right)^H \tag{2.22}$$

$$= \sum_{t=1}^{L} \begin{bmatrix} \left|x_1^t - q_1^t\right|^2 & \left(x_1^t - q_1^t\right)\left(x_2^t - q_2^t\right)^* & \cdots & \left(x_1^t - q_1^t\right)\left(x_{M_T}^t - q_{M_T}^t\right)^* \\ \left(x_2^t - q_2^t\right)\left(x_1^t - q_1^t\right)^* & \left|x_2^t - q_2^t\right|^2 & \cdots & \left(x_2^t - q_2^t\right)\left(x_{M_T}^t - q_{M_T}^t\right)^* \\ \vdots & \vdots & \ddots & \vdots \\ \left(x_{M_T}^t - q_{M_T}^t\right)\left(x_1^t - q_1^t\right)^* & \left(x_{M_T}^t - q_{M_T}^t\right)\left(x_2^t - q_2^t\right)^* & \cdots & \left|x_{M_T}^t - q_{M_T}^t\right|^2 \end{bmatrix} \tag{2.23}$$

The matrix $\mathbf{A}$ is Hermitian and has a square root defined as:

$$B(\underline{\mathbf{x}}, \underline{\mathbf{q}}) = \begin{bmatrix} \underline{x}^1 - \underline{q}^1 & \underline{x}^2 - \underline{q}^2 & \cdots & \underline{x}^L - \underline{q}^L \end{bmatrix} \tag{2.24}$$

$$B\left(\underline{\mathbf{x}}, \underline{\mathbf{q}}\right) = \begin{bmatrix} x_1^1 - q_1^1 & x_1^2 - q_1^2 & \cdots & x_1^L - q_1^L \\ x_2^1 - q_2^1 & x_2^2 - q_2^2 & \cdots & x_2^L - q_2^L \\ \vdots & \vdots & \ddots & \vdots \\ x_{M_T}^1 - q_{M_T}^1 & x_{M_T}^2 - q_{M_T}^2 & \cdots & x_{M_T}^L - q_{M_T}^L \end{bmatrix} \tag{2.25}$$

where, $\mathbf{A} = \mathbf{B}\mathbf{B}^H$ and $\mathbf{B}$ is known as the *difference matrix*.

Note that rank(**A**)=rank(**B**) ≤ M_T. Since **A** is Hermitian, it has r positive eigenvalues, where r is the rank of **A**. For a full rank matrix **A**, the determinant is defined as:

$$\det(\mathbf{A}) = \prod_{i=1}^{M_T} \lambda_i \ ; \text{ where } \lambda_i \text{ is the } i^{\text{th}} \text{ eigenvalue} \tag{2.26}$$

The squared Euclidean distance between two codewords is defined as:

$$d_E^2(\underline{\mathbf{x}}, \underline{\mathbf{q}}) = \left(\underline{\mathbf{x}} - \underline{\mathbf{q}}\right)^H \left(\underline{\mathbf{x}} - \underline{\mathbf{q}}\right) = \sum_{t=1}^{L} \sum_{n=1}^{M_T} \left| x_n^t - q_n^t \right|^2 \tag{2.27}$$

For TCM and MTCM, the effective length (l_e) between any two codewords is defined as the number of distinct symbols between **x** and **q**. However, for STTC, the definition is quite different. The effective length (l_e) for STTC is defined as the number of time instances such that transmitted vector at time t for codeword **x** is different from the transmitted vector at time t for codeword **q** (i.e. $\underline{x}^t \neq \underline{q}^t$). Let the set of time instances $1 \leq t \leq L$ such that $\underline{x}^t \neq \underline{q}^t$ be Ω_{l_e} and $\left|\Omega_{l_e}\right| = l_e$. The product of the squared distance between any two codewords is defined as:

$$d_P^2(\mathbf{x}, \mathbf{q}) = \prod_{t \in \Omega_{l_e}} \left(\underline{x}^t - \underline{q}^t\right)^H \left(\underline{x}^t - \underline{q}^t\right) = \prod_{t \in \Omega_{l_e}} \left(\sum_{n=1}^{M_T} \left| x_n^t - q_n^t \right|^2 \right) \tag{2.28}$$

Tarokh in [Tar98] derived the design criteria of STTC for various fading channels. Over quasi-static Rayleigh fading channels, the pairwise error probability between any two codewords is:

$$P(\underline{\mathbf{x}} \to \underline{\mathbf{q}}) \leq \left(\underbrace{\left(\prod_{i=1}^{r} \lambda_i \right)^{1/r}}_{\text{Coding Gain}} \left(\frac{E_s}{4N_0} \right) \right)^{\overbrace{-rM_R}^{\text{Diversity}}} \tag{2.29}$$

where λ_i is a positive eigenvalue of the **A**(**x**,**q**) matrix of rank r.

The first design criterion over quasi-static Rayleigh fading channels is to maximize the diversity advantage (rM_R) by maximizing the rank of **A** which is equal to the rank **B**. For a full rank, the maximum diversity (M_TM_R) is achieved. To achieve the maximum diversity, the difference matrix **B** must have M_T independent rows and columns. STTC that achieves the maximum diversity is called a full rank code. The second design criterion is to maximize the coding gain by maximizing the minimum of the product of the positive eigenvalues of **A**(**x**,**q**) among all possible codewords. For a full rank matrix **A**, the coding gain between codewords **x** and **q** is equal to the determinant of **A**(**x**,**q**).

Over rapid Rayleigh fading channels, the pairwise error probability is upper bounded by:

$$P(\underline{\mathbf{x}} \to \underline{\mathbf{q}}) \le \prod_{t \in \Omega_{l_e}} \left(\left(\underline{x}^t - \underline{q}^t \right)^H \left(\underline{x}^t - \underline{q}^t \right) \left(\frac{E_s}{4N_0} \right) \right)^{-M_R} = \left(\underbrace{\left(d_P^2(\underline{\mathbf{x}}, \underline{\mathbf{q}}) \right)^{1/l_e}}_{\text{Coding Gain}} \left(\frac{E_s}{4N_0} \right) \right)^{\overbrace{-l_e M_R}^{\text{Diversity}}} \qquad (2.30)$$

To maximize the diversity advantage (l_eM_R), the minimum effective length (l_e) between all pairs of codewords should be maximized. Also, the minimum product of the squared distance among all pairs of codewords should be maximized in order to maximize the coding gain.

Examples of geometrically uniform STTC designed to operate over quasi-static and rapid fading channels are presented next. The 8 state QPSK STTC in Figure 2.8 was presented in [Tar98] for quasi-static Rayleigh fading channels. The average signal energy is normalized to one. The STTC has a full rank over two transmit antennas ($r=2$) and the minimum determinant of the distance matrix **A** is 12. Furthermore, the minimum effective length of this code is two and minimum d_P^2 is 16. The design rules that guarantee full diversity advantage using two transmit antennas are [Tar98]:

- Rule 1: Transitions departing from the same state differ in the second symbol.
- Rule 2: Transitions arriving at the same state differ in the first symbol.

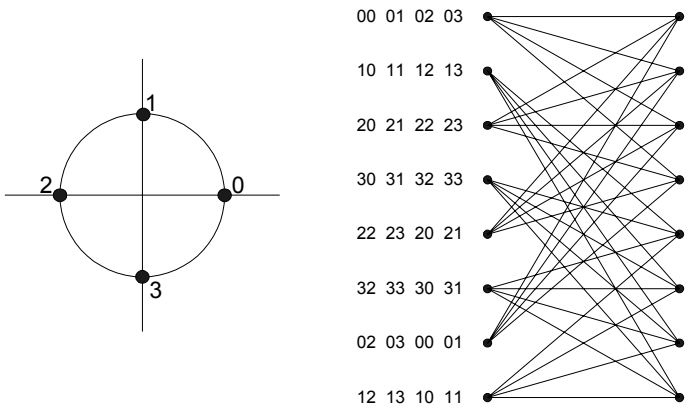

Figure 2.8: 8-state QPSK STTC with two transmit antennas designed for quasi-static Rayleigh fading channels

The other 8-state QPSK STTC in Figure 2.9 was presented in [Zum00] for rapid fading channels where each transmitted symbol fades independently. Mobile channels are usually slow time varying due to the Doppler spread. The channel is transformed into rapid time varying channel by using interleavers with sufficient depth. A signal set partitioning approach was used to maximize the minimum squared product distance (SPD) of the STTC in Figure 2.9. The code has a minimum effective length of two (l_e=2) and a minimum SPD of 24. Also, the minimum determinant of the distance matrix **A** is 4 and the difference matrix **B** has a rank of two (r=2).

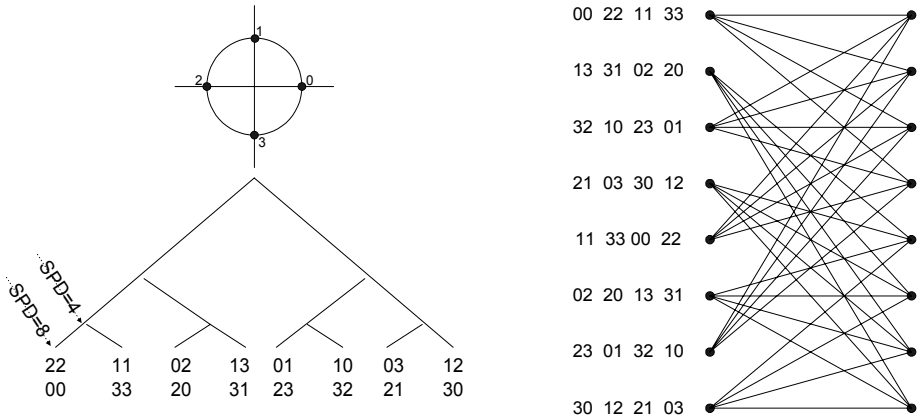

Figure 2.9: 8-state QPSK STTC with two transmit antennas designed for rapid Rayleigh fading channels

A description of the space time trellis encoding and decoding process can be summarized as follows. Assuming a transmission rate of b bps/Hz, the encoder maps b bits onto M_T symbols where each symbol is drawn from a signal constellation Q of size 2^b. The encoder is a finite state machine that jointly performs encoding and signal mapping according to the designed trellis. The M_T coded symbols are transmitted simultaneously through M_T transmit antennas. Under a flat fading assumption, the discrete received signal by M_R receive antennas at time t is:

$$\underline{y}^t = \mathbf{H}^t \underline{x}^t + \underline{\eta}^t \tag{2.31}$$

Over a frame of length L and with channel state information (CSI), the decoder implements a soft Viterbi algorithm that selects the maximum likelihood sequence $\underline{q}^1 \quad \underline{q}^2 \quad \cdots \quad \underline{q}^L$ that minimizes the decision metric:

$$\sum_{t=1}^{L} \left(\underline{y}^t - \mathbf{H}^t \underline{q}^t \right)^H \left(\underline{y}^t - \mathbf{H}^t \underline{q}^t \right) \tag{2.32}$$

Some useful design bounds derived in [Tar98] are given next. Let the signal constellation from which the transmitted symbols are drawn be Q with 2^b elements. A full rank STTC will

have a maximum transmission rate of b bps/Hz. Also, for an STTC with rank r and transmission rate b, the number of states (S) is lower bounded by:

$$S \geq 2^{b(r-1)} \tag{2.33}$$

One major drawback of STTC can be seen form the above equation. The trellis complexity increases exponentially with increasing data rates and increasing STTC rank.

Since the STTC designed in [Tar98] were hand-crafted and were not optimized for coding gain, a lot of research in STTC design had focused on achieving more coding gain. Designs based on a systematic computer-aided search for codes that maximize the minimum determinant criterion was presented in [Bar00][Yan00]. These codes are full rank codes with higher coding gains. A new systematic design approach to maximize the minimum determinant criterion based on set-partitioning and super set of orthogonal space-time block codes was proposed by [Jaf02]. The codes are called super-orthogonal space time trellis codes and they provide full rank, full rate and more coding gains.

The above design criteria for coding gains were derived using a high SNR assumption. Design criteria for moderate and low SNR were recently presented in [Tao01]. They showed that for moderate SNR, the design criterion for maximizing the coding gain is to maximize the minimum of the determinant of **I**+**A(x,q),** where **I** is the identity matrix. Also, for low SNR, the design criteria is to maximize the minimum Euclidian distance (d_E^2) between any two codewords.

2.3.3 Space Time Block Codes

In order to overcome the exponential complexity of STTC, Alamouti in [Ala98] proposed a simple two branch transmit diversity scheme. This scheme achieves full transmit diversity

advantage with linear processing at the receiver. Alamouti's work initiated a new class of space time codes called space time block codes (STBC) [Tar99a]. Before continuing our overview, let us define some common terminologies in space time coding:

- *Full rank code* is a space time code (STC) that has full rank. It has full transmit diversity and is also called a *full diversity code*.
- *Full rate code* is the one that achieves the maximum rate, which is equal to b bps/Hz, where the code symbols are drawn from a constellation set Q of size 2^b.

The main advantage of STBC is that they achieve full diversity with low complexity. By mapping the transmitted symbols to an orthogonal space time transmission matrix, linear processing at the receiver can be implemented. This reduced complexity structure comes at the price of lower transmission rate and coding gain [Tar99a]. For complex constellations such as PSK and QAM, full transmission rate is not possible for more than two transmit antennas. The theory of orthogonal designs for both real and complex constellation is presented in [Tar99a]. A slightly different approach for designing STBC was proposed in [Jaf01] where he used quasi-orthogonal designs that achieved full transmission rates with half of the diversity. The drawback of [Jaf01] approach is the lower diversity and slightly more complex decoder since the decoder works with a pair of transmitted symbols instead of single symbols.

The space time block encoder (STBE) can be described as follows. kb bits arrive at the encoder which selects k symbols from the signal constellation set Q of cardinality 2^b. The selected symbols $(x_1,x_2,\ldots,x_k)$ are mapped to an $L \times M_T$ orthogonal transmission matrix ($\mathbf{O}_{M_T}$), where the i^{th} column represents the transmitted symbols from the i^{th} antenna and the j^{th} row represents the transmitted symbols in the j^{th} time slot. Since k symbols are transmitted during L time slots, the rate (R_s) of STBC is:

$$R_s = \frac{k}{L} \text{ symbols/time slot} \tag{2.34}$$

The maximum transmission rate of STC is equal to one symbol/time slot. For orthogonal STBC, the maximum rate is achieved only for the two transmit antennas case. An example of rate one STBC is given by the following transmission matrix [Ala98]:

$$\mathbf{O}_2 = \begin{pmatrix} x_1 & x_2 \\ -x_2^* & x_1^* \end{pmatrix} \tag{2.35}$$

The above matrix is orthogonal because:

$$\begin{aligned} \mathrm{O}_2^H \mathrm{O}_2 &= D \quad \text{; where } D \text{ is a diagonal matrix} \\ &= \begin{bmatrix} |x_1|^2 + |x_2|^2 & 0 \\ 0 & |x_1|^2 + |x_2|^2 \end{bmatrix} \end{aligned} \tag{2.36}$$

Codes that transmit through three and four antennas with rates 1/2 and 3/4 were designed in [Tar99a].

The receiver should observe the received signals for the whole block length (L). Assuming that the MIMO channel is constant during the transmission of one block, the discrete received signals over the L time slots can be written as:

$$\mathbf{Y}_{M_R \times L} = \underbrace{\mathbf{H}}_{M_R \times M_T} \underbrace{\mathbf{O}^T}_{M_T \times L} + \underbrace{\boldsymbol{\eta}}_{M_R \times L} \tag{2.37}$$

For example, transmitting over 2×2 MIMO channel using $\mathbf{O}_2$ transmission matrix, the received signal over two time slots is:

$$\begin{bmatrix} \underline{y}^1 & \underline{y}^2 \end{bmatrix} = \begin{bmatrix} h_{11} & h_{12} \\ h_{21} & h_{22} \end{bmatrix} \begin{pmatrix} x_1 & -x_2^* \\ x_2 & x_1^* \end{pmatrix} + \begin{bmatrix} \underline{\eta}^1 & \underline{\eta}^2 \end{bmatrix} \tag{2.38}$$

where $\underline{y}^t$ is the $M_R \times 1$ received vector at time $t \in \{1, 2, \ldots, L\}$

h_{mn} is the fading coefficient of the channel connecting receive antenna m

to transmit antenna n.

$\underline{\eta}^t$ is the $M_R \times 1$ AWGN vector at time $t \in \{1, 2, \ldots, L\}$

Due to the orthogonal design, decoding of STBC is easily implemented in two steps. The first is decoupling the received vectors over the whole observation time into estimates of the transmitted symbols using maximum ratio combining (MRC). After that, maximum likelihood detection of the estimated symbols is performed separately. To illustrate the decoding algorithm, let us consider the 2×2 system. We can rewrite (2.38) as:

$$\begin{bmatrix} y_1^1 \\ y_2^1 \\ \left(y_1^2\right)^* \\ \left(y_2^2\right)^* \end{bmatrix} = \begin{bmatrix} h_{11} & h_{12} \\ h_{21} & h_{22} \\ h_{12}^* & -h_{11}^* \\ h_{22}^* & -h_{21}^* \end{bmatrix} \begin{bmatrix} x_1 \\ x_2 \end{bmatrix} + \begin{bmatrix} \eta_1^1 \\ \eta_2^1 \\ \left(\eta_1^2\right)^* \\ \left(\eta_2^2\right)^* \end{bmatrix} \tag{2.39}$$

$$\underline{y}_{es} = \mathbf{H}_{es}\underline{x} + \underline{\eta}_{es} \tag{2.40}$$

where *es* indicates estimation stage and y_m^t and η_m^t indicate the received signal and the AWGN at receive antenna m at time t, respectively.

Since $\mathbf{H}_{es}$ is orthogonal, the transmitted symbols could be easily estimated by decoupling the received signals after multiplying $\underline{y}_{es}$ by $\mathbf{H}_{es}^H$. This corresponds to MRC and results in maximizing SNR of the estimated symbols [Ala98]. The estimated symbols are:

$$\underline{\tilde{x}} = \mathbf{H}_{es}^H \underline{y}_{es} = \mathbf{H}_{es}^H \mathbf{H}\underline{x} + \mathbf{H}_{es}^H \underline{\eta}_{es} \tag{2.41}$$

$$\begin{bmatrix} \tilde{x}_1 \\ \tilde{x}_2 \end{bmatrix} = \begin{bmatrix} |h_{11}|^2 + |h_{12}|^2 + |h_{21}|^2 + |h_{22}|^2 & 0 \\ 0 & |h_{11}|^2 + |h_{12}|^2 + |h_{21}|^2 + |h_{22}|^2 \end{bmatrix} \begin{bmatrix} x_1 \\ x_2 \end{bmatrix} + \mathbf{H}_{es}^H \underline{\eta}_{es} \tag{2.42}$$

Afterwards, the estimated symbols are passed to a maximum likelihood detector that operates on each estimated symbol separately. For example, for detecting $\tilde{x}_1$, the detector will choose symbol $s_i \in Q$ if [Ala98]:

$$\begin{aligned}&\left(|h_{11}|^2+|h_{12}|^2+|h_{21}|^2+|h_{22}|^2-1\right)|s_i|^2+d^2\left(\tilde{x}_1,s_i\right)\\&\le\left(|h_{11}|^2+|h_{12}|^2+|h_{21}|^2+|h_{22}|^2-1\right)|s_k|^2+d^2\left(\tilde{x}_1,s_k\right)\ ;\quad \forall i\neq k\end{aligned} \tag{2.43}$$

for equal energy signals, such as PSK, the above decision criterion is simplified to:

$$d^2\left(\tilde{x}_1,s_i\right)\le d^2\left(\tilde{x}_1,s_k\right)\ ;\quad \forall i\neq k \tag{2.44}$$

where $d^2\left(\tilde{x}_1,s_i\right)$ is the squared Euclidian distance between $\tilde{x}_1$ and s_i.

2.3.4 Differential Space Time Modulation

The previously presented space time systems in this chapter are considered coherent systems. The receiver requires accurate channel state estimation to perform well. This requirement can be met for slowly time varying channels. However, multiple channels are involved in the MIMO channel and thus, multi-channel estimation algorithms are needed. Channel estimation is done based on transmitting training sequences, such as [Tar97][Bud01], or based on blind algorithms, such as [Xu02][Cir02].

Sacrificing some power efficiency, differential schemes could be used to avoid channel estimation. This simplifies and lowers the cost of the receivers. Also, differential detection is more robust when the fading is fast and avoids using training sequences.

The first attempt to detect space time signals without channel estimation was proposed by [Tar98c]. There was no modification of the encoding process. The encoder used STBC with two transmit antennas. However, the detection was performed without channel estimation. Assuming

that the fading is constant over two coded blocks, which is four consecutive symbols for $\mathbf{O}_2$, the detected symbols at time t-1 is used to estimate the channel at the receiver. Then these estimates were used to detect the transmitted symbols at time t. The detection algorithm is classified as joint channel and data estimation and it is not truly differential.

[Tar00] proposed a differential space time scheme where the information bits are differentially encoded and decoded. They designed the scheme for two transmit antennas. The scheme provides full transmit diversity with no channel estimation requirement at the receiver. As a result, performance was worse by 3dB as compared to coherent detection.

Another class of noncoherent MIMO scheme is unitary space time modulation (USTM), which was proposed by Hochwald in [Hoc00a]. It could be detected with or without channel estimation. USTM maps the information bits to a unitary space time block that is drawn from a super constellation which consists of a set of $L \times M_T$ unitary space time blocks, where L denotes the block length over which the fading channel is approximately constant. Unlike STBC, where modulated symbols are mapped to an orthogonal transmission matrix, USTM is concerned with designing constellation sets that consist of unitary matrices that satisfy certain design criteria. It was shown in [Hoc00a] that the modulation performs well either when SNR is high or $L \gg M_T$. Systematic designs of unitary space time constellations were derived in [Hoc00c].

Another differential scheme for multi-transmit antenna systems is differential space time modulation (DSTM) which was proposed independently by [Hoc00b] and [Hug00]. The scheme in [Hoc00b] is called differential unitary space time modulation (DUSTM). The framework is a natural extension of standard differential phase-shift keying commonly used in single antenna systems. The DSTM in [Hug00] is based on unitary group codes which are block codes with a group structure in which each code matrix is square and has equal-energy and orthogonal rows.

The DSTM approach has some advantages over Tarokh's differential scheme. First, DSTM doesn't expand the signal constellation. For example, if QPSK constellation is used with Tarokh's scheme, it will expand the transmitted constellation to 9-QAM. Another advantage is the unified framework that can be applied to any number of transmit antennas. Two transmit DSTM schemes were designed in [Hug00] and [Lia02].

To illustrate the concept of DSTM, we give an example. Consider a system with two transmit antennas and a block length of two, each unitary signal is transmitted over two time slots. Using a QPSK constellation (*Q*), [Hug00] designed a space time unitary group:

$$\Omega = \left\{ \pm \begin{bmatrix} 1 & 0 \\ 0 & 1 \end{bmatrix}, \pm \begin{bmatrix} j & 0 \\ 0 & -j \end{bmatrix}, \pm \begin{bmatrix} 0 & 1 \\ -1 & 0 \end{bmatrix}, \pm \begin{bmatrix} 0 & j \\ j & 0 \end{bmatrix} \right\} \tag{2.45}$$

$$\text{And } \mathbf{D} = \begin{bmatrix} 1 & -1 \\ 1 & 1 \end{bmatrix} \tag{2.46}$$

Let $\mathbf{G} \in \Omega$, then $\mathbf{DG} \in Q^{2x2}$. The set of matrices $\mathbf{D}\Omega = \{\mathbf{DG} : \mathbf{G} \in \Omega\}$ is called a multichannel group code of length *L=2* over the constellation *Q*. Since the cardinality of the above group code is eight, the code transmits three bits over two time slots. Thus, the rate of the space time modulation is defined as:

$$R = \frac{1}{L} \log_2 |\Omega| \text{ b/s/Hz} \tag{2.47}$$

and it is equal to 1.5 b/s/Hz for the above code.

The differential encoding can be summarized as follows. Let the first transmitted block be $\mathbf{X}_0 = \mathbf{D}$. Then three information bits will select $\mathbf{G}_k$ at block time *k*, the transmitter sends the differentially encoded block:

$$\mathbf{X}_k = \mathbf{X}_{k-1}\mathbf{G}_k \ , \quad k = 1, \cdots, K \text{ and } \mathbf{G}_k \in \Omega \tag{2.48}$$

Due to the group structure, $\mathbf{X}_k \in \mathbf{D}\Omega$. Therefore all transmitted blocks are elements of the multichannel group code.

The receiver differentially detects the code. It operates on the current and previous received blocks ($\mathbf{Y}_k$ and $\mathbf{Y}_{k\text{-}1}$). The detector chooses $\tilde{\mathbf{G}}_k$ such that:

$$\tilde{\mathbf{G}}_k = \arg \underbrace{\max}_{\mathbf{G}\in\Omega} \left\{ \mathrm{Re}\left[\mathrm{Tr}\left(\mathbf{G}\mathbf{Y}_k^H \mathbf{Y}_{k-1} \right) \right] \right\} \tag{2.49}$$

where ReTr operator refers to the real part of the trace operator. The block diagram of the differential detector is shown in Figure 2.10. One drawback of DSTM schemes is that the decoding complexity increases exponentially with block length and with transmission rate. The number of required comparisons is $|\Omega| = J = 2^{LR}$.

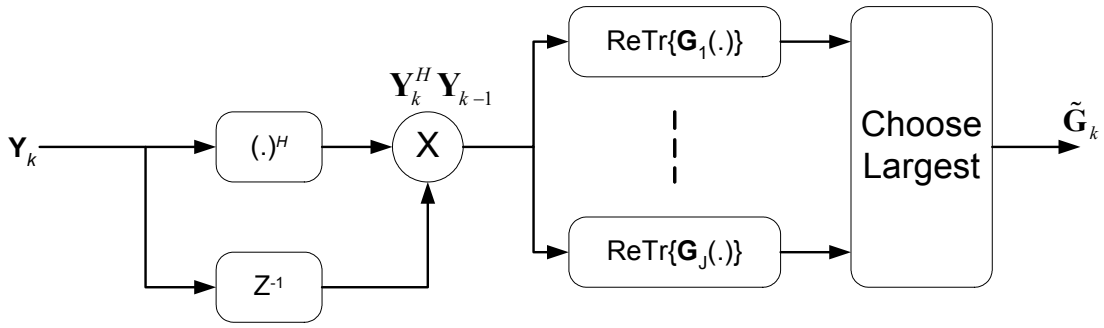

Figure 2.10: Differential space time detector

2.3.5 Comparative Study of Open Loop MIMO Systems

This section evaluates the performance of open loop MIMO communication systems over Rayleigh fading channels. The first part evaluates the performance of STTC and the second part compares STBC and DSTM. The simulated systems have a 2 bps/Hz spectral efficiency.

Performance of STTC over 2x1 and 2x2 MIMO Systems

The simulation uses a frame length of 130 symbols for each transmit antenna. The frame starts and ends with state zero.

Performance over quasi-static channels

The first comparison is done over quasi-static channels with a diversity order of two and four. The diversity order is defined as $Div=rM_R$ where r is the rank of the code and M_R is the number of receive antennas. We refer to Traokh's STTC in **Error! Reference source not found.** as ST-QPSK-Quasi and Zummo's STTC in Figure 2.9 as ST-QPSK-Rapid. Also, we compare the performance of the above two codes with rate 2/3 8PSK trellis codes designed for rapidly fading channels. Recall that the rank of the ST-QPSK-Quasi code is two while it is one for the 8PSK trellis code. We assumed independence between the fade coefficients in order to test the optimal performance of the systems. The simulation result is shown in Figure 2.11. Over SISO channels, the performance of the trellis-coded 8PSK is poor due to the lack of spatial diversity over quasi-static channels. Actually, the uncoded QPSK outperforms the trellis-coded 8PSK by 4dB. This is expected since the channel is quasi-static and trellis-coded 8PSK doesn't have any diversity advantage over this type of channel. However, with multiple receive antenna diversity, the 8PSK trellis code outperform the ST-QPSK-Quasi code by 3 dB. This 3dB is a power penalty because the power is divided between the two transmit antennas. Additionally, STTC provides transmit diversity and coding gains compared with the uncoded QPSK.

Performance over rapidly fading channels.

The second comparison is done over rapid fading channels. This code is compared with the 8PSK trellis code and uncoded QPSK and the results are shown in Figure 2.12. The diversity order is equal to the minimum time diversity (MTD) multiplied by the number of receive

antennas ($Div=LM_R$). Thus, with one receive antenna, $Div=2$ for the 8PSK and the space time codes because both have MTD=2. For a diversity of order four, the space time code has 2×2 diversity while the 8PSK trellis code has 1×2. The results show that the space time code outperforms the 8PSK trellis code. The difference is quit small for a diversity order of two while the difference reaches 1.5 dB for a diversity order of four.

Effect of Minimum Square Product Distance (MSPD)

Figure 2.13 shows the effect of MSPD on the performance of the space time codes over rapidly fading channels. The larger the MSPD, the better the performance as can be seen from the figure.

Effect of Power Mismatch

The performance was tested over ideal conditions where we have assumed perfect channel state estimation and we have assumed spatial and time independence between the fades. Many papers assume that the fade power is equally divided between the paths arriving at each antenna. Let us consider the case where the fade power is not equally divided. This results in a performance degradation as can be seen from Figure 2.14. At an SNR of 14dB and with two transmit and one receive antenna, we see the effect of different path power ratios (PPR). At 0 dB, the fade power is equally split. For power ratios up to 4 dB, the degradation is not significant.

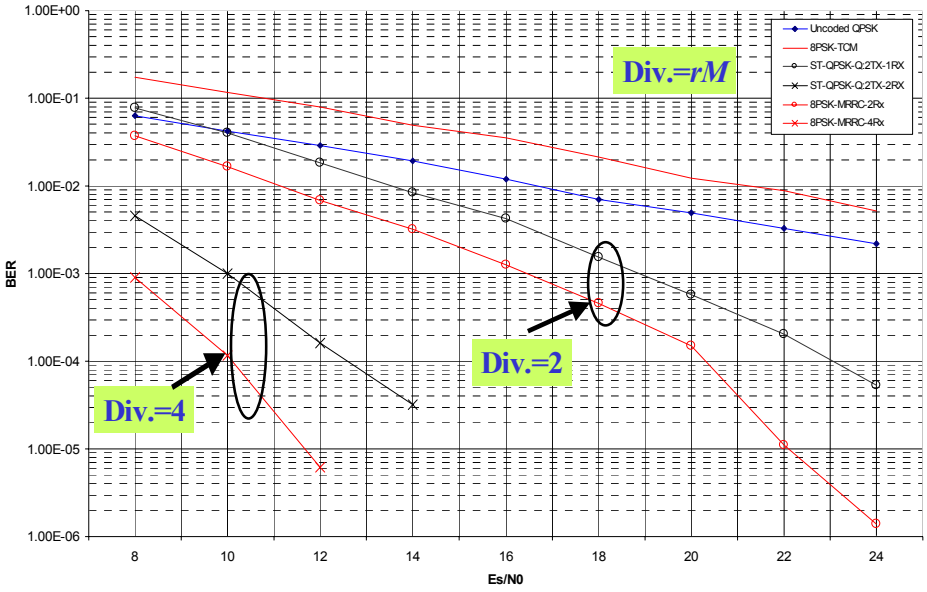

Figure 2.11: Performance comparison of STTC over quasi-static fading channels

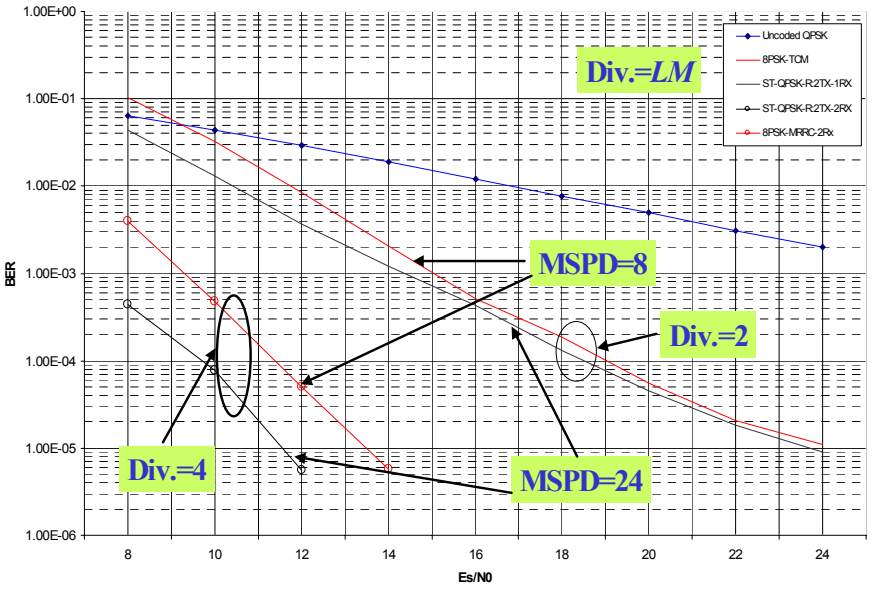

Figure 2.12: Performance comparison of STTC over rapid fading channels

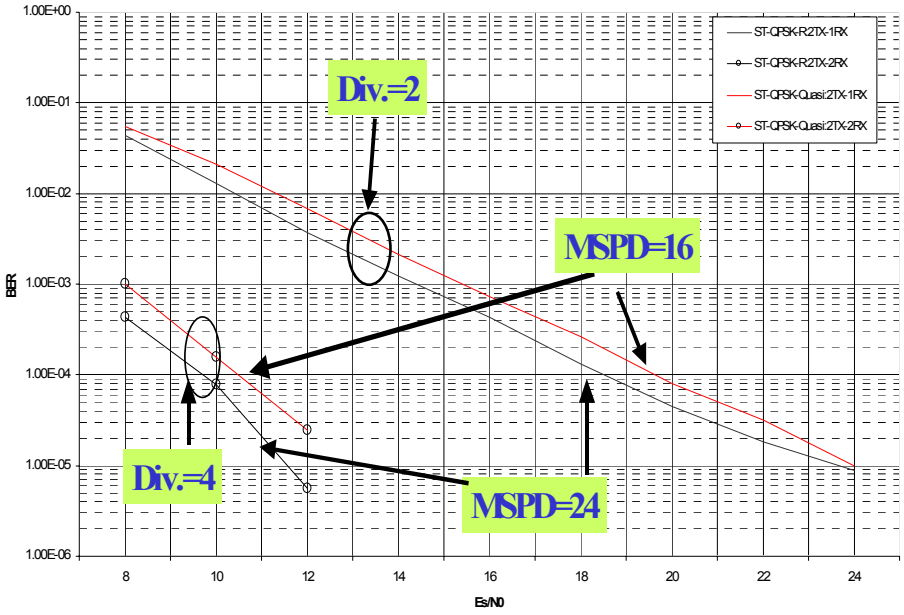

Figure 2.13: The effect of MSPD on the performance of ST codes over rapid fading channels

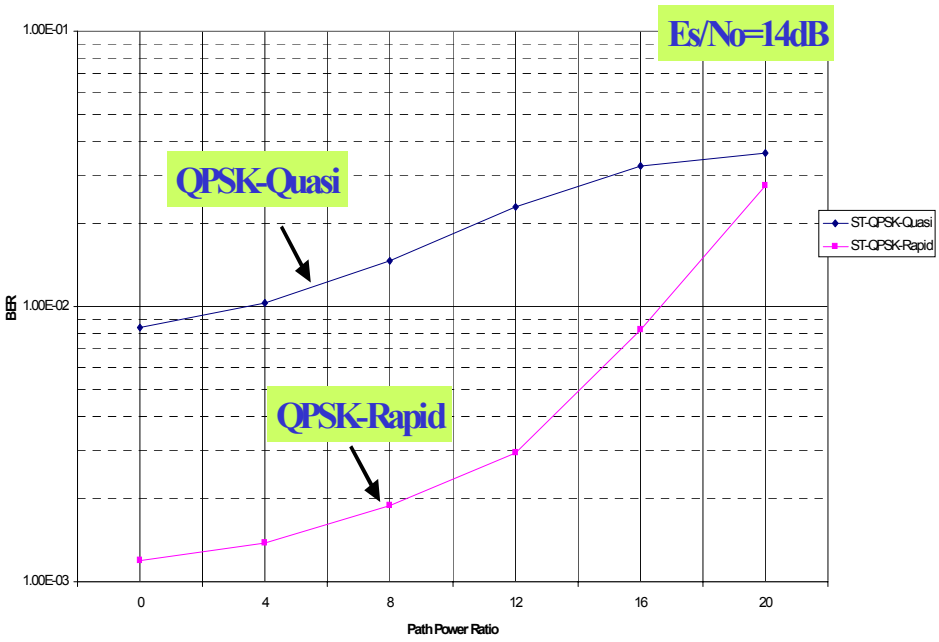

Figure 2.14: Effect of power mismatch on the performance of ST codes

Performance comparison of STBC and DSTM

This section compares the performance between space time block codes (STBC) and differential space time modulation (DSTM). Figure 2.15 compares the performance of 2x1 and 2x2 Alamouti's STBC with DSTM designed by [Hug00]. Since STBC is coherently detected, it outperforms the differential scheme. DSTM shows poor power efficiency since it requires high SNR to perform well.

Performance of STBC versus STTC

Since both STBC and STTC provide full transmit diversity and full rate over two transmit antennas, it is interesting to compare their performances. Over quasi-static fading channels, Figure 2.16 shows the performance of ST-QPSK-Quasi compared to STBC. Over 2x1 MIMO channels, STBC outperforms the trellis code with 8-state while having much less decoding complexity. This shows that the ST-QPSK-Quasi code performs poorly over systems with one receive antenna and at a low number of states. However, over 2×2 MIMO channels, ST-QPSK-Quasi is slightly better than STBC.

The scenario is exactly the opposite over rapidly fading channels. Figure 2.17 shows the performance of ST-QPSK-Rapid compared to STBC. Around 3dB gain is achieved by ST-QPSK-Rapid code. The reason is that trellis codes perform better over rapid fading channels while their performance suffers a lot over highly correlated channels.

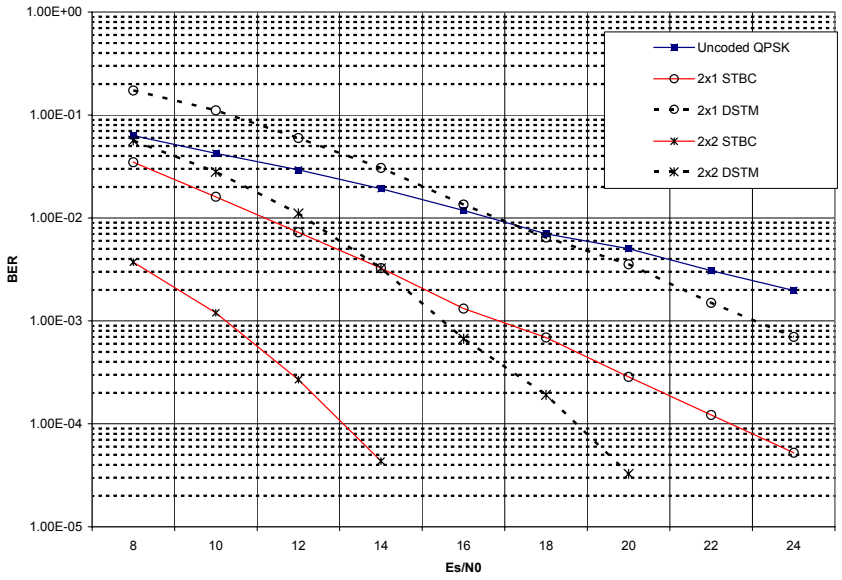

Figure 2.15: Performance comparison of STBC vs. DSTM over 2x1 and 2x2 MIMO channels

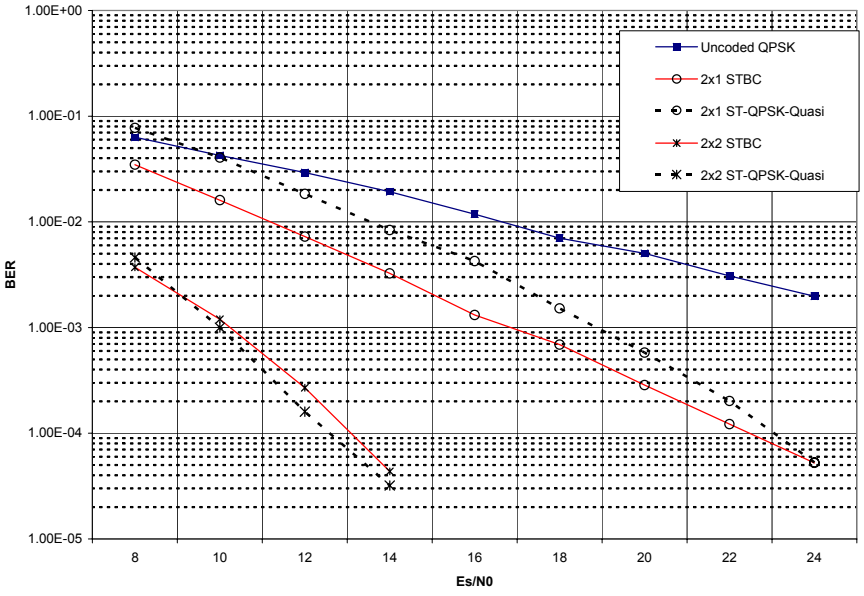

Figure 2.16: Performance comparison STBC vs. STTC over quasi-static Rayleigh fading channels

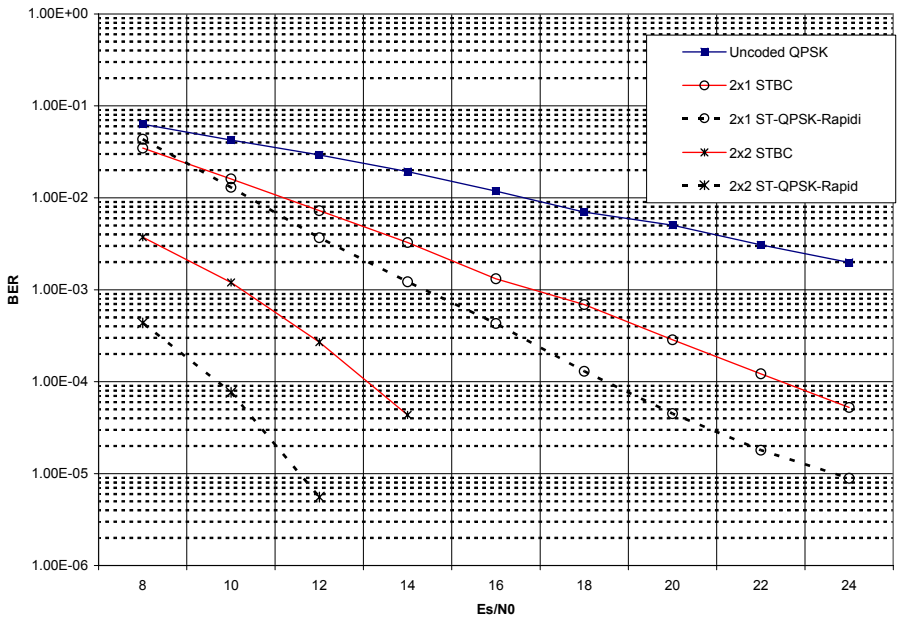

Figure 2.17: Performance comparison of STBC vs. STTC over rapid Rayleigh fading channels

2.4 Chapter Summary

In this chapter, we presented an overview of MIMO channels, MIMO capacity and MIMO communication systems. MIMO communication systems are classified under three categories: layered architectures, space time coding and space time modulation.

The layered architectures achieve very high spectral efficiencies by simultaneously transmitting symbols through all transmit-antennas without introducing any structure at the transmitter to aid detection at the receiver. Thus, multiuser detection algorithms must be used in order to suppress and cancel interfering signals before detecting the desired signal. Although this architecture provides high spectral efficiency, it suffers from poor power efficiency and error propagation. Coding could be easily concatenated with the layered architecture to improve the power efficiency.

Space time coded systems jointly optimize the design of transmit-diversity, data rate and coding gain. They improve the error rate performance of the system by providing diversity.

Schemes that don't require channel estimation at the receiver are unitary space time modulation and differential space time modulation. These schemes directly modulate space time matrices that are drawn from space time constellations that satisfy certain design criteria. The decoding of these schemes increases exponentially with increasing rate or number of transmit antennas. A comparison between these schemes is summarized in Table 2.1.

So far, the presented MIMO communication systems are either using the spatial domain (number of antennas) for spatial multiplexing or for spatial diversity. Spatial multiplexing systems, such as V-BLAST, transmit high data rates but have poor error rate performance due to the lack of diversity. On the other hand, spatial diversity systems, such as space time codes, provide full transmit and receive diversity but with a maximum rate of one symbol/time slot. In this dissertation, we bridge the gap between the two extremes of MIMO systems by assigning some antennas to spatial multiplexing and others to transmit diversity. The total number of transmit antennas is divided into groups and each group is assigned to a space time code. We analyze the capacity of this system, which is termed multi-layered space time code, and show how it compares to other MIMO systems and its preferred region of operation. We also evaluate and compare the information capacity and error rate performance of different multi-layered detection algorithms which are based on multi-user detection theory. The next couple of chapters cover multi-layered systems in more details.

Table 2.1: Comparison between different MIMO communication systems.

	Transmit Diversity	Number of Receive Antennas	Diversity Advantage Over Quasi-Static Fading Channels	Receiver Complexity Increase with increasing number of transmit antennas or/ and transmission rate
BLAST	No	$M_R \geq M_T$	$1 \times (1, 2, \cdots, M_R)$ Earlier detected symbols have lower advantage that later ones	Cubic
STTC	Yes	$M_R \geq 1$	$M_T \times M_R$	Exponential
STBC	Yes	$M_R \geq 1$	$M_T \times M_R$	Linear
DSTM	Yes	$M_R \geq 1$	$M_T \times M_R$	Exponential

Chapter 3
Multi-Layered Space Time Trellis Coded Systems

In this chapter, we propose and study decoding algorithms of a high data rate space time trellis coded architecture. By considering a single user who transmits simultaneously through K parallel space time trellis encoders, the system can provide high spectral efficiencies similar to V-BLAST but with transmit diversity and coding at each layer. The total number of transmit antennas is divided into groups and each group is assigned to a space time trellis code. The transmitter divides the information stream into layers of information and they are encoded and transmitted from each group simultaneously. Since the system is analogous to multiple synchronous users, each transmitting a space time trellis code, the receiver applies multi-user detection (MUD) techniques to decode the received signals. The main contribution of this chapter is developing and comparing three detection algorithms, which are joint detection, group interference nulling and cancellation, and spatial sequence estimation.

3.1 Introduction

To take advantage of the promised capacity of MIMO channels, Foschini proposed the BLAST architecture [Fos96]. It showed a huge increase in spectral efficiencies compared to single input single output (SISO) systems. However, it has poor energy performance and it

doesn't provide any transmit diversity. Furthermore, the number of receive antennas must be at least equal to the number of transmit antennas. That may limit the design for a small receiving end, such as a mobile unit. Another class of MIMO schemes are space time trellis codes (STTC) proposed by [Tar98]. These codes integrate the design of coding, modulation and transmit diversity to fully utilize the MIMO channels without any bandwidth expansions. They are full-rate full-diversity codes but their main drawback is the exponential complexity, in terms of number of states, needed to provide full diversity at a given number of transmit antennas. A spatial multiplexing structure with transmit diversity was proposed by [Tar99] to support high data rate applications. It was a generalized version of BLAST and it was called multi-layered space-time trellis code (MLSTTC) architecture. The encoder is divided into K parallel STTC encoders each transmits through N_G antennas. The decoder uses a spatial interference cancellation technique called serial group interference suppression.

In this chapter, we develop and compare additional decoding algorithms for MLSTTC. This architecture is a tradeoff between diversity and spatial multiplexing. The detection algorithms at the receiver are based on multi-user detection (MUD) techniques. Furthermore, the developed algorithms could be easily adapted to synchronous multi-user STTC systems.

Three classes of MLSTTC receivers are developed. The first is based on joint detection and decoding. An optimum joint MLSTTC decoder is based on a super trellis decoder. It has a huge complexity but it can be built for a small number of layers. The joint receiver complexity is reduced by dividing the detection and decoding process into two stages: a joint detector followed by a trellis decoder for each layer. By applying this, we develop two suboptimal joint receivers. The first one uses a maximum likelihood (ML) hard detector and the second uses a soft-input soft-output (SISO) maximum a posteriori (MAP) detector followed by a SISO-MAP trellis

decoder for each layer. The second algorithm shares soft information iteratively between the two stages. The algorithm is called a soft iterative joint detector. Although the complexity per layer is exponential for the detection stage, it is linear for the decoding stage. The above decoders are quite complex and can only be practically used for a small number of layers.

The second group of multi-layered receivers is based on group interference nulling and cancellation. The complexity of the nulling stage is cubic and the decoding stage is linear but its performance is inferior to the joint detection due to the diversity reduction caused by nulling. Two interference cancellation algorithms are evaluated in this chapter. The first one was proposed by [Tar99] and we call it serial group interference nulling and cancellation (SGINC). This technique serially decodes each layer and it has two main drawbacks: error propagation and unequal diversity advantages for each layer. In order to overcome these disadvantages, we propose a parallel version of the algorithm called parallel group interference nulling and cancellation (PGINC). This algorithm improves the performance of SGINC because parallel cancellation theoretically provides full receive diversity for each layer and the iterative structure reduces the error propagation. However, error propagation greatly limits the diversity of the algorithm.

The third class of MLSTTC receivers is based on spatial sequence estimation (SSE) developed by Maruf in [Moh04] for V-BLAST. In this chapter, we modify the algorithm to an iterative soft SSE for the detection and decoding of MLSTTC. It combines nulling and joint detection and avoids interference cancellation. The main advantage of this algorithm is its flexibility in trading off receive diversity with complexity. Also, it doesn't suffer from error propagation similar to joint detection algorithms but with much less complexity.

3.2 System Description

Encoder

The multi-layered encoder is divided into K parallel groups $\{G_i : i = 1,2,...,K\}$. Each group encodes a layer of information by STTC with N_G transmit antennas. The total number of transmit antennas is M_T. The input stream is divided into K layers of information bits $\{B_i : i = 1,2,...,K\}$. All groups operate simultaneously and the transmission is synchronous. Figure 3.1 shows a block diagram of the system architecture. The N_G transmitted symbols from G_i at time t are represented by the column vector $\mathbf{x}_i^t = (x_{i,1}^t, x_{i,2}^t, \ldots, x_{i,N_G}^t)^T$, where T is the transpose operation. The multi-layered transmitted vector at each instant of time is:

$$\mathbf{x}^t = \begin{bmatrix} \mathbf{x}_1^t & \cdots & \mathbf{x}_K^t \end{bmatrix}^T \tag{3.1}$$

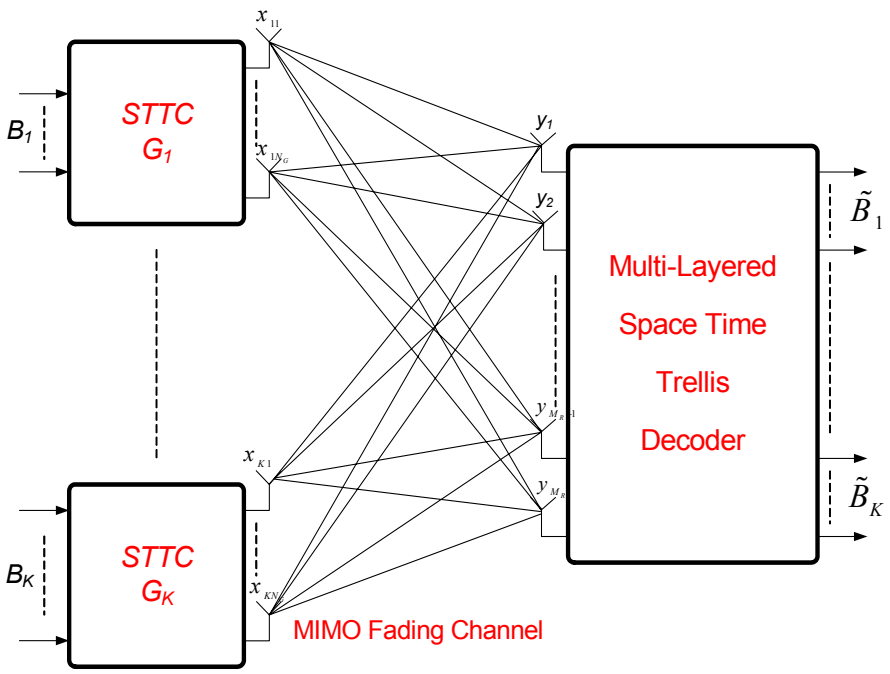

Figure 3.1: Block diagram of the multi-layered space time trellis coding architecture

Discrete Channel Model

The MIMO channel has $M_R \times M_T$ paths arriving at the receiver. To evaluate the optimum performance, we assumed fully independent paths. Each path is a quasi-static fading channel where the fading coefficient is constant over one frame and independent from one frame to another. Each coefficient is a complex Gaussian random variable with mean zero and variance 0.5 per dimension. It has a Rayleigh distributed envelope and a uniformly distributed phase. Let h_{mn} denote the path gain from transmit antenna *n* to receive antenna *m* where $n = 1 \cdots M_T$ and $m = 1 \cdots M_R$, the channel coefficient matrix is:

$$\mathbf{H} = \begin{bmatrix} h_{11} & \cdots & h_{1N_G} & h_{1(N_G+1)} & \cdots & h_{1M_T} \\ \vdots & \vdots & \vdots & \vdots & \vdots & \vdots \\ h_{M_R 1} & \cdots & h_{M_R N_G} & h_{M_R (N_G+1)} & \cdots & h_{M_R M_T} \end{bmatrix} \tag{3.2}$$

$$\mathbf{H} = \begin{bmatrix} \mathbf{H}_1 & \mathbf{H}_2 & \cdots & \mathbf{H}_K \end{bmatrix} \tag{3.3}$$

where $\mathbf{H}_i \in \mathbb{C}^{M_R \times N_G}$ represents the MIMO channel for G_i.

At each receive antenna *m*, AWGN (η_m) is added to the received signal (y_m). It has zero mean and variance of $N_0 / 2$ per dimension. The received vector at time $t = 1, 2, \ldots, L$ is:

$$\mathbf{y}^t = \mathbf{H}\mathbf{x}^t + \boldsymbol{\eta}^t \tag{3.4}$$

where *L* is the frame length of the codeword transmitted from each antenna and

$$\mathbf{y}^t = \begin{bmatrix} y_1 & \cdots & y_{M_R} \end{bmatrix}^T \quad \text{and} \quad \boldsymbol{\eta}^t = \begin{bmatrix} \eta_1^t & \cdots & \eta_{M_R}^t \end{bmatrix}^T$$

3.3 Joint Detection

Two joint detection algorithms are developed in this section to jointly decode MLSTTC. They are the optimum and suboptimal joint decoders. These joint receivers provide full receive antenna diversity while the transmit diversity is equal to each layer diversity. Thus, the diversity order of the joint algorithms is $N_G \times M_R$.

3.3.1 Optimum joint MLSTTC decoder

The optimum joint decoder uses a super trellis to jointly decode all layers. A major drawback is its huge complexity. However, we implement it to be used as a reference for the other proposed decoders. Assume that each group has S states, the super trellis will have S^K states. Each state has $2^{\sum_{i=1}^{K} B_i}$ transitions and each transition corresponds to M_T symbols. Although MLSTTC transmits through M_T antennas, it can't have a rank greater than the rank of each group.

At the receiver, assuming perfect channel state information, the joint decoder selects the maximum likelihood sequence $\tilde{\mathbf{q}}$

where $\tilde{\mathbf{q}} = \left(\mathbf{q}^1, \mathbf{q}^2, \cdots, \mathbf{q}^L\right)$ is the sequence of transmitted vectors for the whole frame
and $\mathbf{q}^t = (\mathbf{q}_1^t, \mathbf{q}_2^t, \ldots, \mathbf{q}_K^t)^T$ is a transmitted vector at time t
and $\mathbf{q}_i^t = (q_{i,1}^t, q_{i,2}^t, \ldots, q_{i,N_G}^t)^T$ is a transmitted vector from G_i

that minimizes the following cumulative decision metric:

$$\sum_{t=1}^{L} \left\| \mathbf{y}^t - \mathbf{H}\mathbf{q}^t \right\|^2 \tag{3.5}$$

3.3.2 Suboptimum joint MLSTTC decoder

The optimum joint decoder suffers from an exponential increase in complexity with an increase in the number of layers. To overcome this drawback, we divide the receiver into two stages: a joint detector followed by a STTC decoder for each layer. Thus, the second stage of the receiver has linear complexity per layer while the first still has exponential complexity. This method is implemented with two algorithms: hard and soft iterative decoding.

Hard decoding

The first suboptimal joint decoder uses a hard decision maximum likelihood (ML) detector at the first stage. The hard decisions are then passed to K parallel STTC decoders as shown in Figure 3.2. The ML detector selects the ML transmitted vector $\tilde{\mathbf{x}}^t$ such that:

$$\tilde{\mathbf{x}}^t = \min_{\mathbf{q}^t} \left\| \mathbf{y}^t - \mathbf{H}\mathbf{q}^t \right\|^2 \tag{3.6}$$

Let Z denote the signal set of each code. Then, the ML detector searches over $|Z|^{M_T}$ possible vectors, where $|Z|$ is the cardinality of the signal set.

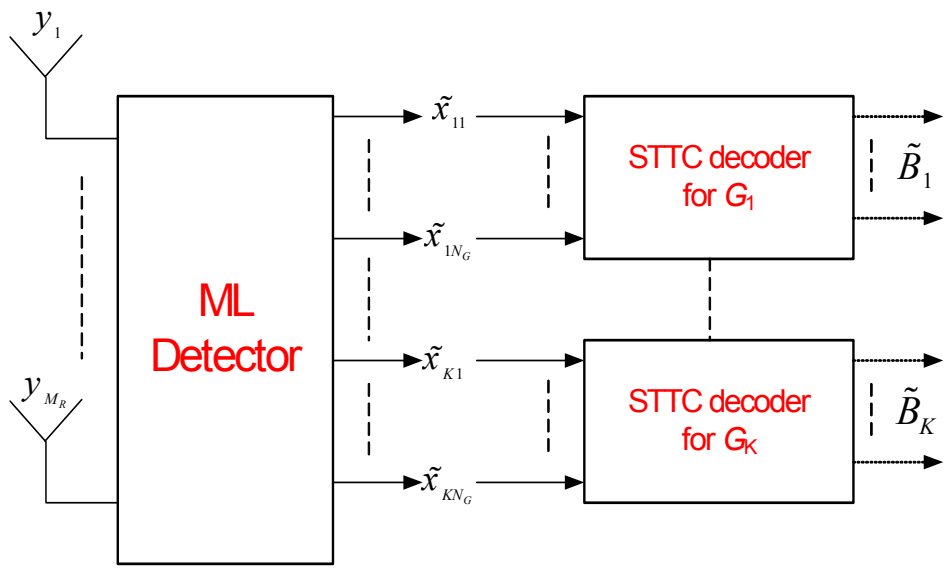

Figure 3.2: Suboptimum joint hard decoding

Soft iterative joint decoder

The second suboptimal joint detector implements a soft in/soft out (SISO) algorithm for the first stage followed by K parallel SISO trellis decoders. The two stages share the soft information iteratively similar to the turbo decoding principle.

SISO detector

The SISO detector used in this algorithm is a MAP detector. The posteriori probability of the transmitted vector $\mathbf{q}^t$ is defined as

$$P(\mathbf{q}^t \mid \mathbf{y}^t) = \frac{P(\mathbf{y}^t \mid \mathbf{q}^t)P(\mathbf{q}^t)}{P(\mathbf{y}^t)} \tag{3.7}$$

Since $P(\mathbf{y}^t)$ is fixed , the posteriori probability is:

$$P(\mathbf{q}^t \mid \mathbf{y}^t) = c \cdot P(\mathbf{y}^t \mid \mathbf{q}^t)P(\mathbf{q}^t) \tag{3.8}$$

where c is a scaling constant such that the $sum\left(P(\mathbf{q}^t \mid \mathbf{y}^t)\right)=1$. Also, $P(\mathbf{q}^t)$ is the a priori probability of the transmitted vector. At the first iteration, the symbols are assumed to be equally probable. At later iterations, the priori probability is fed back from the SISO trellis decoder as an extrinsic probability. The conditional probability of the observation given the transmitted vector is:

$$P(\mathbf{y}^t \mid \mathbf{q}^t) = c_1 \exp(-\frac{\left\|\mathbf{y}^t - \mathbf{H}\mathbf{q}^t\right\|^2}{2\sigma^2}) \tag{3.9}$$

By substituting (3.9) into (3.8), the MAP detector finds the a posteriori probabilities for all $|Z|^{M_T}$ possible transmitted vectors. To proceed to the next stage, marginal posteriori probabilities of the transmitted symbols from each group and from each antenna are calculated. Let $P(\mathbf{q}^t_{k,i} / \mathbf{Y}^t)$ be the marginal posteriori probability vector of size $|Z|$ that represents the a posteriori probabilities of the transmitted symbols from antenna $k \in \{1,2\cdots,N_G\}$ at group G_i. The receiver calculates each element of this vector from the joint posteriori probability by performing the following summation:

$$P(\mathbf{q}^t_{k,i}(j) = z \mid \mathbf{y}^t) = \sum_{\zeta} P(\mathbf{q}^t \mid \mathbf{y}^t) \tag{3.10}$$

where $j = 1,2,\cdots,|Z|$, $z \in Z$ and the sum is performed over the set ζ for which the $(k+(i-1)N_G)^{th}$ symbol of $\mathbf{q}^t$ is equal to signal z.

SISO Space Time Trellis Decoder

K parallel MAP STTC decoders are used in the second stage of the receiver. Each one takes in the marginal a posteriori probabilities of the transmitted symbols calculated in the first stage and generates a new extrinsic probability for the transmitted symbols and decision

probabilities for the information bits. The MAP algorithm is well documented in literature. We have used the algorithm presented in [Mag99] with minor modifications to adjust to STTC. For G_i and at time t+1, the a posteriori probability (APP) of each valid state transition from state s_t to state s_{t+1} is:

$$P[s_t \to s_{t+1} \mid \mathbf{Y}] = \frac{P[s_t \to s_{t+1}, \mathbf{Y}]}{P[\mathbf{Y}]} \tag{3.11}$$

Where **Y** is the vector of observations for the whole frame L. The properties of the Markov process are used to partition the numerator as

$$P[s_t \to s_{t+1}, \mathbf{Y}] = \alpha(s_t)\gamma(s_t \to s_{t+1})\beta(s_{t+1}) \tag{3.12}$$

Where the branch metric is defined as

$$\gamma(s_t \to s_{t+1}) = P[s_{t+1} \mid s_t] \prod_{k=1}^{N_G} P[\mathbf{q}_{k,j}^t (j) = x_k \mid \mathbf{Y}] \tag{3.13}$$

where $P[s_{t+1} \mid s_t]$ is the message (information input) probability which is assumed to be drawn from an i.i.d source. Therefore, $P[s_{t+1} \mid s_t] = 1/2^{B_i}$. Also, $P[\mathbf{q}_{k,j}^t (j) = x_k \mid \mathbf{Y}]$ is the posteriori probability of symbol x_k transmitted from antenna k in G_i at time t. The index j corresponds to the symbol x_k.

Furthermore, the forward probability is defined as

$$\alpha(s_t) = \sum_{\{s_{t-1}\}} \alpha(s_{t-1})\gamma(s_{t-1} \to s_t) \tag{3.14}$$

where the summation is performed over all valid transitions arriving at s_t

The backward probability is defined as

$$\beta(s_t) = \sum_{\{s_{t+1}\}} \beta(s_{t+1})\gamma(s_t \to s_{t+1}) \tag{3.15}$$

Where the summation is performed over all valid transitions going out from s_t.

Then, new extrinsic probabilities of $\mathbf{q}_{k,i}^t$ is:

$$P_{ext}^{dec}(\mathbf{q}_{k,i}^t(j)=z)=c\sum_{\{s_{t-1}\to s_t|x_k=z\}}\alpha(s_{t-1})\beta(s_t)P[s_t\,|\,s_{t-1}] \tag{3.16}$$

where the summation is performed over all valid transitions arriving at s_t such that the transmitted symbol from antenna *k* is equal to *z*.

APP of the information bits is:

$$P(b_i^t=u)=c\sum_{\{s_{t-1}\to s_t|b_i^t=u\}}\alpha(s_{t-1})\gamma(s_{t-1}\to s_t)\beta(s_t) \tag{3.17}$$

Where the summation is performed aver all state transitions at time *t* that correspond to a bit *u*. The new extrinsic probabilities are fed back to the MAP detector and used as priori probabilities.

We calculate the priori probability for $\mathbf{q}^t$ by:

$$P(\mathbf{q}^t)=P([\underbrace{q_1^tq_2^t\cdots q_{N_G}^t}_{\mathbf{q}_1^t}\,q_{N_G+1}^t\cdots q_{M_T}^t])=\prod_{i=1}^{K}\prod_{k=1}^{N_G}P_{ext}^{dec}(\mathbf{q}_{k,i}^t(j)=q_{k+(i-1)N_G}^t) \tag{3.18}$$

The block diagram of the soft iterative joint decoder is shown in Figure 3.3.

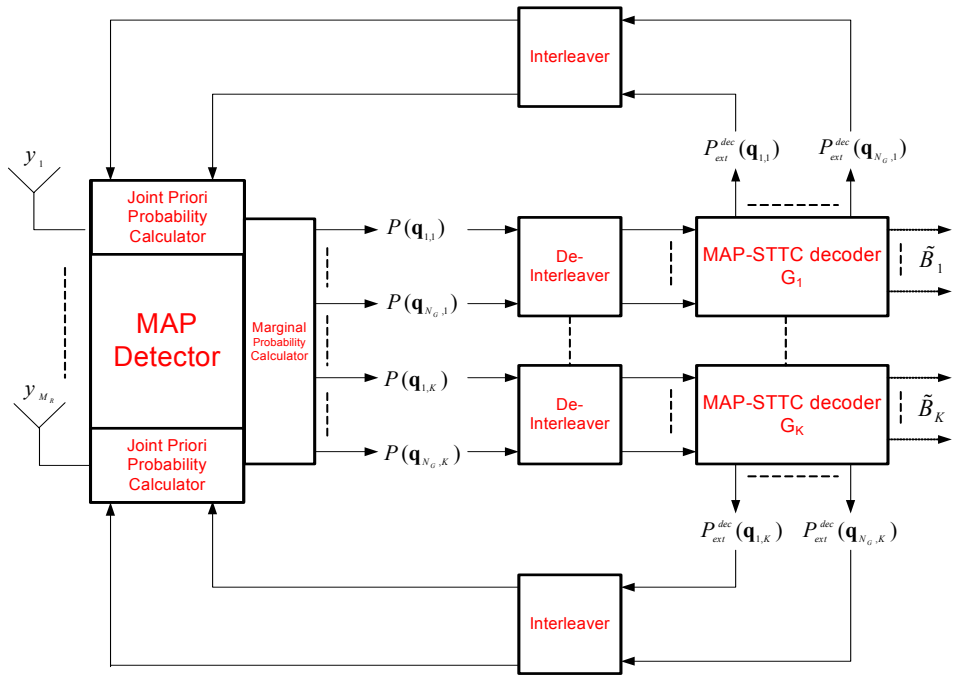

Figure 3.3: Soft iterative joint MLSTTC decoder

3.3.3 Performance Evaluation via Simulation

To test the optimum performance of the proposed decoders, we assume fully independent Rayleigh fading MIMO channels and perfect channel state information. Each path is a quasi-static Rayleigh fading channel which has a constant fading coefficient over the whole frame and is independent from one frame to another. The STTC used in this study for each layer is a rank two 8-state QPSK code designed by [Tar98] for quasi-static Raleigh fading channels. It has 2 bps/Hz efficiency. Its trellis diagram and its corresponding signal set are shown in Figure 3.4.

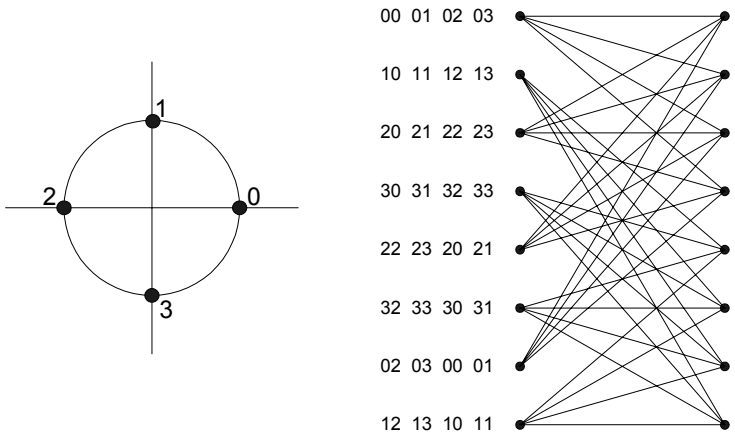

Figure 3.4: Trellis Diagram of rank two QPSK STTC

For a two-layered system, the spectral efficiency is 4 bps/Hz and the total number of transmit antennas is $M_T=4$. Its transmit diversity is two. At the receiver, two receive antennas are used in this section. The number of receive antennas in the joint detection algorithms are not restricted which is an advantage over the interference cancellation receivers.

Figure 3.5 shows the BER performance of the joint detection algorithms versus SNR per receive antenna of the two-layered STTC system. Comparing MLSTTC with uncoded 16QAM shows a huge gain in coding and diversity. This gain is about 19 dB at BER=10^{-3} when compared to the optimal joint detector. The result also illustrates the poor performance of the hard detection algorithm. This performance degradation is a result of using hard decisions at the first stage which throws away valuable information needed by STTC decoder. The performance of the soft iterative joint decoder is also shown in Figure 3.5. With no iterations, this soft decoder outperforms the hard detector by 6dB at BER=10^{-3}. Diminishing returns are observed after two iterations. At that point, the difference between the optimum and the soft iterative detector is around 1.75 dB.

One problem with the proposed soft iterative detector is that the complexity of the first stage is exponential per layer. It can only be practically used for a small number of layers. Next section presents more practical decoding algorithms that are based on spatial interference cancellation.

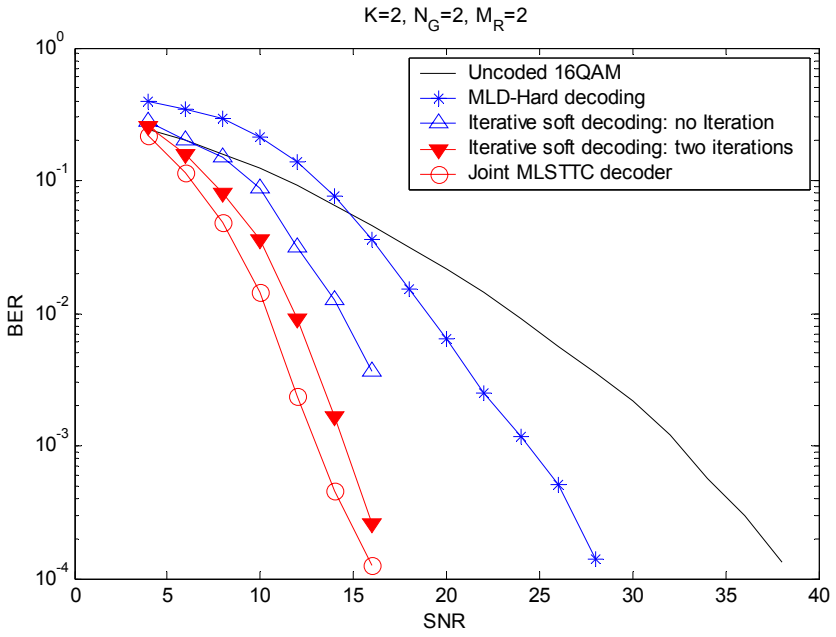

Figure 3.5: Performance of the joint detection algorithm for MLSTTC at 4 bps/Hz over 4x2 MIMO channels.

3.4 Group Interference Nulling and Cancellation

Spatial group inference nulling and cancellation (GINC) algorithms are used in this section to decode each layer. Similar to the suboptimum joint algorithms, there are two stages. The first stage uses interference nulling which has cubic complexity per layer. The second stage performs decoding and interference cancellation and it has linear complexity per layer. This method was originally proposed by Tarokh [Tar99] as an extension to the V-BLAST algorithm and it performs serial group interference nulling and cancellation (SGINC). It reduces the

complexity of the joint decoder with some loss in performance. This method has two drawbacks. The first is that decoding errors propagate from one layer to another. The second is that the diversity advantage is not equal for all layers. The earlier decoded layers have less receive antenna diversity than the later which affects the overall performance. To overcome these drawbacks, we apply iterative parallel processing. The algorithm is called parallel group interference nulling and cancellation (PGINC). The error propagation can be reduced by the iterative structure and each group should theoretically have full receive antenna diversity. However, the results show that this diversity isn't achieved due to error propagations. The following sections describe the serial and parallel algorithms in details.

3.4.1 Serial Group Interference Nulling and Cancellation

Assuming prefect channel state estimation, the idea is to decode G_i while nulling interfering signals from other groups. Then, the algorithm cancels the contribution of the decoded layer from the received signal. After that, the process is serially repeated for each layer. This serial algorithm works best if the layers are arranged from the highest to lowest signal power. Let G_1 be the first group to be decoded. Since it transmits through N_G antennas, there are $M_T - N_G$ interfering signals. For the decoder to successfully null out all other groups, the number of receive antennas must be $M_R \geq M_T - N_G + 1$. The decoder starts by creating the matrix Δ_1 which represents the channel coefficients of $M_T - N_G$ interfering signals. Thus,

$$\Delta_1 = \begin{bmatrix} h_{1(N_G+1)} & h_{1(N_G+2)} & \cdots & h_{1M_T} \\ \vdots & \vdots & \ddots & \vdots \\ h_{M_R(N_G+1)} & h_{M_R(N_G+2)} & \cdots & h_{M_R M_T} \end{bmatrix}_{M_R \times (M_T - N_G)} \tag{3.19}$$

The range of Δ_1 is a subspace of $\mathbb{C}^{M_R}$ that is spanned by $M_T - N_G$ columns and the null space is the orthogonal complement of the range and it is defined as $Null\left[\Delta_1^H\right]$, where *H* denotes the conjugate transpose (Hermitian) [Sch97].

Thus, $$R = Range[\Delta_1] = \{\mathbf{r}: \quad \Delta_1\mathbf{a} = \mathbf{r}; \quad \mathbf{a} \in \mathbb{C}^{M_T} \ and \quad \mathbf{r} \in \mathbb{C}^{M_R}\}$$

$$R^{\perp} = Null[\Delta_1^H] = \{\mathbf{u}: \quad \Delta_1^H\mathbf{u}^H = \mathbf{0}; \quad \mathbf{u} \in \mathbb{C}^{M_R} \ and \quad \mathbf{0} \in \mathbb{C}^{M_T}\}$$

$$= \{\mathbf{u}: \quad \mathbf{u}\Delta_1 = \mathbf{0}; \quad \mathbf{u} \in \mathbb{C}^{M_R} \ and \quad \mathbf{0} \in \mathbb{C}^{M_T}\}$$

The dim($R^{\perp}$) is called the nullity of Δ_1 and the dim(R) is called the rank of Δ_1. Since the range of Δ_1 is spanned by $M_T - N_G$ columns and these columns are linearly independent, $rank[\Delta_1] = M_T - N_G$. Also,

$$Nullity[\Delta_1] + rank[\Delta_1] = M_R$$

$$\Rightarrow \quad Nullity[\Delta_1] = M_R - M_T + N_G \tag{3.20}$$

The decoder finds a set of row vectors $\{\mathbf{u}_i : i = 1, 2, ..., M_R - M_T + N_G; \quad \mathbf{u}_i \in \mathbb{C}^{M_R}\}$ that forms an orthonormal basis of the null space ($R^{\perp}$). Let us define the nulling matrix of interfering groups as:

$$\mathbf{U}_1 = \begin{bmatrix} \mathbf{u}_1 \\ \vdots \\ \mathbf{u}_{M_R - M_T + N_G} \end{bmatrix} \tag{3.21}$$

The decoder nulls out interference by multiplying (3.4) by $\mathbf{U}_1$:

$$\mathbf{U}_1\mathbf{y}^t = \mathbf{U}_1\mathbf{H}\mathbf{x}^t + \mathbf{U}_1\boldsymbol{\eta}^t \tag{3.22}$$

$$\mathbf{U}_1\mathbf{y}^t = \mathbf{U}_1[\mathbf{H}_1 \quad \Delta_1]\cdot\begin{bmatrix}\mathbf{x}_1^t\\ \mathbf{x}_2^t\\ \vdots\\ \mathbf{x}_K^t\end{bmatrix} + \mathbf{U}_1\boldsymbol{\eta}^{\mathbf{t}} \tag{3.23}$$

$$\mathbf{U}_1\mathbf{y}^t = [\mathbf{U}_1\mathbf{H}_1 \quad \mathbf{0} \quad \cdots \quad \mathbf{0}]\cdot\begin{bmatrix}\mathbf{x}_1^t\\ \mathbf{x}_2^t\\ \vdots\\ \mathbf{x}_K^t\end{bmatrix} + \mathbf{U}_1\boldsymbol{\eta}^{\mathbf{t}} \tag{3.24}$$

$$\mathbf{U}_1\mathbf{y}^t = \mathbf{U}_1\mathbf{H}_1\mathbf{x}_1^t + \mathbf{U}_1\boldsymbol{\eta}^{\mathbf{t}} \tag{3.25}$$

$$\tilde{\mathbf{y}}_1^t = \tilde{\mathbf{H}}_1\mathbf{x}_1^t + \tilde{\boldsymbol{\eta}}_1^t \tag{3.26}$$

The noise and the channel characteristics are preserved by this transformation [Tar99]. Let $\widetilde{h}_{ij}$ and $\widetilde{h}_{lk}$ be two different elements of $\tilde{\mathbf{H}}_1$. By the definition of matrix multiplication, $\tilde{h}_{ij} = \mathbf{u}_i\mathbf{w}_j$ and $\tilde{h}_{lk} = \mathbf{u}_l\mathbf{w}_k$ where $\mathbf{w}_j$ and $\mathbf{w}_k$ are the j^{th} and k^{th} columns of $\mathbf{H}_1$. Given Δ_1,

$$E[\tilde{h}_{ij}] = E[\mathbf{u}_i\mathbf{w}_j] = \mathbf{u}_i E[\mathbf{w}_j] = \mathbf{0} \tag{3.27}$$

Thus, the random variable $\widetilde{h}_{ij}$ and $\widetilde{h}_{lk}$ have zero mean. Furthermore,

$$E[\tilde{h}_{ij}\tilde{h}_{lk}^H] = E[\mathbf{u}_i\mathbf{w}_j\mathbf{w}_k^H\mathbf{u}_l^H] = \mathbf{u}_i E[\mathbf{w}_j\mathbf{w}_k^H]\mathbf{u}_l^H = \delta_{jk}\mathbf{u}_i\mathbf{u}_l^H = \delta_{jk}\delta_{il} \tag{3.28}$$

where δ is the kronecker delta function given by $\delta_{jk} = 0$ if $j \neq k$ and $\delta_{jk} = 1$ if $j=k$. Therefore, the elements of $\mathbf{H}_1$ are independent complex Gaussian random variables of variance 0.5 per real dimension. Similarly, the elements of the noise vector are independent complex Gaussian random variables of variance $N_0/2$ per dimension.

After nulling, a trellis decoder decodes G_1 by selecting the sequence

$$\underbrace{q_1^1 q_2^1 \cdots q_{N_G}^1}_{\mathbf{q}_1^t} \cdots q_1^L q_2^L \cdots q_{N_G}^L \qquad \text{where } L \text{ is the frame length}$$

that minimizes the decision metric

$$\sum_{t=1}^{L} \left\| \tilde{\mathbf{y}}_1^t - \tilde{\mathbf{H}}_1 \mathbf{q}_1^t \right\|^2 \tag{3.29}$$

Since $\tilde{\mathbf{H}}_1 \in \mathbb{C}^{(M_R - M_T + N_G) \times N_G}$ and G_i is full rank, it has $N_G \times (N_G + M_R - M_T)$ diversity order.

After that, the detected layer is regenerated and its contribution is subtracted from the received signal. Denote the regenerated codeword by $\tilde{\mathbf{x}}_1^t$, then:

$$\Delta \mathbf{y}^t = \mathbf{y}^t - \mathbf{H}_1 \tilde{\mathbf{x}}_1^t \tag{3.30}$$

$$= \mathbf{H}\mathbf{x}^{\mathbf{t}} + \boldsymbol{\eta}^{\mathbf{t}} - H_1 \tilde{\mathbf{x}}_1^t \tag{3.31}$$

$$= [\mathbf{H}_1 \quad \mathbf{H}_2 \quad \cdots \quad \mathbf{H}_K] \cdot \begin{bmatrix} \mathbf{x}_1^t \\ \mathbf{x}_2^t \\ \vdots \\ \mathbf{x}_K^t \end{bmatrix} - \mathbf{H}_1 \tilde{\mathbf{x}}_1^t + \boldsymbol{\eta}^{\mathbf{t}} \tag{3.32}$$

$$= \mathbf{H}_1 \mathbf{x}_1^t + \mathbf{H}_2 \mathbf{x}_2^t + \cdots + \mathbf{H}_K \mathbf{x}_K^t - \mathbf{H}_1 \tilde{\mathbf{x}}_1^t + \boldsymbol{\eta}^{\mathbf{t}} \tag{3.33}$$

$$= [\mathbf{H}_1 \quad \mathbf{H}_2 \quad \cdots \quad \mathbf{H}_K] \cdot \begin{bmatrix} \mathbf{x}_1^t - \tilde{\mathbf{x}}_1^t \\ \mathbf{x}_2^t \\ \vdots \\ \mathbf{x}_K^t \end{bmatrix} + \boldsymbol{\eta}^{\mathbf{t}} \tag{3.34}$$

If $\mathbf{x}_1^t = \tilde{\mathbf{x}}_1^t$, Then

$$\Delta \mathbf{y}^{\mathbf{t}} = [\mathbf{H}_2 \quad \mathbf{H}_3 \quad \cdots \quad \mathbf{H}_K]_{M_R \times (M_T - N_G)} \cdot \begin{bmatrix} \mathbf{x}_2^t \\ \mathbf{x}_3^t \\ \vdots \\ \mathbf{x}_K^t \end{bmatrix}_{(M_T - N_G) \times 1} + \boldsymbol{\eta}^{\mathbf{t}} \tag{3.35}$$

After cancellation, nulling and space time trellis decoding are repeated to decode G_2 which now has a maximum diversity of $N_G \times (2N_G + M_R - M_T)$. This diversity is highly affected by decoding errors. The nulling, decoding and cancellation process is repeated serially to decode all layers. The i^{th} layer has a maximum diversity of $N_G \times (i \cdot N_G + M_R - M_T)$. Therefore, diversity increases from later decoded layers but error propagation greatly limits the achieved diversity.

To resolve these drawbacks, we proposed an iterative PGINC. The iterative structure with interleaving reduces error propagation and the parallel structure theoretically provides full receive diversity for each layer.

3.4.2 Parallel Group Interference Nulling and Cancellation (PGINC)

The parallel processing consists of parallel inference nulling followed by parallel decoding and interference cancellation. The received vector at time *t* is:

$$\mathbf{y}^t = \mathbf{H}\mathbf{x}^{\mathbf{t}} + \boldsymbol{\eta}^{\mathbf{t}} \tag{3.36}$$

$$= [\mathbf{H}_1 \quad \mathbf{H}_2 \quad \cdots \quad \mathbf{H}_K] \cdot \begin{bmatrix} \mathbf{x}_1^t \\ \mathbf{x}_2^t \\ \vdots \\ \mathbf{x}_K^t \end{bmatrix} + \boldsymbol{\eta}^{\mathbf{t}} \tag{3.37}$$

The decoder finds the nulling matrix for all groups at the same time. For G_i, Δ_i is formed by removing $\mathbf{H}_i$ from the channel matrix $\mathbf{H}$.

$$\Delta_i = \left[\mathbf{H}_1 \quad \cdots \quad \mathbf{H}_{i-1} \quad \mathbf{H}_{i+1} \quad \cdots \quad \mathbf{H}_K\right] \tag{3.38}$$

Then, for G_i, the decoder nulls out all interfering groups:

$$\mathbf{U}_i \mathbf{y}^t = \mathbf{U}_i \mathbf{H}\mathbf{x}^{\mathbf{t}} + \mathbf{U}_i \boldsymbol{\eta}^{\mathbf{t}} \tag{3.39}$$

$$\mathbf{U}_i \mathbf{y}^t = \mathbf{U}_i \begin{bmatrix} \mathbf{H}_1 & \cdots & \mathbf{H}_i & \cdots & \mathbf{H}_K \end{bmatrix} \begin{bmatrix} \mathbf{x}_1^t \\ \vdots \\ \mathbf{x}_i^t \\ \vdots \\ \mathbf{x}_K^t \end{bmatrix} + \mathbf{U}_i \boldsymbol{\eta}^{\mathbf{t}} \tag{3.40}$$

Since $\mathbf{U}_i \mathbf{H}_j = \mathbf{0}$; *when* $i \neq j$

$$\mathbf{U}_i \mathbf{Y}^t = \begin{bmatrix} \mathbf{0} & \cdots & \mathbf{U}_i \mathbf{H}_i & \cdots & \mathbf{0} \end{bmatrix} \begin{bmatrix} \mathbf{x}_1^t \\ \vdots \\ \mathbf{x}_i^t \\ \vdots \\ \mathbf{x}_K^t \end{bmatrix} + \mathbf{U}_i \boldsymbol{\eta}^{\mathbf{t}} \tag{3.41}$$

$$\mathbf{U}_i \mathbf{y}^t = \mathbf{U}_i \mathbf{H}_i \mathbf{x}_i^t + \mathbf{U}_i \boldsymbol{\eta}^{\mathbf{t}} \tag{3.42}$$

$$\tilde{\mathbf{y}}_{i,PIN}^t = \tilde{\mathbf{H}}_i \mathbf{x}_i^t + \tilde{\boldsymbol{\eta}}_i^t \tag{3.43}$$

where $\tilde{\mathbf{H}}_i \in \mathbb{C}^{(M_R - M_T - N_G) \times N_G}$ and (*PIN*) refers to parallel interference nulling stage. The diversity advantage at this stage is $N_G \times (M_R - M_T + N_G)$ for each layer.

The output of PIN stage is passed to *K* parallel trellis decoders. The i^{th} decoder selects the maximum likelihood sequence that minimizes the decision metric:

$$\sum_{t=1}^{L} \left\| \tilde{\mathbf{y}}_{i,PIN}^t - \tilde{\mathbf{H}}_i \mathbf{q}_i^t \right\|^2 \tag{3.44}$$

Let $\tilde{\mathbf{x}}_i^t$ be the selected sequence by decoder *i* at time *t*. Define the matrix Ω_i by:

$$\Omega_i = \mathbf{H} - \begin{bmatrix} \mathbf{0} & \cdots & \mathbf{H}_i & \cdots & \mathbf{0} \end{bmatrix} \tag{3.45}$$

$$= \begin{bmatrix} \mathbf{H}_1 & \cdots & \mathbf{0} & \cdots & \mathbf{H}_K \end{bmatrix} \tag{3.46}$$

For G_i, the decoder cancels interfering groups as:

$$\mathbf{y}_{i,PIC}^{t} = \mathbf{y}^{t} - \Omega_i \tilde{\mathbf{x}}^{t} \tag{3.47}$$

where PIC denotes parallel interference cancellation stage,

$$= \mathbf{H}\mathbf{x}^{t} + \boldsymbol{\eta}^{t} - \Omega_i \tilde{\mathbf{x}}^{t} \tag{3.48}$$

$$= [\mathbf{H}_1 \quad \cdots \quad \mathbf{H}_i \quad \cdots \quad \mathbf{H}_K] \cdot \begin{bmatrix} \mathbf{x}_1^t \\ \vdots \\ \mathbf{x}_i^t \\ \vdots \\ \mathbf{x}_K^t \end{bmatrix} - [\mathbf{H}_1 \quad \cdots \quad \mathbf{0} \quad \cdots \quad \mathbf{H}_K] \cdot \begin{bmatrix} \tilde{\mathbf{x}}_1^t \\ \vdots \\ \tilde{\mathbf{x}}_i^t \\ \vdots \\ \tilde{\mathbf{x}}_K^t \end{bmatrix} + \boldsymbol{\eta}^{t} \tag{3.49}$$

$$= \mathbf{H}_1 \left[\mathbf{x}_1^t - \tilde{\mathbf{x}}_1^t \right] + \cdots + \mathbf{H}_i \mathbf{x}_i^t + \cdots + \mathbf{H}_K \left[\mathbf{x}_K^t - \tilde{\mathbf{x}}_K^t \right] + \boldsymbol{\eta}^{t} \tag{3.50}$$

If $\mathbf{x}_j^t = \tilde{\mathbf{x}}_j^t; \quad \{j \neq i\}$, then perfect cancellation occurs. However, decoding errors can't be avoided and they will limit the performance of the parallel algorithm.

Assuming perfect cancellation, the resulting received vector for G_i is:

$$\mathbf{y}_{i,PIC}^{t} = \mathbf{H}_i \mathbf{x}_i^t + \boldsymbol{\eta}^{t} \tag{3.51}$$

and it is decoded by the i^{th} STTC decoder. Since $\mathbf{H}_i \in \mathbb{C}^{M_R \times N_G}$, G_i benefits from full receive antenna diversity. The parallel interference cancellation and decoding is repeated iteratively until diminishing returns are observed.

3.4.3 Performance Evaluation via Simulation

To evaluate the performance of GINC receivers, we use QPSK STTC as in the previous section. Two layers transmit 4 bps/Hz by two encoders each has two antennas. However, the number of receive antennas must be grater than or equal to three. Thus, the performance of GINC is evaluated over 4×4 quasi-static Rayleigh fading MIMO channels.

Figure 3.6 shows the BER performance of SGINC. The first layer benefits from a diversity order of 2×2 while the second layer should take advantage of 2×4 diversity order after serially canceling the contribution of the first layer from the received vector. However, due to error propagation, this diversity order is not achieved as can be seen from Figure 3.6. By comparing the slope of the BER plot of the second layer with the plot of perfect cancellation case, we see the huge degradation in performance due to error propagation. The performance gain of the second layer is better than the first by 2dB. However, system performance lies between the performances of the two layers. In order to reduce the effect of error propagation and improve the overall system performance, we proposed PGINC. The performance of this iterative parallel receiver is shown in Figure 3.7. With no iterations, the receiver performs PIN followed by a trellis decoder for each layer. At this stage, each layer has a 2×2 diversity order. However, after PIC, each layer should have a diversity order of 2×4. However, error propagation limits the diversity gain. The iterative processing improved the system by 2dB. The performance with perfect cancellation shows the huge effect of errors on the diversity of PGINC.

In order to estimate the loss in performance due to the reduction in complexity, we compare the joint detection algorithms with GINC over 4×4 MIMO quasi-static Rayleigh fading channels. The result is shown in Figure 3.8. Compared to the optimum joint detection, PGINC receiver loses around 4.5dB and SGINC loses 6.6dB.

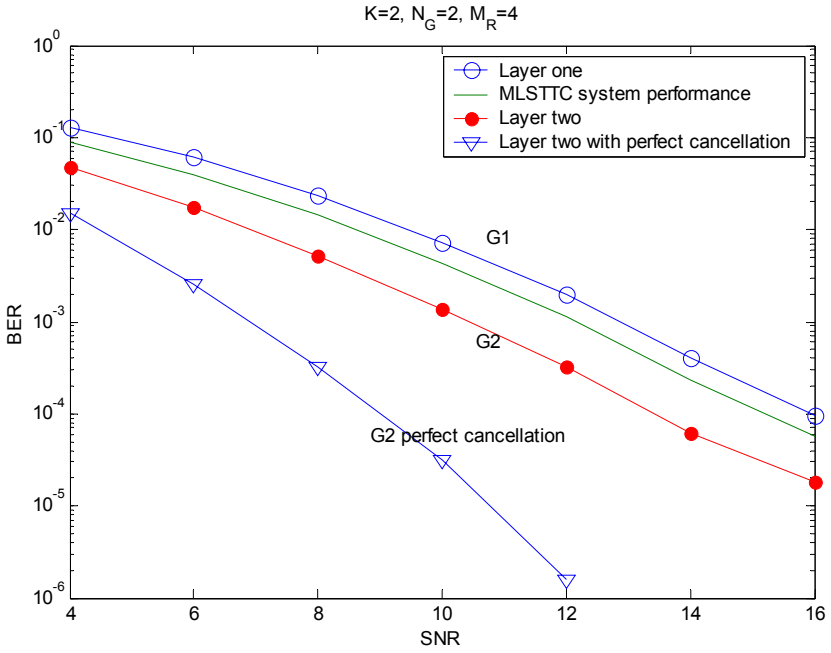

Figure 3.6: Performance of SGINC for 4 bps/Hz MLSTTC with two layers over 4x4 MIMO channels.

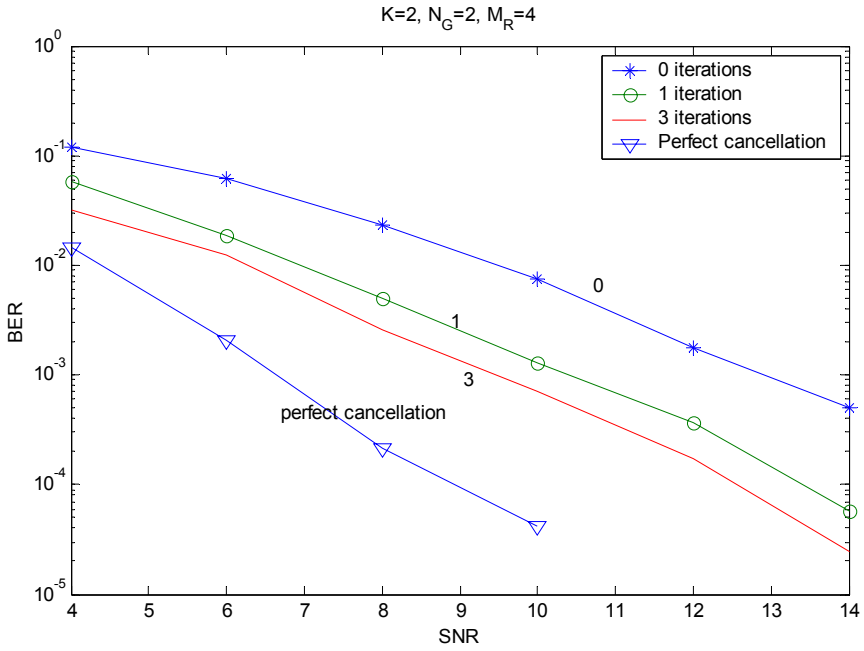

Figure 3.7: Performance of PGINC for 4 bps/Hz MLSTTC with two layers over 4x4 MIMO channels.

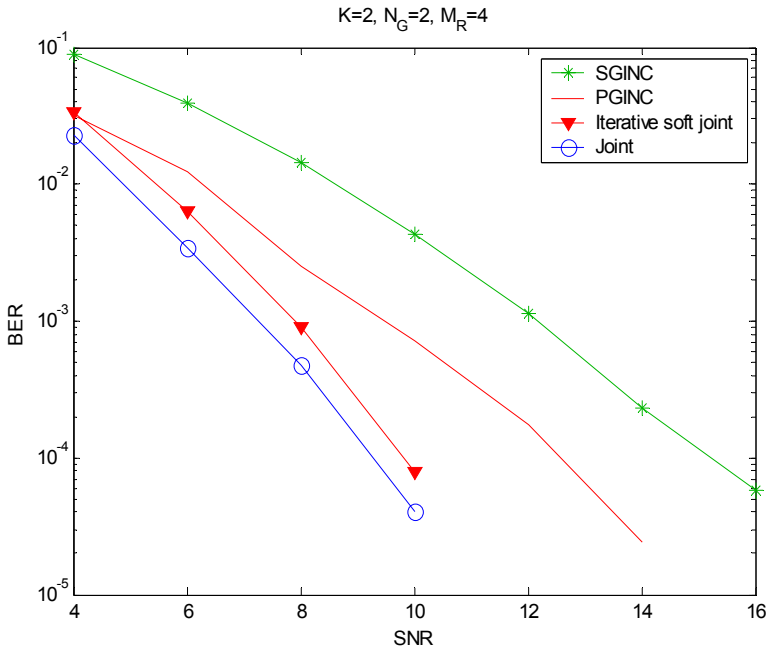

Figure 3.8: Performance comparison of MLSTTC at 4 bps/Hz over 4x4 MIMO channels

3.5 Iterative Spatial Sequence Estimator

A novel spatial sequence estimator (SSE) for V-BLAST is proposed by Maruf in [Moh04]. The algorithm combines group interference nulling and joint detection. It has the flexibility to tradeoff complexity with receive diversity and it doesn't suffer from error propagation. Also, it can work with a number of receive antennas that is smaller than what the V-BLAST algorithm requires. By applying reduced state sequence estimation, complexity can be further reduced with little performance degradation.

We saw in the pervious section the effect of error propagation, which is a result of cancellation, on the achieved diversity. To avoid cancellation and keep the advantages of joint detection, we apply SSE with soft-input soft-output (SISO) maximum a posteriori (MAP) algorithm in the detection stage for MLSTTC. It is an iterative algorithm that shares soft

information with the soft decoding stage. MAP-SSE replaces the MAP detector stage in the soft iterative joint detector in section 3.3. The block diagram for two layers is shown in Figure 3.9. Before explaining the algorithm, we state its main advantages. First, it provides the receiver with the flexibility of trading off complexity with receive diversity and hence the performance. Another advantage is that it doesn't suffer from error propagation. Furthermore, unlike GINC, it can be applied even when the number of receive antennas is smaller than the number of transmit antenna. Also, the trellis description of SSE is a tail-biting trellis. So by employing iterative detection within the estimator, further performance improvements are possible.

In this algorithm, a trellis over space is built for different groups of transmit antennas. The grouping of transmit antennas doesn't have to coincide with the layers of the space time encoder. Actually it is independent of the encoder. The trellis formulation is explained as follows. Let's consider a group of L transmit antennas with $L \le M_T$. The state at the k-th stage, σ_k, describes all possible values taken on by $\mu = L-1$ transmit antennas. Drawing an analogy to an intersymbol interference (ISI) channel, μ corresponds to the memory of the channel while L is the length of the channel. Since the antenna grouping is independent of the encoder, we drop the sub-encoder index *i* and the time index for simplicity. Thus, the transmitted vector from all antennas is $\mathbf{x} = \left([s[1], s[2], \ldots, s[M_T]\right)^T$, where $s[n]$ is the transmitted symbol from antenna *n*. The first stage of the trellis may be initialized as

$$\sigma_1 \triangleq \left(s[\mu], \ldots, s[2], s[1]\right), \quad 0 < \mu < M_T \tag{3.52}$$

The subsequent stages can be derived according to

$$\sigma_{k+1} \triangleq \left(s[t], \sigma_k[1:\mu-1]\right), \quad 1 \le k < M_T \tag{3.53}$$

where

$$t = \mathrm{mod}(\mu + k - 1, M_T + 1) + \left\lfloor (\mu + k - 1) / (M_T + 1) \right\rfloor \tag{3.54}$$

Thus, the number of states at each stage is $|Z|^{L-1}$, where $|Z|$ is the cardinality of the signal set. For successive stages, transmit antennas are grouped in such a way that there is a valid transition between states. Like in any other trellis, for a valid transition from state σ_k to σ_{k+1}, the first $\mu-1$ elements of state σ_k should match the last $\mu-1$ elements of state σ_{k+1}. This is ensured by (3.53). An example trellis is depicted in Figure 3.10. Note that the trellis starts and terminates at the same state description, i.e. the trellis wraps around upon itself. This type of trellis is called *tail-biting* trellis.

Once the trellis is formulated, the received signal component corresponding to each stage is constructed by employing group interference nulling (GIN) technique. It maintains the desired group of signals while suppresses the effect of interfering signals. At any stage of the trellis, all the transmitting antennas except those present in the group are nulled out.

3.5.1 Simulation Result

To evaluate the performance of the SSE algorithm, a simulation study is done for two layered STTC. Each encoder uses the 8-states QPSK STTC with rank two and two transmit antennas. Thus, the transmit diversity of the system is two and the spectral efficiency is 4 bps/Hz. However, the receive diversity depends on the decoding algorithm. Figure 3.11 shows the performance of the system with MAP-SSE with different receive diversity order (RxDiv). Nulling two layers results in RxDiv=2 while the number of states in the SSE trellis is four. Furthermore, nulling one layer greatly improves the performance since RxDiv=3 but the number of states increases to 16, which is still considered low. Since MAP-SSE does not have known states for initialization and termination, most of the errors occur at the trellis edges. By

exploiting the tail-biting feature of the trellis, the forward and backward variables in MAP-SSE are updated using iteration. We call this algorithm an iterative spatial sequence estimator (ISSE). Figure 3.12 shows that 0.5 to 1 dB gain is achieved by ISSE over SSE after one iteration.

The result of comparing SSE performance with the other MLSTTC decoders is shown in Figure 3.13. The result shows that SSE outperforms the GINC algorithms. That is because the SSE algorithm eliminates the error propagation problem. For instance, PGINC should theoretically provide full receive diversity (RxDiv=4). However, due to error propagation, it never achieves that. On the other hand, ISSE gained around 2.5dB at RxDiv=3. Furthermore, the performance of SSE is lower bounded by the joint detection algorithms which correspond to nulling zero layers and providing full receive diversity.

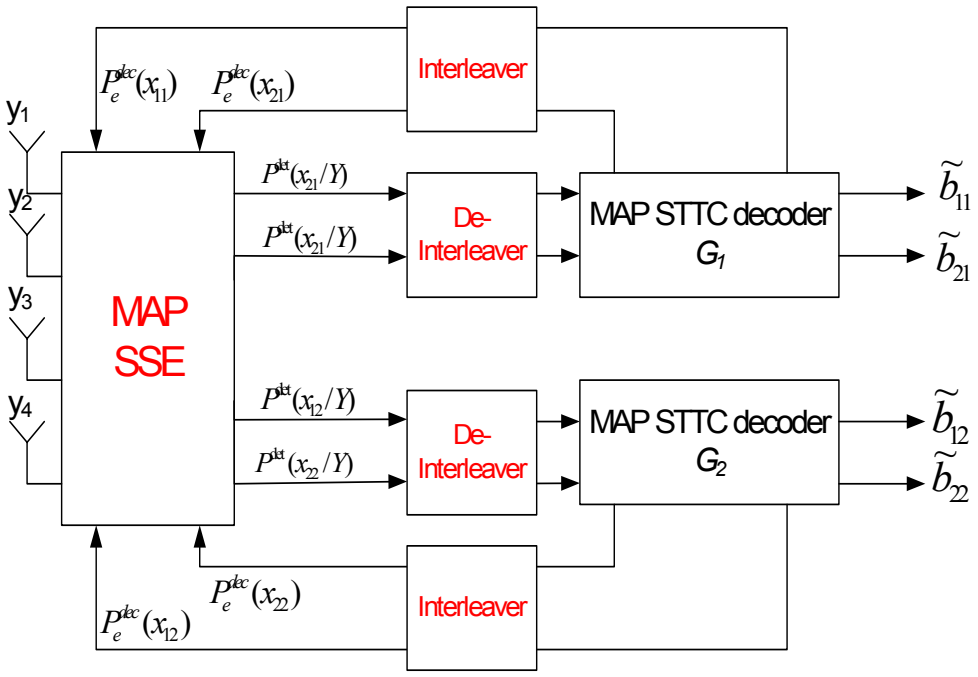

Figure 3.9: Block diagram of iterative soft SSE receiver for two layered STTC systems.

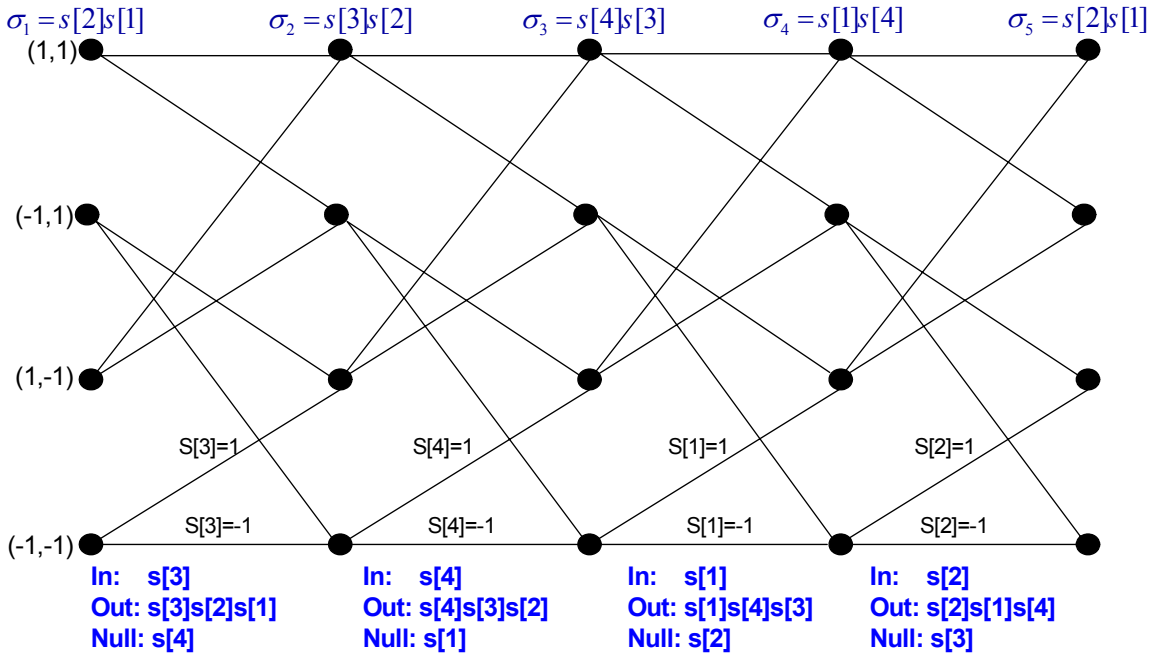

Figure 3.10: SSE trellis diagram for BPSK, M_T=4, L=3

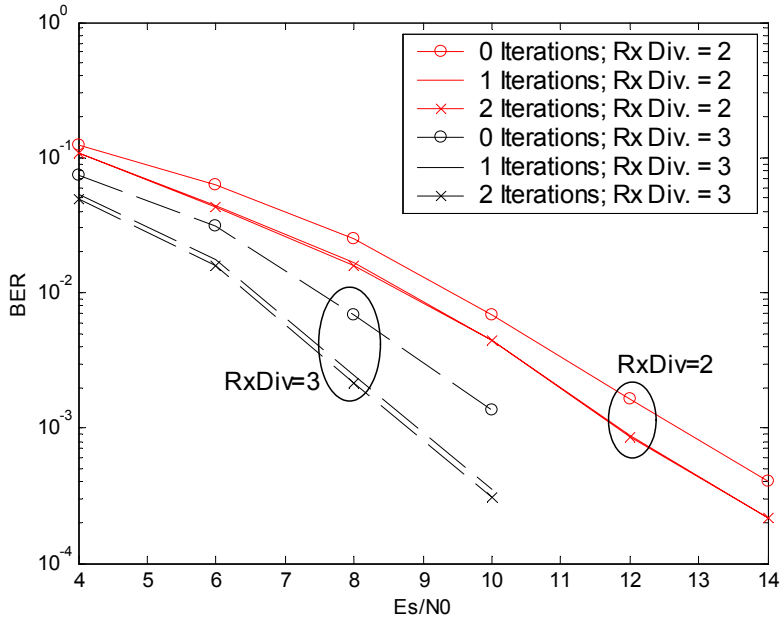

Figure 3.11: Two layered STTC BER performance with iterative soft SSE detection over 4x4 MIMO channels

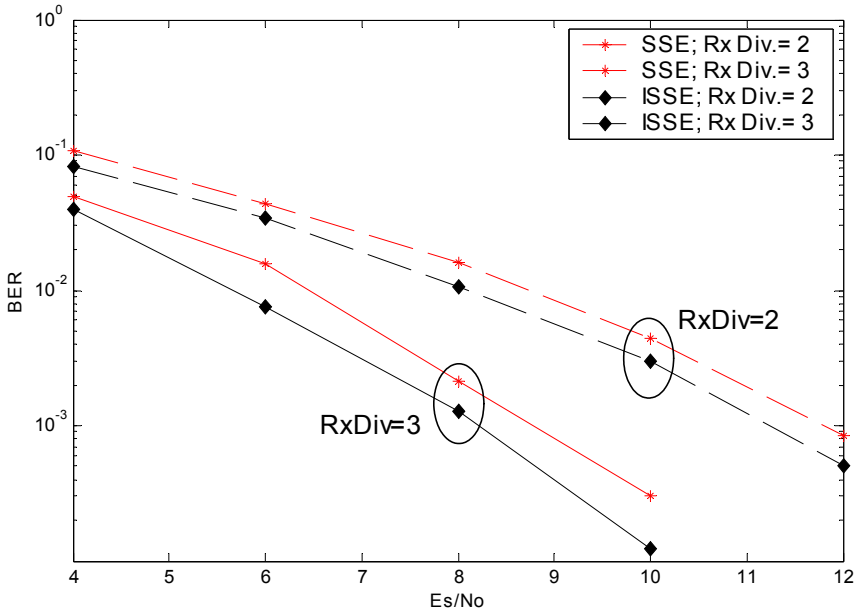

Figure 3.12: Performance comparison of two layered STTC systems with SSE and ISSE detection.

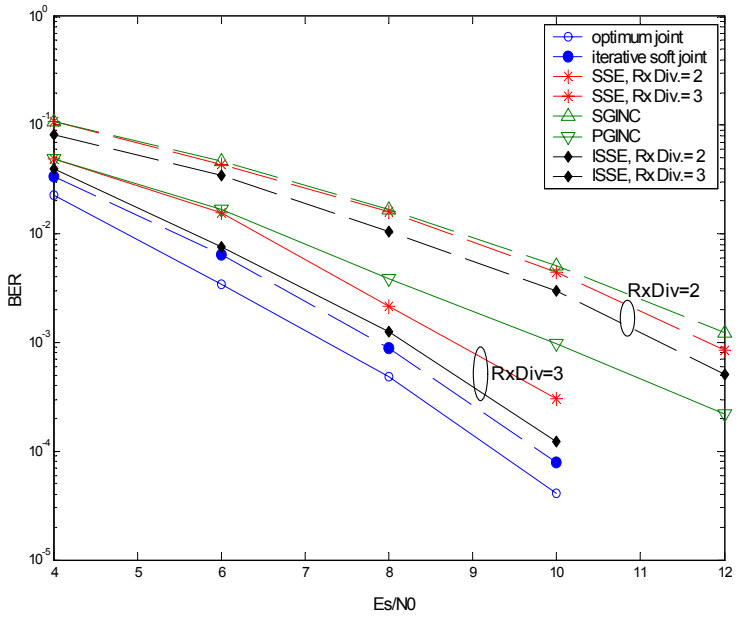

Figure 3.13: Performance comparison of decoding algorithms for two layered STTC systems over 4x4 MIMO channels.

3.6 Chapter Summary

This chapter studies decoding algorithms for multi-layered space time trellis codes. These systems combine spatial multiplexing and STTC to provide transmit diversity and coding gains at each layer without any bandwidth expansion. Three classes of MLSTTC decoders are proposed and evaluated in this chapter. The first uses joint decoding, the second implements more practical receivers based on group interference nulling and cancellation, the third is based on spatial sequence estimation.

Optimum joint detection and suboptimum iterative soft joint detection are studied. They perform the best since they provide full receive diversity for each layer but they suffer from exponential complexity. The second class consists of SGINC and PGINC receivers. Both receivers are implemented in an iterative architecture but the difference is that SGINC iterates in order to decode each layer serially. On the other hand, PGINC decodes all layers at the same time and it iterates to improve the performance of the system. These receivers are less complex than the joint receiver. However, the joint algorithms perform much better. Also, GINC algorithms suffer from diversity reduction caused by nulling and error propagation caused by cancellation. In order to a void cancellation, a soft-input soft-output spatial sequence estimator is proposed in this chapter. The spatial sequence estimator algorithm has the flexibility to tradeoff complexity with receive diversity and it doesn't suffer from error propagation. The algorithm outperforms group interference nulling and cancellation algorithms. However, it still has exponential complexity, in terms of number of states, as a function of group size.

Table 3.1 compares between these receivers in term of complexity per layer, diversity advantage and number of receive antennas required by the receiver. Comparison of the multi-

layered space time coded systems to other open loop MIMO systems is done in Chapter 4 in order to show the advantage of the multi-layered system and its preferred region of operation.

Table 3.1: Comparison of MLSTTC detection algorithms

	Optimum joint	Soft iterative joint	SGINC	PGINC	SSE
Complexity	Exponential per layer	detection stage is exponential and decoding stage is linear per layer	nulling stage is cubic and decoding stage is linear per layer	nulling stage is cubic and decoding stage is linear per layer	detection stage is exponential per group and decoding stage is linear per layer
Diversity order	$N_G \times M_R$	$N_G \times M_R$	For G_i: $N_G \times (i \cdot N_G + M_R - M_T)$	For G_i: $N_G \times M_R$	$N_G \times (M_R - M_T + L)$ where L is the group size
Number of receive Antennas (M)	$M_R \geq 1$	$M_R \geq 1$	If G_i is decoded first $M_R \geq M_T - N_G + 1$	$M_R \geq M_T - N_G + 1$	$M_R \geq 1$

Chapter 4
Outage Capacity of Multi-Layered Space Time Block Coded Systems

In this chapter, we examine the capacity of high data rate open loop MIMO architectures. The first part of the study shows how the multi-layered space time block code (MLSTBC) compares to other MIMO systems, such as V-BLAST and STBC. We focus on the information capacity comparison in order to evaluate the optimal performance of the systems. We show the tradeoffs of these systems and what the advantages of MLSTBC are. The results show that when the number of transmit and receive antennas are equal, MLSTBC is more power efficient than V-BLAST, since it provides more diversity. Furthermore, at low SNR and low outage probabilities, MLSTBC is more spectrally efficient. Thus, it is more suitable for low power wireless data applications.

The second part of this chapter evaluates and compares the information capacity of different detection algorithms for MLSTBC. We compare serial, parallel and joint detection

algorithms. The capacity expression and evaluation for MLSTBC are a unique contribution of this work. This study gives useful insight into the optimal performance of these algorithms and into the spatial multiplexing-diversity tradeoffs of these systems.

Finally, we implement and evaluate the performance of a MLSTBC-OFDM system. This system is robust against frequency selective channels. These type of channels occur at high bandwidth and at high data rates which result in inter-symbol interference that limits the performance of the communication system. This motivates the use of OFDM which transforms the frequency selective channels into parallel flat fading channels.

4.1 Introduction

Multiple-input multiple-output (MIMO) communication systems can offer high data rates through spatial multiplexing and they can improve the link quality through diversity. V-BLAST [Wol98] is a spatial multiplexing scheme that transmits independent layers of information through a MIMO channel. However, it has poor energy performance and doesn't fully exploit the available diversity. On the other hand, space time block coding [Tar99a] provides full transmit and receive diversity but with a maximum code rate of one which is achieved at two transmit antennas.

Combining V-BLAST and STBC results in a layered architecture with transmit diversity in each layer. This is called a multi-layered space time block code (MLSTBC). The idea of this scheme is to demultiplex a single user's data into parallel layers of information. Then, each layer is encoded by STBC. Each code is called a group, because the total number of transmit antennas is divided into groups and each group belongs to one STBC. This architecture was first

considered in [Tar99] but with space time trellis codes (STTC) as the component codes. In a multi-user environment, a multi-user STBC system with minimum mean-squared error (MMSE) detection was studied in [Nag98]. One advantage of using STBC over STTC is that the orthogonal structure and the short code length can be exploited at the receiver to reduce the minimum required number of receive antennas. For MLSTTC, the number of receive antennas should be at least equal to the total number of transmit antennas. However, for MLSTBC, the number of receive antennas is equal to the number of layers.

In this paper, we evaluate and compare the capacities of serial, parallel and joint detection algorithms for MLSTBC. In addition, we compare the serial algorithm with other open loop MIMO transmit techniques, such as V-BLAST, STBC and optimal MIMO, with the same number of transmit and receive antennas. The results of this work show a spatial multiplexing-receive diversity tradeoff as a result of the nulling operation in the detection algorithms. Adding more layers doesn't necessary increase the capacity unless the nulling operation is avoided or by operating at very high SNR. In addition, this work shows that adding a STBC layer on V-BLAST improves the capacity of the MIMO system at low SNR and at low outage probabilities.

4.2 MLSTBC System Model

The MLSTBC transmitter consists of K parallel space time block encoders which are independent and synchronized (Figure 4.1). Each encoder transmits through N_G antennas and the receiver has M_R receive antennas. The total number of transmit antennas is $M_T = K \cdot N_G$. The MIMO channel is assumed to be an independent Rayleigh flat fading MIMO channel where each

coefficient is a complex Gaussian random variable with mean zero and variance of 0.5 per dimension. The received matrix over T time slots, where T is the STBC length, is given by:

$$\begin{aligned}\mathbf{Y} &= \mathbf{HS} + \mathbf{V} \\ &= \begin{bmatrix}\mathbf{H}_1 & \mathbf{H}_2 & \cdots & \mathbf{H}_K\end{bmatrix}\begin{bmatrix}\mathbf{S}_1 \\ \mathbf{S}_2 \\ \vdots \\ \mathbf{S}_K\end{bmatrix} + \mathbf{V}\end{aligned} \tag{4.1}$$

where $\mathbf{H}_i$ is an $M_R \times N_G$ MIMO channel matrix of the i^{th} group and $\mathbf{S}_i$ is the $N_G \times T$ STBC of the i^{th} group. Also, $\mathbf{V}$ is the AWGN matrix over T time slots. Due to the short code length, the receiver rearranges the received matrix to a vector, as done in (2.39) for single STBC. After doing that, we get a discrete MIMO model similar to V-BLAST:

$$\begin{aligned}\mathbf{y} &= \hat{\mathbf{H}}\mathbf{x} + \boldsymbol{\eta} \\ &= \begin{bmatrix}\hat{\mathbf{H}}_1 & \hat{\mathbf{H}}_2 & \cdots & \hat{\mathbf{H}}_K\end{bmatrix}\begin{bmatrix}\mathbf{x}_1 \\ \mathbf{x}_2 \\ \vdots \\ \mathbf{x}_K\end{bmatrix} + \boldsymbol{\eta}\end{aligned} \tag{4.2}$$

where $\mathbf{y}$ is the $M_R \cdot T \times 1$ received vector, $\hat{\mathbf{H}}_i$ is the $M_R \cdot T \times N_G$ orthogonal channels matrix for the i^{th} group, $\mathbf{x}_i$ is the $N_G \times 1$ transmitted symbols from the i^{th} group, and $\boldsymbol{\eta}$ is the $M_R \cdot T \times 1$ AWGN vector.

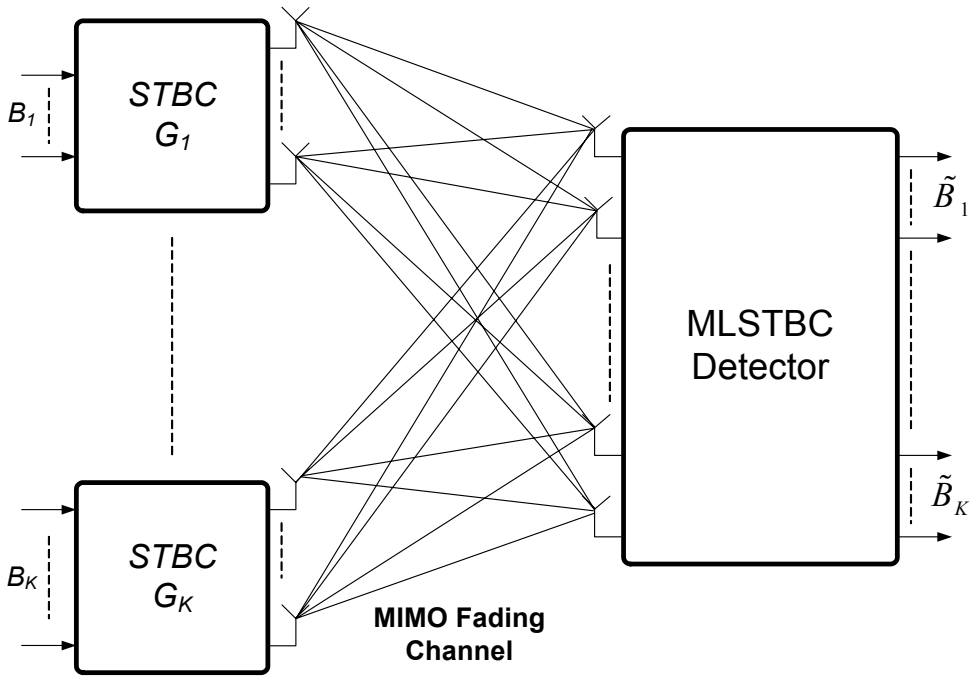

Figure 4.1: MLSTBC black diagram

4.3 Capacity Formulas

The instantaneous capacity of V-BLAST with K layers and with zero forcing interference nulling (ZF) and serial cancellation is given by [Pap02]:

$$C_{VBLAST}^{ZF} = K \cdot \min_{i=1,2,\ldots,K} \left\{ \log_2 \left(1 + \frac{\rho}{K \left\| \mathrm{W}_{ZF,i} \right\|_F^2} \right) \right\} \tag{4.3}$$

where $\mathrm{W}_{\mathrm{ZF},i}$ is the ZF projection vector of the i^{th} layer, ρ is the SNR per receive antenna, and $\left\| (\cdot) \right\|_F^2$ is the squared Frobenius norm.

Furthermore, the instantaneous capacity of an orthogonal STBC of rate r_c and N_G transmit antennas is [San00]:

$$C_{STBC} = r_c \log_2\left(1+\frac{\rho}{N_G}\|\mathbf{H}\|_F^2\right) \tag{4.4}$$

In a MLSTBC system, a serial group interference nulling and cancellation (SGINC) algorithm detects each group separately after canceling previously detected groups and nulling interfering groups. Based on an ordering criterion, assume that the first detected group is the i^{th} group. Then, the algorithm calculates the orthonormal bases of the null space of $\mathcal{H}_i$, where:

$$\mathcal{H}_i = \left[\hat{\mathbf{H}}_1 \quad \cdots \quad \hat{\mathbf{H}}_{i-1} \quad \hat{\mathbf{H}}_{i+1} \quad \cdots \quad \hat{\mathbf{H}}_K\right] \tag{4.5}$$

Denote the orthonormal bases of $\mathcal{H}_i$ by $\mathcal{N}_i$, the received signal for the i^{th} group after nulling is:

$$\tilde{\mathbf{y}}_i = \mathcal{N}_i\mathbf{y} = \tilde{\mathbf{H}}_i\mathbf{x}_i + \tilde{\boldsymbol{\eta}}_i \tag{4.6}$$

where $\tilde{\mathbf{H}}_i$ is the resultant channel matrix after nulling. The post-nulling AWGN vector is white due to the unitary transformation [Tar99]. After that, the contribution of the i^{th} group is subtracted from (4.2) and the process is repeated serially for each group. Different ordering criteria are evaluated and compared next section. The best ordering is based on the Frobenius norm of $\tilde{\mathbf{H}}_i$. The layer with maximum $\|\tilde{\mathbf{H}}_i\|_F^2$ is detected first.

Since MLSTBC is a single user system and the transmitter is not aware of the channel and all groups transmit at the same rate, an outage will occur if an outage happens in any one layer, i.e. “the weakest layer”. Therefore, the instantaneous capacity of a K layered STBC system is:

$$C_{MLSTBC}^{GNIC} = K \cdot \min_{i=1,2,\ldots,K} \left\{ r_c \log_2 \left(1 + \frac{\rho}{K \cdot N_G} \left(\frac{\left\| \tilde{\mathbf{H}}_i \right\|_F^2}{T} \right) \right) \right\} \tag{4.7}$$

where T is the STBC length. The Frobenius norm of $\tilde{\mathbf{H}}_i$ is divided by T because the dimension of the channel matrix has been increased T times after rearranging the original channel matrix as indicated in (4.2). The above formula is also valid for PGINC which was described in Chapter 3 for MLSTTC.

4.3.1 Joint Detection

A joint detector detects all layers jointly using a maximum likelihood (ML) detector. A practical ML detector that has a cubic complexity at high SNR is a sphere decoder (SD). The instantaneous capacity of a joint detector for MLSTBC is:

$$C_{MLSTBC}^{Joint} = \frac{1}{T} \log \left(\det \left[\mathbf{I}_{K \cdot N_G} + \frac{\rho}{K \cdot N_G} \hat{\mathbf{H}}^H \hat{\mathbf{H}} \right] \right) \tag{4.8}$$

where $\hat{\mathbf{H}}$ is defined in (4.2). The capacity is divided by T since the joint detector operates over T symbol periods.

4.4 Comparison of MLSTBC and Open Loop MIMO Systems

This section compares the capacities of the detection algorithms of MLSTBC, V-BLAST and STBC. In addition, the optimal MIMO capacity is included as a reference. We want to show how the MLSTBC compares to these systems and what the advantages of MLSTBC are.

Throughout this study, each group in the MLSTBC system uses Alamouti code [Ala98] with two transmit antennas. The capacity of the different systems is estimated by generating

random complex Gaussian channel realizations from which the instantaneous capacity is calculated and then the capacity probability distribution function (pdf) is approximated.

One main difference between MLSTC and V-BLAST at the same number of transmit-receive antennas is that MLSTBC has more spatial diversity than V-BLAST while V-BLAST has more layers. For example, with a 4×4 MIMO system, MLSTBC has two layers and each layer has a transmit diversity of two. At the receiver, the first detected layer has a receive diversity of three. This is because the detector needs one antenna to null out one interfering layer and the rest provide diversity. On the other hand, V-BLAST has four layers and no transmit diversity. In addition, the first detected layer has no receive diversity because the algorithm needs three antennas to null out three interfering layers.

Figure 4.2 plots The complementary cumulative distribution function (CCDF) of the considered MIMO schemes for 4×4 MIMO channels. The STBC is the orthogonal code of rate ¾ [Tar99a]. The results show that there is a crossover in capacity that is a function of SNR. At low SNR and at low outage probabilities, the capacity of V-BLAST is lower than both STBC and MLSTBC. The reason is that the later schemes provide more diversity which benefits the capacity at low SNR. On the other hand, at high SNR, the capacity of V-BLAST improves significantly and it is higher than MLSTBC for outage probabilities greater than 3%.

The spectral efficiencies of the 4×4 MIMO schemes are shown in Figure 4.3. It shows the tradeoffs between the MLSTBC and V-BLAST systems. First, the spectral efficiency of V-BLAST varies a lot with the outage probability, unlike MLSTBC. For example, at 10 bps/Hz, V-BLAST needs around 9 dB to sustain this rate when going from 10% to 1% outage. On the other hand, MLSTBC needs only 2 dB. This is a result of lack of diversity of V-BLAST. Furthermore, the figure shows that the spectral efficiency rate of increase of V-BLAST is faster than

MLSTBC. Its slope is parallel to the optimal MIMO at high SNR since it is a full spectral multiplexing scheme. However, at low outage probabilities, MLSTBC is more spectral efficient than V-BLAST for a wide range of SNR.

The outage probability as a function of SNR is shown in Figure 4.4 at 4 bps/Hz efficiency. The result reemphasizes the fact that MLSTBC has more diversity than V-BLAST. In the case of 4×4 MIMO channels, the first detected layer has a diversity order of 2×3 while it doesn't have any diversity in V-BLAST. Furthermore, MLSTBC is more power efficient at low and moderate SNR than STBC. That is a result of having diminishing gains with higher diversity orders. Therefore, utilizing some of the antennas for spatial multiplexing doesn't harm the performance.

Figure 4.5 shows the effect of increasing total number of transmit antennas (N) on the spectral efficiency while the number of receive antennas is fixed at eight. The capacities of MLSTBC and V-BLAST first increase when adding more layers as expected but after a certain number of layers, a reduction in capacity occurs especially when $N = 2M$ in MLSTBC and when $N = M$ in V-BLAST. This is a result of receive diversity reduction caused by the nulling operation in the detection algorithms of both systems. In other words, the capacity could be maximized by selecting the best number of layers at a given SNR. As a heuristic rule inferred from the plots, if the intended region of operation is at high SNR, set the number of layers (K) to M-1. On the other hand, if the region of operation is at low and moderate SNR, set K to be equal to $M/2$.

To sum up, MLSTBC is more power efficient than V-BLAST and it has more layers than STBC. The spectral efficiency of V-BLAST is higher at high SNR. However, at moderate and low SNR and at low outage probabilities, MLSTBC is more spectral efficient.

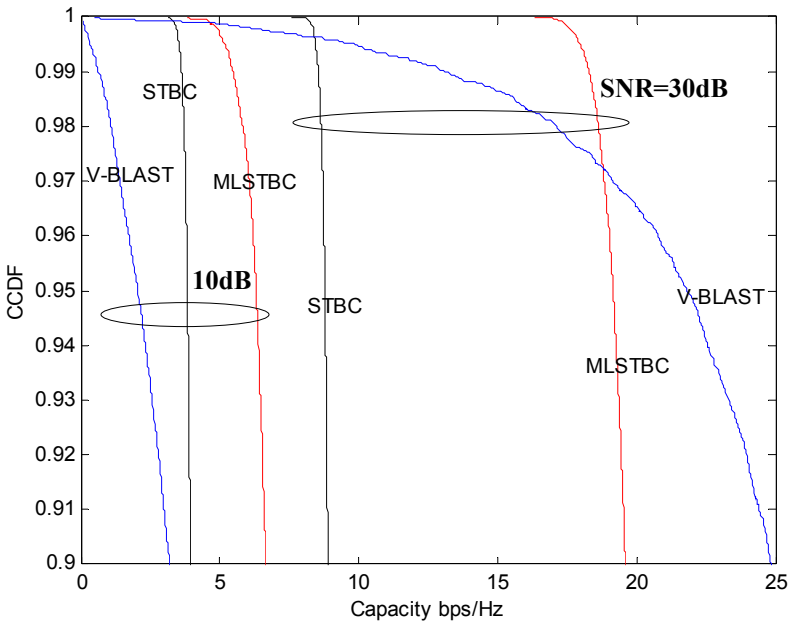

Figure 4.2: Capacity CCDF of MLSTBC , V-BLAST and the STBC at 4×4 MIMO channels

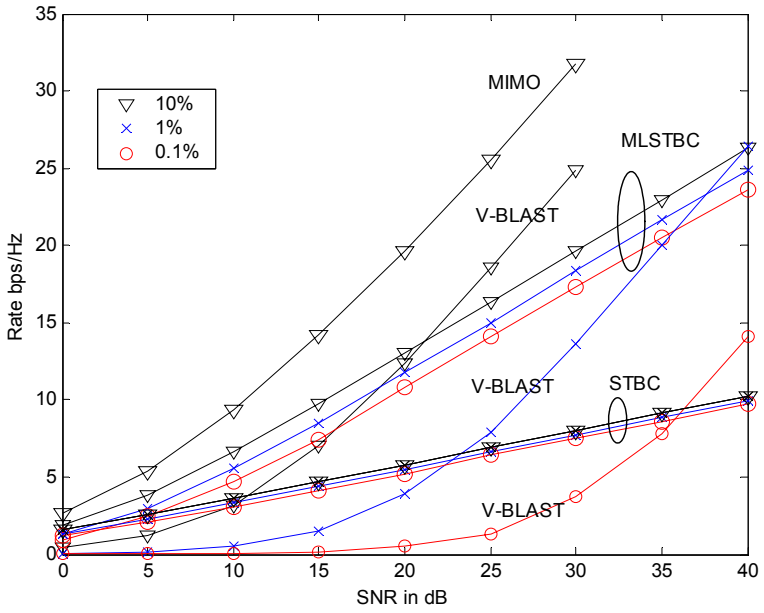

Figure 4.3: Spectral efficiency of MLSTBC, V-BLAST and STBC at 4×4 MIMO channels and at 10, 1, 0.1% outage probabilities.

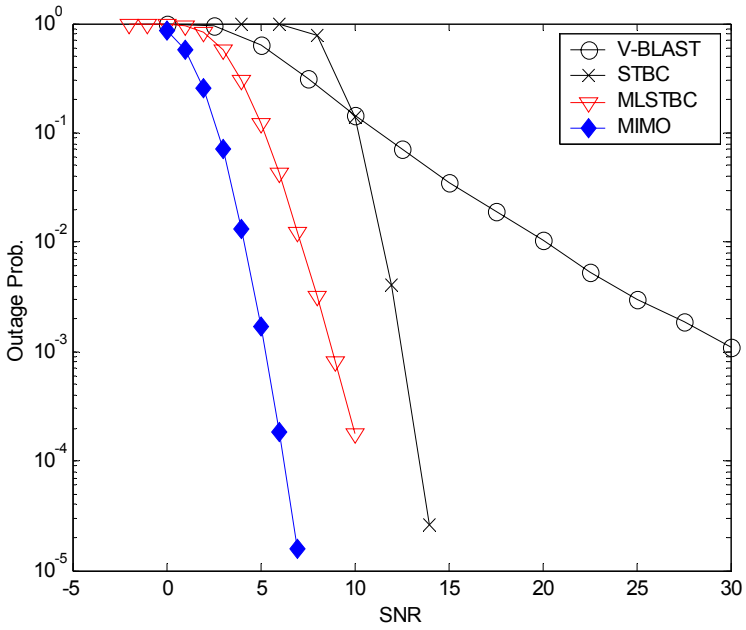

Figure 4.4: Outage probability of MLSTBC, V-BLAST and STBC at 4 bps/Hz and over 4×4 MIMO channels

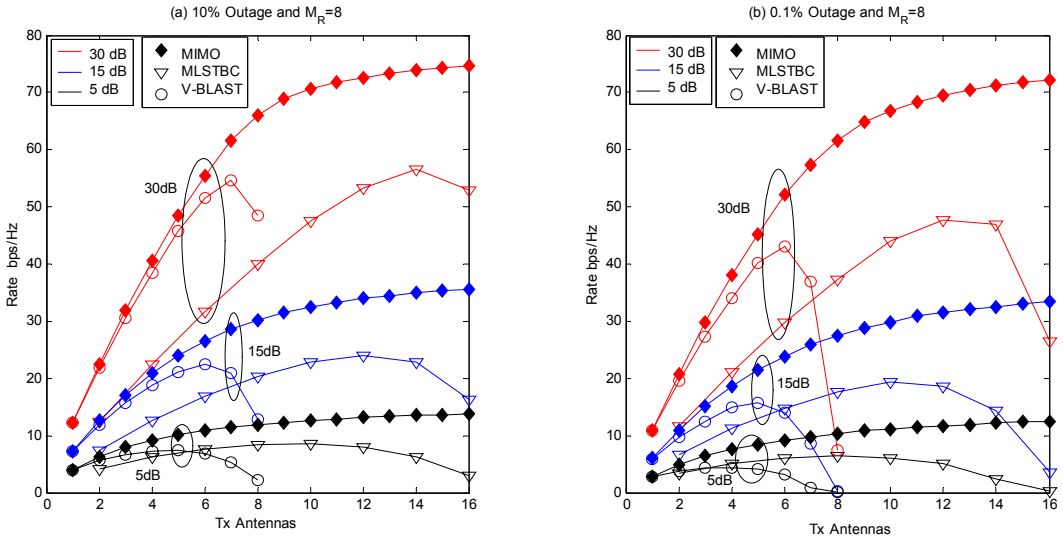

Figure 4.5: Spectral efficiency versus number of transmit antennas for MLSTBC, V-BLAST and the optimal MIMO at eight receive antennas (*M=8*).

4.5 Capacity of MLSTBC Detection Algorithms

In this section, the outage capacities of the MLSTBC detection algorithms are evaluated and compared. We consider serial

4.5.1 SGINC

The CCDF of the MLSTBC capacity for SGINC is shown in Figure 4.6. For this result, the number of receive antennas is eight and the SNR is 10dB. The results show the effect of increasing number of layers (K) while the number of receive antennas is fixed. It is interesting to note that increasing K above a certain limit reduces the capacity. In our case, the capacity starts to back off after K=4. This is a result of a receive diversity and spatial multiplexing tradeoff. When the spatial interference increases by allowing more spatial multiplexing, the nulling operation in the SGINC algorithm needs more antennas to null out the interference and that results in fewer antennas for diversity. Although the capacity in (4.7) is multiplied by K, the size of $\tilde{\mathbf{H}}_i$ for the weakest layer, which is usually the first detected layer, reduces with increasing K. In the simulated case, the receiver has eight receive antennas. It needs one antenna to null out each group. At K=4, three antennas are used to null out three interfering groups and five antennas are used for detecting and providing diversity for the first group. Thus, the diversity order for this layer is 2×5. However, at K=8, the algorithm uses seven antennas to null out seven interfering groups and one antenna is left for detecting the first group. Therefore, no receive diversity is provided in this case and the diversity order is just the transmit diversity of two.

Ordering effect

In this section, we examine the effect of ordering on the MLSTBC capacity. The result is shown in Figures 4.6 and 4.7. We considered two types of ordering. The first is to order based on

the Frobenius norm (FN) of the received channel matrices before nulling (PreFN). The FN measures the MIMO fading power and it is given by:

$$\left\|\mathbf{H}_i\right\|_F^2 = trace\left(\mathbf{H}_i \mathbf{H}_i^H\right) \tag{4.9}$$

The second method is to order based on FN of the postprocessed channel matrices. That is the resultant channel matrix after nulling and we call it (PostFN). This approach adds more processing to the receiver but it greatly improves the outage capacity of SGINC.

The simulation results show a great improvement in the capacity of the serial algorithm with ordering. This is because the capacity is dominated by the minimum capacity of each group which is usually the first detected group. Therefore, by detecting the strongest group first, we increase the capacity of the system. The best ordering technique is the PostFN ordering. In addition, the comparison in Figure 4.7 shows that the ordering gain increases with increasing number of layers.

The previous simulation is done at low SNR (10dB). In order to examine the effect of increasing number of layers at high SNR, we examine CCDF of the multi-layered system with SGINC and with PostFN at 30dB. The result is shown in Figure 4.8. The behavior still similar to low SNR case but the capacity starts to backoff after seven groups. Thus, high SNR compensates for the diversity reduction caused by nulling.

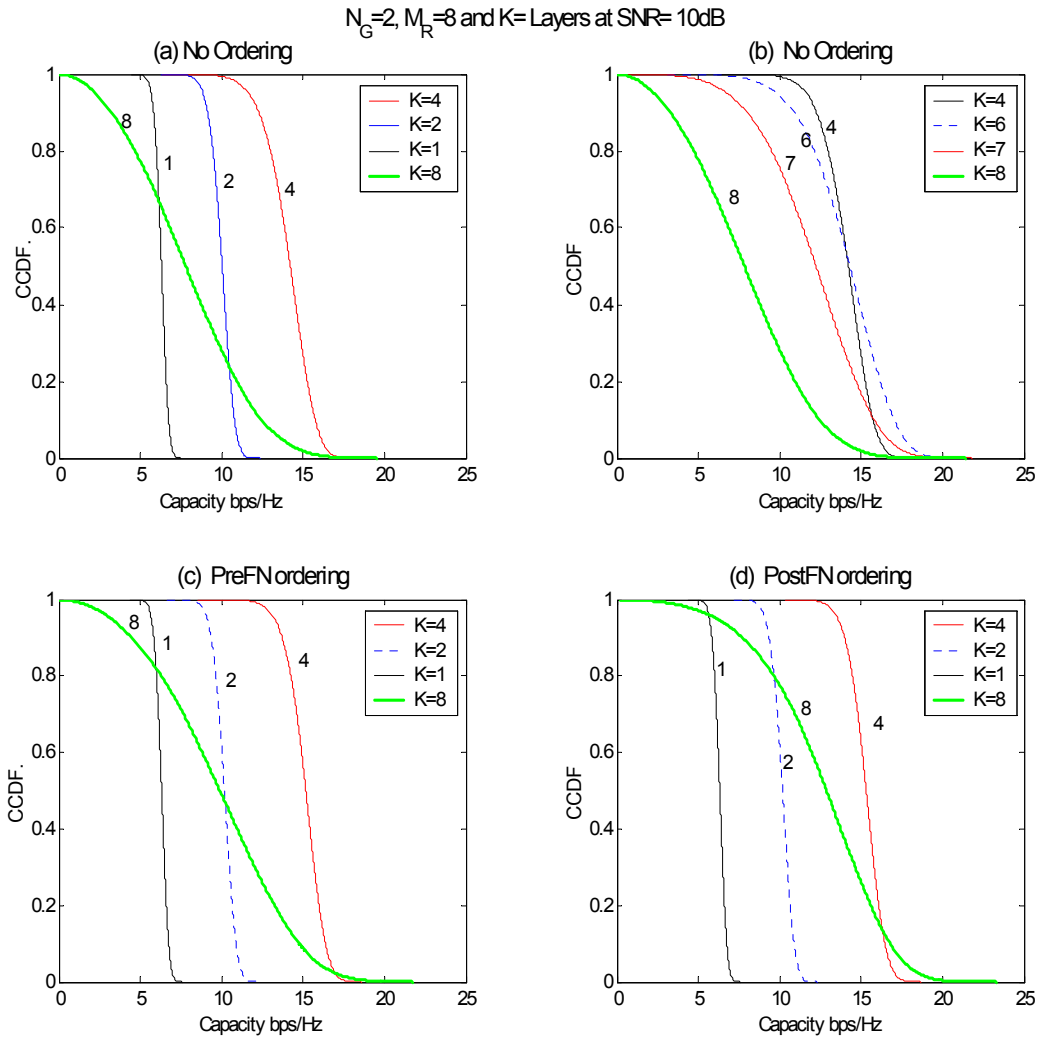

Figure 4.6: Capacity CCDF of SGINC at SNR= 10dB.

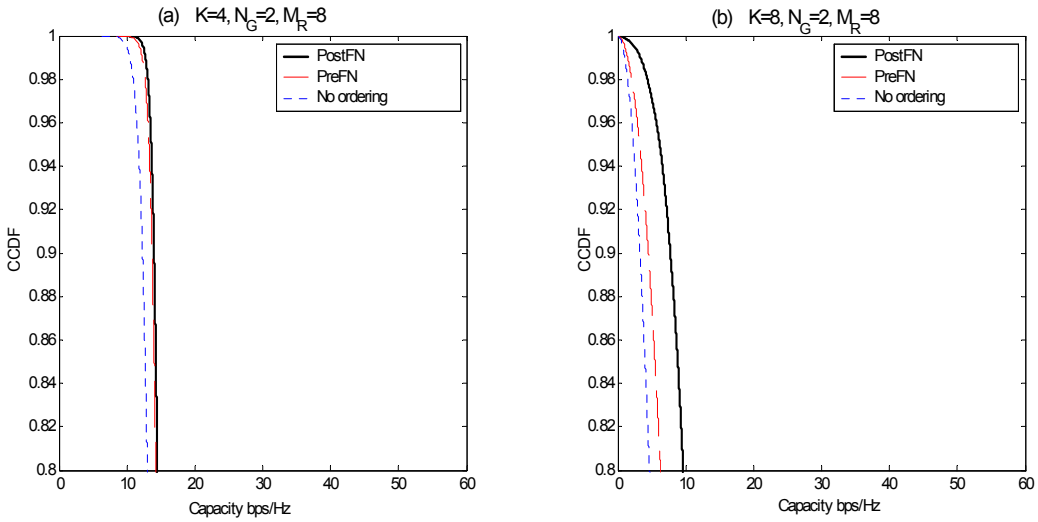

Figure 4.7: Capacity CCDF comparison between different ordering criteria at SNR=10dB.

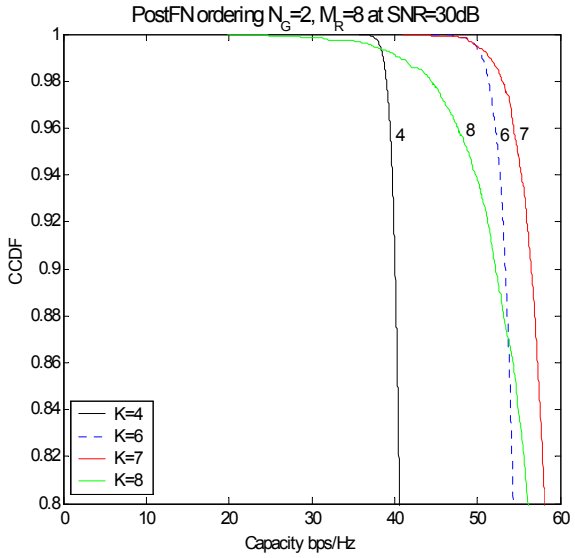

Figure 4.8: Effect of increasing number of layers on capacity CCDF at high SNR (30dB).

4.5.2 PGINC

Parallel processing is applied in this section for the detection of MLSTBC. The algorithm first gets an estimate of the transmitted symbols by a parallel interference nulling stage (PIN) which detects each group separately after nulling all other interference. After that, each group is

detected after subtracting the contribution of all interfering groups from the received signal. This stage is called parallel interference cancellation stage (PIC).

In Figure 4.9, the capacity CCDF of PGINC at eight receive antennas is shown for the two stages. PIN capacity is estimated in Figure 4.9.a. The behavior is similar to SGINC due to the diversity reduction experienced by nulling. However, parallel cancellation overcomes this loss since it provides full receive diversity for each group. Therefore, adding more layers results in more capacity and PIC eliminates the loss in capacity caused by nulling. However, this capacity gain is too optimistic for real systems since we do not consider error propagation in this study which greatly impairs the performance of the GINC algorithms.

The capacity gains obtained from PIC are shown in Figure 4.10. The gain gets higher at higher number of layers.

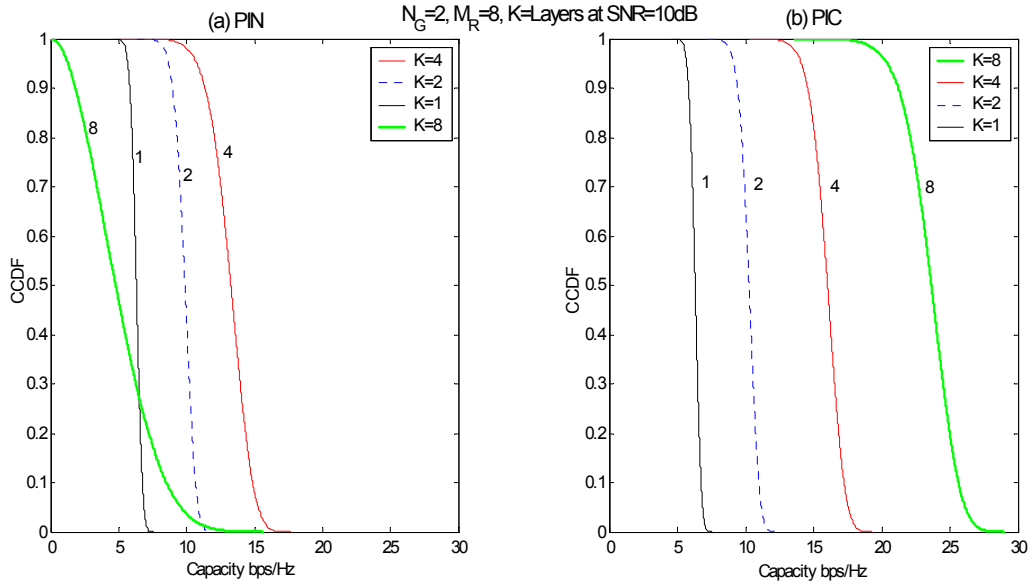

Figure 4.9: Capacity CCDF of PGINC.

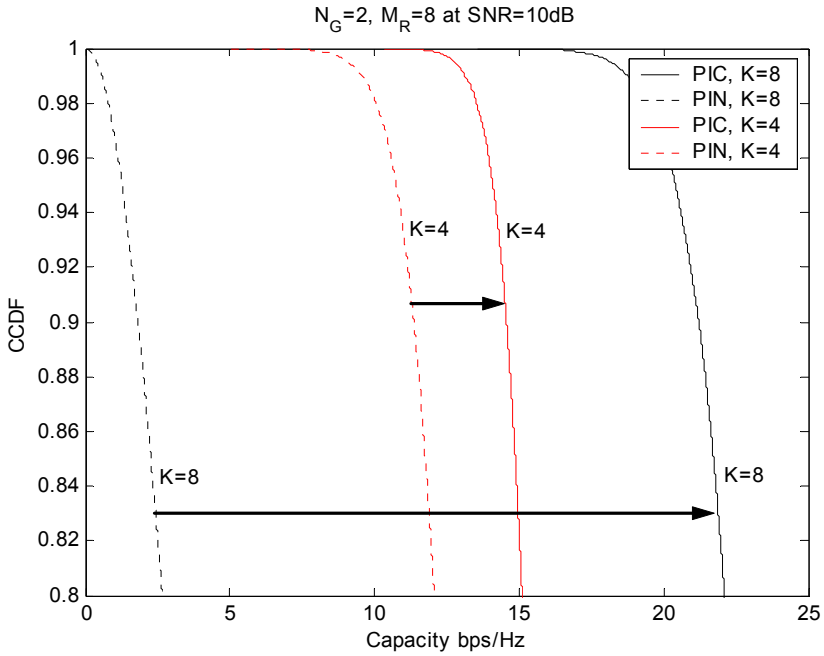

Figure 4.10: Capacity comparison of parallel nulling and parallel cancellation.

4.6 Comparison of MLSTBC detection algorithms

In this section, we compare the capacity of serial, parallel and joint detection algorithms. Also, we examine the spectral efficiency, diversity and the effect of spatial multiplexing on the rate of these algorithms.

4.6.1 CCDF Comparison

The capacity CCDF is compared and the result is shown in Figure 4.11. The joint capacity is based on equation (4.8) and it assumes a joint encoding and decoding scheme. The PGINC capacity is estimated after cancellation so it is the ideal performance assuming no error propagation. The SGINC capacity is for PostFN ordering. The result shows the superiority of PIC over SGINC especially at large number of layers. The joint detection outperform GINC

algorithms except at full multiplexing (K=8) where PIC slightly supports more capacity after 7% outage.

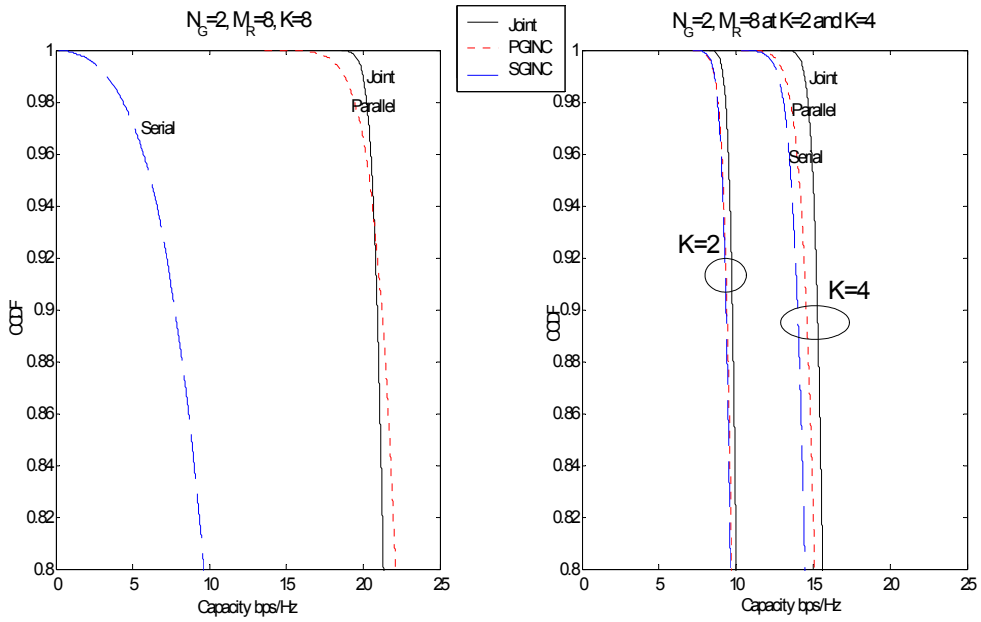

Figure 4.11: CCDF comparison of MLSTBC decoding algorithms at SNR=10dB.

4.6.2 Spectral Efficiency

The spectral efficiency of MLSTBC is investigated in this section as a function of SNR. The results in Figure 4.12 show how the rate scales with SNR for the different detection algorithms. In this simulation, the number of receive antennas is fixed at four and each group uses Alamouti code with two transmit antennas. The rate is estimated at 10% outage and the number of groups is varied from one to four.

The spectral efficiency of GINC is shown Figure 4.12.(a). The spectral efficiency increases with increasing K until K=4. At full spatial multiplexing, the spectral efficiency

experience a reduction in rate at low SNR compared to K=3. After that, it increases rapidly at high SNR.

On the other hand, the spectral efficiencies of PIC and joint detection increase with increasing number of layers. The spectral efficiencies of the parallel and the joint detection algorithms are shown in Figures 4.12.(b) and (c) and they are very close to each other but the PIC has slightly more rate at high SNR.

In Figures 4.11 and 4.12, the capacity and the spectral efficiency of PIC and joint detection are very comparable. The reason is that both PIC and joint detection have the same spatial multiplexing advantage with full receive diversity. They both don't suffer from the drawbacks of the nulling operation. However, PIC detects each layer separately without interference while the joint detector makes decisions jointly. In addition, the comparison shows the effect of having more transmit diversity. The joint detector, which has more transmit diversity, improves the capacity at low outage probability and at low SNR.

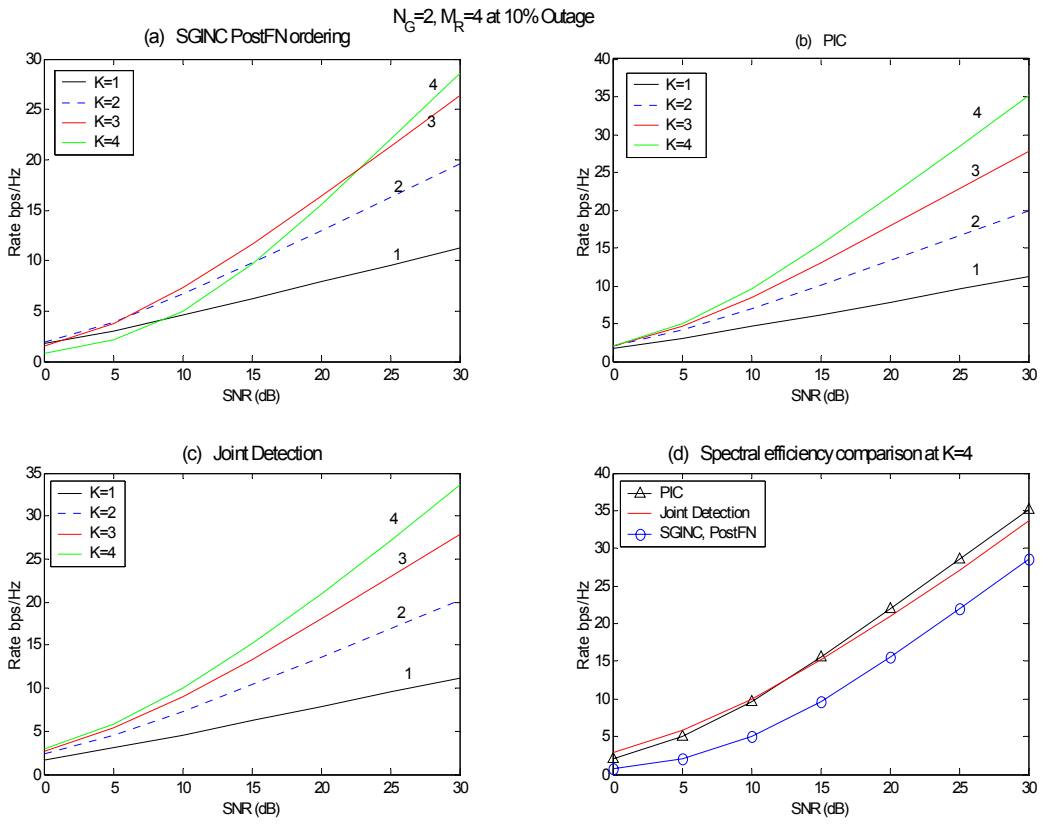

Figure 4.12: Spectral efficiency of MLSTBC at 10% outage.

4.6.3 Outage Probability

Outage probability as a function of SNR is studied in this section. This study shows the diversity advantage of the detection algorithms.

In Figure 4.13, the result is plotted for different detection algorithms at M_R=4 and N_G=2 antennas. The number of layers is varied from one to four and the outage capacity at each case is propositional to the number of layers. Assuming that each group used Alamouti code with QPSK modulation, the outage capacity will be $2K$ bps/Hz.

The outage probabilities of the serial and parallel GINC algorithms are shown in parts (a) and (b) of Figure 4.13, respectively. The diversity of SGINC deceased with increasing number of layers. That is a result of receive diversity reduction caused by nulling. On the other hand, PIC provides full receive diversity for each group. Each group benefits from 2×4 transmit-receive diversity. The shift in the plots with increasing number of groups is a result of increasing data rates which needs more SNR to maintain the same performance.

The performance of joint detection is shown in Figure 4.13.(c). The plots show an increase in diversity advantage with increasing number of layers. That is because the joint detection capacity formula in (4.8) assumes joint encoding and decoding scheme. The diversity advantage of the joint detection under the above assumption is $2K \times M_R$. While joint detection algorithms exist for real systems, such as sphere decoding, the MLSTBC encoding is done for each layer independently. Thus, the actual system has a transmit diversity of two.

Parts (d), (e) and (f) of Figure 4.13 compares the performance of the outage probability of the MLSTBC detection algorithms at different number of groups. The joint detection outperforms the GINC algorithms due to the diversity advantage. Furthermore, the parallel algorithm performs better than the serial. This performance difference increases and became more apparent with increasing number of layers.

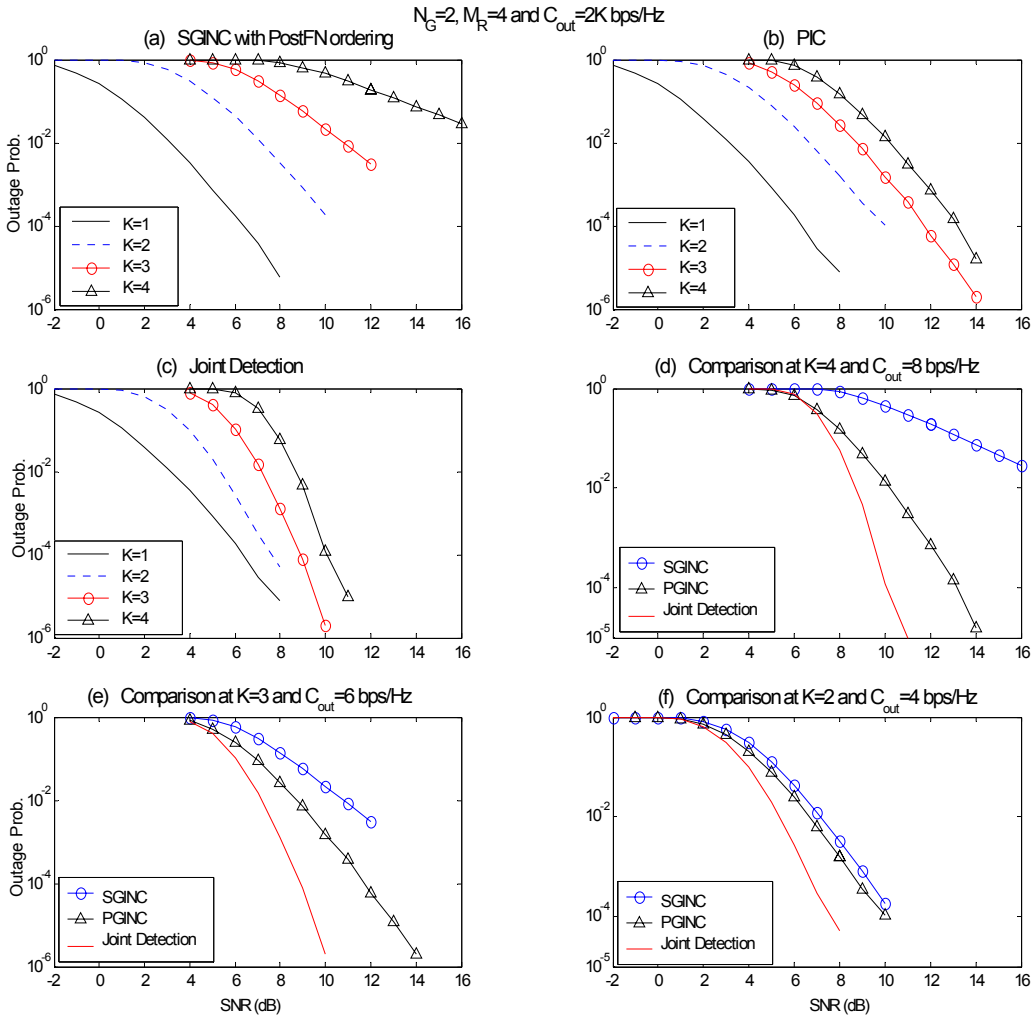

Figure 4.13: Outage probability versus SNR for MLSTBC.

4.6.4 Spatial Multiplexing Effect on Rate

In Figure 4.14, we examine the effect of spatial multiplexing on the spectral efficiency at 10% outage probability. The result reemphasizes the fact that SGINC experiences a capacity reduction after increasing the number of layers above a certain number. Also, another useful insight is that at low SNR, the rate almost doesn't increase with increasing number of layers.

This suggests that in this case, turning off some groups will not reduce the capacity of the system while it will greatly reduce the complexity of the receiver.

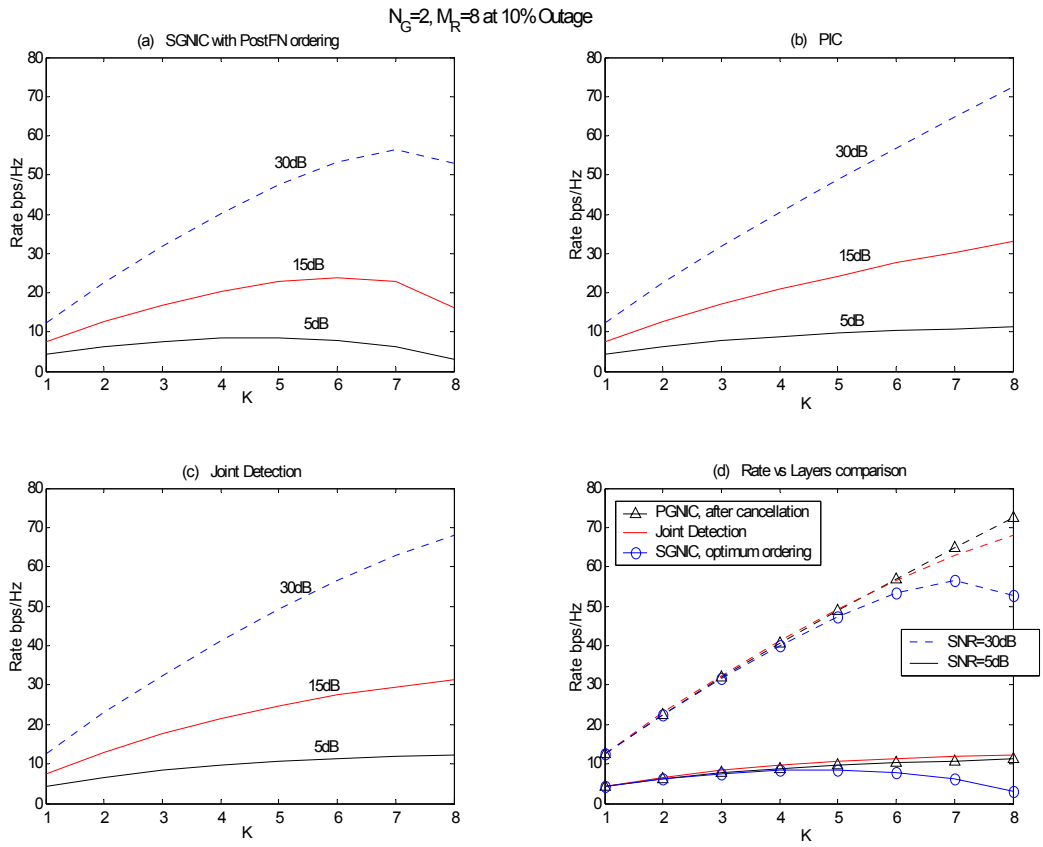

Figure 4.14: Spectral efficiency versus number of layers for MLSTBC.

4.6.5 Spatial Multiplexing Effect on Outage Probability

To study the effect of increasing layers on the outage probability of MLSTBC, the SNR and M_R are fixed and the number of layers is varied. The result is shown in Figure 4.15. Assuming that each group uses QPSK modulation, the outage capacity is $2K$ bps/Hz. The result shows that the outage probability increases with increasing layers. That is due to the increase in

the data rate of the system which needs more energy to sustain the same performance. This could be used as guidelines for adaptive MIMO algorithms that maintain fixed outage probabilities.

A comparison between the different decoding algorithms is shown in Figure 4.15.(d). The result shows the superiority of the joint detection algorithm over GINC to due the diversity advantages as discussed earlier.

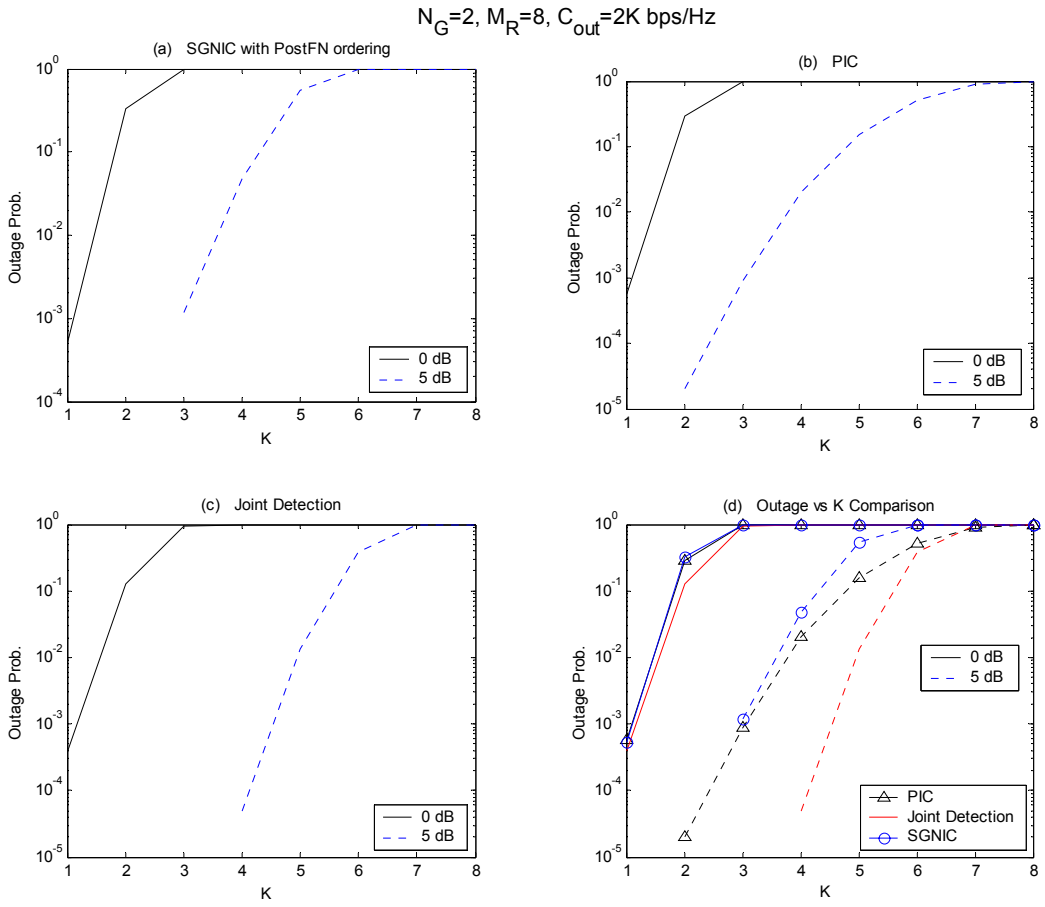

Figure 4.15: Outage probability versus number of layers.

4.7 Performance Evaluation of Detection Algorithms for Multi-layered STBC-OFDM Systems

New high data rate Wireless LANs (WLANs), such as IEEE 802.11a and Hyperlan2, apply orthogonal frequency division multiplexing (OFDM) at the physical layer. This modulation is known to be robust against frequency selective channels (FSC) since it transforms FSC into several parallel flat fading channels. WLAN devices are usually large enough to accommodate multiple antennas both at the transmitter and the receiver. Thus, MIMO communication systems are good candidates for increasing data rates and/ or for providing space time diversity. To increase the data rates of WLAN without adding extra bandwidth, [Gia02] proposed a V-BLAST-OFDM architecture. This approach is a full spatial multiplexing that increases the spectral efficiency of the system. Also, space time coded OFDM was proposed in [Che02][Yan04] to mitigate fading through transmit diversity.

In this section, we implement a MLSTBC system over frequency selective channels. To mitigate the effect of FSC, we concatenate MLSTBC with OFDM. This transforms MIMO FSC into parallel MIMO flat fading channels. The study evaluates and compares the performance of several decoders for MLSTBC-OFDM systems.

4.7.1 MLSTBC-OFDM System Model

In this section, we illustrate the MLSTBC-OFDM system model for two layers. Extension to higher number of layers is straight forward. Each group uses Alamouti STBC [Ala98] and transmits through two antennas and the receiver has two receive antennas as shown in Figure 4.16. Note that $M_R \geq K$, which reduces the required number of receive antennas by half compared

to V-BLAST with the same number of transmit antennas. The information symbols are demultiplexed into two layers, where each layer is assigned to a group. Then it is further divided into two OFDM symbols of length N_c, where N_c is the number of OFDM subcarriers. Using bold face vector notation, each OFDM symbol is denoted by an $N_c \times 1$ column vector $\mathbf{s}_{ki} = \begin{bmatrix} s_{ki,1} & s_{ki,2} & \cdots & s_{ki,N_c} \end{bmatrix}^T$ where k refers to the group number and i refers to the OFDM symbol within that group. The output from each encoder over two OFDM symbol periods is the space time matrix:

$$\mathbf{C}_k = \begin{bmatrix} \mathbf{s}_{k1} & \mathbf{s}_{k2} \\ -\mathbf{s}_{k2}^* & \mathbf{s}_{k1}^* \end{bmatrix} \tag{4.10}$$

After that, each STBC is OFDM modulated before transmission from each antenna. Then, the output is parallel to serial converted and a cyclic prefix (CP) is added to avoid any intersymbol interference (ISI) due to the delay spread of the channel. Figure 4.17 shows the architecture of the STBC-OFDM modulator for a single group.

MIMO FSC is assumed to be constant over transmission of two OFDM symbols. The receiver is equipped with two receive antennas and the received signals over two periods of OFDM symbols for all subcarriers are:

$$\begin{bmatrix} \mathbf{Y}_1^{t_1} & \mathbf{Y}_1^{t_2} \\ \mathbf{Y}_2^{t_1} & \mathbf{Y}_2^{t_2} \end{bmatrix} = \begin{bmatrix} \mathbf{H}_{11} & \mathbf{H}_{12} & \mathbf{H}_{13} & \mathbf{H}_{14} \\ \mathbf{H}_{21} & \mathbf{H}_{22} & \mathbf{H}_{23} & \mathbf{H}_{24} \end{bmatrix} \begin{bmatrix} \mathbf{s}_{11} & -\mathbf{s}_{12}^* \\ \mathbf{s}_{12} & \mathbf{s}_{11}^* \\ \mathbf{s}_{21} & -\mathbf{s}_{22}^* \\ \mathbf{s}_{22} & \mathbf{s}_{21}^* \end{bmatrix} + \begin{bmatrix} \boldsymbol{\eta}_1^{t_1} & \boldsymbol{\eta}_1^{t_2} \\ \boldsymbol{\eta}_2^{t_1} & \boldsymbol{\eta}_2^{t_2} \end{bmatrix} \tag{4.11}$$

where $\mathbf{Y}_m^{t_1} = \begin{bmatrix} y_{m,1}^{t_1} & y_{m,2}^{t_1} & \cdots & y_{m,N_c}^{t_1} \end{bmatrix}^T$ is the OFDM received symbol at time t_1 at antenna m. Similarly, $\boldsymbol{\eta}_m^{t_1}$ is the complex AWGN vector of all subcarriers of zero mean and variance $N_0/2$ per dimension. Furthermore, the OFDM channel matrix in the frequency domain between transmit antennas n and receive antenna m is:

$$\mathbf{H}_{mn} = \begin{bmatrix} h_{mn,1} & 0 & \cdots & 0 \\ 0 & h_{mn,2} & \cdots & 0 \\ \vdots & \vdots & \ddots & \vdots \\ 0 & 0 & \cdots & h_{mn,N_c} \end{bmatrix} \tag{4.12}$$

where $h_{mn,l}$ is the complex Gaussian channel coefficient of the l^{th} subcarrier.

Since OFDM transforms FSC into N_c parallel flat fading channel as apparent in, the MLSTBC detection algorithms are applied on each subcarrier. The MLSTBC received signal at the l^{th} subcarrier is:

$$\begin{bmatrix} y_{1,l}^{t_1} & y_{1,l}^{t_2} \\ y_{2,l}^{t_1} & y_{2,l}^{t_2} \end{bmatrix} = \begin{bmatrix} h_{11,l} & h_{12,l} & h_{13,l} & h_{14,l} \\ h_{21,l} & h_{22,l} & h_{23,l} & h_{24,l} \end{bmatrix} \begin{bmatrix} s_{11,l} & -s_{12,l}^{*} \\ s_{12,l} & s_{11,l}^{*} \\ s_{21,l} & -s_{22,l}^{*} \\ s_{22,l} & s_{21,l}^{*} \end{bmatrix} + \begin{bmatrix} \eta_1^{t_1} & \eta_1^{t_2} \\ \eta_2^{t_1} & \eta_2^{t_2} \end{bmatrix} \tag{4.13}$$

By exploiting the structure of STBC, the received signals over two time periods is rearranged into one vector as:

$$\begin{bmatrix} y_{1,l}^{t_1} \\ y_{2,l}^{t_1} \\ y_{1,l}^{t_2 *} \\ y_{2,l}^{t_2 *} \end{bmatrix} = \begin{bmatrix} h_{11,l} & h_{12,l} & h_{13,l} & h_{14,l} \\ h_{21,l} & h_{22,l} & h_{23,l} & h_{24,l} \\ h_{12,l}^{*} & -h_{11,l}^{*} & h_{14,l}^{*} & -h_{13,l}^{*} \\ h_{22,l}^{*} & -h_{21,l}^{*} & h_{24,l}^{*} & -h_{23,l}^{*} \end{bmatrix} \cdot \begin{bmatrix} s_{11,l} \\ s_{12,l} \\ s_{21,l} \\ s_{22,l} \end{bmatrix} + \begin{bmatrix} \eta_{1,l}^{t_1} \\ \eta_{2,l}^{t_1} \\ \eta_{1,l}^{t_2 *} \\ \eta_{2,l}^{t_2 *} \end{bmatrix} \tag{4.14}$$

$$\begin{aligned} \mathbf{y}_l &= \begin{bmatrix} H_{1,l} & H_{2,l} \end{bmatrix} \mathbf{s}_l + \boldsymbol{\eta}_l \\ \mathbf{y}_l &= \mathbf{H}_l \mathbf{s}_l + \boldsymbol{\eta}_l \end{aligned} \tag{4.15}$$

After that, the multi-layered detection algorithms are applied at each subcarrier. The GINC algorithms are described earlier. The joint detection algorithms is based on the sphere decoder [Dam00]. It has a cubic complexity at high SNR. It will be explained in details in Chapter 5.

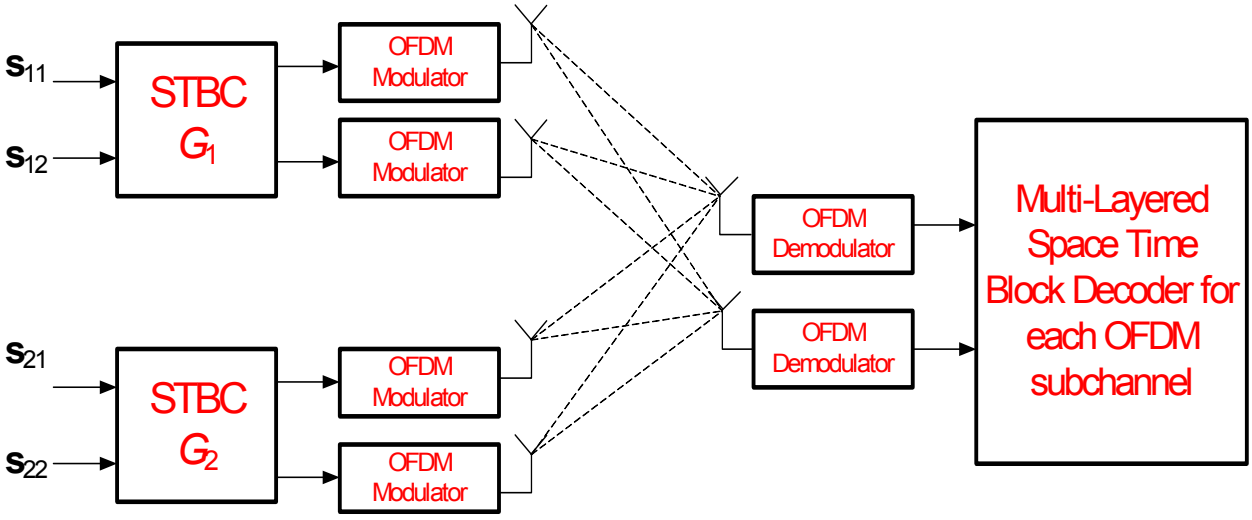

Figure 4.16: Block diagram of MLSTBC-OFDM

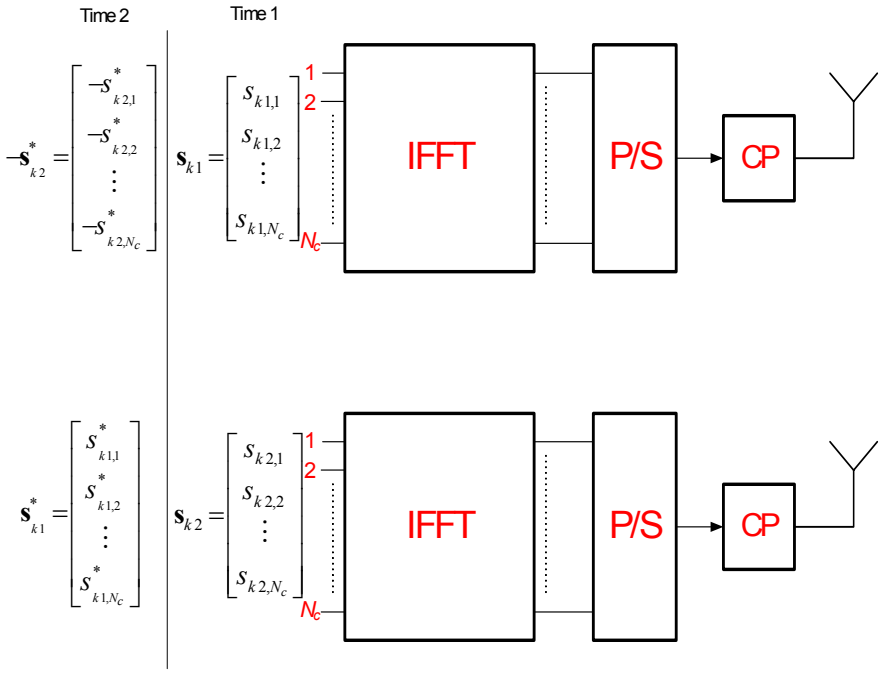

Figure 4.17: Architecture of a single STBC-OFDM transmitter

4.7.2 Simulation Results

In this section, OFDM symbol error rate (SER) is estimated via simulation. An error is counted when at least one of the bits in the whole OFDM symbol is in error. Each OFDM symbol has 64 subcarriers. We use an independent equal path power FSC model of length four. Perfect channel state information is assumed. Also, each layer uses Alamouti full rate code with QPSK modulation. Thus, the rate of each layer is 2bps/Hz and each layer transmits through two antennas and has a transmit diversity of order two.

Figure 4.18 compares the OFDM SER performance of MLSTBC, V-BLAST and STBC over 4x4 MIMO-OFDM channels. The FSC is of length 4. The results show that the MLSTBC is more power efficient than V-BLAST. That is a result of the higher diversity order obtained by the MLSTBC. At 4x4 MIMO channels, the MLSTBC has two layers and each layer has a transmit diversity of order two. At the receiver, one antenna is used to null out interference and three antennas are used for diversity and detection. On the other hand, V-BLAST has four layers and no transmit diversity while the receiver uses three antennas to null out three interfering layers and one antenna is used for the detection of the first layer. Recall that the performance is dominated by the weakest layer. For the case of 4 bps/Hz, the gain is 27dB and it is 19dB for 16 bps/Hz transmission. The reason for this high gain in performance is that the OFDM channel in the frequency domain is highly correlated and a diversity order of 2x3 greatly improves the performance.

The performance of PGINC with four layers and four receive antennas is shown in Figure 4.19. The parallel cancellation should theoretically provide full receive diversity and that requires prefect cancellation. However, due to error propagation, this is not visible without using strong outer codes. PIC improved the system by 2dB compared to PIN. The diversity of PGINC

is dominated by the weakest layer of PIN. The result shows that the slopes of PIC and PIN are parallel. The diversity order of this case is 2×1 since PIN needs three antennas to null three interfering layers.

The effect of ordering on SGINC is shown in Figure 4.20 with four layers and four receive antennas. The results indicate that ordering doesn't increase the diversity but it adds some gain since the strongest layer is detected first. The diversity order of the system is dominated by the first layer which is 2×1 in this case. The best ordering criterion is Post-FN.

Performance comparison of MLSTBC-OFDM detection algorithms with two layers and with two and four receive antennas is shown in Figure 4.21. The number of receive antennas in part (a) is the minimum number required and it is equal to K. The results show that the serial and parallel GINC algorithms provide the same diversity and they perform very close to each other at low number of layers. The diversity advantage of the GINC algorithms is dominated by the first detected layer which has a diversity order of 2×1 in part (a) and 2×3 in part (b). On the other hand, joint detection, using the sphere decoder, provides full receive diversity and doesn't suffer from error propagation. Also, its performance is very close to perfect cancellation case. Furthermore, Figure 4.21.b shows the effect of adding more receive antennas on the performance of the MLSTBC-OFDM detectors. The result shows that they perform very close to each other at low number of layers and at additional receive diversity. That is because, in this case, the weakest layer in the GINC algorithms has a diversity order of 2×3.

The simulation comparison with four layers is shown in Figure 4.22. It depicts the performance of the algorithms at moderate number of layers. In Figure 4.22.a, at M_R=4, the performance of SGINC with Post-FN ordering outperforms PGINC performance after cancellation by around 2dB but still the diversity order is the same for all GINC algorithms. That

is because ordering insures that the strongest layer is detected first while the parallel algorithm is dominated by the weakest layer after PIN. In Figure 4.22.b, the MLSTBC detectors perform within 1dB from each other at eight receive antennas. That is a result of the high diversity order of the first detected layer, which is 2×5 in this case.

To sum up the simulation results, the diversity of GINC algorithms is dominated by the weakest layer which has a diversity order of $2\times(M_R\text{-}K\text{+}1)$. SGINC with Post-FN ordering performs better than the parallel because ordering insures that the strongest layer is detected first. Furthermore, the SD algorithm provides each layer with a diversity order of $2\times M_R$ and it performs the best. Also, when extra receive antennas are added at the receiver, the diversity order of the weakest layer increases and all algorithms perform close to each other.

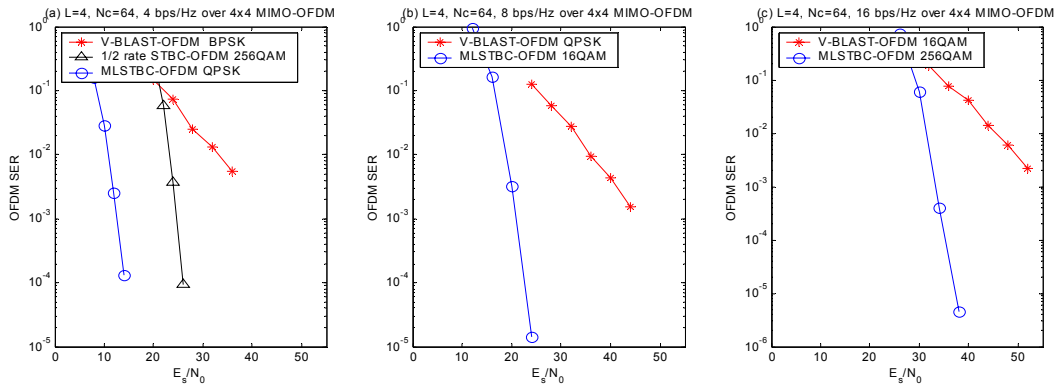

Figure 4.18: OFDM SER comparison of MLSTBC, VBLAST and STBC over 4x4 MIMO channels.

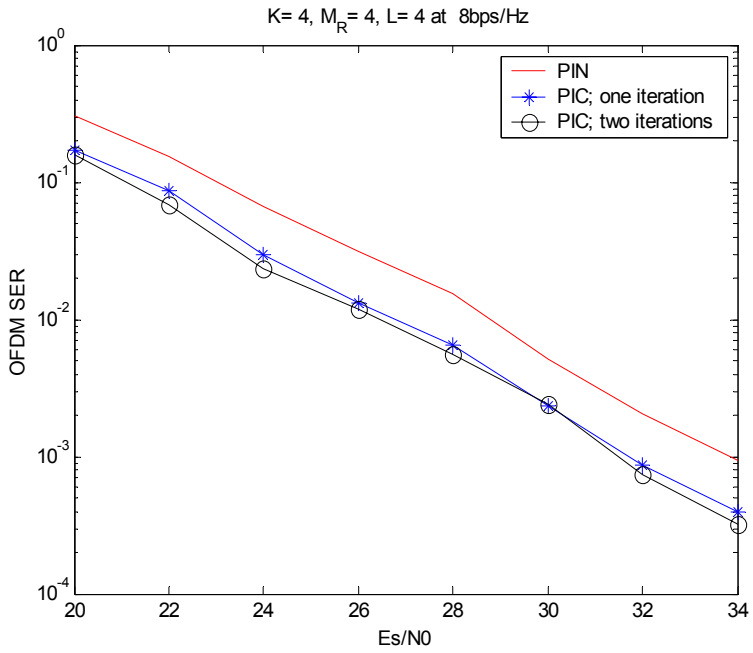

Figure 4.19: Performance of PGINC over 8×4 MIMO channels

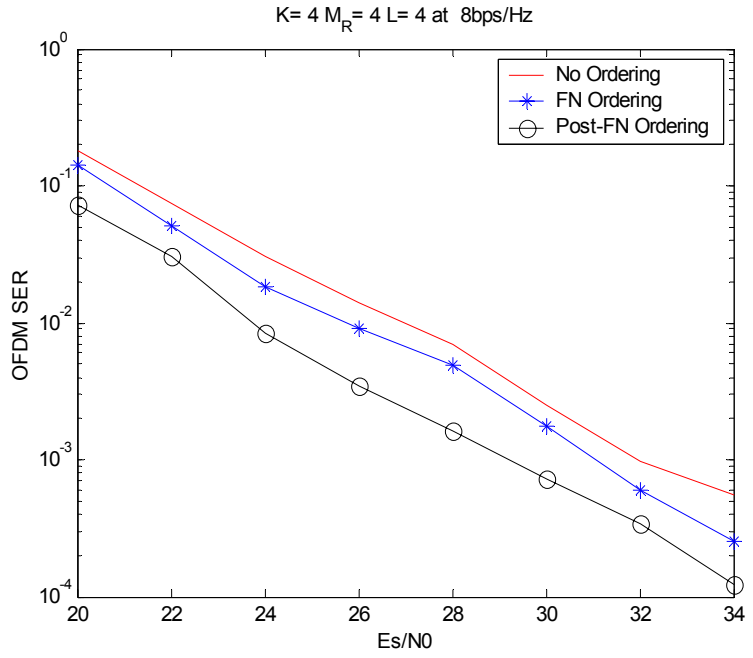

Figure 4.20: Performance of SGINC over 8×4 MIMO channels

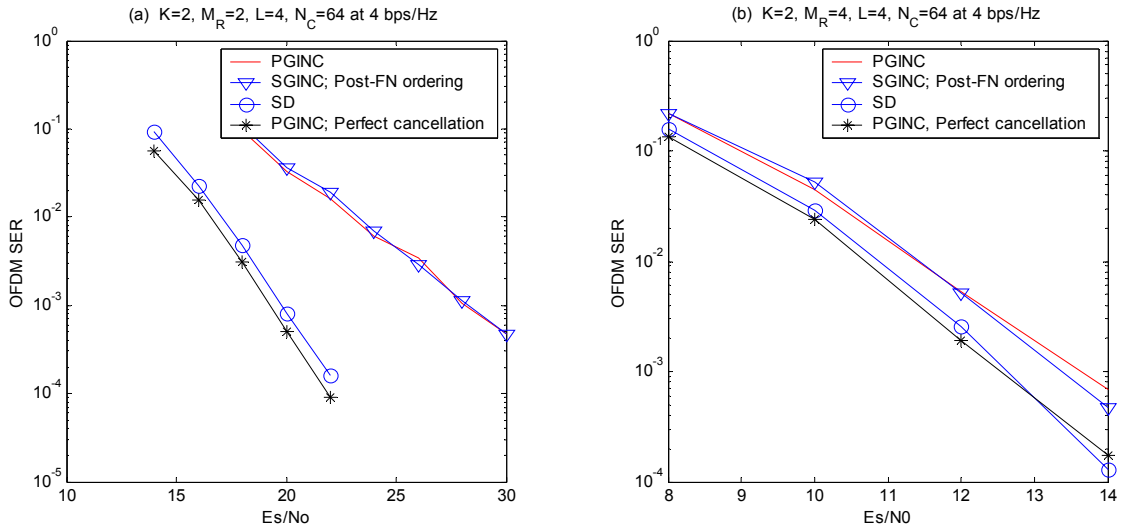

Figure 4.21: Performance comparison of MLSTBC-OFDM detection algorithms over 4×2 and 4×4 MIMO channels

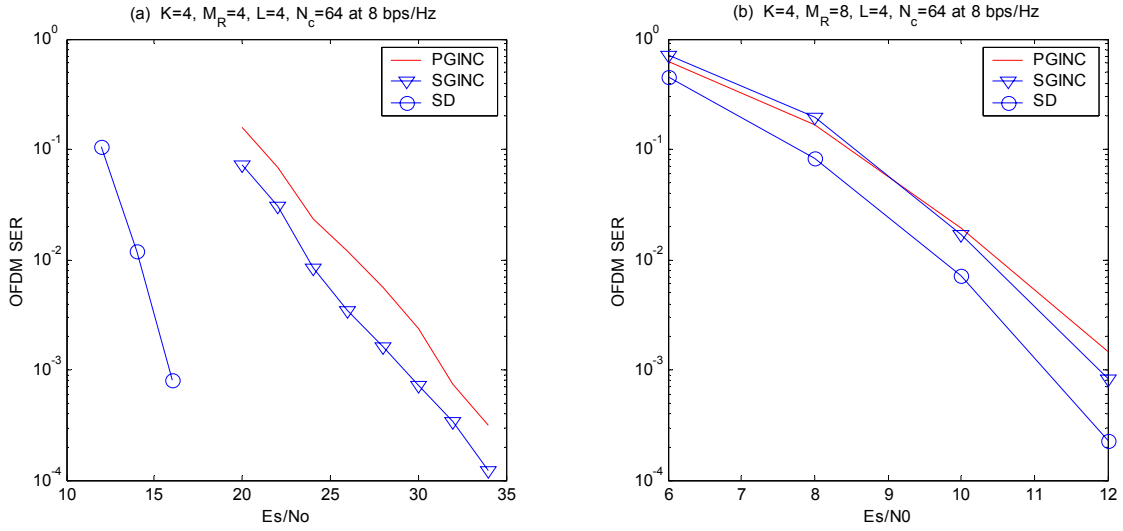

Figure 4.22: Performance comparison of MLSTBC-OFDM detection algorithms over 8×4 and 8×8 MIMO channels

4.8 Chapter Summary

In this chapter, we studied the capacity of different detection algorithms of MLSTBC. The goal is to examine the optimal performance and the spatial multiplexing and diversity tradeoffs and their relation with the detection algorithm. We considered three detection algorithms for MLSTBC; serial group interference nulling and cancellation, parallel group interference nulling and cancellation and joint detection.

The capacity of the serial algorithm of MLSTBC was compared to other open loop transmit techniques at the same number of transmit-receive antennas. The results show that MLSTBC is more spectrally efficient at low SNR and at low outage probabilities than V-BLAST. Furthermore, since MLSTBC has more transmit-receive diversity, it is more power efficient. Therefore, it makes a good candidate for low power high data rate wireless applications. Moreover, the study shows that there is a capacity reduction in MLSTBC and V-BLAST after adding a certain number of layers. That is a result of the nulling operation involved in the detection algorithms.

We also evaluated the performance of multi-layered detection algorithms for MLSTBC systems over frequency selective MIMO channels. The OFDM modulator transforms the frequency selective MIMO channels into parallel flat fading channels in the frequency domain. The OFDM symbol error rate performance of the MLSTBC-OFDM scheme was evaluated and the different detection algorithms were compared. The results show that SGINC with post-FN ordering outperforms PGINC at large number of layers. The diversity of the PGINC algorithm is dominated by the performance after parallel nulling. The joint detector using the sphere decoder outperforms the GINC algorithms since it provides full receive diversity while the diversity order of GINC algorithms is dominated by the first detected layer.

Chapter 5
Application of the Sphere Decoder to MIMO Systems

In this chapter, we study the complexity of a sphere decoder (SD) for MIMO communication systems. Its performance is evaluated for V-BLAST, full-rate full-diversity space time block codes (STBC), and multi-layered STBC system. The results show a huge gain in performance with moderate complexity. Finally, we proposed simple modification of the SD to handle non-rectangular constellations, such as 8PSK.

5.1 Introduction

The sphere decoding (SD) algorithm has received a lot of attention recently because it can achieve maximum likelihood (ML) detection performance with moderate complexity. It was originally proposed by [Poh81] to solve the problem of finding the shortest vector in a lattice and further analyzed by [Fin85]. Viterbo and Boutros, in [Vit99], introduced the algorithm to

communication systems over fading channels. In [Dam00][Cha02][Hoc03], SD was used to improve the performance of V-BLAST through joint detection which provides full receive diversity. Also, it has been applied to the detection of non-orthogonal STBC [Har02][Dam02].

The complexity of the SD is shown in [Fin85] to be polynomial in the dimension of the lattice (m). Analysis and simulation carried out by [Dam01] and [Has01] showed that the average complexity is roughly cubic [$O(m^3)$] at high and moderate SNR and it doesn't depend on the constellation size . For MIMO systems, the dimension of the lattice is $2M_T$, where M_T is the total number of transmit antennas.

In this chapter we examine the effect of spatial multiplexing (number of layers), constellation size, signal to noise ratio (SNR) and the initial random size on the complexity of SD. We also compare the SD complexity with V-BLAST detection algorithm [Wol98]. Furthermore, we propose a modified SD algorithm to handle non-rectangular constellations, such as 8PSK.

5.2 Sphere Decoding Algorithm for MIMO Systems

In this section, we briefly describe the SD algorithm. For more details, the reader is referred to [Vit99][Cha02] or Appendix A.

Assume a vector $\mathbf{x} = (x_1, x_2, \ldots, x_{M_T})^T$, where the symbol x_i is drawn from a constellation Q, is transmitted over an $M_R \times M_T$ MIMO channel, where $M_R = M_T$. The discrete received vector is:

$$\mathbf{y} = \mathbf{H}\mathbf{x} + \boldsymbol{\eta} \tag{5.1}$$

H contains $M_R \times M_T$ i.i.d complex Gaussian channel coefficients of mean zero and variance 0.5 per dimension. Also, $\boldsymbol{\eta}$ is an $M_R \times 1$ of i.i.d complex AWGN of mean zero and variance $N_0/2$ per dimension. The maximum likelihood detector (MLD) selects the vector $\tilde{\mathbf{x}}$ that satisfies the following search criterion:

$$\tilde{\mathbf{x}} = \underbrace{\min \arg}_{\hat{\mathbf{x}} \in Q^{M_T}} \left\{ \left\| \mathbf{y} - \mathbf{H}\hat{\mathbf{x}} \right\|^2 \right\} \tag{5.2}$$

Thus, the complexity of this detector is exponential of $O\left(|Q|^{M_T}\right)$, where $|Q|$ is the cardinality of the signal set. Although, MLD is the optimal in terms of performance and eliminating interference, it has huge complexity. However, after the introduction of SD into communication systems, ML performance can be achieved with moderate complexity.

The mechanism of SD is described as follows: first it sets a hypersphere of initial radius (R) centered at the received vector. Then it searches for one valid point. The search is done sequentially on each coordinate of the transmitted vector with an enumerating process that limits the search range. When SD finds a valid point, it reduces the hypersphere radius so that the new point lies on the surface of the searched sphere. After that, the search is repeated until the closest point near the received vector is found, and that happens when the algorithm results in an empty sphere. However, if the SD doesn't find a valid point inside the initial sphere, it goes back and increases the initial radius and the search is repeated.

The original algorithm described in [Vit99] operates on real lattices only. Although, there is a complex version proposed by [Hoc03], we study the original SD for simplicity. Therefore, the received vector in equation (5.1) is transformed to a real vector as follows:

$$\mathbf{r} = \mathbf{M}\mathbf{u} + \mathbf{v} \tag{5.3}$$

where,

$$\mathbf{r} = \left[\text{real}(\mathbf{y}^T) \ \text{imag}(\mathbf{y}^T) \right]^T$$

$$\mathbf{M} = \begin{bmatrix} \text{real}(\mathbf{H}) & \text{-imag}(\mathbf{H}) \\ \text{imag}(\mathbf{H}) & \text{real}(\mathbf{H}) \end{bmatrix}$$

$$\mathbf{u} = \left[\text{real}(\mathbf{x}^T) \ \text{imag}(\mathbf{x}^T) \right]^T$$

$$\boldsymbol{\upsilon} = \left[\text{real}(\boldsymbol{\eta}^T) \ \text{imag}(\boldsymbol{\eta}^T) \right]^T$$

After that, **r** and **M** are passed to the SD.

The initial radius selection is critical. We will follow the criterion of [Hoc03], which is

$$R = 2\sigma^2 Jn \tag{5.4}$$

where J is an integer, and n is the length of the received vector **r,** and σ^2 is the noise variance.

Figure 5.1 illustrates an example of a SD search over 64QAM constellation. The transmitted signal is denoted x and the received signal is denoted y. In this example, SD only searched over 4 points. The numbers indicate the sequence of the search.

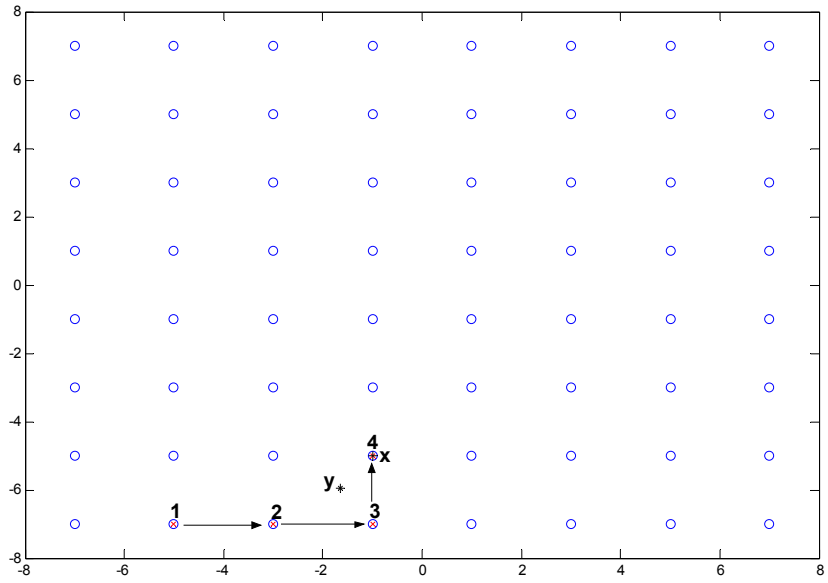

Figure 5.1: Sphere decoding example; 64QAM over a Rayleigh fading channel

5.3 Complexity Study of the Sphere Decoder

In this section, we examine the complexity of SD based on the algorithm described in section 2 using simulation. SD complexity is a random variable. The instantaneous complexity of SD depends on the instantaneous SNR and the transmitted sequence. That greatly challenges the analytical analysis. It has been shown that the average complexity per dimension is cubic at high SNR. Also, the worst case complexity is exponential [Has01].

This study shows the effect of signal dimension, which represents the spatial multiplexing of the MIMO system, constellation, received SNR, and the SD search radius on the complexity. The simulation counts the floating point operations (flops) using Matlab subroutines.

Figure 5.2 shows the relation between the dimension of the transmitted vector from all transmit antennas and the average number of flops per received vector. Since SD operates on real coordinates, the dimension of the vector to be detected is $2M_T$. Thus, the dimension of the vector is twice the spatial multiplexing of MIMO system. The figure compares the complexities of maximum likelihood detection (MLD), V-BLAST detector, and SD. The complexity of MLD increases exponentially with increasing the dimension of the transmitted vector. On the other hand, the average complexity of SD is much lower while it still provides the same performance. Also, the result shows that the SD complexity highly depends on the average SNR. There is a huge difference in complexity at low and high SNR. By curve fitting the estimated average complexity, we found that it is $O\left(M_T^3\right)$ at 20dB and $O\left(M_T^5\right)$ at 5dB. It is interesting to note that the SD complexity at high SNR is slightly lower than the original V-BLAST detector (as presented in [Wol98]). That is because the complexity of V-BLAST is also cubic since it calculates a pseudo inverse of interfering layers to perform nulling each time after cancellation. Moreover, the difference in complexity increases rapidly with increasing M_T as shown in Figure 5.3 at 20dB. Thus, SD operating at high SNR and for large dimension is a good candidate for joint MIMO detection.

To illustrate the effect of SNR on the complexity, we estimated the average complexity at 2×2 and 8×8 MIMO channels. The result is in Figure 5.4 and it shows that for low dimensions, the reduction in flops with increasing SNR is very small while a substantial reduction in complexity is achieved for high dimensions. Also, after a certain threshold, the complexity flatten out indicating that no more substantial reduction in complexity is achieved by increasing SNR.

The initial radius of SD is normally selected to increase the probability of convergence and to reduce the complexity. If the initial search radius is small, the number of flops decreases but the probability of converging to a valid point inside the sphere also decreases. When no valid point is found, the decoder increases the initial radius and searches again which increases the complexity. Figure 5.5 shows the effect of the initial radius on complexity at low and high SNR. The variable J on the x-axis represents the initial radius as in equation (5.4). The result shows that there is also a threshold after which the average complexity is approximately constant. Thus, selecting a large initial search radius doesn't increase the complexity. At low values of J, SD didn't converge and the decoding is repeated several times. However, the simulation shows that at low SNR, this act didn't harm the complexity as severe as at high SNR.

Furthermore, we examine the relation between the complexity and the constellation size. Figure 5.6 compares the complexity of 4×4 MIMO systems with SD when the transmitted symbols are drawn from different QAM constellations. The result shows that the increase in complexity is small at high SNR. That again reemphasizes that the preferred operation region for SD is at high SNR.

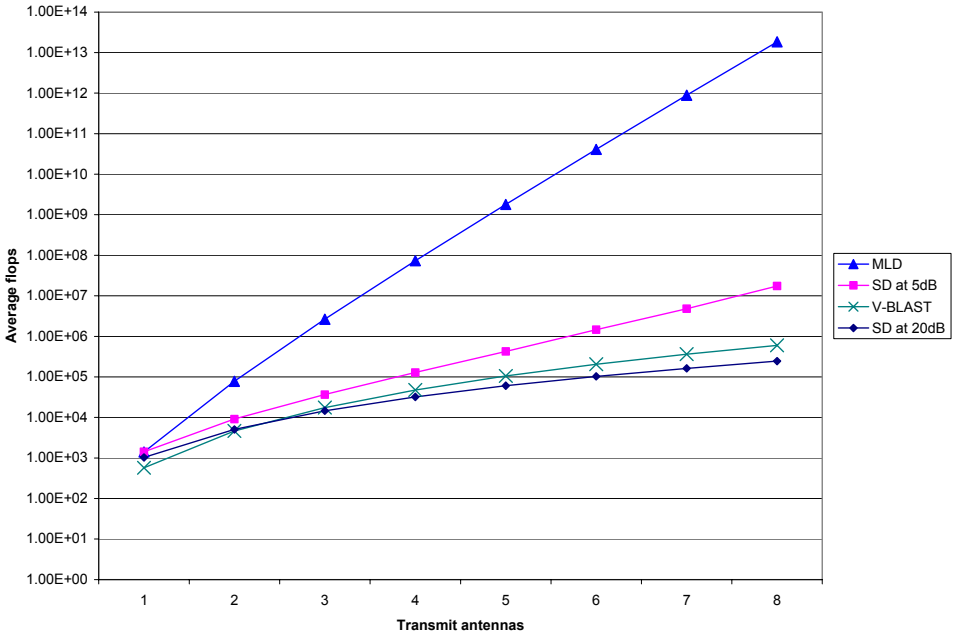

Figure 5.2: SD complexity in flops versus M_T for QPSK MIMO systems.

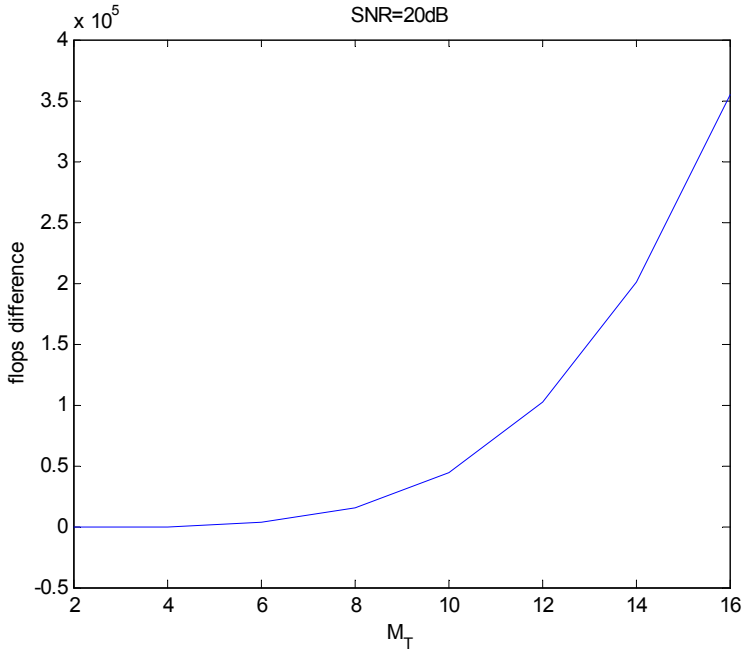

Figure 5.3: Complexity difference in flops between SD and V-BLAST zero forcing detector with ordering

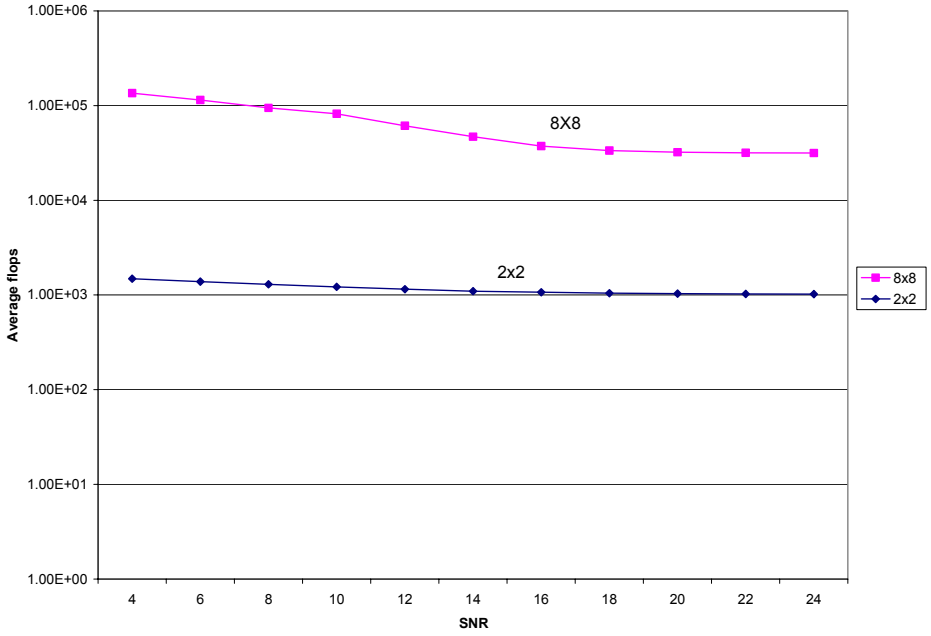

Figure 5.4: SD complexity in flops versus SNR for 2x2 and 8x8 QPSK MIMO systems.

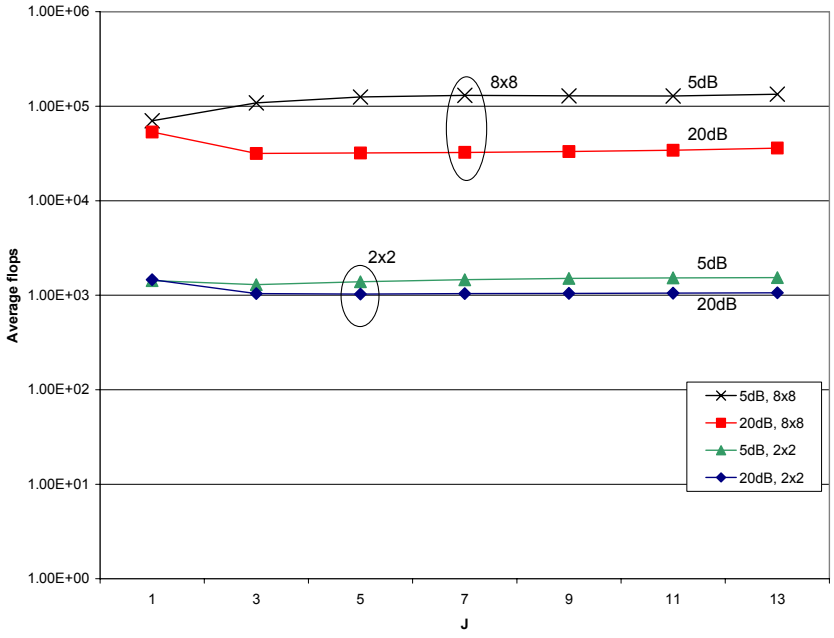

Figure 5.5: SD complexity in flops versus initial search radius for 2x2 and 8x8 QPSK MIMO systems.

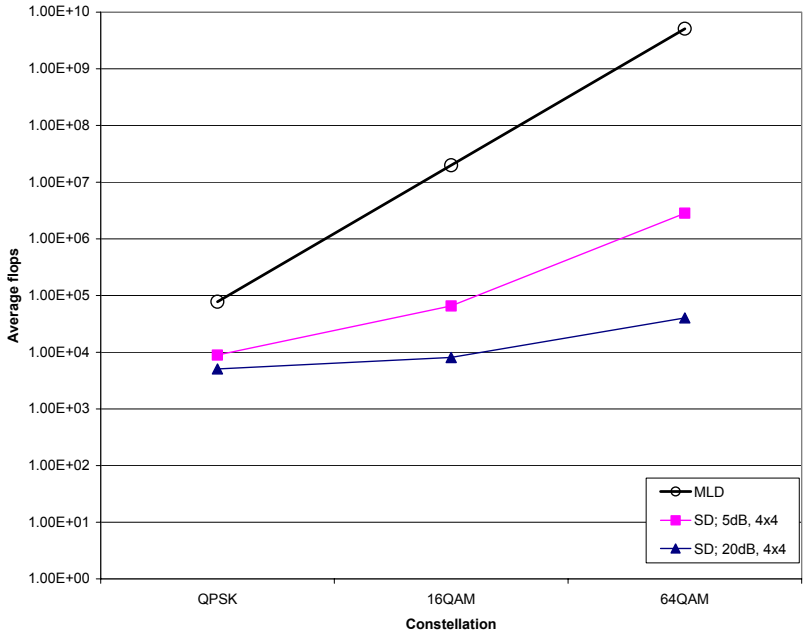

Figure 5.6: SD complexity in flops versus constellation size for 4x4 MIMO systems.

5.4 Modified Sphere Decoder for non-rectangular and Rotated Constellations

In this section, we propose a modification of SD in order to handle non-rectangular constellations, such as M-PSK, and mixed rotated constellations, such as quasi-orthogonal space time block codes with constellation rotation. The original algorithm [Vit99] is designed for rectangular lattices, such as 16QAM. For PSK constellation, the algorithm may converge to an invalid point. To handle this, some researchers [Cha02] proposed to discard the invalid point. However, this is a waste of decoding power and cycles. Others [Hoc03] proposed a complex

version of SD which can handle M-PSK constellation but it is hard to be generalized to mixed rotated constellations.

The modified algorithm is described next. Let $S_{|\mathcal{Q}|}$ be the set of possible values of coordinates of a point **u**. SD searches over a subset of vectors $\mathbf{u} \in S_{|\mathcal{Q}|}^{2M_T}$, which are inside the sphere of radius *R*. For example, for a 2×2 MIMO system with 16-QAM transmitted symbols, the search will be over a subset of real vector $\mathbf{u} \in S_{16}^4$, where $S_{16} = \{-3,-1,1,3\}$. Also, for 8-PSK transmitted symbols, $\mathbf{u} \in S_8^4$, where $S_8 = \{-1,-1/\sqrt{2},0,1/\sqrt{2},1\}$. However, the problem is that not all vectors in S_8^4 are valid, for example, **u**=[-1,-1,-1,-1]^T, and that causes the decoder to converge to an invalid point. To solve this problem, we further subset the possible coordinates and control the enumeration functions in SD so that we always get a valid point. For the 8-PSK example, we will have the following coordinate subsets:

$$S_{8,1} = \{-1/\sqrt{2},1/\sqrt{2}\}, S_{8,2} = \{-1,1\}, \text{ and } S_{8,3} = \{0\}$$

The control on the enumeration function is described as follows: the symbols of the upper half of vector **u**, the imaginary coordinates, are selected from S_8. Then, the symbols of the lower half, the real coordinates, are carefully selected from the three subsets according to the following conditions:

if $u_{i+M_T} \in S_{8,1}$, then $u_i \in S_{8,1}$, where u_i is the i^{th} coordinate of vector **u**.

if $u_{i+M_T} \in S_{8,2}$, then $u_i \in S_{8,3}$

if $u_{i+M_T} \in S_{8,3}$, then $u_i \in S_{8,2}$

by this modification, the search is restricted to valid points.

5.5 Application of Sphere Decoder to MIMO Systems

In this section, we apply SD to three MIMO systems. We evaluate the performance and the diversity advantages of the SD algorithm.

5.5.1 Performance of Spatial Multiplexing with Sphere Decoding

Spatial multiplexing (SM) schemes are high data rate communication architectures that spatially multiplexes transmitted symbols through multiple transmit antennas. V-BLAST is a practical SM scheme that applies spatial interference cancellation algorithms to detect each layer. An optimum receiver would calculate the distant metric of every possible symbol combination and then selects the minimum. This is known as maximum likelihood (ML) detection and it provides full receive diversity and it is completely free of any error propagation. However, it is nearly impossible to be implemented since it has exponential complexity of $O(|Q|^{M_T})$, where $|Q|$ is the cardinality of the signal set from which the symbols are drawn. Therefore, the focus has been on developing low complexity suboptimal detectors. The original V-BLAST detector is based on serial nulling and interference cancellation. This algorithm suffers from poor energy performance due to error propagations and loss of receive diversity advantages as a result of the nulling operation. Parallel processing could be applied on the V-BLAST detector which theoretically should provide full receive diversity advantages. However, error propagation is still a significant factor on the system performance. Since SD can achieve ML performance with moderate complexity, it is a good candidate for SM schemes.

In this section, we compare the performance of SM-SD to V-BLAST with zero forcing (ZF) and MMSE nulling with serial and parallel processing. The BER performance at 4×4 MIMO systems and with QPSK modulation is shown in Figure 5.7.

SD provides full receive diversity and it improves the performance substantially. At BER= 10^{-4}, the energy efficiency improves by 6 dB compared to SIC with ordering and MMSE nulling.

Also, Figure 5.8 shows the performance of 4×4 8PSK SM-SD system using the modified SD presented in section 5.4. This system has 12 bps/Hz efficiency. The modified SD always finds a valid point unlike the original SD when applied to 8PSK.

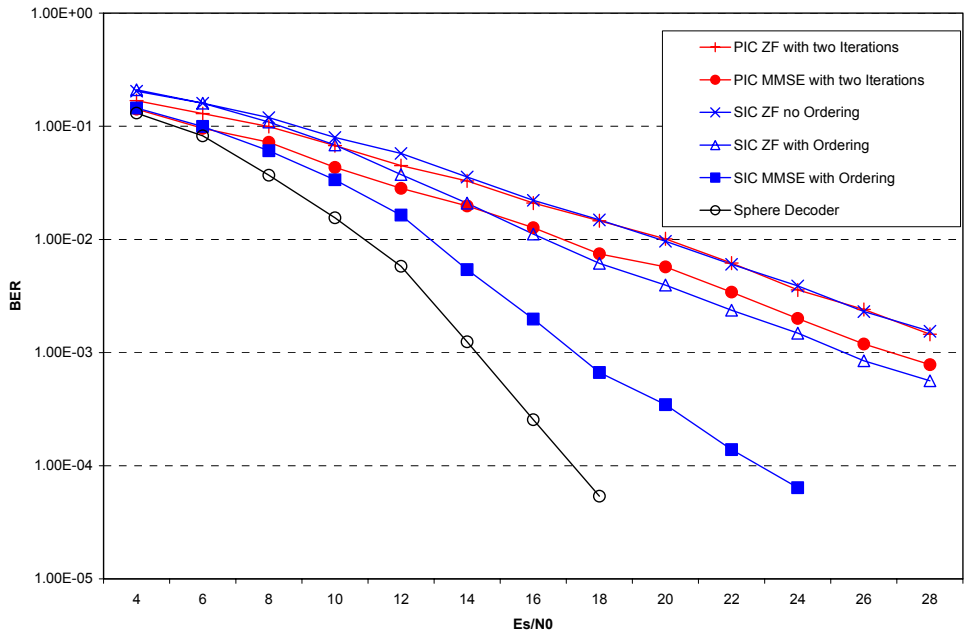

Figure 5.7: Performance of 4x4 QPSK SM with different detection algorithms

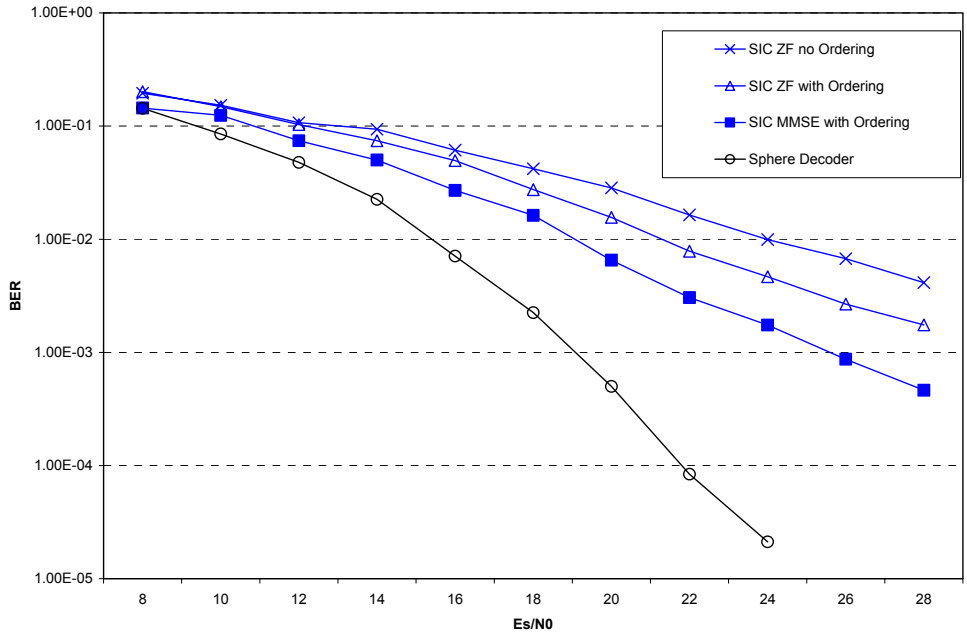

Figure 5.8: Performance of 4x4 8PSK SM with different detection algorithms

5.5.2 Full Rate Full Diversity Space Time Block Codes

Orthogonal STBC provides full transmit diversity with linear detection per transmitted symbol at the receiver [Ala98][Tar99a]. The orthogonal design allows for decoupling the decision statistics for each symbol on which ML detection is applied. However, it is impossible to design orthogonal full rate STBC for more than two transmit antennas [Tar99a].

On the other hand, it is possible to tradeoff rate with diversity by relaxing the orthogonality constraint and allowing more complex processing at the receiver. This is the main idea behind quasi-orthogonal STBC [Jaf01] which achieves full rate with half the transmit diversity. However, the decision statistics can't be uncoupled and ML detection is performed over a pair of symbols. In [Sha03], they rotated the constellation of one of the symbols in order

to improve the distance properties of the decision statistics. It turns out that this rotation made the quasi-orthogonal STBC full rank. That is a full-rate full-diversity STBC for four transmit antennas. Also, full-rate full-diversity nonorthogonal designs have been proposed in [Dam03].

In this section, we apply SD to decode these codes. For example, let us consider the quasi-orthogonal STBC with constellation rotation for four transmit antennas as shown in Figure 5.9. With one receive antenna, the received vector could be modeled as:

$$\mathbf{y} = \begin{bmatrix} h_1 & h_2 & h_3 & h_4 \\ h_2^* & -h_1^* & h_4^* & -h_3^* \\ h_3^* & h_4^* & -h_1^* & -h_2^* \\ h_4 & -h_3 & -h_2 & h_1 \end{bmatrix} \mathbf{x} + \boldsymbol{\eta} \tag{5.5}$$

and that is similar to the MIMO model in equation (5.1) and it is fed to the modified SD since it detects symbols jointly from two different constellations.

Our simulation compares several STBC designed for four transmit antennas at 2 bps/Hz. Figure 5.10 shows the BER performance. The G4 code [Tar99a] is a full-diversity half-rate orthogonal code. The quasi-orthogonal code has full-rate but at half the diversity. We can see that the quasi-orthogonal code provides a diversity of two and it is parallel to Alamouti code (G2). Also, at low and moderate SNR, the quasi-orthogonal code outperforms the orthogonal code since the latter uses a higher constellation (16QAM). Furthermore, rotating half of the symbols of the quasi-orthogonal code makes it of full-diversity and the resultant code performs the best (it is 6dB away from the receive diversity with MRC). The difference is due to splitting the transmit power over four transmit antennas. Also, the figure shows the performance of the nonorthogonal design of [Dam03]. It performs slightly worse than the quasi-orthogonal code with constellation rotation but it has the advantage that the design could be generalized to any constellation and to any number of transmit antennas.

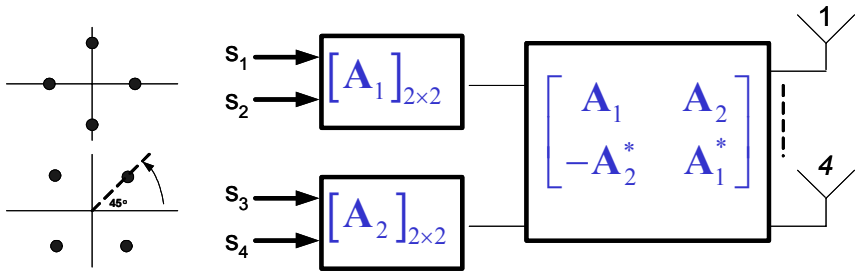

Figure 5.9: Block diagram of quasi-orthogonal STBC with constellation rotation

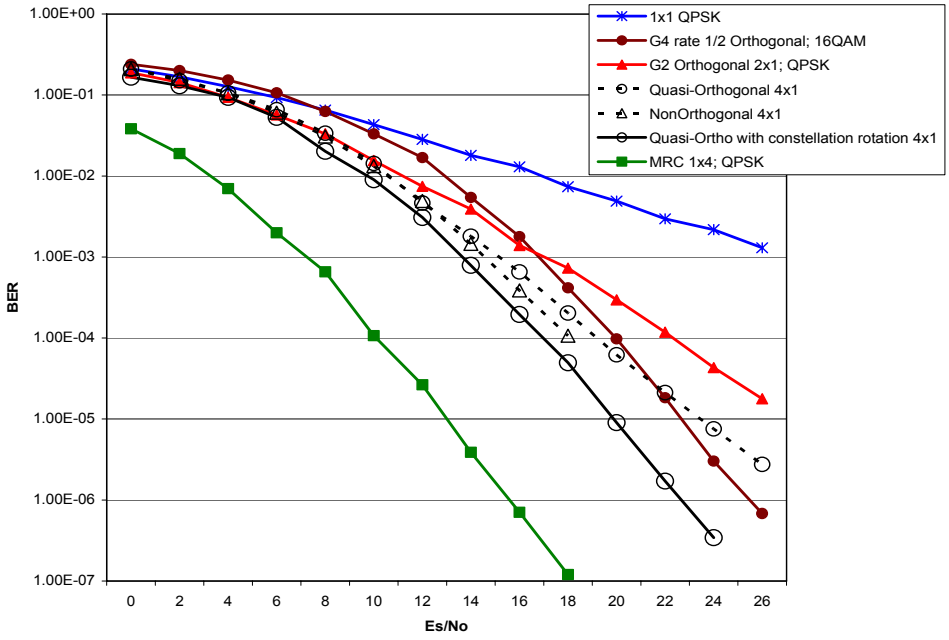

Figure 5.10: Performance of STBC for 4 transmit antennas at 2bps/Hz efficiency

5.5.3 Multi-Layered Space Time Bock Codes with Sphere Decoding

In a previous chapter, we proposed and evaluated the performance of several decoding algorithms for multi-layered space time trellis coded systems. We studied two types of decoders:

group interference nulling and cancellation, and joint detection algorithms. The optimum performance is achieved with joint detection. In this section, we replace the trellis codes with block codes. They provide the same transmit diversity but with much less processing. Additional coding gains could be obtained by concatenating strong outer codes. Another major advantage of using STBC is that the optimum joint detector is easily implemented by SD.

For illustration, we consider two layered system, each transmits Alamouti STBC over two transmit antennas. The spectral efficiency of the system is 4 bps/Hz. Let the number of receive antennas equal two. The received vector over two periods can be written as:

$$\begin{bmatrix} y_1^1 \\ y_2^1 \\ y_1^{2*} \\ y_2^{2*} \end{bmatrix} = \begin{bmatrix} h_{11} & h_{12} & h_{13} & h_{14} \\ h_{21} & h_{22} & h_{23} & h_{24} \\ h_{12}^* & -h_{11}^* & h_{14}^* & -h_{13}^* \\ h_{22}^* & -h_{21}^* & h_{24}^* & -h_{23}^* \end{bmatrix} \cdot \begin{bmatrix} x_{11} \\ x_{21} \\ x_{12} \\ x_{22} \end{bmatrix} + \begin{bmatrix} \eta_1^1 \\ \eta_2^1 \\ \eta_1^{2*} \\ \eta_2^{2*} \end{bmatrix} \tag{5.6}$$

Figure 5.11 shows the BER performance of the two layered QPSK STBC over 4x2 MIMO channels. Joint detection is done by SD and it is compared to parallel group nulling and interference cancellation (PGNIC). The slope of the result shows that SD provides full diversity. About 5dB is gained at BER=10^{-3}.

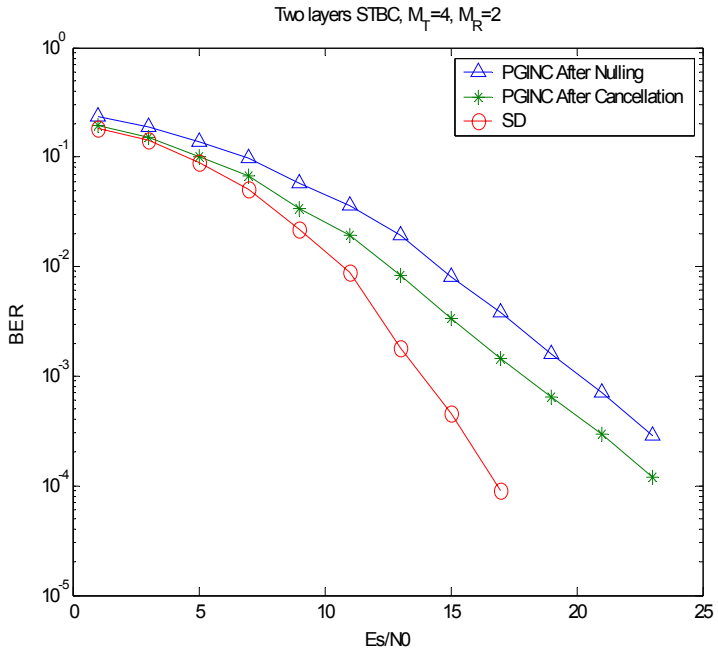

Figure 5.11: Performance of two layers QPSK STBC over 4x2 MIMO channels with sphere decoding.

5.6 Chapter Summary

The complexity of the sphere decoder is studied in this chapter. It has maximum likelihood performance with a cubic complexity at high SNR. We examine the effect of the number of transmit antennas, signal constellation size, SNR and initial radius size on the complexity of the sphere decoder over MIMO channels. Furthermore, we propose a minor modification to SD in order to handle non-rectangular signal sets and mixed constellations. Finally, we illustrate some applications of SD on MIMO systems, such as spatial multiplexing, full rate full diversity STBC and multi-layered STBC.

The complexity results show that the average complexity of SD at high SNR is lower than the original V-BLAST algorithm. The difference increases with increasing number of

layers. Also, the complexity reduction with increasing SNR flattens out after a certain threshold. Moreover, starting the search with a large radius doesn't increase the complexity substantially. Finally, the constellation size affects the SD complexity but the increase is small at high SNR.

Chapter 6
IQ Space Frequency Time Codes for MIMO-OFDM Systems

In this chapter, we study concatenated coding for MIMO-OFDM systems. The proposed concatenated system achieves full spatial and frequency diversity at a much less complexity in terms of number of states. In general, coding for MIMO-OFDM systems is known as space frequency time (SFT) coding since coding is done in the frequency domain.

The chapter starts with an overview of a concatenated trellis coded modulation (TCM) and space time block codes (STBC) system over fading channels. Then we illustrate and describe the benefits of IQ-trellis codes, which are the focus of the study. After that, concatenated SFT codes are compared and evaluated. Finally, a multi-layered SFT coded system is presented. It combines spatial multiplexing with frequency and spatial diversity.

6.1 Concatenating TCM with STBC over Fading Channels

Design of TCM when concatenated with STBC was first considered in [Ala98a] for quasi-static MIMO channels. A block diagram of the concatenated system is shown in Figure 6.1. Under the assumption that the MIMO channel is constant across the whole codeword and using rank r STBC with one receive antenna, it was found that the pairwise error probability (PEP) between codewords **S** and **W** is:

$$P(\mathbf{S} \to \mathbf{W}) \le \frac{1}{\left(\frac{SNR}{8} \sum_{i=0}^{L_c-1} |w_i - s_i|^2 \right)^r} \tag{6.1}$$

where L_c is the TCM codeword length. Note that $\sum_{i=0}^{L_c-1} |w_i - s_i|^2$ is the squared Euclidian distance (D^2) between the two codewords. Denote the free Euclidian distance of the code, which is the minimum squared Euclidian distance, by D_{free}^2, Then,

$$P(\mathbf{S} \to \mathbf{W}) \le \frac{1}{\left(\frac{SNR}{8} D_{free}^2 \right)^r} \tag{6.2}$$

Therefore, the TCM code design criterion when concatenated with STBC over quasi-static fading channels is to maximize D_{free}^2. Thus, TCM designed for AWGN channels are optimal in this case.

On the other hand, when the fade is rapid but is constant across one STBC length (T), and using a T symbol interleaver which treats T symbols as one unit, the PEP will be [Gon02]:

$$P(\mathbf{S} \to \mathbf{W}) \le \frac{1}{\left(\left(\frac{SNR}{8} \right)^{l_\eta} d_p\left(l_\eta\right) \right)^r} \tag{6.3}$$

where η is the set of all i for which $s_i \neq w_i$ or $s_{i+1} \neq w_{i+1}$ and l_η is the number of elements in η. Also, $d_P(l_\eta)$ is the product-sum distance over T consecutive symbols. In the case of Alamouti STBC [Ala98a], it is defined as:

$$d_P(l_\eta) = \prod_{i \in \eta} \left[|w_i - s_i|^2 + |w_{i+1} - s_{i+1}|^2 \right] \tag{6.4}$$

where l_η is the effective length of the error event over span two.

The space time diversity of the concatenated system is rl_η. Since the effective length of the concatenated system is of span two, the original effective length of the TCM is at most the double. In other words, the concatenated system using T symbol interleaving tradeoffs time diversity with spatial transmit diversity. To overcome this drawback, we add simple modifications to the concatenated system. One way to keep the original effective length of the code is to use one symbol based interleaving. Another way is to map two symbols from two different codewords to the STBC while still using two symbols interleaving as illustrated in Figure 6.1.

To decode the concatenated system, a STBC combiner is used to estimate the coded symbols. For Alamouti code, the received STBC signal over two symbol periods with one receive antenna is written as:

$$\begin{bmatrix} y_1^{t_1} \\ y_1^{t_2 *} \end{bmatrix} = \begin{bmatrix} h_{11} & h_{12} \\ h_{12}^* & h_{12}^* \end{bmatrix} \cdot \begin{bmatrix} s_1 \\ s_2 \end{bmatrix} + \begin{bmatrix} \eta_1^{t_1} \\ \eta_1^{t_2 *} \end{bmatrix} \tag{6.5}$$

$$\mathbf{y} = \mathbf{H}\mathbf{s} + \boldsymbol{\eta} \tag{6.6}$$

the STBC combiner multiples the received signal with the Hermitian of **H**. The output is uncoupled estimates of the TCM symbols and they are deinterleaved and decoded by the trellis decoder:

$$\tilde{\mathbf{s}} = \begin{bmatrix} \tilde{s}_1 \\ \tilde{s}_2 \end{bmatrix} = \mathbf{H}^H \mathbf{y} \qquad (6.7)$$

The simulation results of these modifications are shown in Figure 6.2 for a 2bps/Hz system that concatenates a 4-states 8PSK TCM [Jam91] with Alamouti STBC. The minimum effective length of this TCM code is two. Since the STBC is of rank 2, the space time diversity of the concatenated code is four. However, if two symbol interleaving is used, the diversity of the code is reduced to two. The result shows that the one symbol interleaving and the two codewords assignment to STBC keep the time diversity of TCM without any additional complexity. The diversity of the modified system is apparent from the slopes of the plots. On the hand, at high SNR, the diversity of the concatenated system with two symbol interleaving is similar to the uncoded STBC.

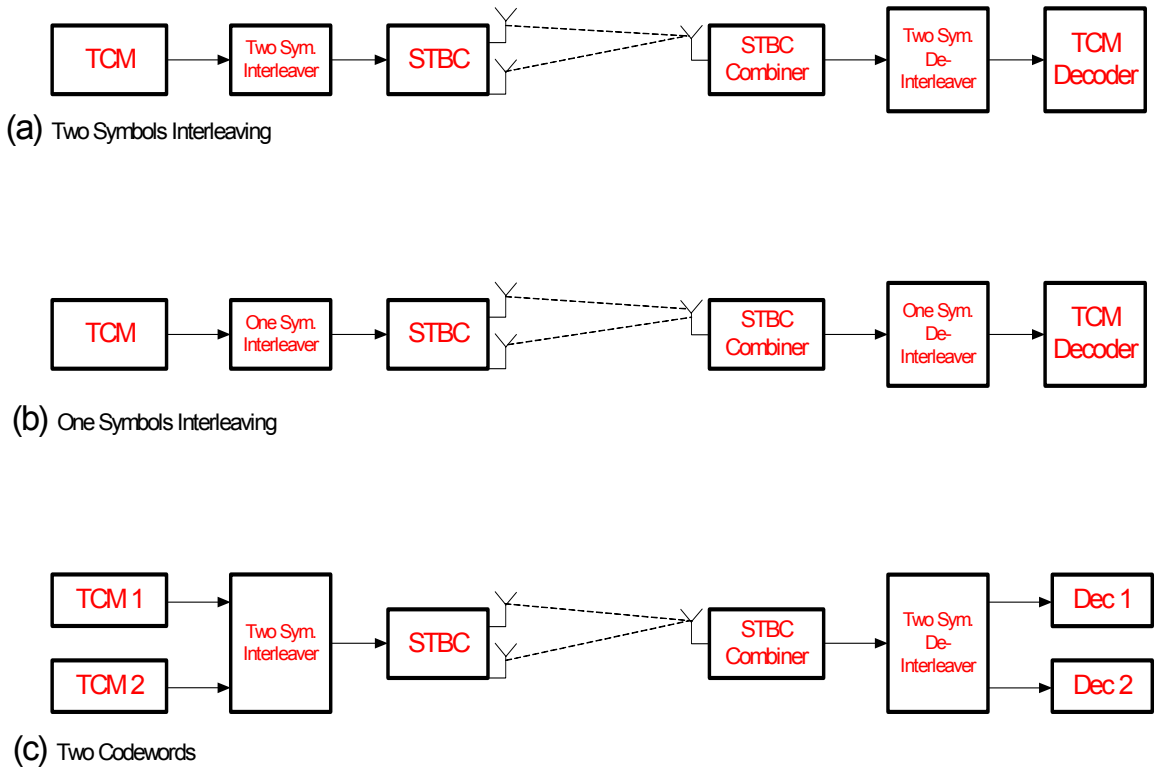

Figure 6.1: Block diagrams of concatenated TCM-STBC codes

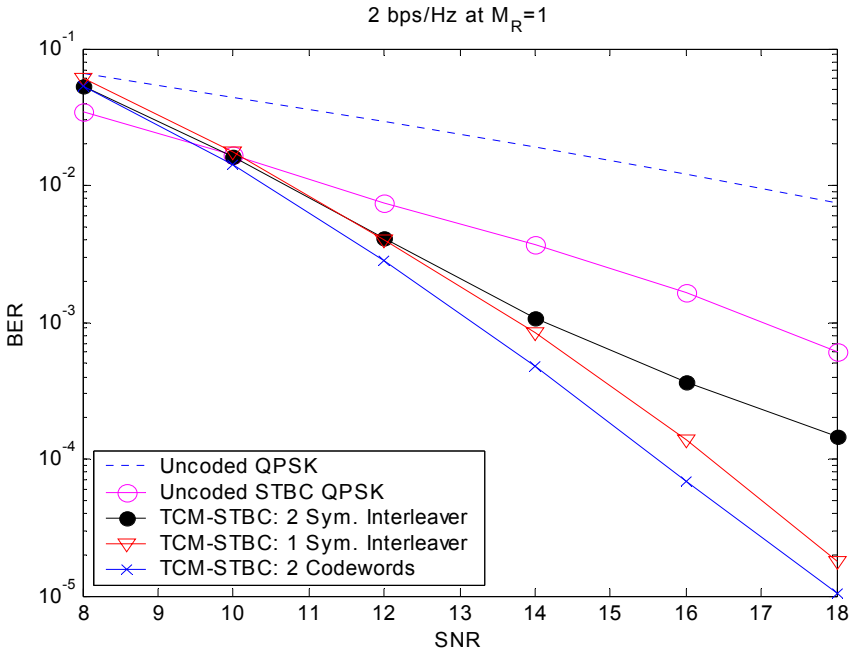

Figure 6.2: Interleaving effect on 4 States 8PSK TCM-STBC

6.2 IQ-Trellis Coded Modulation

An important advantage of the concatenated TCM-STBC is the design separation between temporal and spatial diversity. The spatial diversity is guaranteed by STBC which allows the designer to focus on TCM design to get more temporal diversity. There are a number of trellis code designs that increase the minimum effective length (l_{min}) over fast fading channels. The minimum effect length is known as the time diversity of the code. The first of these is multiple trellis coded modulation (MTCM) [Div88] which increases the effective length by assigning more than one symbol to the output of the trellis. In addition, the effective length of TCM can be increased by using inphase-quadrature (IQ) interleaving with an appropriate design that requires constellation rotation as proposed by [Jel94]. A careful design doubles the effective

length of the TCM code since it will be the number of different coordinates between two codewords rather than the number of different symbols.

Another interesting way to increase the minimum effective length of TCM is to code the inphase and quadrature components by two separate TCM encoders [Als97]. This code is called IQ-TCM. We will implement it in our concatenated system since it shows superior performance improvements over conventional TCM and it is easily implemented from off the shelf codes.

The minimum effective length of TCM is upper bounded by [Als97]:

$$l_{\min} \le \lfloor v / k \rfloor + 1 \qquad (6.8)$$

where v is the number of memory elements in the encoder and k is the number of inputs. Thus, at the same number of states, reducing k increases l_{min}. When k is reduced by a half, l_{min} at most doubles and this is the reason behind the diversity increase of IQ-TCM.

The IQ-TCM design is briefly described next. The encoder divides the input bits into two sets; each set is encoded by a TCM encoder and the output is mapped to an amplitude modulation (AM) signal set. The two parallel encoders produce the IQ components of the quadrature amplitude modulation (QAM) codeword. For example, at 2bps/Hz, IQ-TCM uses two half rate 4-AM trellis codes as shown in Figures 6.3 and 6.4. Each input is trellis coded and mapped to a 4-AM signal set. Then the output is combined to form a 16-QAM signal which is interleaved and transmitted over a Rayleigh fading channel. At 8-states, the IQ-16QAM trellis code provides a time diversity of order four, while it is only two for an 8PSK TCM.

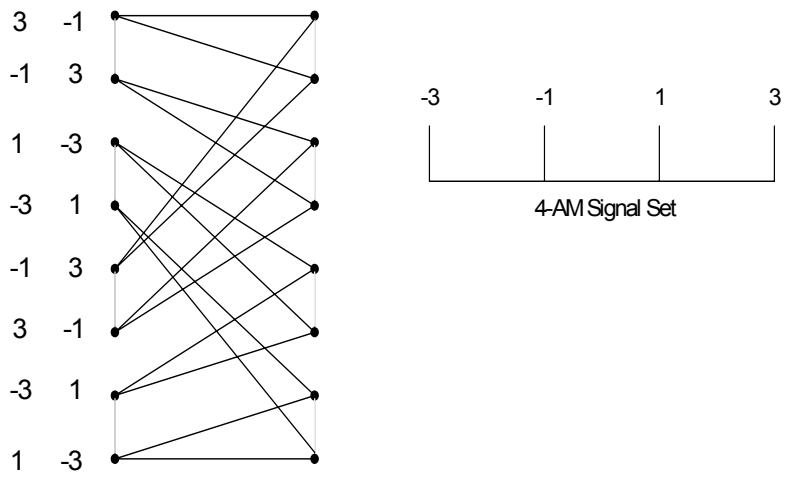

Figure 6.3: 8-states 4AM-TCM

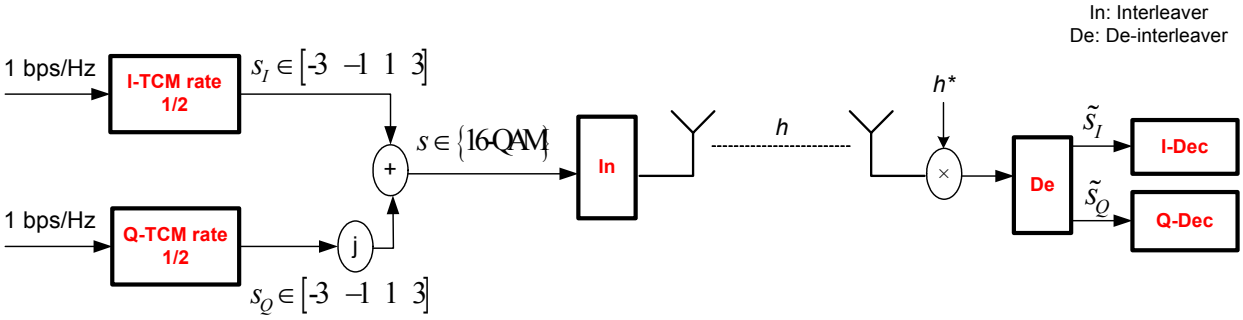

Figure 6.4: Block diagram of 2 bps/Hz IQ-16QAM TCM

6.3 Space Frequency Time Coding for MIMO-OFDM Systems

Coding for MIMO-OFDM systems is the focus of this chapter. Space frequency time (SFT) coding for OFDM applies spatial coding across multiple antennas, frequency coding across OFDM subcarriers and temporal coding across successive OFDM symbols. The first space frequency coding study was done by [Aqr98] where they adapted Tarokh's space time

codes [Tar98] to OFDM with multiple transmit antennas. However, these codes are designed for quasi-static fading channels. Thus, they are not optimized for OFDM channels and couldn't benefit from the available frequency diversity. In [Ben00], it has been shown that the maximum achievable diversity for a MIMO-OFDM system is $M_T L M_R$, where L is the frequency selective channel length and M_T and M_R are the number of transmit and receive antennas, respectively. In order to achieve this diversity, the minimum effective length of the SFT code should be equal to $M_T L$. Thus, the trellis code design criterion is similar to the design over rapid fading channels, which is maximizing the minimum effective length. However, the coding gain depends on the channel and thus optimizing the coding gain is not visible [Ben00]. Furthermore, since the OFDM channel in the frequency domain is highly correlated and slowly varying, interleaving across frequency tones is a vital requirement that allows the code to exploit the available frequency diversity.

To achieve full spatial-frequency diversity, trellis code design needs large number of states. In order to simplify the design and reduce the complexity of the code, [Gon03] proposed to concatenate TCM with STBC. The spatial diversity is guaranteed by STBC while the frequency diversity is achieved by TCM. This separation allows for a less complex, lower number of states, TCM design.

Our main contribution is combining up-to-date design principles for SFT coding and implementing powerful class of trellis codes, which are IQ-TCM. These codes provide larger effective lengths compared to conventional TCM at the same rate and number of states. In addition, we examine the effect of interleaving on the frequency diversity of the concatenated SFT code.

6.3.1 MIMO-OFDM Channel Model in the Frequency Domain

This section presents a MIMO-OFDM channel model in the frequency domain. The fast Fourier transform (FFT) matrix (T) for N_c subcarriers is defined as:

$$\begin{aligned} &\mathbf{T}_{k,j} = \frac{1}{\sqrt{N_c}} \exp\left[-i \frac{2\pi}{N_c} (k-1)(j-1) \right]; \\ &k, j = 0,1,...,N_c - 1 \end{aligned} \tag{6.9}$$

where $\mathbf{T}_{k,j}$ is the *(k,j)* element of $\mathbf{T}$.

A MIMO frequency selective channel (FSC) consists of $M_T \times M_R$ single-input single-output (SISO) FSCs. OFDM transforms the MIMO-FSC into N_c parallel MIMO flat fading channels. Let SISO-FSC between the n^{th} transmit antenna and the m^{th} receive antennas be of length L and denote it as $\mathbf{h}_{mn} = [h_0 \quad h_1 \quad \cdots \quad h_{L-1}]^T$. The OFDM channel in the frequency domain between the n^{th} transmit antenna and the m^{th} receive antenna is:

$$\mathbf{h}^f_{mn} = \mathbf{F}\mathbf{h}_{mn} \tag{6.10}$$

where $\mathbf{F}$ is a partition of $\mathbf{T}$ and it is defined as:

$$\begin{aligned} &\mathbf{F}_{k,l} = \frac{1}{\sqrt{N_c}} \exp\left[-i \frac{2\pi}{N_c} (k-1)(l-1) \right]; \\ &k = 0,1,...,N_c - 1 \\ &l = 0,1,...,L-1 \end{aligned} \tag{6.11}$$

Assume that $\mathbf{h} \sim \mathcal{N}_c(\mathbf{0}, \mathbf{C}_\mathbf{h})$, then the covariance matrix of $\mathbf{h}^f$ will be:

$$\mathbf{C}_{\mathbf{h}^f} = \mathbf{F}\mathbf{C}_\mathbf{h}\mathbf{F}^H \tag{6.12}$$

The correlation coefficient between subcarriers i and j is:

$$\rho_{i,j} = \frac{\mathbf{f}_i \mathbf{C}_\mathbf{h} \mathbf{f}_j^H}{\sqrt{\mathbf{f}_i \mathbf{C}_\mathbf{h} \mathbf{f}_i^H \mathbf{f}_j \mathbf{C}_\mathbf{h} \mathbf{f}_j^H}} \tag{6.13}$$

where $\mathbf{f}_i$, $\mathbf{f}_j$ are the i^{th} and j^{th} row of $\mathbf{F}$, respectively.

Therefore, The OFDM channel in the frequency domain is highly correlated even when the paths of FSC are independent, i.e $\mathbf{C_h}=\mathbf{I}$. The fade rate is slower at low number of paths and it is faster at higher number of paths. To illustrate that, we plotted the OFDM channel in the frequency domain in Figure 6.5 for FSC with independent equal power taps.

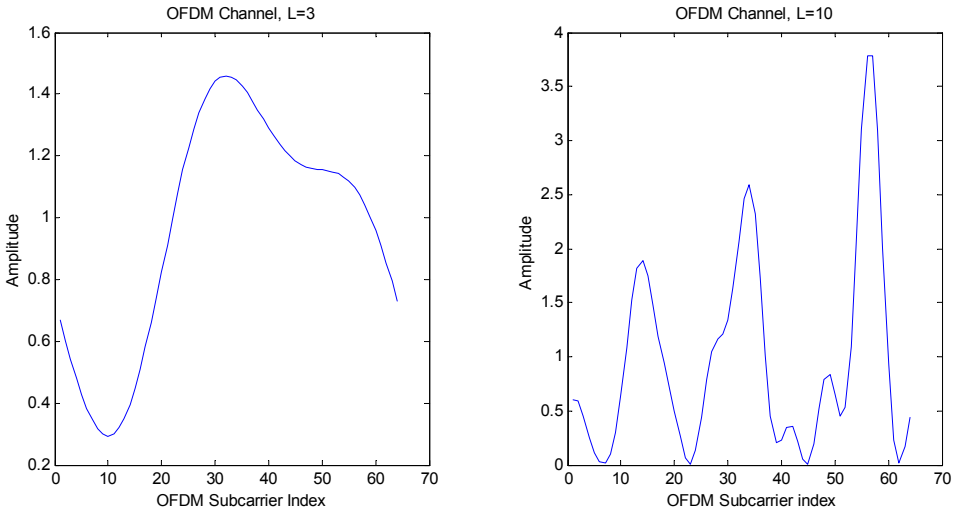

Figure 6.5: Snapshot of an OFDM Channel in the frequency domain

6.3.2 Fading vs AWGN TCM Design

We observed in the literature that few studies [Yon03][Ng03] on concatenated TCM-STBC for MIMO-OFDM systems used Ungerboeck designs which are optimized for AWGN channels. To clarify this, we compare the performance of TCM designed for AWGN channels to those designed for fading channels. Figure 6.6 shows the simulation results of a 2bps/Hz 4-states 8PSK-TCM over a 2x1 MIMO-OFDM channel. The length of FSC is four. Thus the available spatial-frequency diversity is of order eight. The AWGN design [Jam94], which maximizes the minimum Euclidian distance, has a minimum effective length (l_{min}) of one. On the other hand, the fading design [Jam94] criterion is to maximize l_{min} and it has l_{min}=2. The diversity advantage of the fading design is clear from the result. In order to take advantage of the full diversity available for this MIMO-OFDM system at the same spectral efficiency, a 64-states 8PSK-TCM that has l_{min}=4 is needed. In the next section, we will show how to achieve full frequency at just 8-states by using IQ-TCM.

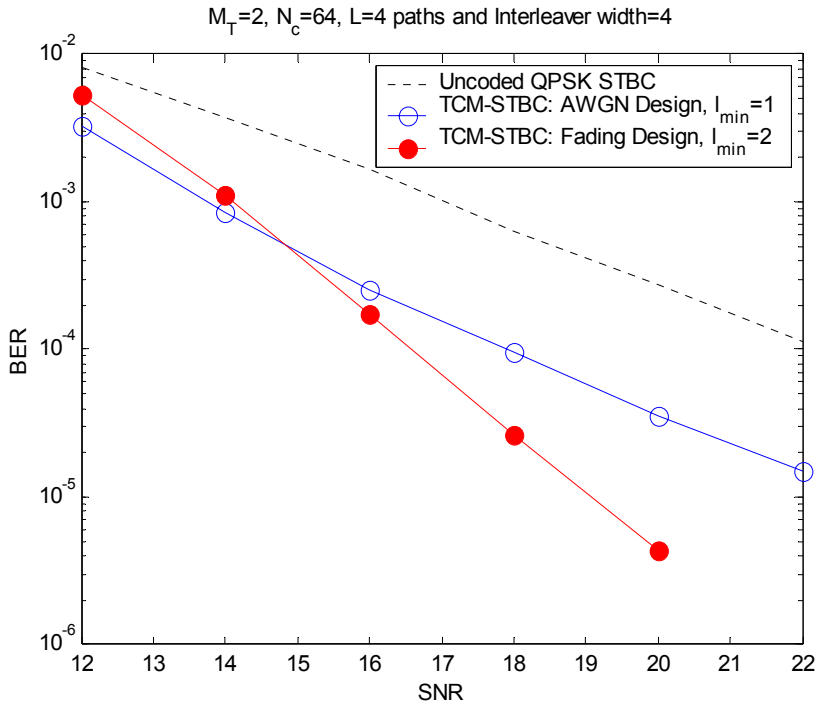

Figure 6.6: Fading vs. AWGN trellis design for 4 States 8PSK TCM-STBC-OFDM system over four taps frequency selective channel at 2bps/Hz efficiency.

6.3.3 IQ-SFT Code

This section describes the IQ-SFT encoder and decoder, which are shown in Figures 6.7 and 6.8, respectively. The IQ trellis encoders output two codewords each is an OFDM symbol of length N_c. Denote the k^{th} IQ-TCM OFDM symbol by $\mathbf{s}_k = \begin{bmatrix} s_{1,k} & \cdots & s_{N_c,k} \end{bmatrix}^T$ where $s_{i,k}$ is the i^{th} IQ-TCM symbol of the k^{th} OFDM symbol. After interleaving, The STBC encodes the two OFDM symbols using Alamouti code at each subcarrier as shown in Figure 6.7. Then the output is OFDM modulated before transmission from each antenna and a cyclic prefix (CP) is added to avoid any intersymbol interference (ISI) due to the delay spread of the channel.

The channel is a MIMO-FSC of length L with equal power paths and each path experience an independent Rayleigh fading. We assume that the channel is constant over two

OFDM symbols. The receiver is equipped with one receive antenna as shown in Figure 6.8. Extension to more than one antenna is straight forward. After FFT, the received signals over two periods in the frequency domain are:

$$\begin{bmatrix} \mathbf{Y}^{t_1} & \mathbf{Y}^{t_2} \end{bmatrix} = \begin{bmatrix} \mathbf{H}_{11} & \mathbf{H}_{12} \end{bmatrix} \begin{bmatrix} \mathbf{s}_1 & -\mathbf{s}_2^* \\ \mathbf{s}_2 & \mathbf{s}_1^* \end{bmatrix} + \begin{bmatrix} \boldsymbol{\eta}^{t_1} & \boldsymbol{\eta}^{t_2} \end{bmatrix} \tag{6.14}$$

where $\mathbf{Y}^{t_1} = \begin{bmatrix} y_1^{t_1} & y_2^{t_1} & \cdots & y_{N_c}^{t_1} \end{bmatrix}^T$ is the OFDM received symbol at time t_1. Similarly, $\boldsymbol{\eta}^{t_1}$ is the complex AWGN vector of all subcarriers of zero mean and variance $N_0/2$ per dimension. Furthermore, the OFDM channel matrix in the frequency domain between transmit antennas n and receive antenna m is:

$$\mathbf{H}_{mn} = \begin{bmatrix} h_{mn,1} & 0 & \cdots & 0 \\ 0 & h_{mn,2} & \cdots & 0 \\ \vdots & \vdots & \ddots & \vdots \\ 0 & 0 & \cdots & h_{mn,N_c} \end{bmatrix} \tag{6.15}$$

where $h_{mn,l}$ is the complex Gaussian channel coefficient of the l^{th} subcarrier of zero mean and variance 0.5 per dimension. The $diag\left(\mathbf{H}_{mn}\right)$ is as defined in (6.10).

Since the OFDM system transforms FSC into N_c parallel flat fading channel as apparent in (6.15), the STBC combiner operates on each subcarrier separately. The STBC received signal at the i^{th} subcarrier is:

$$\begin{bmatrix} y_i^{t_1} & y_i^{t_2} \end{bmatrix} = \begin{bmatrix} h_{11,i} & h_{12,i} \end{bmatrix} \begin{bmatrix} s_{1,i} & -s_{2,i}^* \\ s_{2,i} & s_{1,i}^* \end{bmatrix} + \begin{bmatrix} \eta_i^{t_1} & \eta_i^{t_2} \end{bmatrix} \tag{6.16}$$

it is rearranged into:

$$\begin{bmatrix} y_i^{t_1} \\ y_i^{t_2*} \end{bmatrix} = \begin{bmatrix} h_{11,i} & h_{12,i} \\ h_{12,i}^* & h_{12,i}^* \end{bmatrix} \cdot \begin{bmatrix} s_{1,i} \\ s_{2,i} \end{bmatrix} + \begin{bmatrix} \eta_i^{t_1} \\ \eta_i^{t_2*} \end{bmatrix} \tag{6.17}$$

After that a STBC combiner is used to estimate the IQ coded symbols as illustrated in (6.7). Then the uncoupled estimates are deinterleaved and passed to the IQ-trellis decoders.

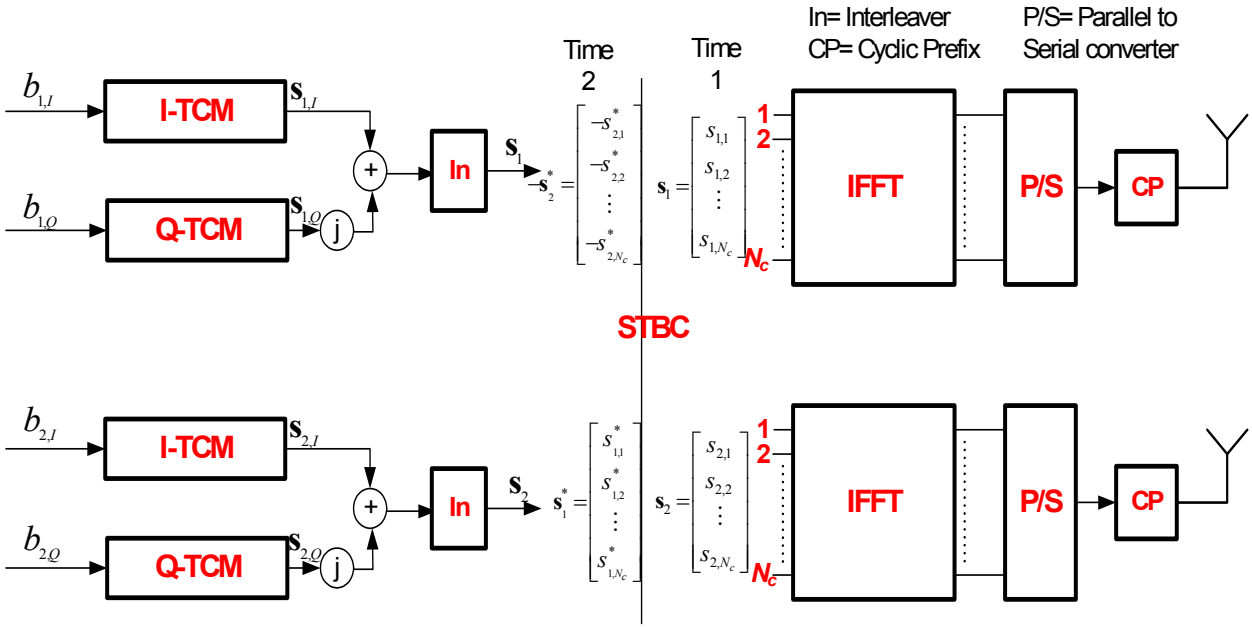

Figure 6.7: Block Diagram of IQ-SFT Encoder

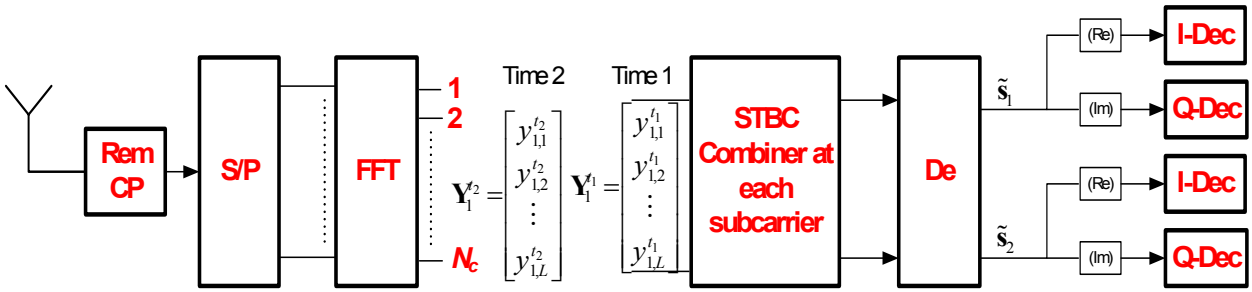

Figure 6.8: Block Diagram of IQ-SFT Decoder at one receive antenna

6.4 Performance Comparison of SFT Codes

This section compares the performance of the IQ-SFT code with other codes at 2 bps/Hz efficiency. The IQ concatenated code uses the IQ-16QAM TCM code as described in Figure 6.3. Its performance is compared to a conventional 8PSK TCM code designed for rapid fading channels [Jam94] and to Tarokh's STTC. Table 6.1 calculates the complexity of the SFT codes needed to achieve full spatial-frequency diversity ($M_T L M_R$). Since Tarokh's STTC is a joint design, it needs to have at least $l_{min}=M_T L$ to achieve full diversity. On the other hand, the concatenated TCM-STBC provides spatial diversity by STBC and frequency diversity by TCM. This explains the huge reduction in complexity of the concatenated codes compared to Tarokh's code. In addition, the IQ codes further reduce the number of states of conventional TCM by factor of power of two. If the number of states for the IQ-16QAM code is x, then it is x^2 for the 8PSK TCM code.

The BER performance of the SFT codes over four taps FSC is shown in Figure 6.9. The codes have 8-states and the receiver has one antenna. The interleaver is a block interleaver of width four. At 8-states, the frequency diversity of the IQ code is four while it is two for the 8PSK and Tarokh's QPSK codes. Thus, the IQ TCM-STBC code achieves full diversity of order 8 while the conventional TCM-STBC code provides a diversity of order 4. Tarokh's QPSK code only achieves a diversity of order 2 and its slope is parallel to the uncoded STBC.

For FSC of length two, the BER performance is shown in Figure 6.10. In this case, the maximum frequency diversity available is two and it is achieved by both concatenated schemes.

Therefore, there are no additional diversity gains for the IQ code as apparent from the parallel slopes. However, the IQ code adds some coding gain (around 1.5dB at BER=10^{-4}).

Table 6.1: Complexity of SFT codes at 2bps/Hz and M_T=2 transmit antennas

FCS Length	Minimum number of states to achieve full diversity ($M_T L M_R$)		
L	Tarokh QPSK	8PSK	IQ-16QAM
2	64	4	2
3	1024	16	4
4	16384	64	8
5	262144	256	16
6	4194304	1024	32
7	67108864	4096	64

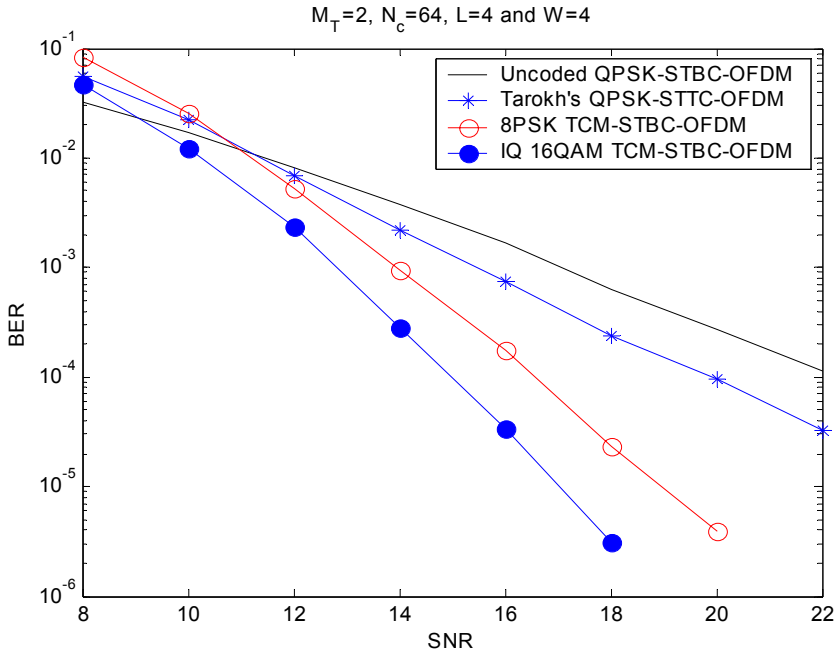

Figure 6.9: Performance comparison of 8 States SFT codes over four taps frequency selective channels.

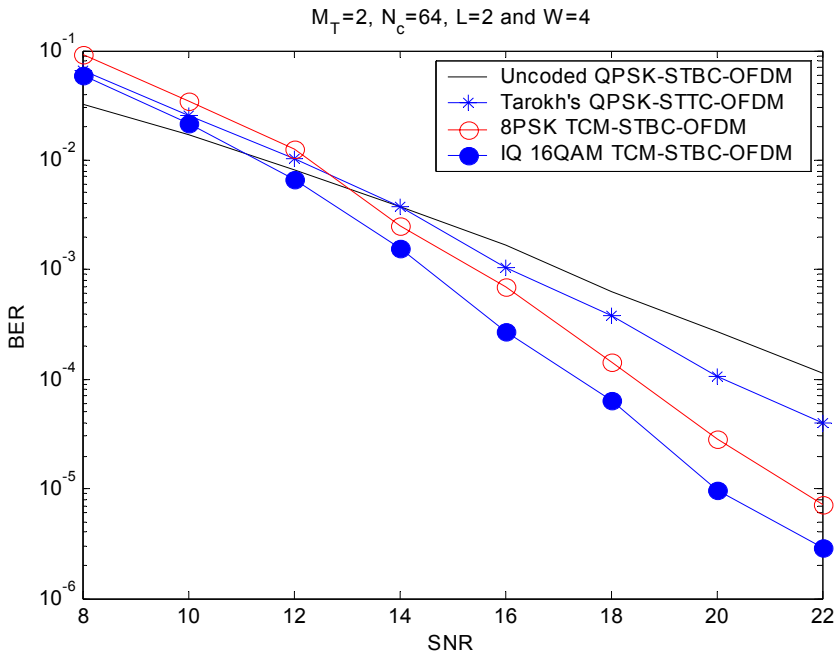

Figure 6.10: Performance comparison of 8 States SFT codes over two taps frequency selective channels.

6.4.1 Interleaving Effect

The effect of interleaving on the frequency diversity is investigated in this chapter. We consider a block interleaver and examine the effect of its width. A block interleaver read symbols row by row and output them column by column. We consider width lengths of power two so that it divides N_c.

The effect of a block interleaver width at four rays FSC, N_c=64 subcarriers and over 2×1 MIMO-OFDM channels is shown in Figure 6.11. The simulated SFT code is the 8-states IQ-16QAM TCM-STBC and it can take full advantage of the available spatial-frequency diversity. However, the result shows that the diversity obtained is highly dependent on the interleaver width (W). The best performance is at W=4 and 8.

It has been shown in [Wan04] that the optimal interleave in a SF coded OFDM system should separate any consecutive codeword symbols by a multiple of N_c / L in order to maximize the coding gain, which is impossible to build [Wan04]. However, a block interleaver with a width of L and a depth of N_c / L will separate successive symbols by N_c / L or $N_c - N_c / L - 1$. Therefore, a block interleaver with a width of L is nearly optimal. However, after examining the interleaver design for a few cases, we found that a width of L is not always the best choice. This happens if the FSC has low number of rays. Specifically, at L=2 paths and N_c=64 subcarriers, the simulation result doesn't support the claim that the best block interleaver width should be two, as can be interpreted from Figure 6.12. The coded system got more gain and diversity at width of four and eight. However, in other cases, such as L=4 and 8 in Figures 6.11 and 6.13, respectively, the best performance happens at W=L in additional to other width values such as 2L.

As an attempt to explain the effect of interleaving, we examine the channel correlation in the frequency domain as a function of the distance between OFDM bins, as shown in Figures 6.14 to 6.16. We assumed that the FSC rays are independent and have equal power. Thus, the correlation matrix ($\mathbf{C}_h$) in (6.12) is the identity matrix. The plots are for the correlation between the channel coefficient of the first subcarrier and all others ($\boldsymbol{\rho}_1$). The correlation vectors starting with other subcarriers are cyclically shifted version of $\boldsymbol{\rho}_1$. These figures show the effect of interleaving on the correlation. By sitting the block interleaver width to *L*, the correlations between $\mathbf{h}^f(1)$ and the next *L*-1 values are zero, as can be seen in Figures 6.14 and 6.15. However, this isn't always the best interleaver design as we saw with the case of two rays FSC. The reason might be that there is a high transition between the correlation values in the case of *L*=2 and W=2 (Figure 6.14). For example, $\rho_{12} = 0$ and $\rho_{13} = 0.9976$. On the other hand, at *L*=2 and W=4 (Figure 6.16), the correlation between $\mathbf{h}^f(1)$ and the next three subcarriers is low and it doesn't jump to high values until the fifth subcarrier. This may explain the performance improvement at W=4.

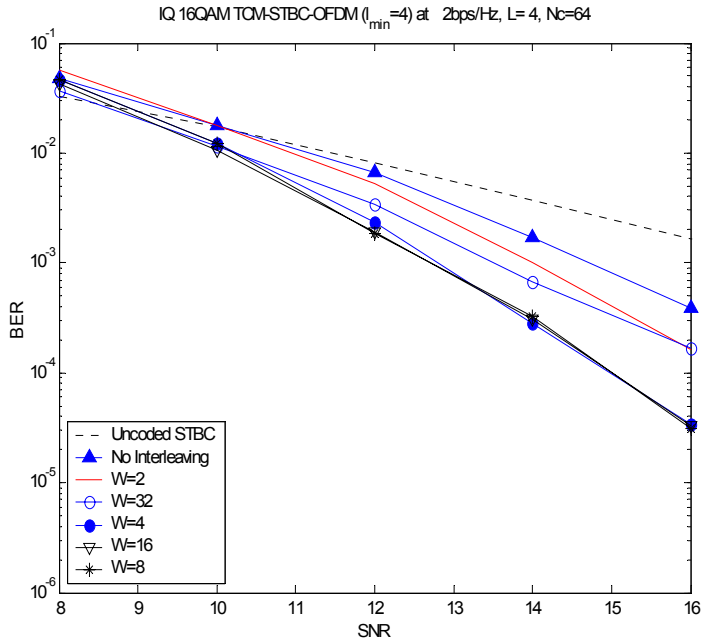

Figure 6.11: Effect of interleaving on the diversity and gain of the IQ-TCM-STBC-OFDM system at 2x1 MIMO channels and at four rays FSC.

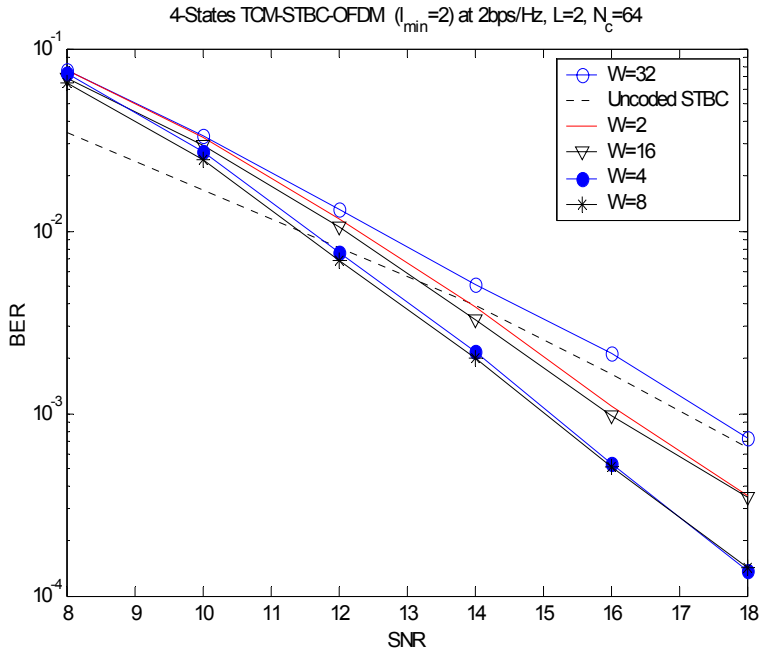

Figure 6.12: Interleaving effect of 4-states TCM-STBC-OFDM at a two rays frequency selective channel

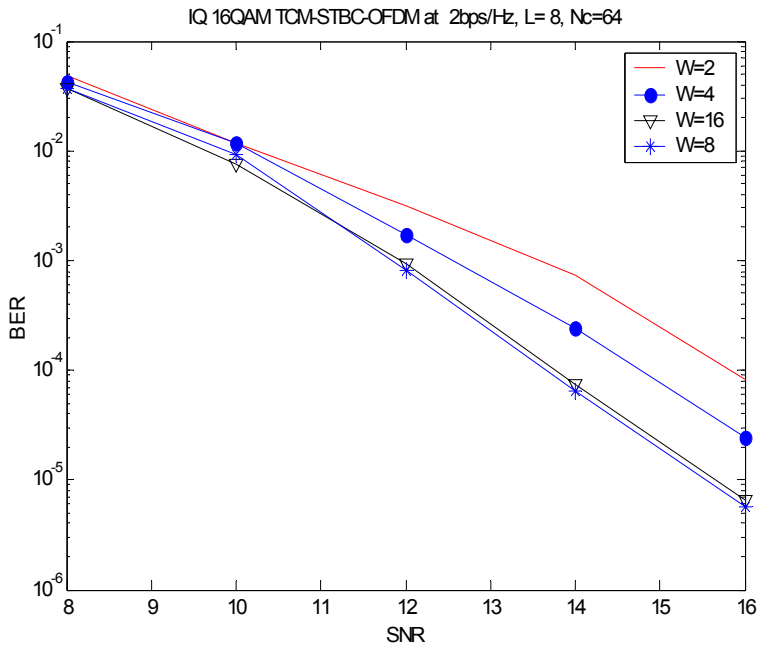

Figure 6.13: Effect of interleaving on the diversity and gain of the IQ-TCM-STBC-OFDM system at 2x1 MIMO channels and at eight rays FSC.

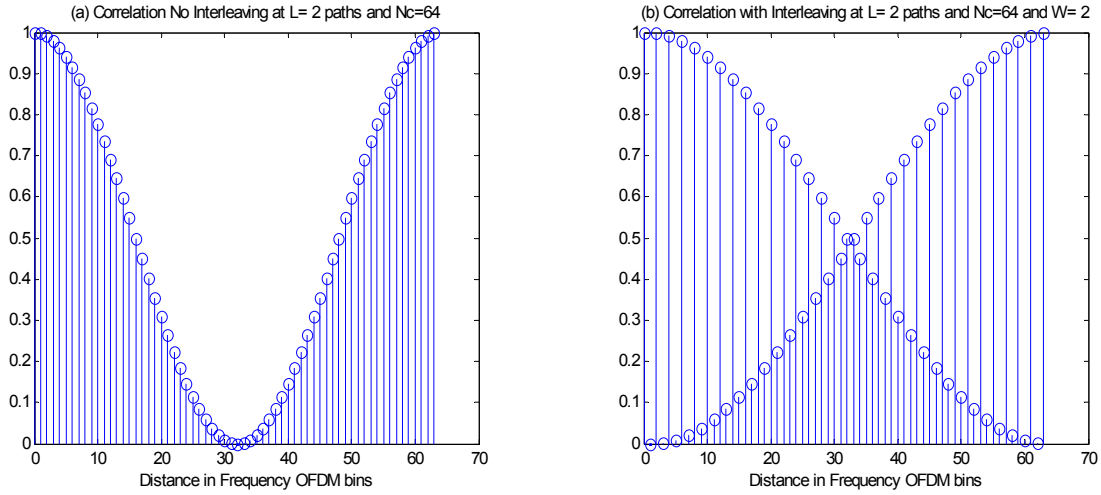

Figure 6.14: Correlation of the channel coefficient in the frequency domain for a two rays independent FSC and 64 subcarriers and an interleaver width of two.

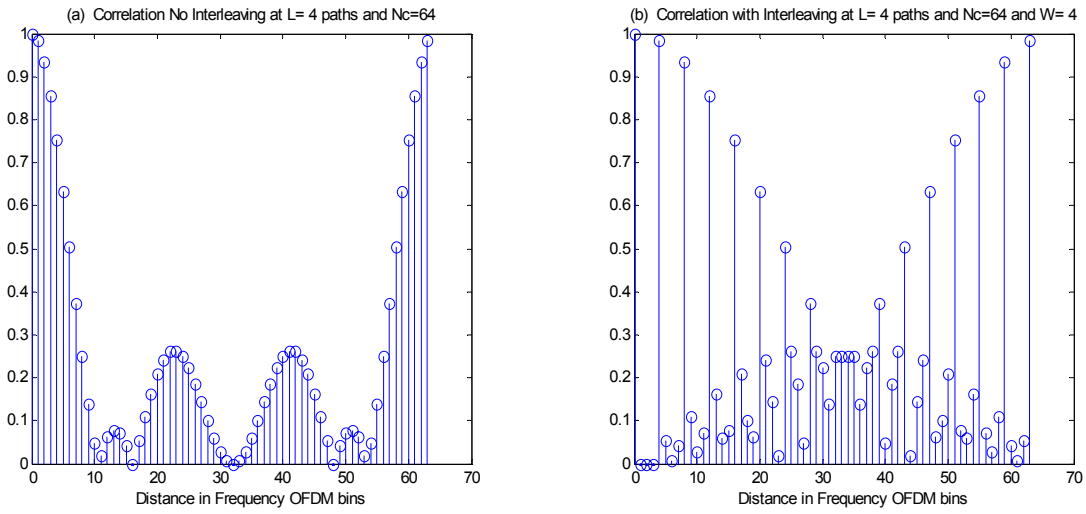

Figure 6.15: Correlation of the channel coefficient in the frequency domain for a four rays independent FSC and 64 subcarriers and an interleaver width of four.

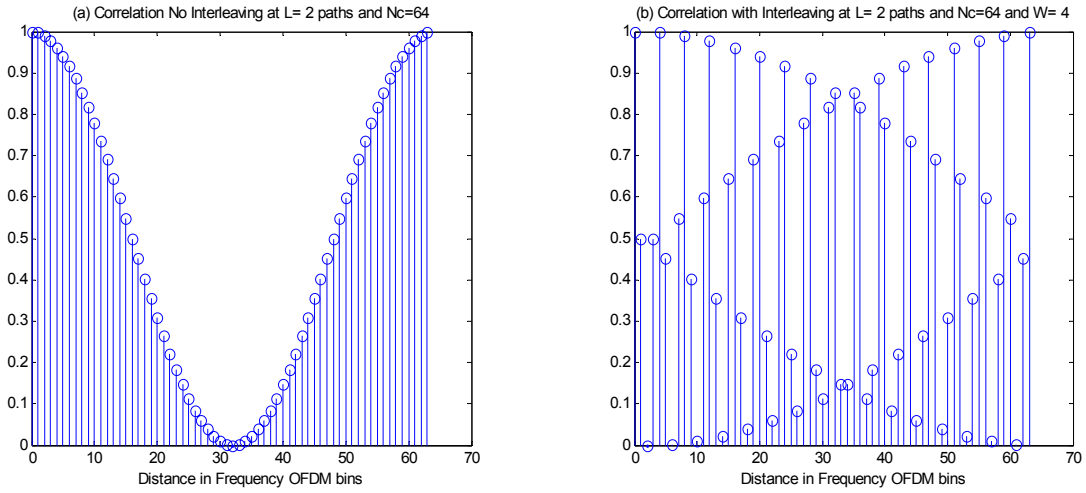

Figure 6.16: Correlation of the channel coefficient in the frequency domain for a two rays independent FSC and 64 subcarriers and an interleaver width of four.

6.5 Multi-Layered IQ-SFT Coded Systems

We evaluated the performance of several detection algorithms for MLSTBC-OFDM systems in a previous chapter. However, we didn't exploit the available frequency diversity in the frequency selective channel. Therefore, we concatenate bandwidth efficient codes that take advantage of this diversity without sacrificing the data rate. That is the motivation behind concatenating IQ-TCM with the MLSTBC-OFDM system and we refer to it as multi-layered IQ space frequency time codes (MLIQSFT).

6.5.1 System Model

The MLIQSFT coded system consists of K parallel IQ-SFT codes. Each code is described in details in Figure 6.7. . Each encoder consists of N_G antennas and is called a group. Thus, the total number of transmit antennas is M_T=$K \cdot N_G$. The receiver has M_R receive antennas. The information bits encoded by each encoder are called a layer. A bock diagram of the multi-layered system is shown in Figure 6.17. At the receiver and after OFDM demodulation, the multi-layered received signal at the i^{th} subcarrier over T time slots, where T is the STBC length, is:

$$\begin{aligned}\mathbf{y}_i &= \mathbf{H}_i \mathbf{x}_i + \boldsymbol{\eta}_i \\ &= \begin{bmatrix}\mathbf{H}_{1,i} & \mathbf{H}_{2,i} & \cdots & \mathbf{H}_{K,i}\end{bmatrix} \begin{bmatrix}\mathbf{x}_{1,i} \\ \mathbf{x}_{2,i} \\ \vdots \\ \mathbf{x}_{K,i}\end{bmatrix} + \boldsymbol{\eta}_i\end{aligned} \tag{6.18}$$

where $\mathbf{y}_i$ is an $M_R \cdot T \times 1$ received signal, $\mathbf{H}_{k,i}$ is an $M_R \cdot T \times N_G$ orthogonal channel matrix for the k^{th} group, $\mathbf{x}_{k,i}$ is the $N_G \times 1$ transmitted symbols from the k^{th} group, which are the IQ-trellis coded symbols, and $\boldsymbol{\eta}_i$ is an $M_R \cdot T \times 1$ AWGN vector. To get to the above model, we used the

property of the short code length to rearrange the received matrix to a vector as done in (6.17) for a single group.

In the next section, different multi-layered detection techniques will be compared. They have one common operation which is group interference nulling. It needs to be done at each subcarrier since the MIMO channel at each frequency tone is different. Based on an ordering criterion, assume that the first detected group is the k^{th} group. Then, the algorithm calculates the orthonormal bases of the null space of $\mathcal{H}_{k,i}$, which is the channel matrix of all interfering groups at the i^{th} subcarrier:

$$\mathcal{H}_{k,i} = \left[\mathbf{H}_{1,i} \quad \cdots \quad \mathbf{H}_{k-1,i} \quad \mathbf{H}_{k+1,i} \quad \cdots \quad \mathbf{H}_{K,i} \right] \tag{6.19}$$

Denote the orthonormal bases of $\mathcal{H}_{k,i}$ by $\mathcal{N}_{k,i}$, the received signal for the k^{th} group after nulling is:

$$\tilde{\mathbf{y}}_{k,i} = \mathcal{N}_{k,i} \mathbf{y}_i = \tilde{\mathbf{H}}_{k,i} \mathbf{x}_{k,i} + \tilde{\boldsymbol{\eta}}_{k,i} \tag{6.20}$$

where $\tilde{\mathbf{H}}_{k,i}$ is the resultant channel matrix after nulling. Then, the STBC combiner is used to estimate the IQ-TCM symbols at the i^{th} subcarrier. The Frobenius norm (FN) of the k^{th} group at the i^{th} subcarrier is defined as:

$$\text{FN}_{k,i} = \frac{1}{T} \left\| \tilde{\mathbf{H}}_{k,i} \right\|_F^2, \text{ where } \left\| \mathbf{A} \right\|_F^2 = trace\left(\mathbf{A}^H \mathbf{A} \right) \tag{6.21}$$

FN is divided by T because the dimension of the channel matrix has been increased T times after rearranging the original channel matrix.

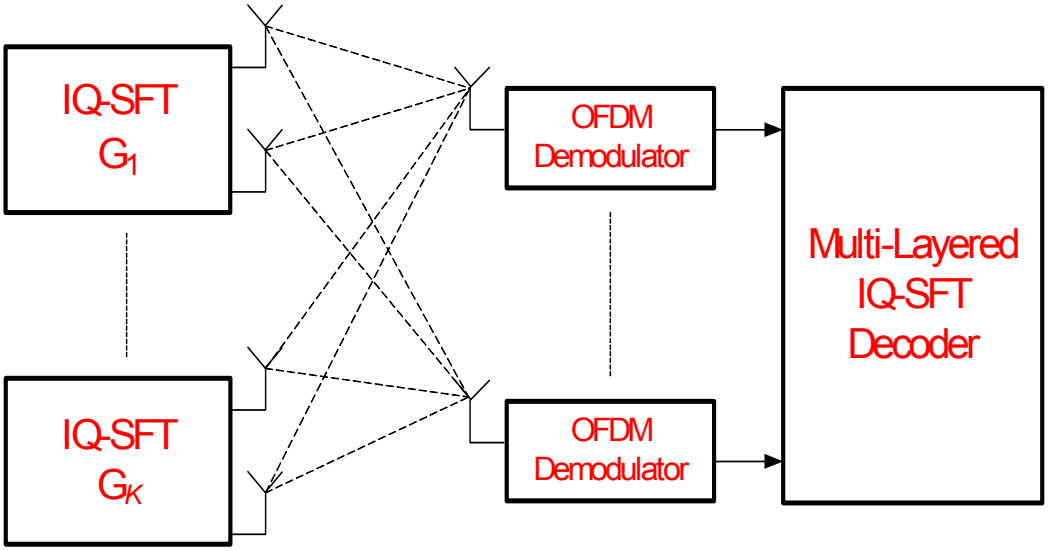

Figure 6.17: Block diagram of a MLIQSFT coded system

6.5.2 Multi-Layered Detection Algorithms

Serial and parallel detection algorithms are described in this section. We also present and compare different ordering criteria for the serial algorithm.

Serial interference nulling/ decoding and cancellation

This algorithm operates on the MIMO received signal in the frequency domain after FFT. This algorithm serially nulls out interfering OFDM symbols without ordering as described in Figure 6.18. Ordering is not a straight forward operation because each subcarrier has a different channel and the ordering needed to be done at the OFDM symbol level since each OFDM symbol is a codeword. Different ordering criteria are discussed in the next section.

At each subcarrier, the algorithm calculates the orthonormal bases of the null space of the interfering groups. After that, an STBC combiner is used to uncouple the space time symbols at each subcarrier. These soft outputs and the channel information are passed to the IQ-trellis decoders. Then, the symbols of the first layer are regenerated and their contributions are subtracted from the received signal. This process is repeated serially to detect each IQ coded layer.

Ordering criteria

Ordering is very essential in serial processing since detecting strong layers first result in less error propagations to successive layers and hence improves the performance of the system. In this section, we propose and evaluate the performance of several ordering criteria. They are described as follows:

- Post-nulling ordering with hard detection: In this method, ordering is done at each subcarrier using the SGINC algorithm, which is descried in Chapter 4. The algorithm performs ordering and detection based on maximum post-processing Frobenius norm of each layer at each subcarrier. It is the same as the uncoded MLSTBC-OFDM detection. Thus, the output of the multi-layered detection stage is hard symbols which are interleaved and passed to the IQ-trellis decodes. Obviously, the drawback of this approach is the hard detection and the separation between interference nulling and cancellation and IQ-trellis decoding. This hard detection approach severely degrades the performance of the decoder.
- MaxMin FN: this approach orders whole OFDM symbols instead of per carrier bases. The serial nulling/ decoding and cancellation algorithm is similar to the unordered case which has the advantage of soft symbol decoding. The algorithm first calculates

FNs of the MIMO channels at each subcarrier for all groups then the group that has the maximum minimum FN is detected first. Therefore, this method takes into account the worst case scenario. After selecting the best layer based on this ordering criterion, the interfering layers are nulled out and the soft output from the STBC combiner is passed to the IQ-trellis decoder and the process continues as described in Figure 6.18. FNs of the MIMO channels can be calculated pre-nulling or post-nulling. Post-nulling is more complex since the algorithm nulls at each subcarrier. The system performance is compared for these two approaches.

- MaxAverage FN: this ordering criterion is similar to the MaxMin FN but instead of selecting the min FN, the algorithm calculates the average FN and orders based on it.
- Blind power allocation: this method doesn't do ordering at the receiver. Instead, the power at the transmitter is distributed unequally among the groups such that the first detected group has the highest power. It pre-selects the order of detection. This compensate for the less receive diversity advantage for earlier detected groups. Since the consider systems in this study are open loop, the power allocation is done blindly without channel state knowledge, similar to [Tar99]. The power is distributed so that there is a 3dB difference between consecutive groups. Meanwhile, the sum is constant and equal to a single transmit antenna power. Group k is multiplied by the following power allocation factor:

$$w_k = \sqrt{\alpha 2^{K-k}}; \text{ where } \alpha = \frac{1}{N_G \sum_{k=1}^{K} 2^{K-k}} \tag{6.22}$$

Parallel nulling/ decoding and cancellation

The parallel processing doesn't need ordering. It nulls all groups at the same time as illustrated in Figure 6.19. Then, each group space time symbols are uncoupled and estimated by the STBC combiner. After de-interleaving, the output of the combiner is decoded by the IQ trellis decoder. Then the codewords are regenerated and interleaved. After that, parallel cancellation is done at each subcarrier. The output of the cancellation stage is de-interleaved and IQ trellis decoded. This iterative parallel processing is repeated until diminishing returns are observed.

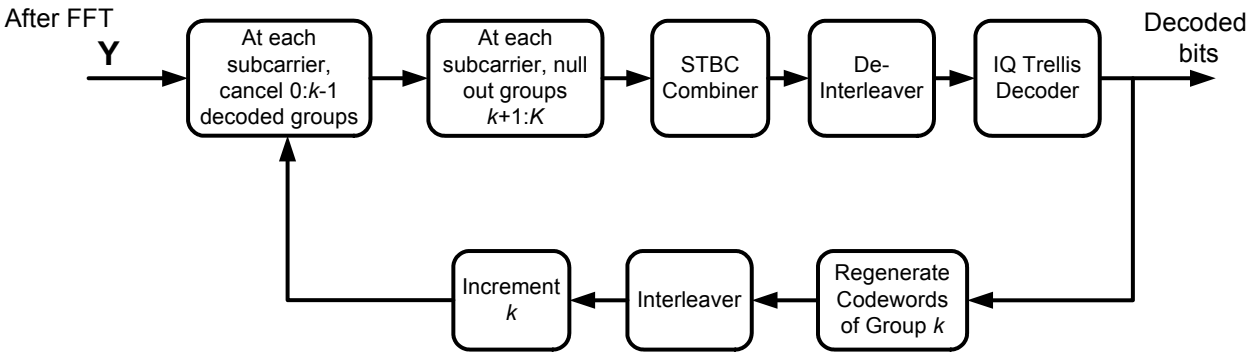

Figure 6.18: Block diagram of the serial soft nulling/ decoding and cancellation algorithm

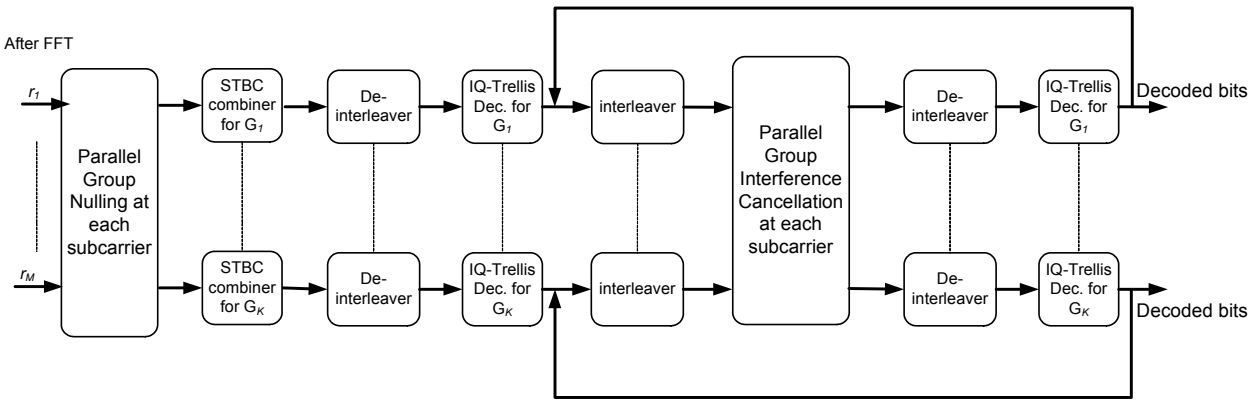

Figure 6.19: Block diagram of the parallel nulling/ decoding and cancellation algorithm

6.5.3 Simulation Results

In this section, we evaluate the BER performance of the MLIQSFT detection algorithms. The serial detection algorithms are compared in Figure 6.20. The hard nulling with ordering performs worse than no ordering because the trellis decoder suffers from hard detection. The result also shows that the different ordering criteria, which are at the receiver, perform very close to each other. Thus, performing ordering based on pre-FN is more computational efficient while its performance is very close to the post-FN ordering. On the other hand, power allocation at the transmitter performs the best with less complexity than ordering since the order is fixed. This shows that the unequal power allocation greatly benefits the serial detection and cancellation algorithm. At BER of 10^{-3}, around 1dB is gained by ordering and around 2dB is gained by the blind power allocation at the transmitter.

Performance with parallel detection and cancellation is shown in Figure 6.21. The iterative processing gives diminishing returns after four iterations. It gains around 4.5 dB after

four iterations compared to no iterations. When it is compared to the ideal performance of no cancellation, it is 6 dB far. Perfect cancellation is a lower bound and it has full receive diversity.

Figure 6.22 compares the performance of the serial and parallel processing for the MLIQSFT codes. The parallel processing at four iterations gained around 1dB compared to the serial with power allocation. The diversity advantage of the IQ coded system is apparent from the result when compared to the uncoded MLSTBC-OFDM system. The coded plots have sharper slopes as a result of achieving full frequency diversity.

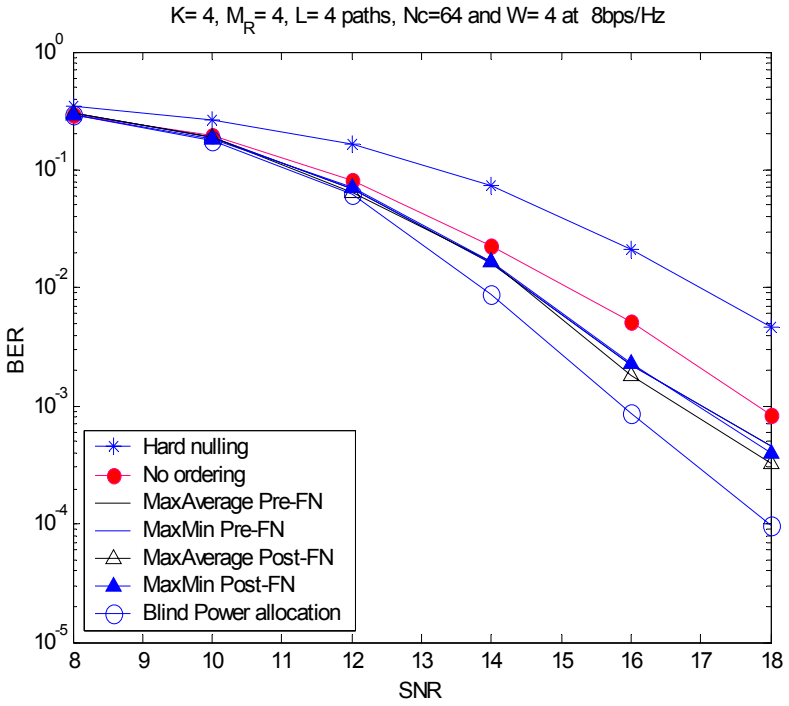

Figure 6.20: Performance comparison of serial detection algorithms for MLIQSFT codes

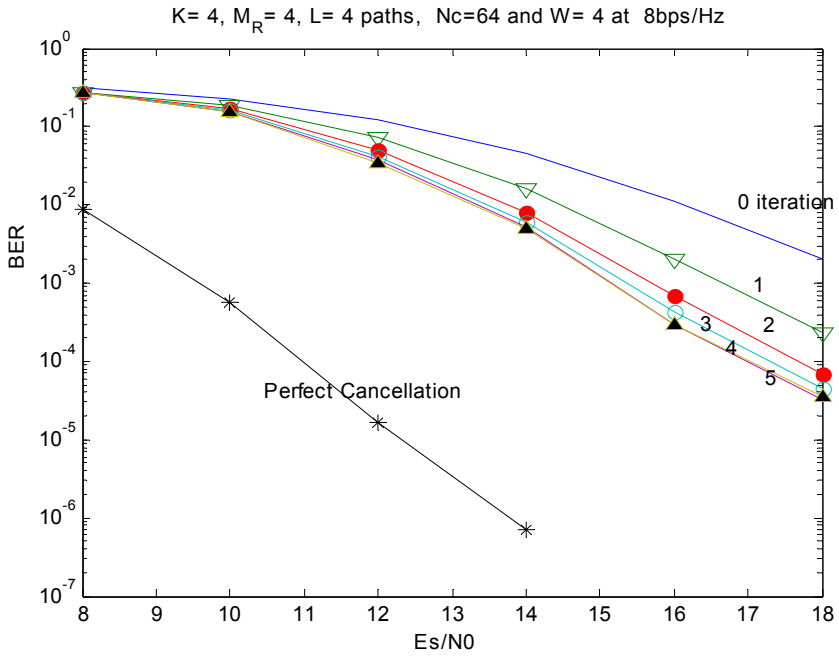

Figure 6.21: Performance of MLIQSFT codes with parallel iterative detection

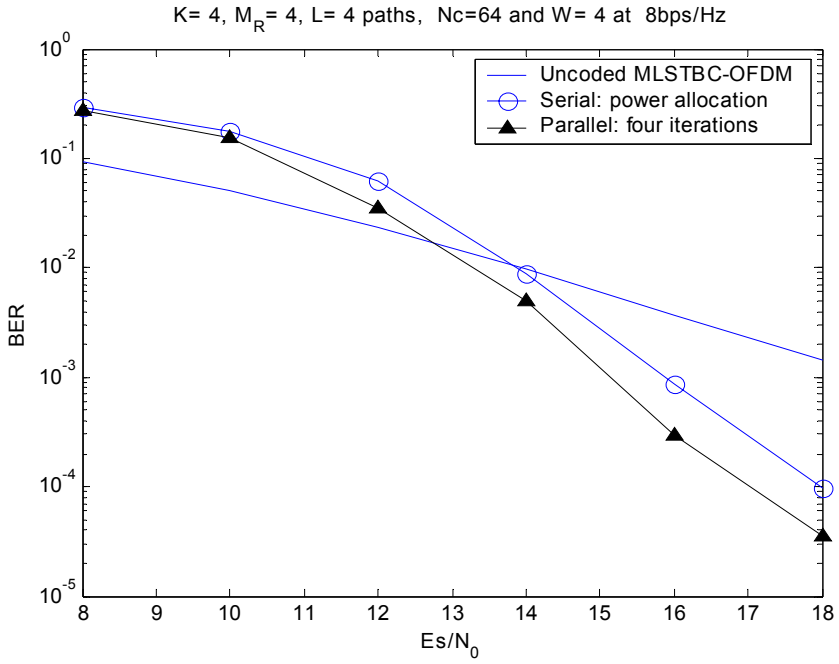

Figure 6.22: Performance comparison of serial and parallel detection for MLIQSFT codes.

6.6 Chapter Summary

In this chapter, we considered the design of bandwidth efficient space frequency time codes for MIMO-OFDM systems. Our approach was to concatenate trellis codes with space time block codes. The concatenated system separates frequency coding from space time coding and it has much lower complexity than a joint design. The design criterion of the trellis code is to have large minimum effective length in order to capture the available frequency diversity. In order to provide larger effective lengths at a low complexity, we adapted IQ-trellis codes which were originally designed for rapid fading channels. In addition, interleaving is very essential in order to mitigate for the highly correlated OFDM channel in the frequency domain. Therefore, we examined the effect of interleaving on the performance of the codes and on the achieved diversity. Finally, we compared and evaluated the performance of serial and parallel detection algorithms for multi-layered IQ space frequency time codes. This multi-layered architecture is a spatial multiplexing scheme with spatial and frequency diversity at each layer.

The main results of this study show the performance improvements of IQ-TCM over conventional TCM at the same number of states and spectral efficiency. The reason for that is the larger effective length of IQ-TCM. Also, the simulation results emphasize the importance of an appropriate interleaver design since there is a great loss in performance and diversity if the block interleaver is not designed carefully. Finally, the multi-layered IQ-coded scheme performs much better than the uncoded one. The parallel processing slightly outperforms the other detection algorithms.

Chapter 7
Uplink Scheduling for Multiuser Systems with Spatial Multiplexing

In this chapter, we study uplink scheduling for multiple user systems employing spatial multiplexing where the application is delay-tolerant. The scheduler selects one user at a time based on a scheduling criterion that depends on the detection algorithm. Each user spatially multiplexes his data over the transmit antennas. This spatial multiplexing (SM) scheme provides high data rates while a multi-user diversity obtained from scheduling improves the performance of the uplink system. Both V-BLAST detector and the sphere decoder are considered. The main results of this study show that the scheduler that maximizes the optimal MIMO capacity doesn't work well for a V-BLAST system. Instead, we find that a scheduler that maximizes the V-BLAST capacity is one which is derived specifically from the V-BLAST detection algorithm. Furthermore, we investigate suboptimal schedulers and their performance. In addition, we look into scheduling for SM with sphere decoding and we find that in this case, using MIMO capacity as the scheduling criterion is the best.

7.1 Introduction

Until recently, most of the studies on MIMO techniques have focused on optimizing the physical layer. However, in a multiuser environment, optimizing the physical layer for each user doesn't necessarily optimize the system performance nor does it take advantage of the statistical independence of the fading channels among the users. Furthermore, different users have different needs in terms of data rates, power limits and Quality of Service (QoS). These requirements make scheduling an important technique for optimizing the performance of a communication system and utilizing the system resources efficiently. Since the physical link of each user is a fading channel, and it is usually independent from one user to another, scheduling transmission to the user with the best channel conditions at each time leads to a form of selection diversity known as multiuser diversity. In general, schedulers are designed to maximize system throughput, capacity, and minimize error rates, but they also should provide fairness to users and minimize packet delays. In addition, scheduling is used to minimize interference, adapt to traffic loads, and satisfy a quality-of-service (QoS) requirement.

Scheduling is sometimes classified under radio resource management, cross-layer optimization or multiuser diversity. In single-input single-output (SISO) systems, where each mobile and the base station have one antenna, it was shown that selecting the user who has the maximum signal to noise ratio (MaxSNR) maximizes the total information capacity of the uplink system [Kno95]. Similar results were also found for the downlink from the base station to the mobile unit [Tse97]. This scheduler is known as MaxSNR scheduling. Over MIMO channels, most of the studies are based on theoretical information capacity [Hea01] [Air03] [Rea04] and on

the downlink, which is the broadcast channel from the base station to the mobile unit. It has been shown in [Goz03] that space time block coding (STBC) and scheduling aren't a good match. In fact, scheduling to a user with single antenna outperforms scheduling using STBC. The reason is that STBC averages the fades while the scheduler tends to benefit from high peaks in the fading channel. In addition, multiuser diversity obtained from scheduling is much higher than the spatial diversity of STBC, so STBC diversity doesn't add much benefit. On the other hand, spatial multiplexing (SM) schemes are more synergistic with scheduling. That is because they provide high data rates while the scheduler compensates for the lack of diversity by providing multiuser selection diversity.

In a MIMO system, scheduling could be done to a single user or multiple users. Scheduling to multiple users (i.e allowing more than one user to transmit or receive at the same time) is shown to be optimal in terms of maximizing system capacity and throughput. In [Hea01], downlink scheduling to multiple users improved the average throughput compared to single user scheduling. Furthermore, the optimal uplink MIMO scheduling based on an information theoretical approach was considered in [Lau02]. They showed that the scheduler should allocate all the power to at most M_R users, where M_R is the number of receive antennas at the base station. Also, they found that the optimal power resource allocation is water-filling in space and time. In [Air03], the authors found that multiuser scheduling reduces the average delay experienced by the users compared to single-user scheduling. In [Shi03], the scheduler selects K users at a time and it cycles through groups of users in a round robin (RR) fashion. Thus, it provides diversity through multiple antennas while it insures fairness through RR scheduling.

In this chapter, we investigate scheduling on the uplink, where users employ V-BLAST. We focus on single-user scheduling. Although it is not optimal, it is more practical and easily

implemented. The search space for best transmission is much less than the multiuser case and a multiuser diversity of order K, where K is the number of users, can be achieved. Also, the multiuser scheduling requires strict synchronization among the different users. Thus, our scheduler selects one user at a time based on a certain criterion. Each user spatially multiplexes their data over the transmit antennas to provide high data rates while the multiuser diversity obtained from scheduling improves the performance of the uplink. Our main contribution in this work is finding the capacity maximization scheduling criteria for V-BLAST uplink users. Also, we show that the optimal MIMO capacity criterion doesn't work well for V-BLAST. The V-BLAST maximum capacity scheduler is derived specifically from its detection algorithm. Furthermore, we investigate the performance of suboptimal scheduling criteria that are based on the MIMO channel matrix directly. Finally, we look into scheduling for spatial multiplexing with sphere decoding and in this case, scheduling based on maximum MIMO capacity provides the best performance.

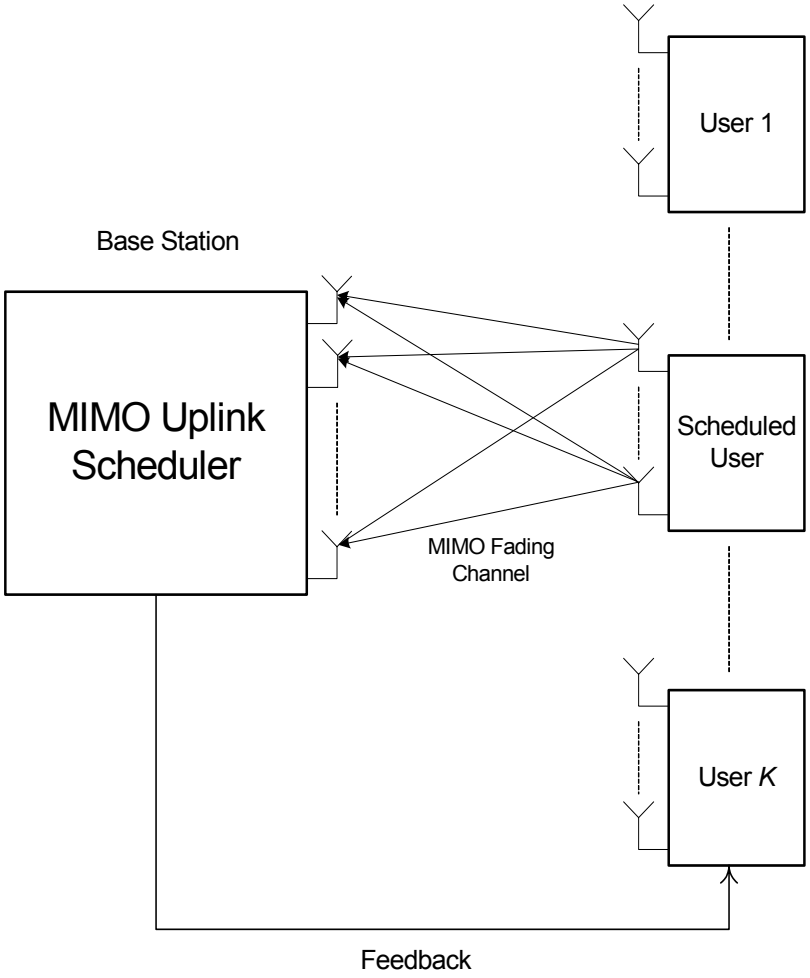

Figure 7.1: Uplink MIMO Scheduling

7.2 System Model

We consider scheduling for a single user at a time. The average SNR is assumed to be the same for all users; they are either at similar distance or they use loose power control. There are K users and each user transmits through M_T transmit antennas and the base station receiver has M_R receive antennas. The MIMO channel is assumed to be an independent Rayleigh flat fading MIMO channel where each coefficient is an i.i.d complex Gaussian random variable with zero mean and unit variance. The received signal from user k is:

$$\mathbf{y}_k = \mathbf{H}_k \mathbf{x}_k + \boldsymbol{\eta}_k \tag{8.1}$$

where $\mathbf{y}_k$ is an $M_R \times 1$ received vector, $\mathbf{H}_k$ is an $M_R \times M_T$ MIMO channel matrix for the k^{th} user, $\mathbf{x}_k$ is an $M_T \times 1$ transmitted symbols from user k, and $\boldsymbol{\eta}_k$ is an $M_R \times 1$ i.i.d complex AWGN vector of zero mean and variance $N_0/2$ per dimension.

7.3 Optimal MIMO scheduling

Assuming that optimal MIMO encoder and decoder are available, the optimal MIMO scheduler selects the user whose channel matrix maximizes MIMO capacity:

$$\begin{aligned} C_{\max} &= \max_{k=1,2,\ldots,K} C_k \ ; \text{where} \\ C_k &= \log_2\left(\det\left(\mathbf{I}_{M_R} + \frac{SNR}{M_T}\mathbf{H}_k\mathbf{H}_k^H\right)\right) \end{aligned} \tag{8.2}$$

where $\mathbf{I}_{M_R}$ is the identity matrix and $\mathbf{A}^H$ is the conjugate-transpose (Hermitian) of $\mathbf{A}$.

Assuming that $M_T \leq M_R$, then:

$$C_k = \sum_{n=1}^{M_T} \log_2\left(1 + \frac{SNR}{M_T}\lambda_n(\mathbf{H}_k)\right) \tag{8.3}$$

where $\lambda_n(\mathbf{H}_k)$ is the n^{th} eigenvalue of $\mathbf{H}_k\mathbf{H}_k^H$. The maximum capacity is achieved when the channel is orthogonal [Fos98] and in this case, $\lambda_n(\mathbf{H}_k) = \|\mathbf{H}_k\|_F^2$, for $n = 1,\ldots,M_T$, where $\|(\cdot)\|_F^2$ is the squared Frobenius norm. Then, the MIMO capacity will be:

$$C_k = M_T \log_2\left(1 + \frac{SNR}{M_T}\|H_k\|_F^2\right) \tag{8.4}$$

When $\mathbf{H}_k$ is orthogonal, the eigenspread of $\mathbf{H}_k\mathbf{H}_k^H$ will be one. The eigenspread is defined as the ratio of the largest eigenvalue to the smallest. This fact results in an eigenspread scheduling criterion, which will be explained in the next section.

7.4 V-BLAST Scheduling

V-BLAST [Wol98] is a practical MIMO architecture that spatially multiplexes transmitted data over multiple transmit antennas. Data transmitted from each antenna is called a layer of information. At the receiver, a serial interference nulling and cancellation algorithm is used to detect each layer. Although V-BLAST is a full spatial multiplexing scheme, it has poor energy performance because of the lack of spatial diversity. Therefore, it makes a good match with scheduling since multiuser diversity obtained improves the performance significantly.

This section proposes and evaluates scheduling algorithms for uplink V-BLAST users. It has been shown that in single antenna systems, selecting the user that has the maximum SNR (MaxSNR) is optimal [Kno95] and it maximizes the system information capacity. However, the MaxSNR scheduler is not optimal for V-BLAST users as will be seen later from the simulation results. The reason is that, unlike SISO systems, the received SNR $\left(trace(\mathbf{H}_k \mathbf{H}_k^H)\right)$ doesn't reflect directly the capacity of MIMO systems. Moreover, scheduling based on maximization of MIMO channel capacity as in (8.2) is also not optimal for V-BLAST since its detection algorithm is suboptimal. Since V-BLAST is an open loop system and all layers have the same rate, an outage in capacity will occur if an outage happens in at least one layer. Therefore, the V-BLAST capacity is dominated by the weakest layer and it is given by [Pap02]:

$$C_{VBLAST}^{ZF} = M_T \cdot \min_{i=1,2,\ldots,M_T} \left\{ \log_2 \left(1 + \frac{SNR}{M_T \left\| \mathrm{W}_{ZF,i} \right\|^2} \right) \right\} \qquad (8.5)$$

where $\mathrm{W}_{ZF,i}$ is the ZF projection row for the i^{th} layer and M_T is the number of layers (transmit antennas). Recall that the V-BLAST detector performs a series of interference nulling and

cancellation operations. At the n^{th} stage, let $\mathbf{H}_n$ be the MIMO channel matrix after canceling the n-1 detected layers. Then, the ZF matrix at this stage is:

$$\mathrm{W}_{ZF} = \left(\mathbf{H}_n^H \mathbf{H}_n\right)^{-1} \mathbf{H}_n^H \tag{8.6}$$

Based on the V-BLAST ordering criteria, the strongest layer for detection at this stage is the one with:

$$\left\|\mathrm{W}_{ZF,i}\right\|^2 = \min\left(diag\left(\left[\mathbf{H}_n^H \mathbf{H}_n\right]^{-1}\right)\right) \tag{8.7}$$

and its post-processing SNR is:

$$SNR_i^{ZF} = \frac{SNR}{M_T \left\|\mathrm{W}_{ZF,i}\right\|^2} \tag{8.8}$$

Therefore, the layer that determines the capacity of V-BLAST is the one with largest norm of the ZF projection row. Let $w_k = \max_{i=1,2,\ldots,M_T}\left\{\left\|\mathrm{W}_{ZF,i}^k\right\|^2\right\}$ be the value for user k, then the scheduler that maximizes the V-BLAST capacity will select the user with minimum w_k. In other words, the capacity maximization scheduling for V-BLAST is to select the user with largest post-processing SNR of his weakest layer. However, this scheduler needs to perform ZF nulling and ordering to the channel matrices of all users before selecting the best user, which requires a lot of computations. Therefore, we examine other suboptimal schedulers that are based on the received MIMO channels before V-BLAST processing. These schedulers don't take into account the V-BLAST structure. The first one chooses the user with the largest MIMO channel power $\left(trace\left(\mathbf{H}_k \mathbf{H}_k^H\right)\right)$ and we will refer to it as MaxSNR scheduler, which mimics the optimal scheduler for single antenna systems. The next scheduler measures the eigenspread of $\mathbf{H}_k \mathbf{H}_k^H$ and selects the user with the minimum eigenspread (MinES). The eigenspread is defined as:

$$s = \frac{\lambda_{\max}}{\lambda_{\min}} \tag{8.9}$$

where $\lambda_{\max}$ and $\lambda_{\min}$ are the largest and smallest eigenvalues of $\mathbf{H}_k \mathbf{H}_k^H$, respectively. The eigenspread gives insight into the orthogonality of the channel. The smaller the value of *s*, the closer the matrix is to be orthogonal. The minimum value of *s* is one, and it occurs when the channel matrix is orthogonal. The eigenspread is related to the condition number of $\mathbf{H}_k$ as:

$$\begin{aligned} s &= \text{cond}(\mathbf{H}_k)^2 \\ \text{where, } \text{cond}(\mathbf{H}_k) &= \frac{\rho_{\max}}{\rho_{\min}} \end{aligned} \tag{8.10}$$

where $\rho_{\max}$ and $\rho_{\min}$ are the largest and smallest singular values of $\mathbf{H}_k$. From this relation, we derive a scheduler that takes into account both the channel power and the eigenspread of $\mathbf{H}_k$. It selects the user that has the largest minimum singular value of $\mathbf{H}_k$. From (8.10), we have:

$$\begin{aligned} \frac{\rho_{\max}}{\rho_{\min}} &= \sqrt{s} \\ \rho_{\min} &= \frac{\rho_{\max}}{\sqrt{s}} \end{aligned} \tag{8.11}$$

Thus, selecting the largest $\rho_{\min}$ means selecting a large $\rho_{\max}$, which measures the norm of $\mathbf{H}_k$ and hence the power, and a small eigenspread (*s*). We will refer to this scheduler as MaxMinSV.

To summarize, the scheduling algorithms considered for V-BLAST are:

1- MaxVBLASTCapc: select the user with $\min_{k=1,\ldots,K} \{w_k\}$, where $w_k = \max_{i=1,2,\ldots,M_T} \left\{ \left\| \mathrm{W}_{ZF,i}^k \right\|^2 \right\}$ and $\mathrm{W}_{ZF,i}$ is defined in (8.7).

2- MinES: select the user with minimum eigenspread of $\mathbf{H}_k \mathbf{H}_k^H$ as defined in defined in (8.9).

3- MaxMinSV: select the user with maximum minimum singularvalue of $\mathbf{H}_k$.

4- MaxSNR: select the user with maximum Frobenius norm of $\mathbf{H}_k$ $\left(trace(\mathbf{H}_k \mathbf{H}_k^H)\right)$.

5- RR: round-robin scheduling allows each user to transmit in a time-division fashion.

7.5 Simulation Results

The BER performance of the wireless uplink system with scheduling is shown in Figure 7.2. The MaxSNR scheduler captures very little multiuser diversity and it gains around 1dB compared to the RR algorithm. On the other hand, the best scheduler is the one that maximizes V-BLAST capacity (MaxVBLASTCapc) by selecting the user who has the strongest weakest layer as described earlier. The MinES and the MaxMinSV schedulers capture the multiuser diversity but MaxMinSV provides more gain since it takes into account the power of the MIMO channel. They perform very close to MaxVBLASTCapc which has more diversity at high SNRs (sharper slope). The result in this figure also shows that using maximum MIMO capacity as the scheduling criterion, as in (8.2), doesn't perform very well for V-BLAST. The reason for that is the suboptimality of the V-BLAST detection algorithm.

The complementary cumulative distribution function (CCDF) of the capacity of V-BLAST uplink scheduling is shown in Figure 7.3. The result shows that the MaxMinSV and MinES schedulers perform very close to the MaxVBLASTCapc scheduler.

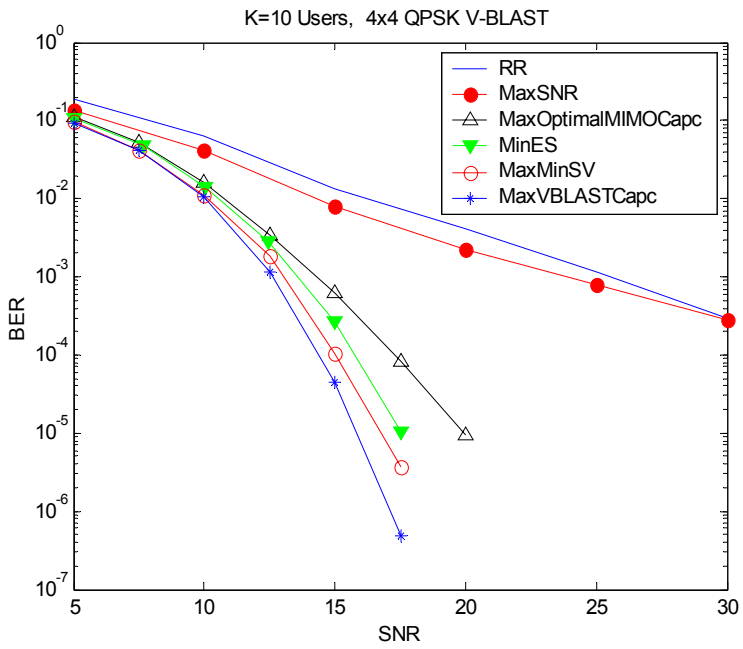

Figure 7.2: Aggregate BER of 4x4 QPSK V-BLAST users with uplink scheduling

Figure 7.4 shows the capacity gains of uplink V-BLAST scheduling at 10% outage versus number of users. The optimal MIMO capacity scheduling, as defined in (8.2), is estimated by assuming the availability of optimal MIMO modems. Therefore, it provides an upper bound for the V-BLAST scheduling algorithms. However, when using RR scheduling with optimal MIMO modems, the rates provided by V-BLAST with scheduling are higher when the number of users is greater than five. The reason is that V-BLAST with scheduling captures K-fold diversity, where K is the number of users, in addition to being a full spatial multiplexing scheme while the optimal MIMO system with RR scheduling is a spatial multiplexing system with spatial diversity only. Furthermore, the MaxVBLASTCapc scheduler approaches optimal MIMO scheduling at a large number of users. Thus, scheduling greatly improves the capacity of the uplink system even with suboptimal detectors. The results in this figure also illustrate the poor performance of MaxSNR scheduling. It has very little gains even at high number of users.

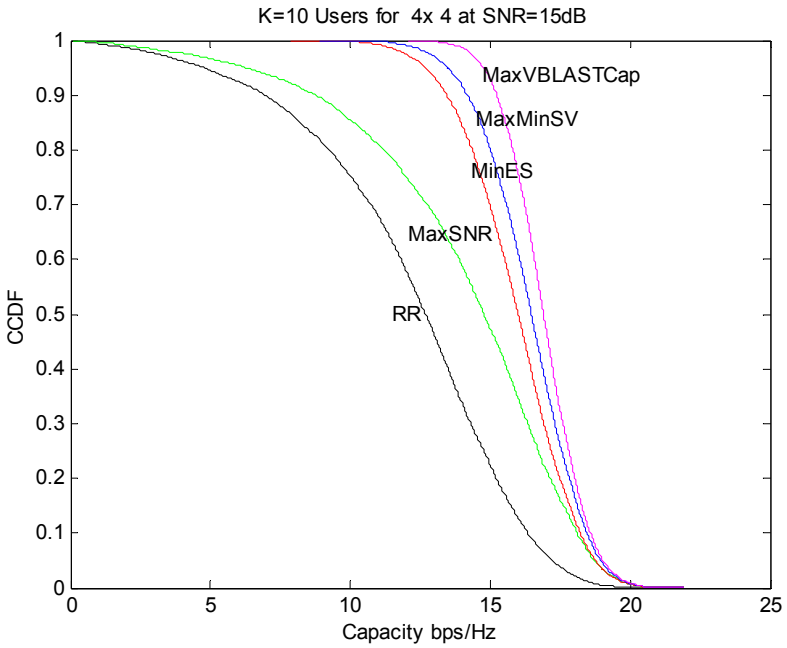

Figure 7.3: Capacity CCDF of 4x4 V-BLAST with uplink scheduling

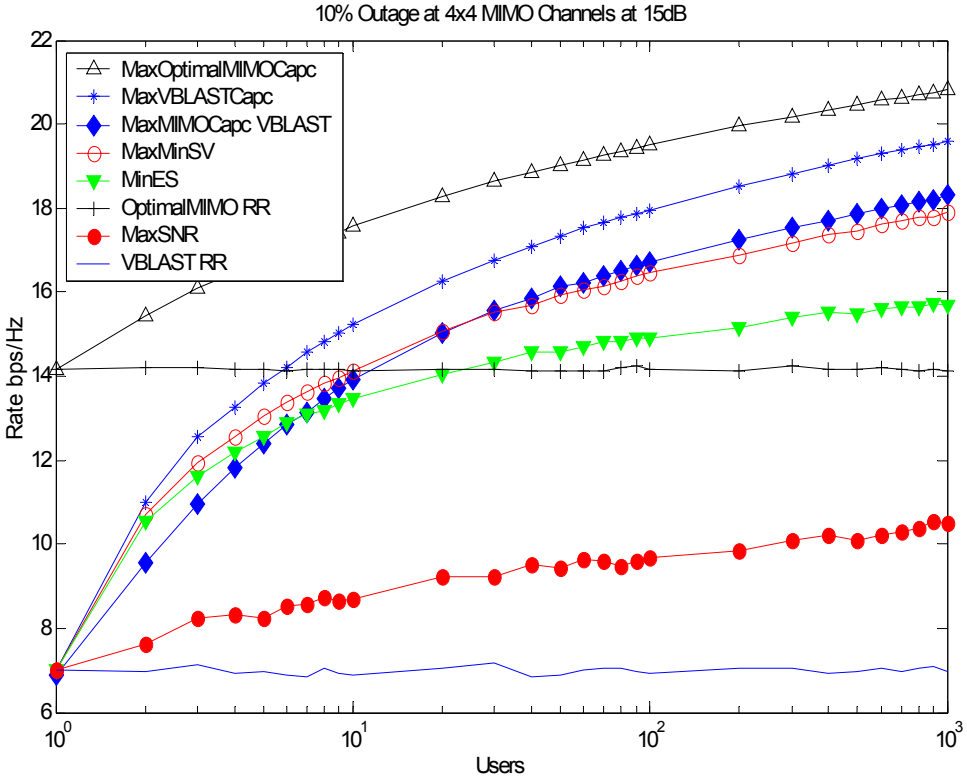

Figure 7.4: Capacity versus number of users at 4x4 MIMO channels and at 10% Outage probability

7.6 Effect of Suboptimal Detection

To further examine the effect of using less complex receivers for spatial multiplexing (SM) users with uplink scheduling, we consider two suboptimal receivers. The first one removes the ordering process from the V-BLAST algorithm and the second one is a simple ZF receiver. The rational is that the multiuser diversity may overcome the weakness of the suboptimal algorithms.

Similar to (8.5), the capacity of a spatial multiplexing system with ZF receiver for user k is:

$$C^{k}_{SM-ZF} = M_T \cdot \min_{i=1,2,\ldots,M_T} \left\{ \log_2 \left(1 + \frac{SNR}{M_T \left\| \mathrm{W}^{k}_{SM-ZF,i} \right\|^2} \right) \right\} \tag{8.12}$$

$$\text{where} \quad \left\| \mathrm{W}^{k}_{SM-ZF,i} \right\|^2 = \left[\left(\mathbf{H}_k^H \mathbf{H}_k \right)^{-1} \right]_{ii}$$

Figure 7.5 compares the capacity of SM schemes with uplink scheduling versus the number of users for different detectors. The result shows the loss in rate due to using simpler SM detection. Since the multi-user diversity order is high, we expect that the loss in rate will be small. The result indicates a small loss in capacity at a large number of users. When the number of transmit and receive antennas is low, such as 2×2, the loss is not substantial.

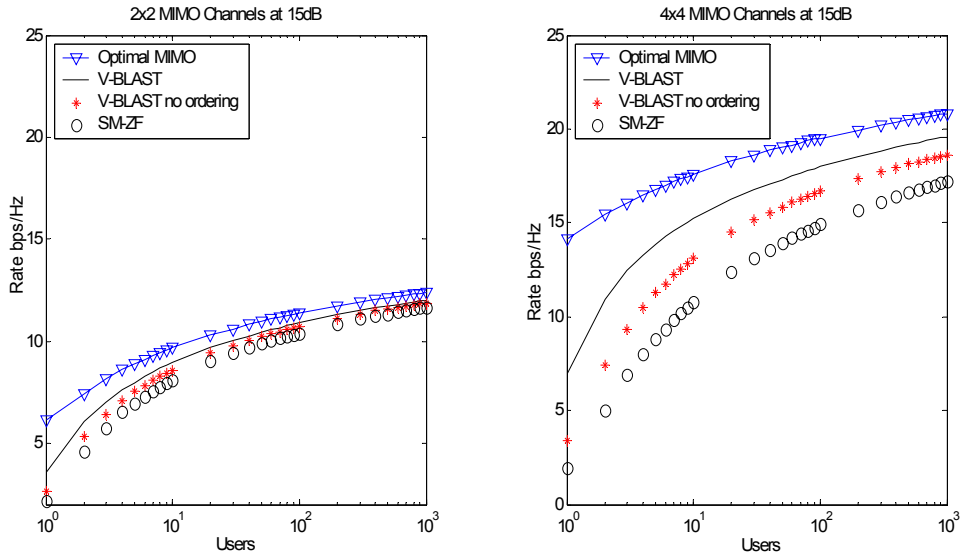

Figure 7.5: Capacity versus number of users at 10% Outage probability for suboptimal detectors

7.7 Advantage of V-BLAST over SISO and SIMO systems

The simulation results in Figure 7.6 show the advantage of V-BLAST over receive diversity and single-input single-output (SISO) systems. The optimal scheduler that maximizes the capacity for SISO and single-input multiple-output (SIMO) systems is to select the user that has maximum SNR $\max_{k=1,2,\ldots,K} \left\{ h_k^H h_k \right\}$. Although V-BLAST is a suboptimal detector and it suffers from noise enhancement and error propagation, it boosts capacity by over 100% compared to SISO and MISO systems. Furthermore, its capacity increases logarithmically with number of users, similar to the behavior of MIMO systems when the number of transmit antennas exceeds number of receive antennas. Moreover, the BER performance of V-BLAST outperforms MRC by 8 dB at low BERs as shown in Figure 7.7.

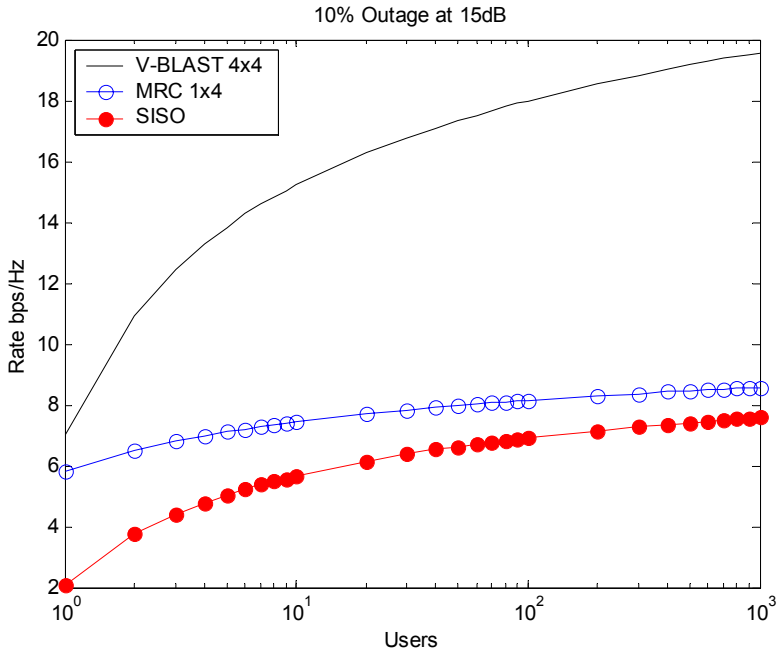

Figure 7.6: Spectral advantage of V-BLAST over receive diversity and SISO systems with uplink scheduling

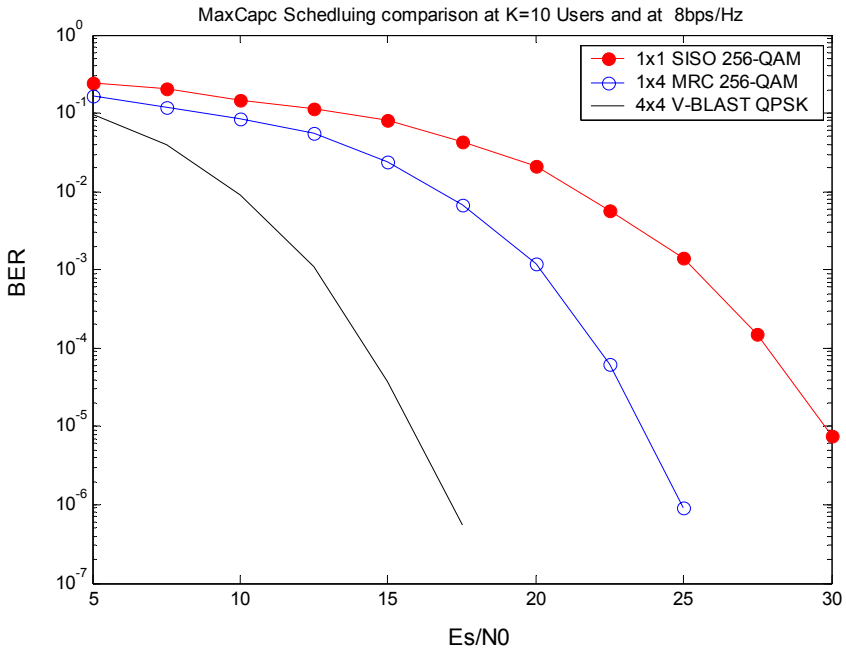

Figure 7.7: BER Comparison of V-BLAST and MRC with uplink scheduling

7.8 Spatial Multiplexing with Sphere Decoding

A sphere decoder (SD) is a maximum likelihood (ML) detector that provides full receive diversity for spatial multiplexing systems with cubic average complexity at high SNRs. In this section, we examine few scheduling algorithms for spatial multiplexing with sphere decoding (SM-SD). The scheduler that maximizes MIMO capacity, as described in (8.2), is the optimal for SD. Other schedulers are described earlier. The BER performance is shown in Figure 7.8. The key difference between SD and V-BLAST is the receive diversity advantage due to ML detection. This may reduce the importance of scheduling. However, compared to RR scheduling, multiuser diversity still gives some gains in BER performance, around 3dB at 10 users.

Figure 7.9 shows the capacity gains of SM-SD with different scheduling criteria at 10% outage as a function of number of users. Notice that the performance of the MaxSNR scheduler with SD is much better than with V-BLAST. This is a result of the full receive diversity advantage of SD.

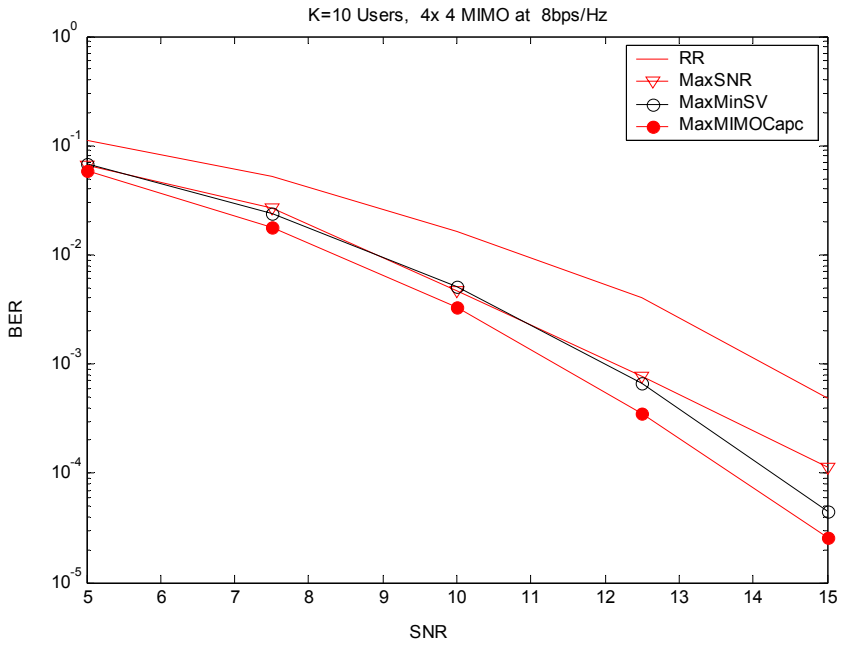

Figure 7.8: Sphere Decoder scheduling for 4x4 spatial multiplexing uplink users

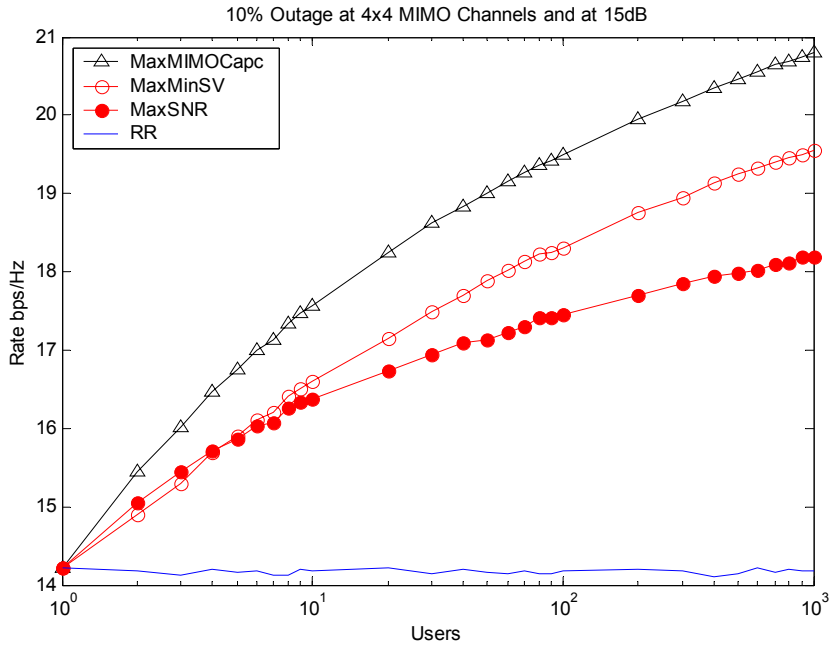

Figure 7.9: Capacity versus number of users at 4x4 MIMO channels and at 10% Outage probability for SM-SD

7.9 Chapter Summary

This chapter compared and evaluated the performance of several scheduling algorithms for the uplink scheduling of V-BLAST users. The scheduler selects one user at a time and each user spatially multiplexes his data over the transmit antennas. The basic scheduling technique is known as round-robin in which each user is allowed to transmit in an ordered fashion without taking any advantage of the channel variations and statistics.

The main contribution of this chapter is finding the optimal scheduler that maximizes V-BLAST capacity for uplink single user scheduling. It selects the user that has the maximum post-processing SNR of the weakest layer. It needs to perform nulling and ordering for each MIMO channel matrix in order to evaluate this criterion. A suboptimal scheduler that performs very close to the optimal is to schedule to the user that has the maximum minimum singular value of the MIMO channel. This criterion takes into account the eigenspread of the MIMO channel and its power at the same time. The eigenspread of the MIMO channel measures how close it is to orthogonality because orthogonal channels maximize the MIMO capacity.

Furthermore, we showed that scheduling based on maximum MIMO capacity is not optimal for V-BLAST. That is due to the suboptimality of the V-BLAST detection algorithm while the MIMO capacity criterion assumes optimal encoding and decoding. Furthermore, scheduling for V-BLAST users outperforms optimal MIMO users with round-robin scheduling. This greatly emphasizes the capacity gains that scheduling offers to wireless uplink systems. Moreover, comparing V-BLAST to less complex MIMO receivers, such as a zero forcing filter, shows that there is a small loss in capacity at a large number of users. When the number of transmit-receive antennas is low, such as 2×2, the loss is negligible. In addition, comparing the capacity of scheduling for V-BLAST with SISO and SIMO systems, we find huge gains in

capacity. Finally, we studied scheduling for a spatial multiplexing system when using a sphere decoder (SD) at the receiver. Since SD is a maximum likelihood receiver, scheduling to a user who maximizes the MIMO channel capacity performs the best. However, the gains of scheduling in this case are less significant since SD already provides full receive diversity to the MIMO system.

Chapter 8
Conclusion

This dissertation focused on three advances in MIMO communication systems. The first studied a combined spatial multiplexing and space time coding architecture in order to bridge the gab between these two MIMO systems. In this system, the information is divided into layers and each layer is encoded by a space time code. This is known as multi-layered space time coded system. Both space time trellis codes (STTC) and block codes (STBC) are used as the layer codes. Due to the short code length of STBC, the number of receive antennas should be at least equal to the number of layers. On the other hand, it is equal to the total number of transmit antennas for STTC case. We study three classes of decoding algorithms for multi-layered space time trellis codes (MLSTTC). The first uses joint decoding, the second implements more practical receivers based on group interference nulling and cancellation, the third is based on spatial sequence estimation. The joint detection algorithms perform the best since they provide full receive diversity for each layer and they don't suffer from error propagation. The second class consists of serial and parallel group interference nulling and cancellation (SGINC, PGINC). Both receivers are implemented in an iterative architecture but SGINC decodes each layer

serially, whereas PGINC decodes all layers simultaneously. Further, PGINC iterates cancellation to improve the performance of the system. These receivers are less complex than the joint receiver. However, they suffer from diversity reduction caused by nulling and error propagation caused by cancellation. PGINC should theoretically achieve full receive diversity. However, due to error propagation, we found that the diversity is dominated by the nulling stage. In order to avoid cancellation, a soft-input soft-output spatial sequence estimator was proposed. The spatial sequence estimator algorithm has the flexibility to tradeoff complexity with receive diversity and doesn't suffer from error propagation. The algorithm outperforms the group interference nulling and cancellation algorithms.

In order to show how the multi-layered system compares to other open loop MIMO systems, the serial algorithm capacity for multi-layered STBC (MLSTBC) is compared to V-BLAST and STBC at the same number of transmit-receive antennas. The results show that MLSTBC is more spectrally efficient at low SNR and at low outage probabilities than V-BLAST. Furthermore, since MLSTBC has more transmit-receive diversity, it is more power efficient. Therefore, it makes a good candidate for low power data applications. Moreover, the study shows that there is a capacity reduction in MLSTBC and V-BLAST after adding a certain number of layers. This is a result of the nulling operation involved in the detection algorithms and demonstrates that there is a spatial multiplexing and diversity tradeoff. We also studied the capacity of the MLSTBC algorithms in order to examine the optimal performance of these algorithms. The goal was to examine the optimal performance, the spatial multiplexing and diversity tradeoffs and their relation to the detection algorithm. The result shows that the diversity of the group inference nulling and cancellation algorithms is dominated by the first

detected layer. Ordering improves the performance of the serial algorithm but it doesn't increase the diversity.

The second part of this dissertation focused on MIMO-OFDM systems. We first evaluated the performance of multi-layered detection algorithms for MLSTBC over frequency selective MIMO channels. The OFDM modulator transforms the frequency selective MIMO channels into parallel flat fading channels in the frequency domain. The OFDM symbol error rate performance of the MLSTBC-OFDM scheme was evaluated and the different detection algorithms were compared. The results showed that SGINC with post-Frobenius norm ordering outperforms PGINC at a large number of layers. The joint detector using the sphere decoder outperforms the GINC algorithms since it provides full receive diversity while the diversity order of GINC algorithms is dominated by the first detected layer. We also consider the design of bandwidth efficient space frequency time codes for MIMO-OFDM systems. Our approach was to concatenate trellis codes with space time block codes. The concatenated system separates frequency coding from space time coding and has much lower complexity than a joint design. The design criterion of the trellis code is to have large minimum effective length in order to capture the available frequency diversity. In order to provide larger effective lengths at low complexity, we adapted IQ-trellis codes which were originally designed for rapidly fading channels. In addition, we found that interleaving is essential in order to mitigate highly correlated OFDM channels in the frequency domain. Toward that end, we examined the effect of block interleaving on the performance of the codes and on the achieved diversity. Finally, we compared and evaluated the performance of serial and parallel detection algorithms for multi-layered IQ space frequency time codes. This multi-layered architecture is a spatial multiplexing scheme with spatial and frequency diversity at each layer. The main results of this study show

the performance improvements of IQ-TCM over conventional TCM at the same number of states and spectral efficiency. The reason for the improvement is the larger effective length of IQ-TCM. Also, the simulation results emphasize the importance of an appropriate interleaver design since there is a great loss in performance and diversity if the block interleaver is not designed carefully. Finally, the multi-layered IQ-coded scheme performed much better than the uncoded one. The parallel processing slightly outperforms the other detection algorithms.

The last part of this dissertation proposed and compared uplink scheduling algorithms multiple user systems employing spatial multiplexing. The scheduler selects one user at a time for transmission and each user spatially multiplexes his data over the transmit antennas. The basic scheduling technique is known as round-robin scheduling where each user is allowed to transmit in an ordered fashion without taking any advantage of the channel variation or statistics. The main contribution of this chapter is finding the optimal scheduler that maximizes V-BLAST capacity for uplink single user scheduling. It selects the user that has the maximum post-processing SNR of the weakest layer. It needs to perform nulling and ordering for each MIMO channel matrix in order to evaluate this criterion. A suboptimal scheduler that performs very close to the optimal is to schedule to the user that has the maximum minimum singular value of the MIMO channel. This criterion takes into account the eigenspread of the MIMO channel and its power at the same time. The eigenspread of the MIMO channel measures how close it is to orthogonality because orthogonal channels maximize the MIMO capacity. Furthermore, we showed that scheduling based on maximum MIMO capacity is not optimal for V-BLAST. That is due to the suboptimality of the V-BLAST detection algorithm while the MIMO capacity criterion assumes optimal encoding and decoding. Furthermore, optimal scheduling for V-BLAST users outperforms optimal MIMO users with round-robin scheduling. This greatly

emphasizes the capacity gains that scheduling offers to wireless uplink systems. Moreover, comparing V-BLAST to less complex MIMO receivers, such as a zero forcing filter, we found that there is a small loss in capacity at a large number of users. However, when the number of transmit-receive antennas is low, such as 2×2, the loss is negligible. In addition, comparing the capacity of scheduling for V-BLAST with SISO and SIMO systems, we find huge gains in capacity. Finally, we studied scheduling for a spatial multiplexing system when using a sphere decoder (SD) at the receiver. Since SD is a maximum likelihood receiver, scheduling to a user who maximizes the MIMO channel capacity performs the best. However, the gains of scheduling in this case are less significant since SD already provides full receive diversity to the MIMO system.

Appendix A

The sphere decoder searches for the closest point or the shortest vector in a lattice. A lattice is the set of points generated by a generator matrix **M** as:

$$\Lambda(\mathbf{M}) \equiv \left\{ \mathbf{Mu};\ \mathbf{u} \in \mathbb{Z}^n \right\} \tag{A.1}$$

where $\mathbb{Z}$ is the ring of integers and $\mathbf{M} \in \mathbb{R}^{m \times n}$, where $m \geq n$. The columns of **M** are linearly independent and they form the basis vectors for Λ. Also, u is the coordinate of the lattice point. For example, for 16-QAM constellation, $\mathbf{u} \in \{-3, -1, 1, 3\}$. Although the formal definition is for integer coordinates, it could be generalizes for real coordinates such as in 8PSK.

Assume that the received vector is

$$\mathbf{r} = \mathbf{Mu} + \mathbf{v} \tag{A.2}$$

the SD searches through points in the lattice Λ inside a sphere of radius $\sqrt{C}$. The search for the closest point will be:

$$\underbrace{\min}_{\mathbf{x} \in \Lambda} \left\| \mathbf{r} - \mathbf{Mx} \right\|^2 \tag{A.3}$$

it is similar to the search of the shortest vector in Λ:

$$\underbrace{\min}_{\mathbf{w} \in \mathbf{r} - \Lambda} \left\| \mathbf{w} \right\|^2 \tag{A.4}$$

By left multiplying the received vector in (A.2) by the pseudo-inverse $\mathbf{M}^\dagger$, we get

$$\begin{aligned} \mathbf{M}^\dagger \mathbf{r} &= \mathbf{M}^\dagger \mathbf{Mu} + \mathbf{M}^\dagger \mathbf{v} \\ \boldsymbol{\rho} &= \mathbf{u} + \boldsymbol{\varepsilon} \end{aligned} \tag{A.5}$$

thus, we can write $\mathbf{w} = \mathbf{M}\boldsymbol{\varepsilon}$, where $\boldsymbol{\varepsilon} \in \mathbb{R}^n$. Also, $\mathbf{r} = \mathbf{M}\boldsymbol{\rho}$, where $\boldsymbol{\rho} \in \mathbb{R}^n$.

The search for the shortest vector in equation (A.5) can be rewritten as:

$$Q(\boldsymbol{\varepsilon}) = \|\mathbf{w}\|^2 = \boldsymbol{\varepsilon}^T \mathbf{M}^T \mathbf{M}\boldsymbol{\varepsilon} = \boldsymbol{\varepsilon}^T \mathbf{G}\boldsymbol{\varepsilon} = \sum_{i=1}^{n}\sum_{j=1}^{n} g_{ij}\varepsilon_i\varepsilon_j \le C \tag{A.6}$$

where $\mathbf{G} = \mathbf{M}^T\mathbf{M}$ is the Gram matrix. The above representation transformed the sphere of radius C and centered at the received vector to an ellipsoid centered at the origin of the new coordinate system defined by ε.

Cholesky's factorization could be applied on **G** and it gives us $\mathbf{G} = \mathbf{R}^T\mathbf{R}$, where **R** is an upper triangular matrix. Then,

$$Q(\boldsymbol{\varepsilon}) = \boldsymbol{\varepsilon}^T \mathbf{R}^T \mathbf{R}\boldsymbol{\varepsilon} = \|\mathbf{R}\boldsymbol{\varepsilon}\|^2 = \sum_{i=1}^{n}\left(r_{ii}\varepsilon_i + \sum_{j=i+1}^{n} r_{ij}\varepsilon_j \right)^2 \le C \tag{A.7}$$

let $q_{ii} = r_{ii}^2$ and $q_{ij} = r_{ij} / r_{ii}$, then

$$Q(\boldsymbol{\varepsilon}) = \sum_{i=1}^{n} q_{ii}\left(\varepsilon_i + \sum_{j=i+1}^{n} q_{ij}\varepsilon_j \right)^2 \le C \tag{A.8}$$

By solving the above inequality for each coordinate, the algorithm finds the possible range for each coordinate. Starting from ε_n we get:

$$q_{nn}\varepsilon_n^2 \le C \tag{A.9}$$

then, after some steps, we get

$$-\sqrt{\frac{C}{q_{ii}}} \le \varepsilon_n \le \sqrt{\frac{C}{q_{ii}}} \tag{A.10}$$

substituting $\varepsilon_n = \rho_n - u_n$ and solving for u_n we get

$$\left\lceil -\sqrt{\frac{C}{q_{ii}}} + \rho_n \right\rceil \le u_n \le \left\lfloor \sqrt{\frac{C}{q_{ii}}} + \rho_n \right\rfloor \tag{A.11}$$

where $\lfloor x \rfloor$ is the greatest integer less than x and $\lceil x \rceil$ is the smallest integer greater than x and u_n is the n^{th} integer coordinate of the lattice Λ. Similarly, the i^{th} integer coordinate will have the following bounds:

$$\left\lceil -\sqrt{\frac{1}{q_{ii}}\left(C-\sum_{l=i+1}^{n} q_{ll}\left(\varepsilon_l+\sum_{j=l+1}^{n} q_{lj}\varepsilon_j\right)^2\right)}+\rho_i+\sum_{j=i+1}^{n} q_{ij}\varepsilon_j \right\rceil \leq u_i \leq \left\lfloor \sqrt{\frac{1}{q_{ii}}\left(C-\sum_{l=i+1}^{n} q_{ll}\left(\varepsilon_l+\sum_{j=l+1}^{n} q_{lj}\varepsilon_j\right)^2\right)}+\rho_i+\sum_{j=i+1}^{n} q_{ij}\varepsilon_j \right\rfloor \tag{A.12}$$

the above calculations could be done recursively. Let

$$S_i = \rho_i + \sum_{l=i+1}^{n} q_{il}\varepsilon_j \tag{A.13}$$

$$\begin{aligned} T_{i-1} &= C - \sum_{l=i}^{n} q_{ll}\left(\varepsilon_l+\sum_{j=l+1}^{n} q_{lj}\varepsilon_j\right)^2 \\ T_{i-1} &= T_i - q_{ii}(S_i-u_i)^2 \end{aligned} \tag{A.14}$$

Thus, the i^{th} coordinate will be bounded by:

$$\left\lceil -\sqrt{\frac{T_i}{q_{ii}}}+S_i \right\rceil \leq u_i \leq \left\lfloor \sqrt{\frac{T_i}{q_{ii}}}+S_i \right\rfloor \tag{A.15}$$

the SD algorithm could be described as follows: based on the initial radius C, the decoder will finds the bounds for the n^{th} coordinate of the vector **u**. Then, it will select the first candidate and based on it, it will find the bounds for the n-1 coordinate and this will continue until at some coordinate if no possible values are found inside the bounds, the algorithm will go back to the previous coordinate and select another candidate. If it happens that no valid point could be found inside this radius, the algorithm will increase the radius and starts again. When a valid point is found, its distant from the center (the received vector) will be:

$$\tilde{d}^2 = C - T_1 + q_{11}(S_1 - u_1)^2 \qquad \text{(A.16)}$$

and this distance will be the radius for next search. In other words, the radius of the sphere will be reduced until it reaches the maximum likelihood point.

The flowchart of the SD algorithm is shown in Figure A.1. The function Q-Chol(**G**) calculates the Cholesky factorization of **G** and transform it to the coefficients $\{q_{ik}\}$ as in (A.5). The set $\mathcal{S}$ contains the possible values of each coordinate. For example, for 16QAM signals, $\mathcal{S}$={-3,-1,1,3}. The functions $\underline{Q}$ and $\bar{Q}$ finds the upper and the lower bounds of the i^{th} coordinate as in (A.15). Furthermore, the function enum lists the possible values of the i^{th} coordinate from L_i to U_i and the function length outputs the number of these possible values.

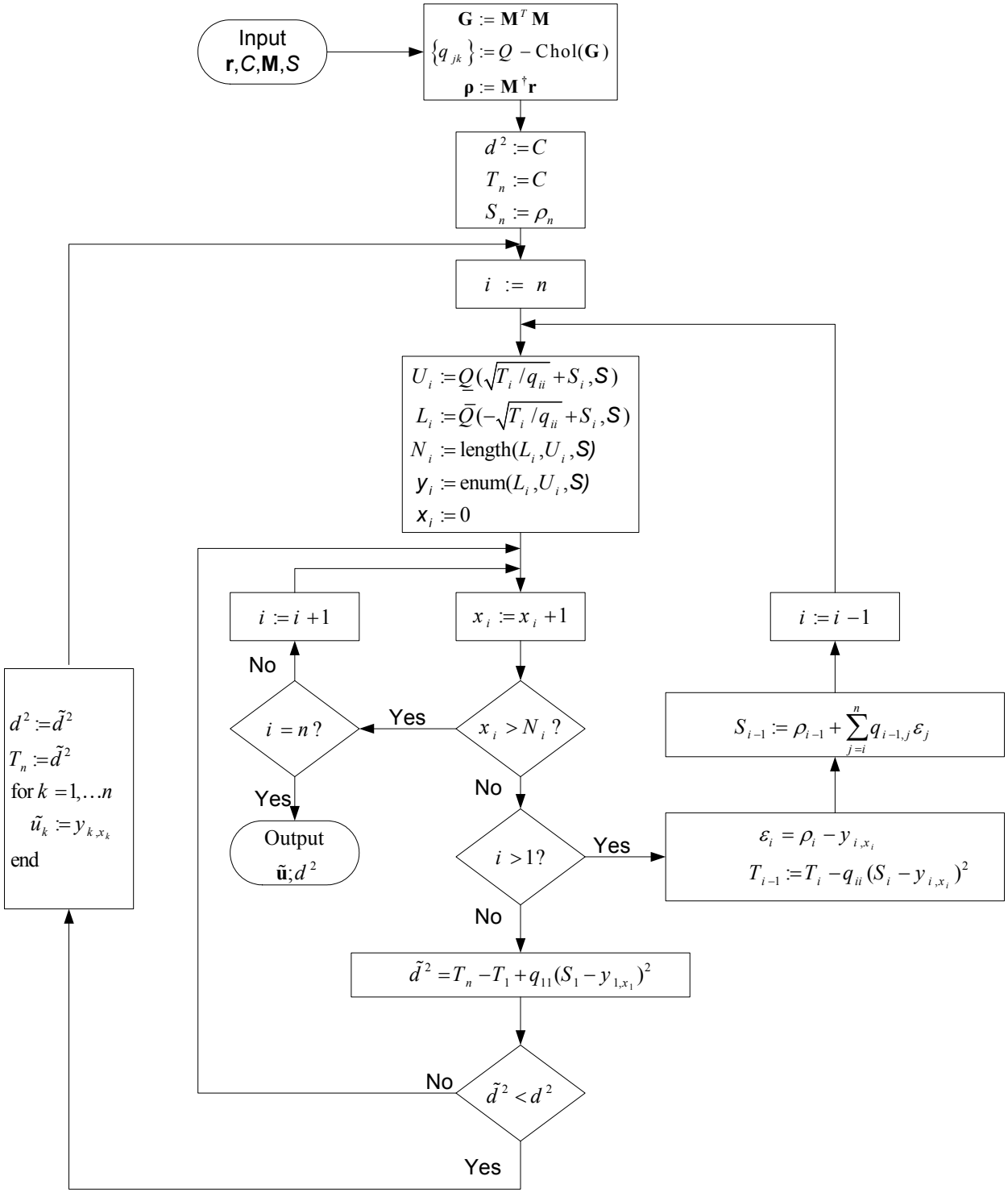

Figure A.1: Flowchart of the sphere decoding algorithm

Bibliography

[3GPP99] 3GPP RAN WG1, Physical layer-General Description, V2.0.0, April 1999.

[Ahm02] Y. Ahmed, R. M. Buehrer, and J. H. Reed, "Space-time block codes for eight transmit antennas," *IEEE Thirty-Sixth Asilomar Conference on Signals, Systems and Computers*, vol. 2, pp. 1359-1363, Nov. 2002.

[Air03] M. Airy, S. Shakkattai and R. W. Jr. Heath, "Spatially greedy scheduling in multi-user MIMO wireless systems," *Signals, Systems and Computers, 2003. Conference Record of the Thirty-Seventh Asilomar Conference on*, vol. 1, pp. 982 – 986, 9-12 Nov. 2003.

[Ala98] S. Alamouti, "A Simple Transmit Diversity Technique for Wireless Communications," *IEEE J. Select. Areas Comm.* vol.16, no.8. Oct. 1998

[Ala98a] S. V. Alamouti, V. Tarokh, and P. Poon, "Trellis-Coded Modulation and Transmit Diversity: Design Criteria and Performance Evaluation," *IEEE International Conference on Universal Personal Communications, 1998,* vol. 1, pp. 703– 707, Oct. 1998.

[Alg04] S. Al-Ghadhban and B. Woerner, "Iterative Joint and Interference Nulling/Cancellation Decoding Algorithms for Multi-Group Space Time Trellis Coded Systems," *IEEE WCNC. 2004*, vol. 4, pp. 2317-2322, 21-25 March 2004.

[Als97] S. A. Al-Semari and T. E. Fuja, "I-Q TCM: Reliable Communication over the Rayleigh Fading Channel Close to the Cutoff Rate," IEEE Trans. on Information Theory, vol. 43, pp. 250-262, Jan. 1997.

[Aqr98] D. Agrawal, V. Tarokh, A. Naguib and N. Seshadri, "Space-Time Coded OFDM for High Data-Rate Wireless Communication Over Wideband Channels," *IEEE Vehicular Technology Conference 1998*, vol. 3, pp. 2232 – 2236, May 1998.

[Bar00] Stephan Baro, Gerhard Bauch, and Axel Hansmann, "Improved Codes for Space-Time Trellis Coded Modulation". *IEEE Communications Letters*, vol. 4, no. 1, Jan. 2000.

[Ben00] Ben Lu and X. Wang, "Space-Time Code Design in OFDM Systems," *IEEE GLOBECOM '00*, vol. 2, pp. 1000 – 1004, 27 Nov.-1 Dec. 2000

[Ben00a] Ben Lu; Xiaodong Wang. "Iterative receivers for multiuser space-time coding systems," *IEEE Journal on Selected Areas in Communications*, vol. 18, Issue: 11, pp. 2322 -2335, Nov 2000.

[Bud01] C. Budianu and L. Tong, "Channel estimation for space-time orthogonal block codes", *IEEE ICC 2001,* vol. 4, pp. 1127-1131, 2001.

[Bue02] R. M. Buehrer, "The impact of angular energy distribution on spatial correlation," *IEEE 56th. VTC Fall 2002,* vol. 2, pp. 1173 -1177, 2002.

[Cha01] Changjiang Xu; Hongjun Xu; Kyung Sup Kwak. "The application of space-time codes in CDMA systems", *IEEE 53rd VTC Spring 2001*, vol. 2 , pp. 1415 -1419, 2001.

[Cha02] A. M Chan and Inkyu Lee, "A new reduced-complexity sphere decoder for multiple antenna systems," *IEEE International Conference on Communications, 2002*, vol. 1, pp. 460 -464, 28 April-2 May 2002.

[Che02] Jian Cheng, Haifeng Wang and Shixin Cheng; "Space-Time Block Coded Transmit Diversity for OFDM system in Mobile Channels," *Personal, Indoor and Mobile Radio Communications, 2002. The 13th IEEE International Symposium on* , Volume: 1 , 15-18 Sept. 2002 Pages:208 - 211 vol.1

[Che03] Z. Chen, J. Yuan, B. Vucetic, and Z. Zhou, "Performance of Alamouti scheme with transmit antenna selection," *Electron Lett.,* vol. 39, no. 23, pp. 1666-1668, Nov. 2003.

[Cir02] H. A. Cirpan and E. Panayirci, "Blind channel estimation for space-time coding systems with Baum-Welch algorithm", *IEEE ICC 2002*, vol. 3, pp. 1579-1583, 2002.

[Cor02] G. Corral-Briones, C. Rodriguez, and C. Marques, "Non-iterative joint decoding of space-time codes and multiuser interference in asynchronous DS-CDMA systems", *IEEE WCNC2002.* vol. 1 , pp. 94 -98, 17-21 Mar 2002.

[Cov91] T. M. Cover, J. A. Thomas, *Elements of Information theory*, John Wiley & Sons, Inc., 1991.

[Dab00] A. G. Dabak, S. Hosur, T. Schmidl, and C. Sengupta, **"**A comparison of the open loop transmit diversity schemes for third generation wireless systems," *IEEE WCNC 2000*, vol.1, pp. 437-442, 2000.

[Dam00] M. O. Damen, A. Chkeif, and J.-C. Belfiore, *"*Lattice code decoder for space-time codes", *Communications Letters, IEEE*, vol. 4 Issue: 5, pp. 161 -163, May 2000.

[Dam01] M. O. Damen, K. Abed-Meraim, M. S. Lemdani, "Further results on the sphere decoder", *Information Theory, 2001. Proceedings. 2001 IEEE International Symposium on*, pp. 333, 24-29 June 2001.

[Dam02] M. O. Damen, K. Abed-Meraim, J.-C Belfiore, "Diagonal algebraic space-time block codes", *Information Theory, IEEE Transactions on*, Volume: 48 Issue: 3, March 2002 Page(s): 628 -636

[Dam03] M. O. Damen, H. El Gamal and N. C. Beaulieu, "On the design of quasi-orthogonal constellations: Filling the empty threads," *IEEE VTC Fall 03 Orlando Fl,* Oct. 2003

[DaS01] M.J. Da Silva, A. Taffin, S. Lasaulce, and S. Buljore, "Closed loop transmit diversity enhancements for UMTS narrowband and wideband D-CDMA," *Vehicular Technology Conference, 2001. VTC 2001 Spring. IEEE VTS 53rd*, vol.3, pp. 1963-1967, 2001.

[Div88] D. Divsalar and M. K. Simon, "Multiple Trellis Coded Modulation (MTCM)," *IEEE Trans. Commun.*, vol. COM-36, pp. 410-419, Apr. 1988.

[Fin85] U. Fincke and M. Pohst, "Improved methods for calculating vectors of short length in a lattice, including a complexity analysis," *Math. Computation*, vol. 44, pp. 463-471, Apr. 1985.

[Fos96] G. J. Foschini "Layered Space Time Architecture for wireless communication in a fading environment when using multielement antennas," *Bell Lab. Technical Journal*. vol. 1, no. 2, Autumn 1996.

[Fos98] G. J. Foschini and M. J. Gan, "On Limits of Wireless Communications in a Fading Environment when using Multiple Antennas," *Wireless Personal Communications*. Vol. 6, pp. 311-335, March 1998.

[Fos99] G. Foschini, G. Golden, R. Valenzuela, and P. Wolniansky. "Simplified Processing for High Spectral Efficiency Wireless Communication Employing Multi-Element Arrays". *IEEE Journal on selected areas in Communications.* vol. 17, no. 11, Nov. 1999.

[Gam01] H. El Gamal and R. Hammons, "A New Approach to Layered Space-Time Coding and Signal Processing". *IEEE Transaction on Information Theory.* vol. 47, no. 6, pp. 2321-2334, September 2001.

[Ge02] H. Ge, K. D. Wong, M. Barton, and J. C. Liberti, "Statistical characterization of multiple-input multiple-output (MIMO) channel capacity**".** *IEEE Wireless Communications and Networking Conference,* vol. 2, pp. 789 -793, Mar 2002.

[Gia02] Luca Giangaspero, et al. "Co-Channel Interference Cancellation Based on MIMO OFDM Systems," *IEEE Wireless Communications Magazine*, pp. 8-17, Dec. 2002.

[Gon02] Yi Gong and Khaled Ben Letaief, "Concatenated Space-Time Block Coding with Trellis Coded Modulation in Fading Channels," *IEEE Transaction on Wireless Communications*, vol. 1, no. 4, pp. 580-590, Oct. 2002.

[Gon03] Yi Gong and Khaled Ben Letaief, "An Efficient Space-Frequency Coded OFDM System for Broadband Wireless Communications," *IEEE Trans. on Commun.*, vol. 52, pp. 2019-2029, Nov. 2003.

[Goz03] Ran Gozali, R M. Buehrer and B. D. Woerner, "The Impact of Multiuser Diversity on Space-Time Block Coding," *IEEE Comm. Letters*, vol. 7, no 5, pp. 213:215, May 2003

[Har02] L. B. Harchegani, A. R. Ghaderipoor, S. H. Jamali, K., Dolatyar, "New sphere decoding for block space-time codes", *ICASSP'02*, vol. 4, pp. IV-4170, 13-17 May 2002.

[Has01] B. Hassibi and H. Vikalo, *"*On the expected complexity of sphere decoding", *Signals, Systems and Computers, 2001. Conference Record of the Thirty-Fifth Asilomar Conference on*, vol. 2, pp. 1051 -1055, 4-7 Nov. 2001.

[Hea01] R. W. Jr. Heath, M. Airy and A.J. Paulraj, "Multiuser diversity for MIMO wireless systems with linear receivers," Signal, Systems and Computers 2001, Conference Record of the Thirty-Fifth Asilomar Conference on, vol. 2, pp. 1194-1199, 2001.

[Her02] M. Hernandez, M. Collados, G. Janssen, "Space-time coded soft-iterative multiuser receivers for WCDMA", *Vehicular Technology Conference, 2002. VTC Spring 2002. IEEE 55th* , vol. 1, pp. 120 -124, 2002.

[Hoc99] B. Hochwald, T. Marzetta and C. Papadias, "A Novel Space Time Spreading Scheme for Wireless CDMA systems." *37th Annual Allterton Conference on Communication, Control and Computing*, Urbana, IL, Sept. 1999.

[Hoc00a] B. Hochwald and T. Marzetta, "Unitary Space-Time Modulation for Multiple-Antenna Communications in Rayleigh Flat Fading", *IEEE Trans. On Information Theory,* vol. 46, no. 2, pp. 543-564, March 2000.

[Hoc00b] Hochwald, B. M. and Wim Sweldens. "Differential Unitary Space-Time Modulation", *IEEE Trans. On Communications,* VOL. 48, NO. 12, December 2000. Pages:2041-2052

[Hoc00c] Hochwald, B. M.; Marzetta, T. L.; Richardson, T. J; Sweldens, W.; and R. Urbanke. "Systematic Design of Unitary Space-Time Constellations", *IEEE Trans. On Information Theory,* VOL. 46, NO. 6, September 2000. Pages: 1962-1973

[Hoc03] Hochwald, B.M.; ten Brink, S.; "Achieving near-capacity on a multiple-antenna channel", *Communications, IEEE Transactions on*, vol. 51 Issue: 3, pp. 389 -399, March 2003

[Hon02] Hongbin Li, "Semi-blind multiuser receiver for space-time coded CDMA systems," *IEEE International Conference on Acoustics, Speech, and Signal Processing, 2002*, vol. 3, pp. 2401-2404, 2002.

[Hug00] Hughes, Brian L. "Differential Space-Time Modulation", *IEEE Trans. on Information Theory,* vol. 46, NO. 7, pp. 2567-2578, November 2000.

[Jal99] Jalloul, L.M.A.; Rohani, K.; Kuchi, K.; Chen, J.; "Performance analysis of CDMA transmit diversity methods," *Vehicular Technology Conference, 1999. VTC 1999 - Fall. IEEE VTS 50th* , vol. 3 , pp. 1326 -1330, 1999.

[Jam94] H. Jamali and T. Le-Ngoc. *Coded-Modulation Technique for Fading Channels.* Kluwer Academic Publisher 1994.

[Jam91] H. Jamali and T. Le-Ngoc, "A new 4-state 8PSK scheme for fast fading shadowed mobile radio channels," *IEEE Trans. Vech. Technol*, vol. 40, pp. 216-222, Jan. 1991.

[Jaf01] Hamid Jafarkhani. "A Quasi-Orthogonal Space-Time Blcok Code". *IEEE Trans. On Communications*, vol. 49, no. 1, January 2001.

[Jaf02] H. Jafarkhani, N. Seshadri, "Super-orthogonal space-time trellis codes," *IEEE Transactions on Information Theory*, vol. 49, Issue 4, pp. 937-950, April 2003.

[Jay01] S. K. Jayaweera and H. V. Poor, "Iterative multiuser detection for space-time coded synchronous CDMA", *IEEE 54th*,*VTC 2001 Fall,* vol. 4, pp. 2736-2739, 2001.

[Jel94] B. D. Jelecic and S. Roy, "Design of Trellis Coded QAM for Flat Fading and AWGN Channels," *IEEE Trans. on Vech. Technol*., vol. 44, pp. 192-201, Feb. 1994.

[Ker02] J. P. Kermoal, L. Stchumacher, K. I. Pedersen, P. Mogensen, F. Frederiksen. "A Stochastic MIMO Radio Channel Model With Experimental Validation". *IEEE Journal on Selected Areas in Communications,* vol. 20, no. 6, August 2002

[Kha01] M. A. Khalighi, J.-M Brossier, G. V Jourdain, and K. Raoof, "Water filling capacity of Rayleigh MIMO channels," *12th IEEE International Symposium on Personal, Indoor and Mobile Radio Communications*, vol. 1, pp. A-155-A-158, Sep 2001.

[Kie02] M. Kiessling, J. Speidel, I. Viering, M. Reinhardt, "A closed-form bound on correlated MIMO channel capacity" *IEEE 56th Vehicular Technology Conference,* vol. 2, pp. 859 -863, 2002.

[Kno95] R. Knopp and P. Humblet, "Information capacity and power control in single cell multiuser communications," *Proc. IEEE Int. Computer Conf. (ICC'95),* Seattle, WA, June 1995.

[Lau02] V. K.N. Lau, Y. Liu and T. A Chen, "Optimal Multi-user Space Time Scheduling for Wireless Communications," *IEEE 56th VTC 2002-Fall. 2002*, vol. 4, pp. 1939-1942, 24-28 Sept. 2002.

[Lia02] Xue-Bin Liang and Xiang-Gen Xia. "Unitary Signal Constellations for Differential Sapce-Time Modulation with Two Transmit Antennas: Parametric Codes, Optimal

Designs, and Bounds". *IEEE Trans. on Information Theory,* vol. 48, no. 8, pp. 2291-2322, August 2002.

[Luc99] Downlink diversity improvements through space-time spreading, Lucent Technologies, Aug. 1999.

[Mag99] P. Magniez and Duhamel, "Turbo-Equalization applied to Trellis-Coded-Modulation," *IEEE VTC 1999-Fal,* vol. 5, pp. 2556-2560.

[Mis02] A. Mishra, S. Ganesh, and U. B. Desai, "Blind space-time multiuser detector," *IEEE International Symposium on Circuits and Systems, 2002*, vol. 1 , pp. I-697-I-700, 2002.

[Moh04] M. Mohammad, S. Al-Ghadhban, B. Woerner, and W. Tranter "Spatial Sequence Estimation Based Decoding Algorithm for V-BLAST" *VTC2004-Fall. 2004 IEEE 60th* , vol. 3, pp. 1875 – 1879, 26-29 Sept. 2004

[Moh04a] M. Mohammad, S. Al-Ghadhban, B. Woerner, and W. Tranter. "Comparing Decoding Algorithms for Multi-Layer Space-Time Block Codes," *SoutheastCon, 2004. Proceedings. IEEE*, pp. 147 – 152

[Nag98] A. Naguib, N. Seshadri, and A.R. Calderbank, "Applications of Space-Time Block Codes and Interference Suppression for High Capacity and High Data Rate Wireless Systems," *Signals, Systems & Computers, 1998. Conference Record of the Thirty-Second Asilomar Conference on* ,vol. 2 , pp. 1803-1810, 1-4 Nov. 1998.

[Ng03] S. X. Ng, T. H. Liew and L. Hanzo, "Space-Time Block Coded and IQ-interleaved TCM, TTCM, BICM and BICM-ID Assisted OFDM," *IEEE 58th VTC 2003-Fall*, vol 3, pp. 1492 – 1496, 6-9 Oct. 2003.

[Ong01] E. N. Onggosanusi, A. Gatherer, A. G. Dabak, and S. Hosur, **"**Performance analysis of closed-loop transmit diversity in the presence of feedback delay," *Communications, IEEE Transactions on* , vol. 49, Issue: 9 , pp. 1618 -1630, Sep 2001.

[Ped00] K. Pedersen, J. Andersen, J Kermoal and P. Mogensen. " A Stochastic Multiple-Input Multiple-Output Radio Channel Model for Evaluation of Space-Time Coding Algorithms". *IEEE 52nd VTS-Fall VTC 2000*, vol. 2 , pp. 893-897, 2000 .

[Pap99] C. Papadias, B. Hochwald, T. Marzetta, M. Buehrer and R. Soni, "Space Time Spreading for CDMA systems," *6th Workshop on Smart Antennas in Wireless Mobile Communications,* Stanford, CA, July 1999.

[Pap02] C. Papadias and G. J. Foschini, "On the Capacity of Certain Space-Time Coding Schemes," *EURASIP Journal on Applied Signal Processing 2002*, Vol. 5, pp. 447-458, May 2002.

[Poh81] M. Pohst, "On The Computation of lattice vectors of minimal length, successive minima and reduced basis with applications," *ACM SIGSAM*, vol. 15., pp. 37-44, 1981.

[Rap96] Rappaport, Theodore. *Wireless Communications, Principles and Practice*. Prentice Hall, Inc. 1996.

[Rea04] M. Realp and A.I Perez-Neira, "Cross-layer MAC scheduling for multiple antenna systems," *Global Telecommunications Conference, 2004. GLOBECOM '04. IEEE*, vol. 5, pp. 3352 – 3356, 29 Nov.-3 Dec. 2004.

[Rey02] D. Reynolds, W. Xiaodong, and H. V. Poor, "Blind adaptive space-time multiuser detection with multiple transmitter and receiver antennas," *IEEE Transactions on Signal Processing,* vol.50, Issue: 6, pp. 1261 -1276, June 2002.

[Roh97] K. Rohani and L. Jalloul, "Orthogonal Transmit Diversity for Direct Spread CDMA," *ETSI SMG2 Wideband CDMA Concept Group*, Sept. 15-17, 1997.

[Roh99] K. Rohani, M. Harrison, K. Kuchi, "A comparison of base station transmit diversity methods for third generation cellular standards," *Vehicular Technology Conference, 1999 IEEE 49th* , vol.1, pp. 351 -355, Jul 1999.

[San00] S. Sandhu and A. Paulraj, "Space-Time Block Codes: A Capacity Perspective," *IEEE Comm. Letters*, vol. 4, no. 12, pp. 384:386, December 2000.

[Sch97] Schott, James R., *Matrix Analysis for statistics*. New York : John Wiley, c1997.

[Sha03] N. Sharma and C. B. Papadias, " Improved quasi-orthogonal codes thorough constellation rotation," *vol. 51, IEEE Trans. Commun., pp. 332-335*, March 2003.

[Shi99] D. Shiu and J. M. Kahn, "Layered Space-Time Codes for Wireless Communications using Multiple Transmit Antennas", *Proc. of IEEE Intl. Conf. on Commun.*, pp. 436-440, Vancouver, B.C., June 6-10, 1999.

[Shi03] Oh-Soon Shin and Kwang Bok Lee, "Antenna-Assisted Round Robin Scheduling for MIMO Cellular Systems," *IEEE Comm. Letters*, vol. 7, no 3, pp. 109:111, March 2003.

[Son04] R. A. Soni and R. M. Buehrer, "On the performance of open-loop transmit diversity techniques for IS-2000 systems: a comparative study," *IEEE Transactions on Wireless Communications*, vol. 3, pp. 1602-1615, 2004.

[Ste00] B. Steiner, “Performance aspects of Transmit Antenna Diversity (TxAD) Techniques for UTRA-TDD”, *Proc. IEEE VTC Spring 2000, Japan,* pp 1165-1169.

[Tar97] V. Tarokh, A. F. Naguib, N. Seshadri, A. R. Calderbank, “Space-time codes for high data rate wireless communication: mismatch analysis,” *IEEE ICC 97 Montreal,* vol. 1, pp. 309 -313, 18-12 Jun 1997.

[Tar98] V. Tarokh, N. Seshadri and A.R. Calderbank, “Space-Time Codes for High Data Rates Wireless Communications: Performance Criterion and Code Construction,” *IEEE Transactions on Information Theory,* Vol 44, Number 2, pp. 744-765, Mar. 1998.

[Tar98b] V. Tarokh, and T.K.Y. Lo, “Principal ratio combining for fixed wireless applications when transmitter diversity is employed” *Universal Personal Communications, 1998. ICUPC '98. IEEE 1998 International Conference on* , Volume: 2 , 1998. Page(s): 907 -909 vol.2

[Tar98c] V. Tarokh, S.M Alamouti, and P. Poon. “New detection scheme for transmit diversity with no channel estimation,” in *Proc. IEEE Int. Conf. Universal Personal Commun.,* 1998

[Tar99] V. Tarokh, A. Naguib, N. Seshadri, A.R. Calderbank, "Combined array processing and space-time coding ", *Information Theory, IEEE Transactions on,* vol. 45, pp. 1121 -1128, May 1999.

[Tar99a] V. Tarokh, H. Jafarkhani, and A. R. Calderbank, “Space-Time Block Codes from Orthogonal Designs”. *IEEE Trans. On Information Theory*, VOL. 45, NO. 5, July 1999.

[Tar00] V. Tarokh and H. Jafarkhani, “A Differential Detection Scheme for Transmit Diversity”. *IEEE Journal on Selected Areas in Communications,* vol. 18, no. 7, July 2000.

[Tao01] M. Tao and R. S. Cheng, “Improved Design Criteria and New Trellis Codes for Space-Time Coded Modulation in Slow Flat Fading Channels.” *IEEE Communication Letters,* vol.5, no. 7, July 2001.

[Tel95] Telater, “Capacity of multi antenna Gaussian Channels,” *AT&T-Bell Labs Internal Tech. Memo.*, June 1995.

[Tex98] Space-time block coded transmit antenna diversity for WCDMA, Texas Instruments, Dec. 1998

[Tho01] S. Thoen, L. Perre, B. Gyselinckx, and M. Engels, "Performance analysis of combined transmit –SC/ receive-MRC," *IEEE Trans. Commun.,* vol. 49 no. 1, pp. 5-8, Jan. 2001.

[Tsa02] Jainn-An Tsai, *Combined Space-Time Diversity and Interference Cancellation for MIMO Wireless Systems*. Dissertation submitted to the faculty of Virginia Polytechnic Institute and State University in partial fulfillment of the degree of Philosophy in Electrical Engineering. May 2002.

[Tse97] D. N. C. Tse, "Optimal power allocation over parallel Gaussian channels," *Proc. Int. Symp. Infrmation Theory*, Ulm, Germany, June 1997.

[Tra02] T. A. Tran and A. B. Sesay, "Combined space-time trellis-coded modulation and group multiuser detection," *IEEE 55th VTC Spring 2002*, vol. 3, pp. 1369-1373, 2002.

[Ung82] G. Ungerboeck, "Channel coding with multilevel/phase signals," *IEEE Transactions on Information Theory*, vol. 28, Issue: 1, pp. 55-67, Jan 1982.

[Vit99] E. Viterbo and J. Bouros, *"*A universal lattice code decoder for fading channels," *IEEE Transactions on Information Theory*, vol. 45, Issue: 5, pp. 1639 -1642, July 1999.

[Vie01] I. Viering, M. Reinhardt and T. Frey, "Statistical Modeling of spatially correlated MIMO channels," *ISPACS 2001*, Nashville, November, 2001.

[Wan04] X. Wang, Y. R. Shayan, and M. Zeg, "On the Code and Interleaver Design of Broadband OFDM Systems," *IEEE Communication Letters*, vol. 8, pp. 653-655, Nov. 2004.

[Wit93] A. Wittneben, "A new bandwidth efficient transmit antenna modulation diversity scheme for linear digital modulation," *in Proc. IEEE'ICC,* 1993, pp. 1630-1634.

[Wol98] P. W. Wolniansky, G. J. Foschini, G. D. Golden, and R. A. Yalenzuela, "V-BLAST: an architecture for realizing very high data rates over the rich-scattering wireless channels," *Proc. ISSSE-98,* Pisa, Italy, pp. 295-300, Sept. 29, 1998.

[Wub01] D. Wubben, R. Bohnke, J. Rinas, V. Kuhn, and K. D Kammeyer, "Efficient algorithm for decoding layered space-time codes," *Electronics Letters* , vol. 37, Issue: 22, pp. 1348 – 1350, 25 Oct 2001.

[Xia00] C. Xiaodong and A. N. Akansu, "Multicarrier CDMA systems with transmit diversity", *Vehicular Technology Conference, 2000. IEEE VTS-Fall VTC 2000*. 52nd , vol. 6, pp. 2817-2821, 2000.

[Xu02] X. Changjiang and T. Le-Ngoc, "Joint channel estimation and decoding of space-time block codes", *Vehicular Technology Conference, 2002. Proceedings. VTC 2002-Fall. 2002 IEEE 56th* , Volume: 3 , 2002 Page(s): 1540 -1544 vol.3

[Xug01] Lu Xuguang and Li Hongbin, "Blind multiuser detection for space-time coded CDMA systems," *IEEE International Conference on Acoustics, Speech, and Signal,* vol. 4, pp. 2313 -2316, 2001.

[Yan00] Q. Yan and R.S. Blum, "Optimum space-time convolutional codes," *In Proc. WCNC,* Sept 2000.

[Yan04] Guang-Hua Yang, Dongxu Shen and V.O.K Li. "UEP for Video Transmission in Space-Time Coded OFDM Systems," *INFOCOM 2004. Twenty-third AnnualJoint Conference of the IEEE Computer and Communications Societies*, vol. 2, pp. 1200 - 1210, March 7-11, 2004

[Yon03] T. Yong, W. Junli, L. Tao, and Y. Guangxin, "Concatenated Space-Time Block Code with Trellis Coded Modulation in OFDM System," *IEEE ICCT 2003*, vol. 2, pp. 1194 – 1197, 9-11 April 2003.

[Yum00] Yumin Zhang; Blum, R.S. "Multistage multiuser detection for CDMA with space-time coding", *Statistical Signal and Array Processing, 2000. Proceedings of the Tenth IEEE Workshop on*, pp. 1-5, 2000.

[Zhi01] L. Zhiqiang and G. B. Giannakis, "Space-time block-coded multiple access through frequency-selective fading channels", *Communications, IEEE Transactions on* , vol. 49, Issue: 6, pp. 1033-1044, June 2001.

[Zhi03] L. Zheng and D. Tse, "Diversity and Multiplexing: A Fundamental Tradeoff in Multiple-Antenna Channala," *IEEE Trans. on Information Theory*, vol. 49, no. 5, May 2003.

[Zum00] S. A. Zummo and S. Al-Semari, "Space-Time Coded QPSK for Rapid Fading Channels" *Personal, Indoor and Mobile Radio Communications, 2000. PIMRC 2000. The 11th IEEE International Symposium on* , vol. 1, pp. 504-508, 2000.

Vita

Samir Al-Ghadhban was born on Feb. 03, 1975 in Khobar, Saudi Arabia. In 1997, he was awarded Bachelor of Science degree in Electrical Engineering with highest honors from King Fahd University of Petroleum and Minerals (KFUPM). In 2000, he received his Master of Science degree in Electrical Engineering from KFUPM with focus on wireless communications. In 2000, he received a scholarship from KFUPM and joined Virginia Tech PhD program in Electrical Engineering. He joined mobile portable and radio group (MPRG) in 2000 until graduation. He will receive his PhD in Electrical Engineering on Dec. 2005 from Virginia Tech. His current interests are in MIMO systems, space frequency time coding and scheduling.

Through his academic life, he has been awarded many honor certificates. In 1992, he received Prince Mohammed bin Fahd award for high achievement in secondary school over the Eastern Province in Saudi Arabia. In 1997, he received the IEEE student award for highest in major GPA and KFUPM award for highest honors.